WELDING Journal

February 2004

Welding Aluminum and the New Ford GT

Advantages of Electron Beam Welding

PUBLISHED BY THE AMERICAN WELDING SOCIETY TO ADVANCE THE SCIENCE, TECHNOLOGY AND APPLICATION OF WELDING

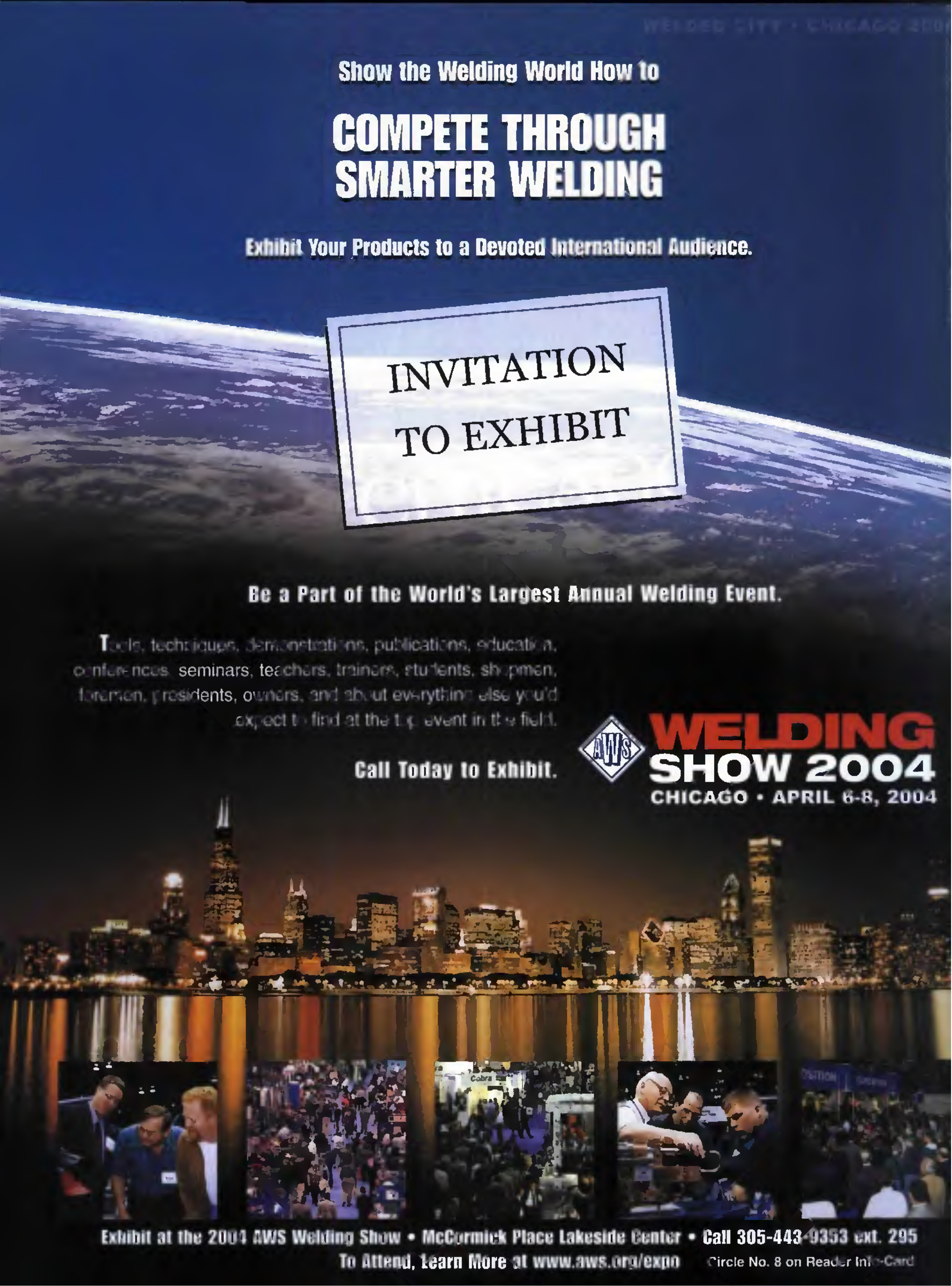

Show the Welding World How to
COMPETE THROUGH SMARTER WELDING
Exhibit Your Products to a Devoted International Audience.
INVITATION TO EXHIBIT
Be a Part of the World's Largest Annual Welding Event.
Tools, techniques, demonstrations, publications, education, conferences, seminars, teachers, trainers, students, shopmen, foremen, presidents, owners, and about everything else you'd expect to find at the top event in the field.
Call Today to Exhibit.
AWS
WELDING SHOW 2004
CHICAGO • APRIL 6-8, 2004
Exhibit at the 2004 AWS Welding Show • McCormick Place Lakeside Center • Call 305-443-9353 ext. 295
To Attend, Learn More at www.aws.org/expo
Circle No. 8 on Reader Info-Card

CONTENTS

February 2004 • Volume 83 • Number 2

AWS Web site *http://www.aws.org*

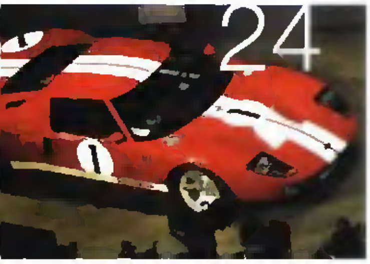

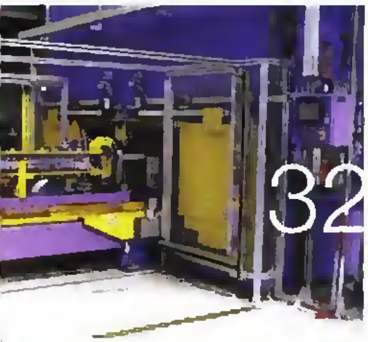

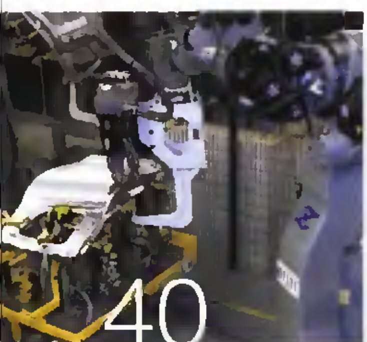

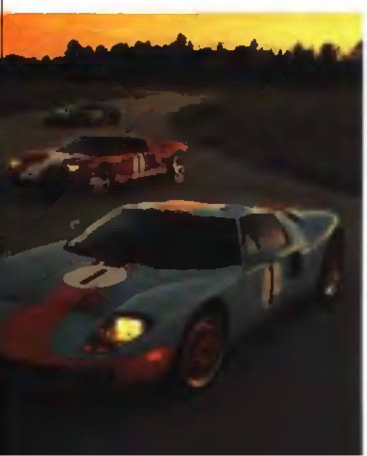

Features

Welding Research Supplement

Cover picture provided by Ford Motor Co.

Departments

Welding Journal (ISSN 0043-2296) is published monthly by the American Welding Society for $90.00 per year in the United States and possessions, $130 per year in foreign countries: $6.00 per single issue for AWS members and $8.00 per single issue for nonmembers. American Welding Society is located at 550 NW LeJeune Rd., Miami, FL 33126-5671; telephone (305) 443-9353. Periodicals postage paid in Miami, Fla., and additional mailing offices. **POSTMASTER:** Send address changes to Welding Journal, 550 NW LeJeune Rd., Miami, FL 33126-5671.

BY HUGH K. WEBSTER
AWS WASHINGTON GOVERNMENT AFFAIRS OFFICE

2003 Congress Produced Most Bills Ever

The first session of the 108th Congress, which ended in December, introduced almost 7000 pieces of legislation, the most ever by any Congress. Of these, only 159, or less than 3%, were actually enacted into law.

Proposed Greenhouse Gas Emissions Guidelines

The U.S. Department of Energy has released proposed guidelines for the voluntary reporting of greenhouse gas emissions and reduction efforts. These guidelines are related to the Department of Energy's registry program and are consistent with the current Administration's voluntary efforts to reduce U.S. greenhouse gas emissions. The guidelines, which are subject to a 60-day comment period, are available on the Department of Energy's Web site, *www.doe.gov*.

Manufacturing Competitiveness Costs Study Released

External, nonproduction costs add approximately 22% to unit labor costs of U.S. manufacturers (nearly $5 per hour worked) relative to their major foreign competitors, and are the primary competitive challenge facing manufacturers and their workers, according to "How Structural Costs Imposed on U.S. Manufacturers Harm Workers and Threaten Competitiveness," a new study sponsored by the National Association of Manufacturers and the Manufacturers Alliance/MAPI. The external costs referred to include taxes, health care and pension benefits, regulatory compliance, litigation, and energy.

Structural expenses such as taxes, benefits, regulatory compliance, litigation, and energy add nearly $5 per hour worked to U.S. manufacturing costs, threatening competitiveness.

OSHA to Renew Random Audit Program

The U.S. Occupational Safety and Health Administration (OSHA), for the third consecutive year, will conduct a random audit of 250 employers to ensure data being submitted to OSHA are accurate and in compliance with applicable regulations. The program should last approximately 12 months. Certain businesses will be excluded, including those with less than 40 employees, and those that currently participate in OSHA's Voluntary Protection Programs. Companies in the construction industry are expected to be excluded from audits under this program as well, since they were overrepresented last year.

Manufacturing Assistance Report Delayed

A highly anticipated and long-awaited report from the Department of Commerce identifying methods of strengthening manufacturing in the United States that was originally scheduled to be issued in September has been postponed for several months. In March 2003, Commerce announced its "Pro-Growth Manufacturing Agenda," which would include this report as well as establishment of a new assistant secretary level position within Commerce to focus on the manufacturing sector. Numerous workshops were conducted by Commerce officials with manufacturing executives throughout the country in order to better understand their concerns and possible solutions. Regarding the assistant secretary position, the exact duties have not been identified, but it is expected that this person will be a primary advocate for manufacturing within the federal government.

Campaign Finance Ruling May Bring More Regulation

The U.S. Supreme Court's recent decision upholding almost all of the provisions of the McCain-Feingold campaign reform law is expected to bring more government regulation of federal elections. Even though the margin of victory was 5-4, the case was a strong endorsement of the legal authority of Congress to regulate election financing. And while the ban on so-called soft money is expected to greatly increase the influence of political action committees, these entities can also expect that their higher profile will result in increased oversight and restrictions from Congress.

State Ergonomics Rules Rejected

After a bruising battle, a public referendum in the state of Washington to drop government regulations on ergonomics has passed. While this is a state issue, advocates on both sides from throughout the United States participated and watched this matter closely, and the result is expected to resonate as other states consider such rules. Washington had been only the second state — the other being California — to adopt ergonomics regulations. Federal rules were issued in 2001 but later overturned by Congress.

OSHA Announces Criteria for Priority Enforcement Cases

The U.S. Occupational Safety and Health Administration has issued a memorandum identifying the criteria that will qualify a case a "priority enforcement case" and therefore merit particular attention from OSHA. Specifically, an OSHA inspection that uncovers any of the following criteria will qualify:

- A fatality inspection in which OSHA finds a high-gravity serious violation related to the death;
- An inspection that results in three or more high-gravity serious violations;
- An inspection that results in two failure-to-abate notices where the underlying violations were classified as high-gravity serious;
- A fatality inspection in which OSHA finds that willful violation of a standard caused the death of the employee. ◆

Contact the AWS Washington Government Affairs Office at 1747 Pennsylvania Ave. NW, Washington, DC 20006; e-mail hwebster@wc-b.com; *FAX (202) 835-0243.*


SMOOTH FEEDING
SuperArc™
Premium MIG Wire with MicroGuard Ultra surface treatment.
MORE of What You Need in a MIG Wire.
MORE EFFICIENCY thanks to a smoother arc and reduced cleaning time.
MORE PRODUCTION thanks to a smoother feed and less downtime.
MORE PEACE OF MIND thanks to Lincoln Electric's 100% Satisfaction Guarantee.
Why Buy Anything Else?
SMOOTH ARC
LINCOLN® ELECTRIC
THE WELDING EXPERTS
The Lincoln Electric Company Cleveland, Ohio U.S.A.
216-481-8100 www.lincolnelectric.com
Circle No. 29 on Reader Info-Card

PRESS TIME NEWS

GE Aircraft Engines Acquires Agfa's Nondestructive Examination Unit

GE Aircraft Engines (GEAE), Evendale, Ohio, recently completed its acquisition of the Agfa-Gevaert Nondestructive Testing business unit, following receipt of all required regulatory approvals. Agfa NDT will be combined with GEAE's Nondestructive Testing business unit and will be renamed GE Inspection Technologies.

The company will be based in Hürth, Germany, and will have 1000 employees at more than 25 facilities in 25 countries worldwide. Jeff Nagel has been named president of GE Inspection Technologies. He has served as general manager of Business Development at GEAE since 2001 and previously served as president of GE Home Electric Products.

The purchase also includes a supply agreement for GE Inspection Technologies to become the exclusive seller of Agfa NDT X-ray film. Agfa will retain its X-ray film production.

GE Inspection Technologies offers radiographic, ultrasonic, eddy current, and other inspection-related products.

"GE has a strong history in the development of nondestructive inspection technology and equipment to support its businesses," said David Calhoun, president and CEO of GE Transportation. "For example, GEAE has been using GE Medical Systems' technology to enhance the productivity of our operations for years. The purchase of Agfa NDT provides GE with a platform on which to become a global leader in technology-driven inspection products that will deliver customer productivity, quality, and safety."

Lincoln Electric to Expand Welding Gun Product Line and Manufacturing Capabilities

Lincoln Electric Holdings, Inc., Cleveland, Ohio, recently announced plans to invest up to $10 million to expand its Magnum® welding gun product line and manufacturing capabilities in welding accessories. The company's aim is to dramatically increase its share of the worldwide welding gun market.

"Automation, robotics, and other high-production welding systems are increasing demand for high-quality welding guns," said John M. Stropki, executive vice president and chief operating officer. "To meet this demand, we are planning a new facility that will incorporate the manufacture of high-technology welding gun products. We also plan to refocus the efforts of our best research, design, and manufacturing engineers to this endeavor."

Lincoln plans to enhance its current line of Magnum® guns for the gas metal arc, flux cored arc, and submerged arc welding markets, and to invest in new designs for both steel and aluminum welding systems.

Seminar to Feature Presentations on Cutting-Edge Automotive Steel Technologies

The American Iron and Steel Institute (AISI) has scheduled its third Great Designs in Steel Seminar for Wednesday, February 18, at the Laurel Manor Conference and Banquet Center in Livonia, Mich. The free seminar begins at 7:00 a.m. with registration and continental breakfast. Attendees can also register online at *www.autosteel.org* by clicking on the seminar's promotional banner and following the path to "Register Online."

Automotive engineers will make most of the presentations, which will be divided among three concurrent tracks. The presentations will conclude at 3:30 p.m. Exhibits supporting the presentations will be available throughout the day.

Several presentations will focus on advanced high-strength steels, which are more durable than other steels but have less mass. Among the welding-related topics scheduled for the seminar are sessions on gas metal arc welding of advanced high-strength steels, dual-phase steel applications in tailor-welded blank technology, robust schedules for spot welding zinc-coated high-strength automotive steels, and impact modeling of spot welds in high-strength steels.

WELDING Journal

Publisher *Jeff Weber*

Editorial
Editor/Editorial Director *Andrew Cullison*
Senior Editor *Mary Ruth Johnsen*
Associate Editor *Susan Campbell*
Associate Editor *Ross Hancock*
Peer Review Coordinator *Doreen Kubish*

Graphics and Production
Production Editor *Zaida Chavez*

Advertising
National Sales Director *Rob Saltzstein*
Advertising Sales Promotion Coordinator *Lea Garrigan*
Advertising Production *Frank Wilson*

Subscriptions
Leidy Brigman
American Welding Society
550 NW LeJeune Rd., Miami, FL 33126
(800) 443-9353, ext. 453
leidy@aws.org

STRENGTH THROUGH INNOVATION

CUTMASTER 1Series – Experience the power of 1

Our exciting new CUTMASTER™ 1Series™ plasma cutting systems feature Thermal Dynamics'® revolutionary 1Torch – the only plasma cutting torch with easy-to-use ATC™ Quick Disconnect, standardized consumable parts, and performance optimized cutting tips. The CUTMASTER 1Series family of plasma systems gives you the power and precision for any plasma cutting need, from 3/8" to 1-1/4" maximum cut capacity. And 1Series start technology eliminates HF electronic interference that can occur with other designs.

Choose from CUTMASTER 1Series models 38, 51, 81 or 101, and discover the new dimension of flexibility, value, and performance that only CUTMASTER from Thermal Dynamics can provide.

For more information about the new **CUTMASTER 1Series** line and other Thermal Dynamics plasma cutting products, contact your local distributor or call
(800) 752-7621
www.thermal-dynamics.com

Circle No. 75 on Reader Info-Card

A THERMADYNE Company

Building a Foundation for the Future of Welding Education

The Education Committee (EC) has been very active in making welding education better not only for the balance of this decade but beyond. I'd like to tell you about some of the committee's objectives and accomplishments.

One of our first objectives was to improve communication for educators, students, and prospective students with the AWS Education Department. The recently updated Education Department Web site (*www.aws.org/education/*) provides a great amount of information 24 hours a day, 7 days a week with easy access worldwide. Their e-mail address *education@aws.org* and (800) 443-9353 ext. 229 phone number provide two more direct routes to the departmental staff. Current initiatives of the Education Department to create additional lines of communication are its participation at events like the ACTE convention, SkillsUSA convention, and the Educators booth, Plummer Memorial Lecture, and Education Program at the AWS Show. The first of a new quarterly newsletter to the 550+ SENSE welding programs is due out shortly.

A second initiative is to provide a directory of all welding education programs in the United States on the Web site. Currently, an interactive map on the site identifies and provides contact information for all of the AWS SENSE programs by state. The map will soon be expanded to include all U.S. welding programs by state and education level. This will not only help students locate a program at a specific level of welding education but one that is nearby.

A third initiative will recognize excellence in the following four categories: welding students, graduates, educators, and programs. Each month the AWS Education Department Web site will feature one or more person(s) or schools from each of these categories, including photos and other information. This showcase will include students from middle school, high school, postsecondary certificate, two-year technical, welding engineering technology, and welding engineering undergraduate, graduate, and doctorate programs. The intention of this new section of the Education Web site is to provide the following:

- Potential students will be given insight into the accomplishments of higher education level students
- Insight for advanced students into graduates' work experiences and challenges
- All students can learn about the programs available that can help them pursue an education and career in the field of welding
- Greater recognition for District and National Educator of the Year recipients
- Recognition of educational institutions committed to raising the level of welding skills, knowledge, and research.

A fourth objective is to update AWS documents and programs that support welding education. The update of B5.5, *Specification for the Qualification of Welding Educators*, is in the B5E Subcommittee for review and approval. This update better aligns this document with 2004 state and local requirements for welding educators. The modularization of QC-10, *Specification for Qualification and Certification of Entry Level Welders*, is in its second ballot in EC, and the modularization of EG2.0, *Guide for the Training and Qualification of Welding Personnel: Entry Level Welder*, has been prepared for its first ballot by the EC. These two documents will enable Entry Level students, despite the reduced contact hour constraints of welding education in 2004, to be better prepared for going directly into industry and improve the transition of students continuing their welding education. It addresses new state and federal requirements for documentation of student accomplishments for graduation.

I hope this information gives you some insight into the Education Committee's activities and that you consider this a personal invitation to join the AWS Education Committee or to become an active supporter of welding education through your local AWS Section.

Dennis Klingman
Chair, AWS Education Committee

STRENGTH THROUGH INNOVATION

'Next Generation' Power Performance

Thermal Arc introduces a new line of high-performance portable welding power sources for STICK, TIG, MIG and arc gouging (CAG) applications. We've improved the technology and value of our P-Wee®, Pro-Lite®, Pro-Plus® and Pro-Wave® power supply products, combining the very best in user convenience, portability, reliability and job-site versatility.

Thermal Arc offers a variety of 'Next Generation' models, all featuring:

- Simplified user interface with push-button controls
- Easy set-up and ability to store frequently used programs
- Voltage Reduction Device for maximum safety
- Durable, stackable case design
- Hassle-free, 3-year Thermal Arc warranty

See why Thermal Arc is the leader in arc welding technology. For more details, contact your local distributor or call Thermal Arc

(800) 255-5846

www.thermalarc.com

THERMAL ARC®

Circle No. 34 on Reader Info-Card

A THERMADYNE Company

New Women's Business Center Sites Open in Seven States

The U.S. Small Business Administration (SBA) recently added 11 new sites, in 7 states, to its Women's Business Center (WBC) program. The centers provide long-term training, counseling, and mentoring services to women entrepreneurs who want to start or grow small businesses.

The 11 new sites will share $1,650,000 in SBA funding, to be distributed among the centers. Each site is required to match a portion of the federal funds with private contributions, and services are tailored to the community in which each site is located. The program provides funding for an initial five-year term.

The WBC program now has 91 centers in 48 states, the District of Columbia, Puerto Rico, the Virgin Islands, and American Samoa. For more information, visit the Office of Women's Business Ownership's home page at *www.sba.gov/financing/special/women.html*. There is also an online Women's Business Center that can be reached at *www.onlinewbc.gov/*.

Worldwide Laser Market to Cross $3 Billion by 2008

The worldwide market for all types of lasers was estimated to be just over $2 billion in 2003 and should rise at an average annual growth rate (AAGR) of 9.1%, making it cross $3 billion by 2008, according to a recent report from Business Communications Co., Inc.

Diode-pumped, solid-state lasers will show the strongest growth, rising at an AAGR of 14.8% to $490.5 million in 2008. However, lamp-pumped lasers will continue to constitute the largest market, growing at a rate of 8% to reach $980.9 million by 2008, according to the report.

The report,GB-292, Solid State, Gas and Dye Lasers: Outlook for the Future, states use of lasers of various types will increase and dominate a number of fields. Cost of the report is $3750. For more information, contact Business Communications Co., Inc., 25 Van Zant St., Norwalk, CT 06855; telephone (203) 853-4266, ; e-mail *publisher@bccresearch.com*.

Miller Electric Celebrates 75th Anniversary; Commissions Anniversary 'Chopper'

Miller Electric Mfg. Co., Appleton, Wis., recently started its 75th anniversary celebration with the delivery of a motorcycle it commissioned Orange County Choppers (OCC) to design and build.

The company employs approximately 1200 people in Wisconsin. It began in 1929 in the basement of Niels Miller's Appleton home after he recognized a need for a small, affordable arc welding machine that would operate on the type of electricity available in rural Wisconsin.

Paul Teutul, owner of Orange County Choppers, rides the Miller 75th anniversary chopper inside Miller's Appleton, Wis., headquarters.

Delivery of the Miller chopper on December 12, 2003, marked the start of a yearlong celebration, explained Vickie Rhiner, manager, marketing, Miller Electric. Detailed information on the chopper, Miller's history, and customer appreciation events can be found on a new Web site *www.MillerWelds.com/75years*. Rhiner said the company plans to update the site every four to six weeks and that the biggest events will not be immediately announced.

To officially turn over the Miller chopper, OCC owner Paul Teutul, Sr., and chief designer and fabricator Paul Teutul, Jr., visited Miller's headquarters, signed autographs, and toured the manufacturing facility as part of filming for a cable TV show. An episode of *American Choppers,* airing early this month on the Discovery Channel, chronicles the building of the motorcycle.

The Miller Electric chopper features a Stars and Stripes design meant to embody the American spirit and freedom to ride. Orange County Choppers exclusively uses Miller brand power sources and welding helmets, and Paul, Jr., learned to weld using one of the company's machines.

BOC to Provide Gases and Equipment for Discovery Channel's 'Thunder Races'

Leopard Films of the United Kingdom has asked BOC North America, Murray Hill, N.J., to provide welding gases and hard goods for the welding and cutting machines used in *Thunder Races*, a series shown on the Discovery Channel in the U.K. and Europe.

The premise of *Thunder Races* is that three teams of three car fanatics/mechanical engineering experts are given $1000 and 24 hours to buy an old wreck and spare parts and then convert it into a vehicle they race at the end of the show. Each week the teams build a different type of vehicle — dune buggies, monster trucks, etc. Because of the extreme stress the vehicles endure, welding is a critical element in their success or failure.

California Tool and Welding Supply, a BOC distributor, has been working with Leopard Films in Las Vegas, Nev., as it films an American special of the show that will be shown early this year on Discovery's The Learning Channel. The distributor will supply cylinder gases and welding hard goods to the film crew and *Thunder Races* contestants.

Robotics Industry Up 28% in First Nine Months of 2003

New orders for industrial robots increased 28% through September 2003, according to figures released by Robotic Industries Association (RIA), the industry's trade group.

North American robotics suppliers received orders for 10,051 robots valued at $698.2 million from North American manufacturing companies in the first nine months of the year. Manufacturing companies from outside North America ordered an additional 331 robots valued at $29.3 million. The combined total of 10,382 robots valued at $727.5 million represents an increase of 28% in units and 15% in dollars over the same period in 2002.

"While it's too early to declare that the robotics industry is on the road to new record sales, we're very encouraged by the fact that nearly as many robots have been ordered through three quarters of 2003 as were ordered in the entire year of 2002," said Donald A. Vincent, RIA executive vice president.

Material handling continues to be the largest application area for robotics, followed by spot welding, arc welding, coating and dispensing, assembly, and material removal.

Wolf Robotics Purchases ABB's Welding Systems Division

Wolf Robotics recently purchased the assets of ABB's Welding Systems Division in Ft. Collins, Colo. The new company is part of the Rimrock group, currently ABB's largest strategic partner for robot automation.

The welding and cutting business has operated in Ft. Collins for nearly 60 years as Heath Engineering, ESAB Automation, and, for the past 11 years, as ABB. Dave Prosser will stay on as vice president and general manager, and approximately 25 people from the former ABB division have joined Wolf Robotics.

Wolf Robotics will offer a full range of products to the nonautomotive, general industry segment, and services that will include production consulting, technical service, parts, training, preventive maintenance, and programming.

Industry Notes

- MKS Instruments, Inc., Andover, Mass., recently opened an office in Shanghai to expand its local support in China. The office includes a calibration center and spare parts warehouse and can provide customer training. Garret Lin, general man-

— *continued on page 73*


Heat up your business
with the newest techniques & equipment
HOT SHOW HIGHLIGHTS:
▪ More than 400 exhibits
▪ Free Sessions
▪ Thousands of experts and highly-trained technical representatives
▪ Hundreds of live demos
▪ 2.6 million tons of equipment
▪ Seven special-interest Pavilions
▪ $2,500 First Prize for Best Welder in the First AWS Professional Welding Competition
▪ Show-only deep discounts on select exhibitor products
▪ And much more
REGISTER FREE ONLINE AT
WWW.AWS.ORG/EXPO
OR CALL TOLL-FREE 877-868-5290
AWS
WELDING
SHOW 2004
Sponsored by the American Welding Society
APRIL 6–8, 2004 ▪ CHICAGO, ILLINOIS
McCORMICK PLACE ▪ LAKESIDE CENTER
Circle No. 15 on Reader Info-Card


ESAB
PAC

Seven Truths for Welding and Joining Education

An educator presents his ideas on what he feels will shape the future of welding and joining education

BY ROBERT W. MESSLER, JR.

Joining, especially the process of welding, is faced with profound changes that have begun to transform materials science in ways that challenge conventional wisdom and best practice. At the same time, an increasingly global economy is forcing changes in the way manufacturing must take place to provide the volume, diversity, flexibility, responsiveness, quality, and cost competitiveness of products demanded by increasingly sophisticated and fickle consumers. Yet, ironically, manufacturing has seemingly lost some of its appeal as a career path for young engineers and technologists compared to research, product design, technical service, patent law, business, and entrepreneurship. Finally, postsecondary education has either not changed at all, enough, or in suitably appropriate ways to address these other changes to appropriately educate the future generations of technological thinkers and practitioners. The problem in postsecondary education is as much one of failure to fully recognize the profoundness and pervasiveness of the just-mentioned changes as it is a seemingly institutionalized resistance to accepting or responding to any change well or quickly.

Very Real Changes

Since the Stone Age[1], materials have been undergoing change with a progressively accelerating rate. The Bronze Age followed the 100,000-year-long Stone Age and lasted 4000 years until the dawn of the Iron Age, which lasted less than 2000 years, from about 100 B.C. to at least the 1700s. Since the Iron Age, we have experienced, but not (at least yet) formally named, ages dominated by steel, aluminum, superalloys, titanium, and long-range ordered alloys (or intermetallics) among metals; with overlapping parallel ages of plastics, semiconductors, high-temperature superconductors, and, now, nanocrystalline materials. At this very moment, we are experiencing the dawn of what may be the most profound of all ages, the age of tissue engineering (Refs. 1, 2). Clearly, any and every change in material demands an appropriate, corresponding change in processing, including joining in general, and welding in particular. Joining is, after all, the most important of all processes in manufacturing and construction, for without joining, nothing of great size, shape complexity, impressive functionality, or economy would exist (Ref. 3).

Manufacturing has been undergoing changes since the dawn of the Industrial Age, which first appeared in Europe and the new America between 1760 and 1790. In the last few decades, however, the rate and profoundness of change have been staggering. Quality, rather than quantity, became the measure of success; quantity with quality at low cost became the measure of productivity. The consumer demanded products; manufacturers didn't force unwanted choices on consumers. Automation has become more than a means to higher productivity, it has increasingly become the only means to produce some products — products involving too much repetitiveness to stimulate human beings, too much complexity to rely on typical workforces, too much hazard to expose humans to, or too small a size to rely on human dexterity. As a result, automation has become the "saving grace" of, not the "threat" to, the common worker, and embedded quality assurance has become a necessity rather than a perceived luxury.

Yet, even with the increased sophistication demanded of manufacturing, it has lost some, if not much, of its appeal to young engineers, as well as to current students in postsecondary education and the feed-streams from middle and secondary schools. The appeal of self-employment, independence, freedom to work at home, or wherever one wants (as opposed to where manufacturing centers have tended to be), business, service, and entrepreneurship have lured young people away from manufacturing. This allure has undoubtedly been helped (if not forced) by parents who want more for their children than they had for themselves, especially parents who lost jobs in the manufacturing sector, often just at the time they were sending their children to college.

While there have been changes in materials, in manufacturing, and in the appeal of manufacturing as a career, there have not been comparable, or offsetting, changes in postsecondary education. Colleges and universities have tended to adjust their curricula to the new world of service, not the unrecognized new world of manufacturing. Increasing numbers of faculty who never worked in industry, no less in manufacturing, drive the development of new courses tied to their research interests as much or more than to industry's interests. Materials curricula tend to try to cover all materials to the exclusion of depth in any material or focus on one material to the exclusion of other materials. They tend to gloss over processing — if they cover it — and they ignore joining because they

ROBERT W. MESSLER, JR., is Professor of Materials Science & Engineering, Director of Materials Joining, and Associate Dean for Academic & Student Affairs for the School of Engineering at Rensselaer Polytechnic Institute, Troy, N.Y.

Based on a paper presented at the AWS Annual Meeting and Convention, April 8–10, 2003, Detroit, Mich.

1. The Stone Age is the earliest period of time in which humans were known to employ tools made exclusively from stone, spanning from about 100,000 to 4000 B.C., for most of what is now the developed world.

either don't recognize its importance or understand its practice. All in all, it is more a lack of understanding what has changed and what is needed than simply not caring or responding. There is also the problem of not knowing how to respond.

So let's look at what must change in postsecondary education, as the foundation for and genesis of future designers and practitioners in manufacturing, in general, and joining and welding, in particular.

The Seven Truths

It is contended here that there are seven factors at play that are so basic, so ingrained, and so pervasive that they should be treated as "truths" just as certain "givens" are treated as truths in logic. These truths arise outside of education, but they profoundly affect what is needed from education.

Truth #1: The majority of problems encountered in joining in practice arise from the lack of application of existing knowledge, not a lack of knowledge.

This is not a cry to stop seeking new knowledge through research. It is simply a statement of fact that must be changed. Otherwise, if we don't use what we know, why seek to know more?

Anyone who has conducted a failure analysis for a product or process knows the root cause was virtually always avoidable if existing knowledge had only been employed. Welds in high-strength steels crack because of hydrogen-induced embrittlement arising from failure to properly preclean using well-established procedures, failure to employ commercially available recommended low-hydrogen electrodes, failure to employ needed and recommended preheat, or failure to postweld heat treat using well-established procedures. No fundamental knowledge was missing. Existing knowledge was simply not employed out of ignorance or neglect.

This is a matter of education. New designers, process engineers, and practitioners need to know the theory and then employ it. Increased attention needs to be given to case studies. The risks of circumventing best practice need to be fully appreciated. The education of a joining specialist or welding engineer must be centered on a strong foundation in theory, with appropriate accommodation of (or accounting for) faulty assumptions, imposed constraints, special circumstances, or lack of complete knowledge.

Truth #2: Poor quality in practice often results because high quality is not the basis for reward, gross output is.

If a shoemaker is paid for how many pairs of shoes he/she makes, he/she will make a lot of pairs of shoes, many of which may be of poor quality. If a welder is paid for how much he/she welds (in meters or feet, kilograms or pounds), lots of rod will get "burned." If industry wants quality because customers want quality or because the criticality of the structure or product demands quality, then quality not quantity must be the measure of success *and* the basis for reward.

Workers need to be rewarded for their "net quality" output not their "gross" output, with the emphasis on quality not quantity or speed. Education must instill in students that productivity is a measure of the efficiency with which output of acceptable quality is created not the sheer quantity of output.

Truth #3: Automation will increasingly be forced over manual processing.

The increasing sophistication of products, the greater demands on performance, global competitiveness, and a shrinking force of skilled tradespeople will continue to force automation to replace and eventually predominate over manual processing. As materials become increasingly "engineered" in their composition and microstructure, they will need to be processed more carefully, and robots will have to replace human beings. As speed with quality becomes the measure of productivity (see Truth #2), processes will have to be automated, employing embedded sensing for continuous monitoring and adaptive control. As fewer and fewer young people are attracted into the skilled trades for the allure of (and societal pressure to obtain) a college education, the workforce of such people will continue to shrink.

Automation will become the preferred approach for routine product manufacture and the necessary approach for highly sophisticated product manufacture. Human beings will be used for their creativity and adaptability, not their utility. Education will have to focus on teaching how processes work and how they can be controlled, not on how they can be performed as a trade. Troubleshooting will be a key skill, not burning rods.

Truth #4: For automated processes, overcontrol is as problematic as undercontrol or lack of control.

Surely there are examples where an automated process has not been sufficiently controlled; examples where knowledge of what to do, of what to control and how to control it, existed but was not followed (see Truth #1). But, there is also a tendency to overcontrol processes. Give a welder four knobs to turn, and that person will turn all four knobs. Give the welder one knob (like on a synergic power supply) and he/she will turn that one. Sometimes the knob turning is more out of a sense of guilt from not doing something than out of any real need.

The future world to be dominated by automated processing (see Truth #3) needs a new paradigm of "minimal essential control" vs. "total control." Perhaps an analogy will help make the point. An equine veterinarian knows everything there is to know about how a horse works, including the detailed mechanics, kinematics, and physiology of what makes a horse run fast. A jockey knows how to make a horse run fast, but rarely knows much about the detailed mechanics, kinematics, and physiology of the horse. The jockey effectively controls a complex system using a simple process of coaxing with verbal chortles and properly placed and timed cracks of a whip. This is minimal essential control. A veterinarian on a horse would almost certainly attempt total control and, in the process, overcontrol to no advantage, if not a disadvantage.

Education of welding engineers must emphasize control to achieve the desired end, not as an end in itself. Minimal essential control needs to be seen as proper not deficient. Control needs to be focused on outcome, not input. If the microstructure in and around a weld must be of a certain type for the weld to be considered of high quality, then we must learn to sense weld microstructure, not voltage, current, and travel speed.

Truth #5: Quality begins as a mindset, must be pervasive throughout manufacturing, and must be assessed in situ not post facto.

We must learn how to sense and monitor what really matters, rather than what doesn't matter but is easy to sense and monitor. Voltage, current, and travel speed are important parameters to produce a weld, and are indirectly responsible for at least some key characteristics of a weld for it to be considered of high quality, but they are not enough. Perhaps they are easy to monitor, so we monitor them out of guilt not to do so, as much as a lack of knowledge of knowing how to monitor what is really important (i.e., Truth 4).

Education must focus on the concept of total quality control, not as the result of overcontrol, but as the result of proper embedded control. A model to be emulated in welding is the "pop" thermometer in Frank Perdue's chickens. The weld is done, and done properly, when something "embedded" to monitor the weld indicates the weld has been done well.

Truth #6: The technology of joining will

become more important than the practice of welding; an enabling technology not just a pragmatic process.

Among a community of welders, this probably sounds like heresy. It's not meant to. It's just reality. Welding is a process for joining — an important one but not the only one. The proliferation of synthetic polymers, the yet-to-be realized full potential of composites, the emergence of nanomaterials and nano-structures, and the life-altering promise of tissue engineering will challenge joining more than just welding.

Education needs to not just respond to this "truth," it must anticipate and lead the needed change. Education in joining technology as an enabling technology, not just as a pragmatic manufacturing process must begin immediately, not later (Ref. 4).

Truth #7: The practitioners of joining will become more sophisticated as the process becomes more sophisticated.

Many of us learned to perform calculations needed to solve engineering problems using a slide rule. Some of us learned to do so using a handheld calculator and others a laptop computer. We all are good problem solvers — using the same basic knowledge but different tools. As joining becomes more an enabling technology than simply a pragmatic process (i.e., Truth # 6), the knowledge needed in practice will change but not nearly as much as the tools. In the future, scientists, engineers, and physicians will increasingly replace hard-hatted riveters and helmeted welders for the most sophisticated and high-value-added joining. That's not scary; it's progress.

Summary

Joining is changing because materials are changing. Welding is changing, because knowledge is changing. Education must change because knowledge is what drives and sustains change. As educators we are challenged — if not charged — to lead, not follow this change. To lead, we must embrace the changes not just face them. We must accept certain factors as "truths" and respond accordingly, logically, eventually leading the change, not reacting to it. ◆

References

1. Messler, R. W., Jr. 1996. The challenges for joining to keep pace with advancing materials and designs. *Materials & Design* 16(5): 261–269.

2. Messler, R. W., Jr. 2000. Joining technologies: Where to go from here not to be left behind? *J. of Assembly Automation* 20(2): 99–100.

3. Messler, R. W., Jr. 1993. *Joining of Advanced Materials.* Stoneham, Mass.: Butterworth-Heinemann.

4. Messler, R. W., Jr. 2003. Joining comes of age: From pragmatic process to enabling technology. *J. of Assembly Automation* 23(2): [t.b.d.].

Do You Have Some News to Tell Us?

If you have a news item that might interest the readers of the *Welding Journal*, send it to the following address:

Welding Journal Dept.
Attn: Mary Ruth Johnsen
550 NW LeJeune Rd.
Miami, FL 33126.

Items can also be sent via FAX to (305) 443-7404 or by e-mail to *mjohnsen@aws.org*.

Welding Generator Provides Excess Power

The Ranger™ 10,000 multiprocess welding machine includes a full-kVA 120 V/240 V outlet plus four 120-V outlets to power up to 10,000 W of plasma arc cutting machines, grinders, lights, and tools. It provides up to 225 A of AC/DC welding power for SMAW, GTAW, GMAW, and FCAW.

The Lincoln Electric Co. 100
22801 St. Clair Ave., Cleveland, OH 44117-1199

Electrostatic Air Cleaner Removes Oil and Smoke

The Air Boss® Model 75 electrostatic air-purification system is available in various capacity ranges for removing oil mist and smoke from plant facilities. The product is factory assembled, allowing the customer to quickly connect it to ductwork, power, and plumbing.

Trion Inc. 101
101 McNeill Rd., Sanford, NC 27330

Helmet Features Flip-Up Lens

The FlexView welding helmet/respirator system features a spring-mounted, retractable autodarkening lens that can be lifted, while a large, clear polycarbonate lens provides face protection during weld preparation, inspection, and grinding. A powered air-purifying respirator creates a positive atmosphere of filtered air that is 25-times cleaner than the air outside of the helmet. Assorted filters can be stacked in the respirator to provide additional protection against specific vapors.

Hornell, Inc. 102
2374 Edison Blvd., Twinsburg, OH 44087

Flame Spray Wire Produced in Larger Size

PMet 844 is a ⅛-in., cored, Ni-20Al wire designed as a bond coat for use with 420 stainless steel, aluminum bronze, and other flame spray coatings. The product is supplied on 10-lb spools.

Polymet Corp. 103
10073 Commerce Park Dr., Cincinnati, OH 45246

Laser CMM Has a 165-Foot Range

The Advantage Tracker portable coordinate measuring machine (CMM) has a 165-ft range and features a 72-µm accuracy at 20 ft. The product has a remote voice-command system and can be mounted in any position — vertical, horizontal, or upside-down.

Faru Technologies 104
125 Technology Park, Lake Mary, FL 32746

Purge Dam Materials Flush Away in Water

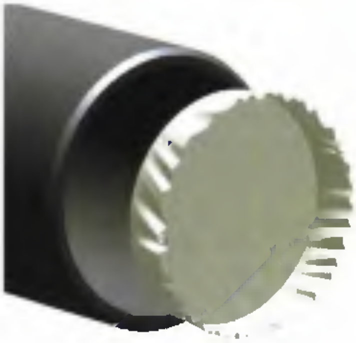

The company's water-soluble purge paper and dam-holding tape products are used to dam inert gases during the gas tungsen arc (GTA) welding of steel or aluminum pipes. After welding, the paper and tape can be flushed away with water or steam, leaving no harmful residue.

Aquasol Corp. 105
1576 Sweet Home Rd., Amherst, NY 14228

Mat Reduces Fatigue and Withstands Spatter

The Spatter-Mat was specifically designed for welding areas to alleviate leg and back stress from standing and working. The ½-in.-thick mat features a buoyant sponge base with a pebbled rubber surface that repels sparks, hot metal shards, and spatter while providing traction.

Wilson Industries, Inc. 106
123 Explorer St., Pomona, CA 91768

Diesel Welding Generators Operate at Low Speed

The PRO 300 multiprocess welding generator features a 22-hp, water-cooled

Circle No. 38 on Reader Info-Card

Caterpillar diesel engine producing 300 A at 100% duty cycle with a welding output range of 20 to 410 A. The engine runs at 1800 rpm for longevity. The unit also delivers 12 kW of power for lights and power tools.

Miller Electric Mfg. Co. 107
P.O. Box 100, Lithonia, GA 30058

Gas Regulator Handles High Inlet Pressure

The BelGas Type P39 high-pressure gas regulator features a forged brass body and a stainless steel diaphragm. Equipped with

Circle No. 37 on Reader Info-Card

Circle No. 2 on Reader Info-Card

¼-in. FNPT ports, the unit handles an inlet pressure of 5500 lb/in^2, with outlet ranges of 0–120, 0–150, 0–225, and 0–500 lb/in^2.

Marsh Bellofram 108
State Rt. 2, Box 305, Newell, WV 26050

Articulated Hose System Offers Flexibility

The Maxiflex universal articulated hose system allows positioning of cooling and cleaning fluids, gases, and vacuum delivery in grinding, milling, and other industrial applications. The ¼-in.- or ½-in.-diameter hoses are nonconductive, resistant to chemicals, and not subject to vibrational repositioning.

Wiha Quality Tools 109
1348 Dundas Cir., Monticello, MN 55362-8434

Robot Optimized for Parts Finishing

The DX1350 six-axis robot is optimized for material removal, deburring, and parts finishing applications such as grinding and sanding. The robot can bring the process tool to the workpiece or bring the workpiece to a fixed tool.

Motoman Inc. 110
805 Liberty Lane, West Carrollton, OH 45449

Tool Preps Oxygen-Cut Steam Pipes for Welding

The Prepzilla Millhog® pipe-milling and end-prep tool clamps to the inside of the torched ends of oxyfuel-cut steam lines and removes the heat-affected zone. After producing a square end, the tool can

— *continued on page 73*

ROBOTIC WELDING OF

Innovative aluminum frame-welding technologies are incorporated in the Ford GT

BY CARL OCCHIALINI

Sixteen months is not much time to design and produce a production-ready, street-legal, totally modern reincarnation of one of racing's most legendary vehicles — in fact, it's unheard of. But when the chairman of Ford Motor Co., William Clay "Bill" Ford, Jr., told his design and engineering teams that he wanted the new Ford GT ready for him to drive in the company's June 16, 2003, centennial parade, it became "job one."

The original Ford GT40 gained its reputation after former chairman and CEO Henry Ford II became determined to end the dominance of European auto manufacturers in international racing. In 1966, the GT40 swept first, second, and third places at the 24 Hours of Le Mans, the most prestigious of all international racing events. At the same time, Ford dethroned Ferrari, which had won the previous six races. The GT40 would end up winning first place for four consecutive years. Before the GT40, no American car had won the event.

While the new Ford GT maintains the image of the original with its low profile, curving lines, and mid-mounted engine, it grew slightly in size. The new GT is 18-inches longer, nearly a foot wider, and 4-inches higher than its predecessor. The engine, Ford's largest 5.4-liter, supercharged V-8 generates 500 horsepower and 500 ft-

---

CARL OCCHIALINI is Automotive Manager, Technical Sales, The Lincoln Electric Company, Cleveland, Ohio.

ALUMINUM SPACE FRAMES SPEEDS INTRODUCTION OF SPORTS CAR

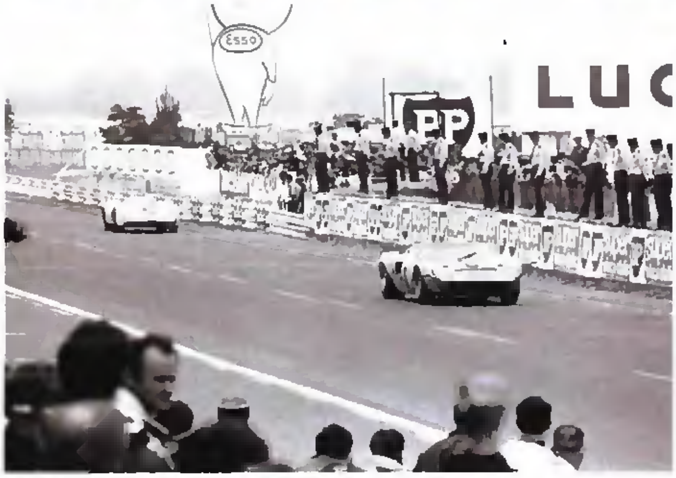

A sixties-era Ford GT40 at 24 Hours of LeMans, 1969, just a few lengths ahead of a Porsche 908, with one lap to go.

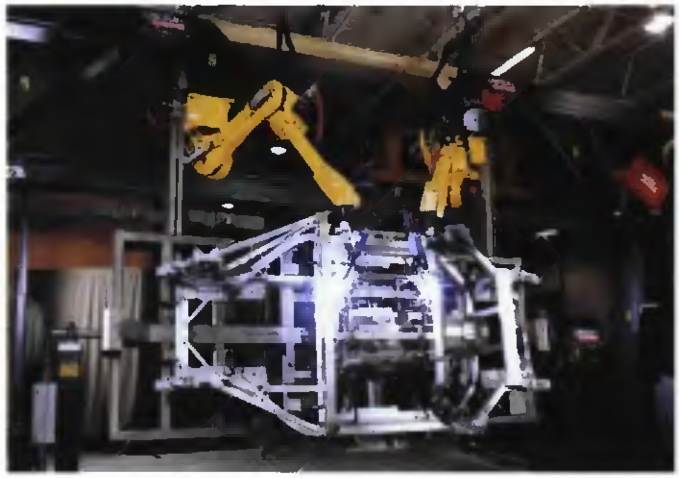

Two inverted welding robots work on a frame mounted to a rotating fixture.

lb of torque — power almost identical to that of the Le Mans-winning legend.

To accomplish this feat of engineering mastery on such a tight timeline, 30 engineers were selected from the top of their respective departments within the Ford Motor Co., and given an off-site Detroit, Mich., location where they could focus on the task at hand.

Subcontractor Metro Technologies, Ltd., had previously called in The Lincoln Electric Co. on another aluminum frame project for Ford called the Think vehicle. The Think was a highly engineered electric concept car. On the Think project, partners Lincoln and Metro were able to demonstrate their expertise on aluminum-framed vehicles, so when it came time to look for welding partners on the Ford GT project, Lincoln and Metro were given the task.

And quite a task it was — joining 35 aluminum extrusions, seven complex castings, two semisolid formed castings, and several stampings with more than 450 aluminum welds, each one unique, to make up the hybrid aluminum space frame. Attempting that many robotic welds on an aluminum automobile frame was a venture into uncharted territory.

Rick Tepper, robotic welding coordinator for Metro, said his team was able to complete the daunting task through teamwork and comprehensive analysis.

"Once Metro Technologies received the job, we worked with MVS (vehicle stampings and assemblies designer Mayflower Vehicle Systems) to develop a space frame design that was both structurally sound and capable of being manufactured. We applied knowledge from previous programs and developed a team of Tier 2 aluminum suppliers for additional support and expertise."

Tepper and his team, together with Lincoln as a source of welding expertise, also brought to the project years of collective experience from working on myriad aluminum welding projects.

"Weld shrinkage or distortion can be a major factor when working with aluminum," Tepper said, "but we knew by experience and experimentation how to weld these frames and keep distortion to within a couple of millimeters on the entire frame.

"We're talking about a high-performance vehicle pushing 500 horsepower and going 0 to 60 in four seconds with a top speed around 200 miles per hour," Tepper added. "That's why the welds have to be spot on."

The key to manufacturing an aluminum frame with such a high number of welds is sequencing, according to Tepper. By sequencing the robots to weld alternate sides of the frame, it allows an area to cool down before accepting another

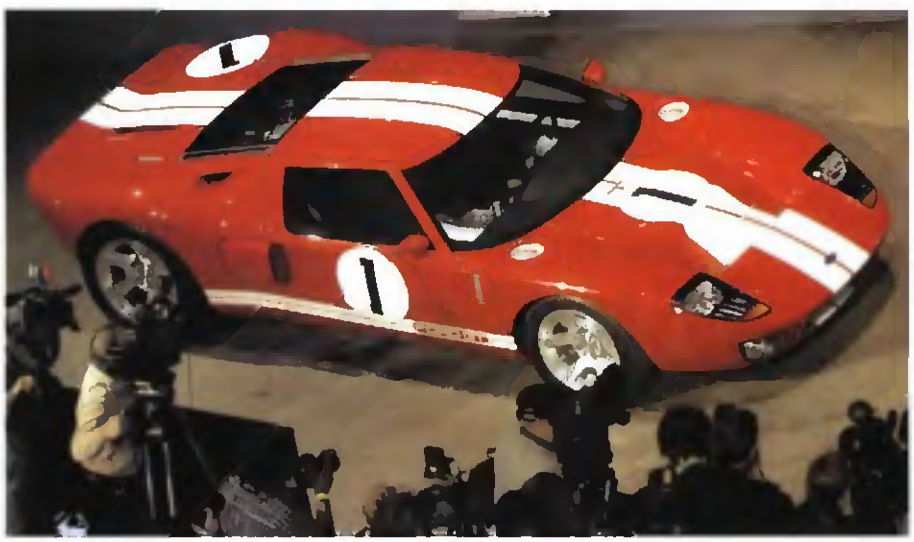

Equipped with a 500-horsepower mid-mounted engine, the Ford GT accelerates from zero to 60 in four seconds, with a top speed of about 200 miles per hour.

weld, thereby reducing distortion and controlling shrinkage.

To complete the job, Lincoln and Metro assembled four robotic cells utilizing a total of five robots. Lincoln's Power Wave® 455M power sources were mated with FANUC® 120iLB six-axis robots with the longest available reach of 70 inches and capable of high-speed movements. Each of these cells makes 100 to 125 welds. Rotating positioners were used to hold the parts under the robots to reduce cycle times.

To complete welding operations, the team chose Lincoln's SuperGlaze™ 1.2-mm 4043 aluminum gas metal arc welding (GMAW) wire. The 4043 alloy can be tricky to feed because of its softness. To manage the feeding challenges, a Binzel® torch was used in conjunction with an MK Products® push-pull system. Argon was used as the shielding gas. All of these components were then integrated by Lincoln Electric, providing Metro with a single welding partner to take responsibility for the welding cells, equipment, and operation.

Before the welding began, Tom Larkins, applications engineer at Lincoln Electric Automations Div., utilized the Delmia UltraArc® robotic arc welding simulation program to determine the logistics of the project. By programming three-dimensional, virtual models of the robots, torches, cabling, and the parts to be welded, real-world placements of each component could be factored, as could the movements of the robots to reach hard-to-access weld placements and avoid collisions.

"We used this as a tool as to whether or not specific components of the project would work," Larkins said. "Without this validation, the costs and timeline associated with the project would have been greatly extended."

With the information provided by the program, it was up to Lincoln's robotic technologist, Marty Sidall, to program the actual robots.

"There were a lot of challenges with the robots running upside-down, and it was difficult to get the torch into certain areas for some of the welds," Sidall said. "In order to reach every single weld in the program, we were really pushing these robots to their limits of positioning, and the placement of the parts had to be precise."

The frequent design changes also created programming challenges for Sidall. When one of the robot's 40 to 50 weld positions had to be altered, it created a domino effect in the programming in that the entire sequence after that weld had to be altered. Adding to the complexities of the programming was the fact that two robots were welding simultaneously in the same cell, which required "handshake communications." In these cells, if a weld sequence were altered, it would have to be altered on both robots.

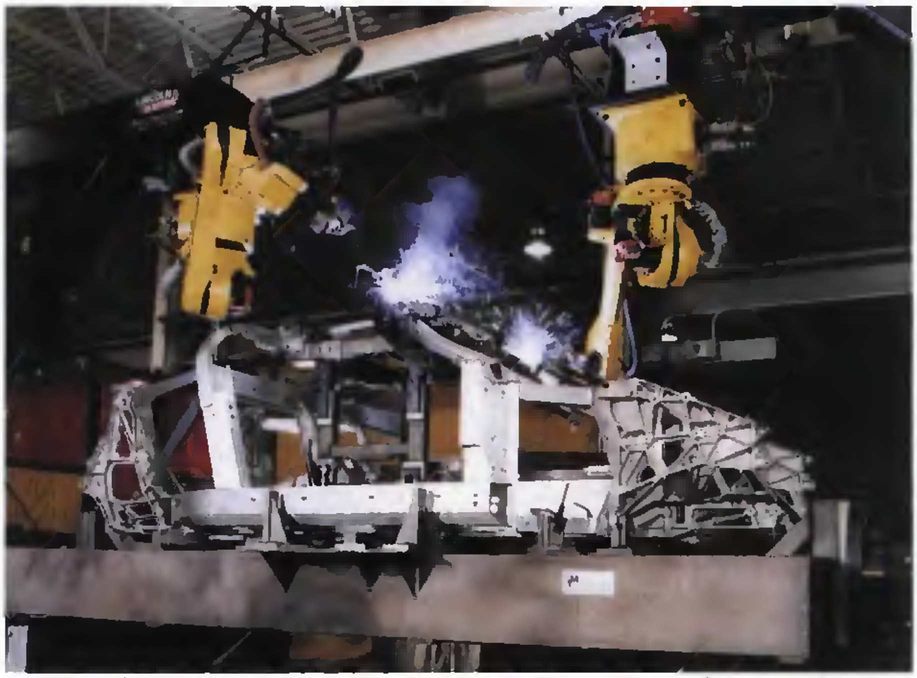

Robotic welding cells for the Ford GT are equipped with a rotating workpiece positioner.

"You not only have to program the robots to do the welds, you have to program them to know each other's location to avoid collisions," said Sidall.

To do this, Sidall programmed one of the robots as the "dumb" robot, which would return to a perch position before the other robot would resume its sequence.

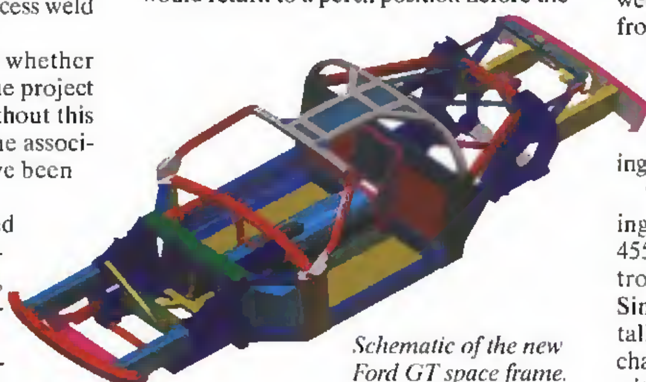

Schematic of the new Ford GT space frame.

Additionally, because there were so many welds to complete, the clamps and tooling holding the parts to be welded were often getting in the way of the robots and the weld gun.

"Hats off to Metro," Sidall said. "They were right in there at a moment's notice, bending and cutting clamps and relocating clamp handles to allow for the robots to do their job."

All said and done, the programming of the robots for each cell took about six weeks.

Cell one utilizes one robot with what could be called a "double Ferris wheel," where two fixtures revolve around each other and individually spin at the same time. Front and rear bumper mounts, transmission assemblies, and miscellaneous stabilizing bars are mounted in this cell.

Cells two and three each utilize two inverted robots, hanging from overhead, to allow for more range of motion. Rear subassemblies and primary castings are welded in cell two while cell three welds front assemblies.

Cell four utilizes two more inverted robots to weld together the front and rear assemblies and attach the cockpit, or greenhouse, completing the frame.

The Ford GT Spaceframe Manufacturing Team chose to use the Power Wave 455M because of its technology that controls and shapes the output waveform. Since the waveform may be shaped digitally, using software without the need to change electrical components, equipment with waveform control can deliver customized results for almost any application, improving productivity, quality, and operator appeal on a wide range of materials. These capabilities provide users with a versatile and upgradable welding system.

Tepper said the technology was integral in allowing Metro to achieve the welds necessary on the 6061 T6 extruded aluminum ranging in thickness from 1.5 to 8 mm, with 3 mm being the most common size. The machine allows for a lower-amperage welding procedure to be used, critical when distortion control is required for welding thin-gauge aluminum. Also, the digitally controlled inverter power source is capable of sophisticated arc starting procedures that help to reduce the risk of starting porosity and contribute to a flat, attractive weld bead profile. It also provides seamless arc welding process changes from GMAW to pulse or Pulse-on-Pulse™ from one weld to the next with minimal spatter.

As for interfacing with the Lincoln equipment, Tepper said, "Actually, the robots, together with Lincoln's control panels, are pretty easy to use. Once we developed our welding procedures, we didn't have any problems."

Tepper said by the time they welded the fourth frame, they were running "production intent," or parts intended for use in actual production, featuring weaved welds and all.

Three months prior to the centennial celebration deadline, nine prototypes of the finished car hit the road to test various components. By the June 16 deadline, three production models were ready and were driven, one by Bill Ford, to kick off the company's centennial celebration.

Two of the original three GTs have been dedicated "media cars" and are currently making the circuit of leading automobile media outlets where they are driven and reviewed by journalists. An additional 15 GTs were built for crash tests and other studies.

With the completion of the first 18 GTs, the robotic welding cells and other production mechanisms are being dismantled and shipped to Milford Fabricating Co. in Detroit. Milford, a subsidiary of the Budd Co., will handle production of the vehicles.

The plan is to build eight GTs per day, five days a week for two and a half years — a grand total of 4500 GTs expected to retail at $140,000–150,000. If initial feedback from the automotive press is any indication, the GTs should be zipping off the showroom floor as fast as their 500-horsepower engines can take them. ◆

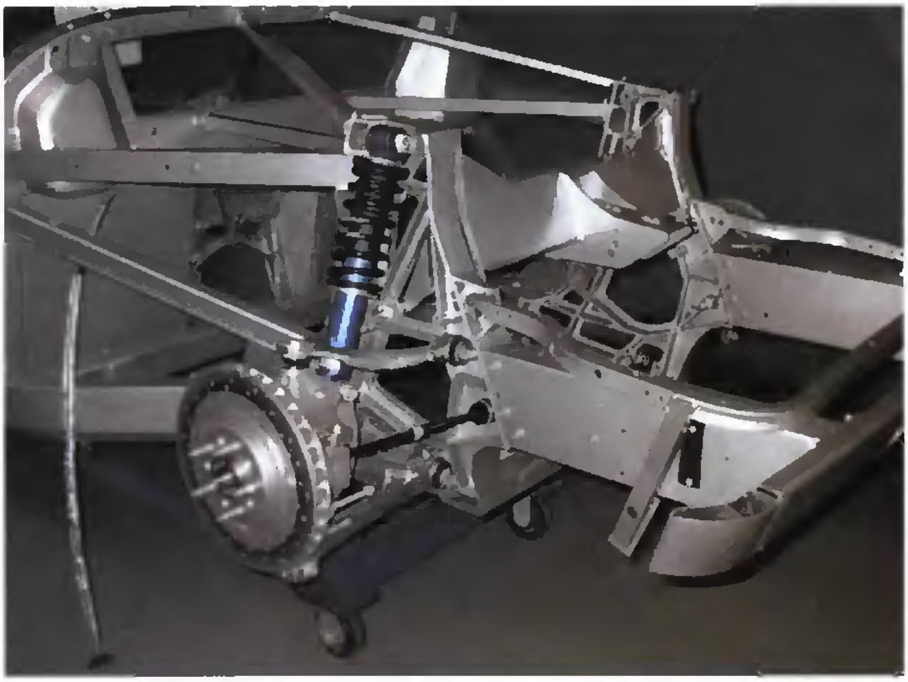

Side-rear view of the car's aluminum frame with wheel suspension.

Fig. 1 — The Joint Venture is being used by the U.S. military for evaluation and demonstration trials.

New Developments in Aluminum Shipbuilding

Welded aluminum meets the needs of a changing military

BY TONY ANDERSON

This article was inspired by current activities within the U.S. military, the extraordinary developments in aluminum shipbuilding that have been taking place in Australia, and the creation of new high-strength aluminum alloys, primarily in Europe, for the shipbuilding industry.

A recent visit to Incat Tasmania Pty. Ltd. (shipbuilding), off the southeast coast of Australia, revealed a manufacturer that has taken aluminum shipbuilding to exciting new levels. In 1977, it launched its first high-speed catamaran, and today it is manufacturing the new generation of 98-meter (322-ft) wave-piercers, which are being evaluated by the United States military. Incat has constructed more than 50 vessels of various lengths. The company's first passenger/vehicle ferry was delivered in 1990, a 74-meter (243-ft) wave-piercing catamaran with a maximum deadweight capacity of 200 metric tons (440,000 lb). The more recent 98-meter Evolution 10B range has a deadweight four times that amount.

While Incat-built ferries initially revolutionized transport links around the U.K., today its ships operate in North and South America, Australasia, the Mediterranean, and throughout Europe. Incat's extensive shipbuilding activity is conducted from a modern facility with over 32,000 m^2 under cover, located at Hobart's Prince of Wales Bay in Tasmania.

Aluminum Welded Ships within the U.S. Military

In response to great interest from the U.S. military in high-speed craft, Incat, via its U.S. affiliate, Incat USA, formed a strategic alliance with an American shipyard to market and build innovative craft designs for military and commercial markets. The Bollinger/Incat USA strategic alliance combines Incat, the premier builder of the world's

Fig. 2 — The Spearhead, one of a new generation of 98-meter wave-piercers, has been deployed in the Persian Gulf.

fastest vehicle/passenger ferries, with Bollinger, a proven builder of a variety of high-speed, reliable, and efficient patrol boats for the U.S. Navy and Coast Guard.

The U.S. government has awarded Bollinger/Incat USA, New Orleans, La., the charter for a high-speed craft (HSC) for a multiservice program operated by various arms of the military. The HSC vessel, now known as *Joint Venture* HSV-X1 (Fig. 1), is being used for evaluation and demonstration trials to assess the usefulness of such technology in military and Coast Guard applications. The *Joint Venture* was selected as the optimum vessel to deliver the best performance for the scope of work required by the military. Undergoing a major refit with innovative design and construction, the craft was upgraded and fitted with military enhancements such as a helicopter deck, stern quarter ramp, rigid-hulled inflatable boat, deployment gantry crane, troop facilities for 363 personnel, crew accommodation, storage facilities, medical facilities, and long-range fuel tanks. As the *Joint Venture* continues to excel in her experimental role, Incat's intention to see the military potential of such craft realized took another step forward in September 2002 with the sale of USAV TSV-1X *Spearhead* to Bollinger/Incat USA for charter to the U.S. Army.

Spearhead (Fig. 2) is the U.S. Army's first theater support vessel (TSV) and is part of the Advanced Concept Technology Demonstrator program by the office of the secretary of defense and the U.S. Army. *Spearhead* is being used to demonstrate and evaluate its ability to perform during certain mission scenarios, to assess its usefulness to the U.S. military, and to refine the requirements for the next generation of Army watercraft. The TSV is critical to the Army's ability to perform its Title 10, intratheater mission. *Spearhead* is utilized on missions to maximize its speed and flexibility and is needed for both sustainment deliveries and the movement of Army prepositioned stocks and troop units. Theater support vessels promise to change the way the U.S. Army gets to the fight. They will allow the Army to quickly deliver intact packages of combat-ready soldiers and leaders with their equipment and supplies, enabling them to "fight off the ramp" if necessary. Delivering intact units within a theater also will reduce the need for a large-scale onshore reception, staging, onward movement, and integration of soldiers, vehicles, and equipment within the battle space. The future vessels promise to transport units within a theater of operation in hours instead of days. The TSV will support the Army Transformation goal of deploying a combat-ready brigade anywhere in the world within 96 hours, a division in 120 hours, and five divisions within 30 days. Speed, coupled with a large cargo capacity, will provide greater payload throughput at long ranges as well as the ability to rapidly reposition and mass assets within a theater of operations.

Just three weeks after the awarding of the contract for *Spearhead* came another, separate, order from the U.S. military. Military Sealift Command is the contracting arm that has leased a 98-meter craft from Bollinger/Incat USA to support U.S. Navy Mine Warfare Command. The craft, HSV-X2 *Swift*, was constructed at the Hobart, Tasmania, shipyard and will be stationed in Ingleside, Tex. The ship is capable of maintaining an average speed of 35 knots or greater loaded with 500 short tons (453,600 kg) consisting of 350 personnel and military equipment. A minimum operating range of 1100 nautical miles at 35 knots is required by the contract, as is a minimum transit range of 4000 nautical miles at an average speed of 20 knots. Furthermore, the craft must be capable of 24-hour operations at slow speeds (3–10 knots) for small boat and helicopter operations.

It will be fitted with a stern ramp capable of on/off loading directly astern or to the starboard quarter. The ramp is capable of loading/unloading a multitude of military vehicles up to and including battle tanks of up to 140,000 lb (63,500 kg). The ramp is also capable of launch and recovery of amphibious assault vehicles. To achieve this, the ramp tip end can be submerged, allowing the amphibious vehicles to drive on and off.

The ship is also capable of launch and recovery of small boats and unmanned vehicles up to 10,400 kg (23,000 lb) while underway.

TONY ANDERSON (tanderson@alcotec.com) *is Technical Director of AlcoTec Wire Corp., Traverse City, Mich.; Chairman of the Aluminum Association Technical Advisory Committee for Welding and Joining; Chairman of the AWS D10H Subcommittee on Aluminum Piping; Chairman of the AWS D3A Subcommittee on Aluminum Hull Welding; Chairman of the AWS/SAE Subcommittee on Automotive Arc Welding of Aluminum; and Vice Chairman of AWS D1G Subcommittee 7 on Aluminum Structures.*

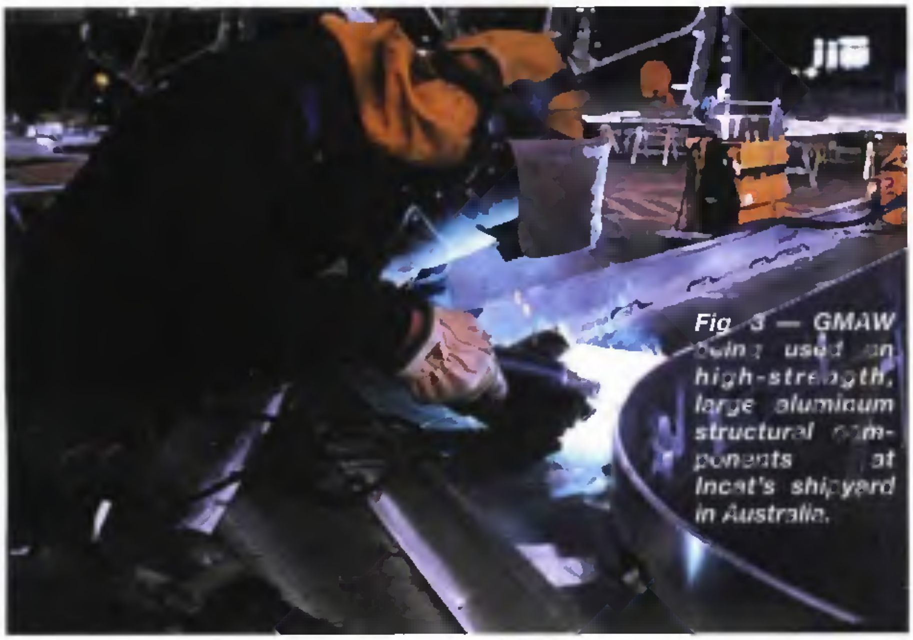

Fig. 3 — GMAW being used on high-strength, large aluminum structural components at Incat's shipyard in Australia.

The vessel is fitted with a NAVAIR-certified helicopter deck for operation of MH-60S, CH-46, UH-1, and AH-1 helicopters. An area protected from the weather for storage and maintenance of two MH-60S helicopters is provided, as is a Carriage Stream Tow and Recovery System (CSTARS). This helo deck has the capacity to transfer equipment up to 2720 kg (6000 lb) to and from the vehicle deck.

New Developments in High-Strength Aluminum Alloys for Marine Applications

Until fairly recently, the most popular base metal used for aluminum shipbuilding, 5083, had very little rivalry from other alloys. The 5083 base alloy was first registered with the Aluminum Association in 1954, and while often referred to as a marine aluminum alloy, it has been used for many applications other than shipbuilding. The popularity of the 5083 alloy within the shipbuilding industry has been largely based on its availability and also its ability to provide excellent strength, corrosion resistance, formability, and weldability characteristics. Other lower-strength alloys such as 5052 and 5086 have been used for the manufacture of usually smaller, lower-stressed, and typically inland lake boats, but 5083 has been predominant in the manufacture of oceangoing vessels.

In recent years, progress has been achieved by aluminum producers in the development of improved aluminum alloys specifically targeted at the shipbuilding industry. In 1995 the aluminum manufacturer Pechiney of France registered the aluminum Alloy 5383 and promoted this material to the shipbuilding industry as having improvements over 5083 alloy. These improvements provided potential for significant weight savings in the design of aluminum vessels and included a minimum of 15% increase in the postweld yield strength, improvements in corrosion properties, and a 10% increase in fatigue strength. These developments, coupled with formability, bending, cutting, and weldability characteristics at least equal to that of 5083, made the 5383 alloy very attractive to designers and manufacturers who were pushing the limits to produce bigger and faster aluminum ships.

More recently, in 1999, the aluminum manufacturer Corus Aluminum Walzprodukte GmbH in Koblenz, Germany, registered the aluminum base Alloy 5059 (Alustar) with the American Aluminum Association. This alloy was also developed as an advanced material for the shipbuilding industry, providing significant improvements in strength over the traditional 5083 alloy. The 5059 alloy is promoted by Corus as providing improvements in minimum mechanical properties over Alloy 5083. These improvements are referenced as being a 26% increase in yield strength before welding and a 28% increase in yield strength (with respect to Alloy 5083) after welding of H321/H116 temper plates of the AA5059 (Alustar alloy).

Welding the New Aluminum Alloys

The welding procedures used for these high-strength alloys are very similar to the procedures used for welding the more traditional 5083 base metals. The 5183 filler metal and the 5556 filler metal are both suitable for welding 5383 and 5059 base metals. These alloys are predominantly welded with the gas metal arc welding (GMAW) process using both pure argon and a mixture of argon/helium shielding gas — Fig. 3. The addition of helium of up to 75% is not uncommon and is useful when welding thicker sections. The helium content provides higher heat during the welding operations, which assists in combating the excessive heat sink when welding thick plate. The extra heat associated with the helium shielding gas also helps to reduce porosity levels. This is very useful when welding the more critical joints such as hull plates that are often subjected to radiographic inspection.

The design strengths of these alloys are available from the material manufacturers; however, there would appear to be few as-welded strength values incorporated in current welding specifications. Certainly these relatively new base alloys are not listed materials within the AWS D1.2, *Structural Welding Code — Aluminum*, and consequently no minimum tensile strength requirements are included in this code. If this material continues to be used for welded structures there will be a need to address this situation by establishing appropriate tensile strength values and including them in the appropriate welding codes.

Early testing on the 5059 (Alustar) base alloy indicated that problems could be encountered relating to the weld metal not being capable of obtaining the minimum tensile strength of the base material heat-affected zone. One method used to improve the weld tensile strength was to increase the amount of alloying elements drawn from the plate material into the weld. This was assisted by the use of helium additions to the shielding gas, which produces a broader penetration profile that incorporates more of the base material. The use of 5556 filler metal rather than the 5183 filler metal can also help increase the strength of the deposited weld material.

Obviously these high-performance vessels require high-quality welding. The training of welders, development of appropriate welding procedures, and implementation of suitable testing techniques are essential in producing such a high-performance product.

The Future

With the increasing demand to create larger and faster ships, particularly for military service, and the development of new, improved, high-performance aluminum base materials, it is apparent that aluminum welding has acquired an interesting and important place within the shipbuilding industry. Also, with the pending introduction of this unique technology into the United States, it is important that designers, manufacturers, and, particularly, welders and welding engineers are adequately trained and familiar with this new technology. ◆

EBW of Aluminum Breaks Out of the Vacuum

Applying electron beam welding directly in atmosphere boosts aluminum welding productivity

BY KLAUS-RAINER SCHULZE AND DONALD E. POWERS

KLAUS-RAINER SCHULZE is with PTR Praezisionstechnik GmbH, Maintal, Germany, and DONALD E. POWERS is with PTR-Precision Technologies, Inc., Enfield, Conn.

Electron beam welding (EBW) is a high-energy-density beam welding method that is recognized as providing the capacity to achieve higher weld speeds, lower heat inputs, and greater depth-to-width aspect ratios than most other fusion-type welding methods. However, while generally recognized as having the capability to provide these desirable process characteristics while being utilized in some form of vacuum environment, it is not as commonly recognized that the EBW process can also be employed for use on workpieces located outside a vacuum environment (i.e., directly in atmosphere) — Fig. 1. This nonvacuum means of electron beam welding eliminates the necessity of having to evacuate a workpiece's surroundings before initiating welding, thereby reducing the overall cycle time required for producing parts.

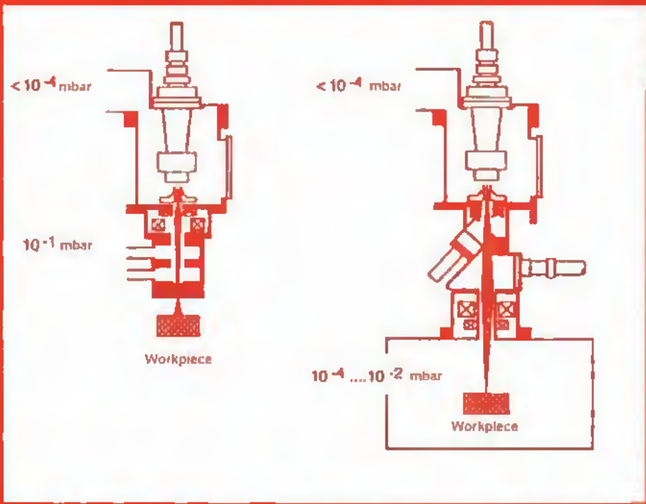

Fig. 1 — Electron beam welding directly in atmosphere and under vacuum.

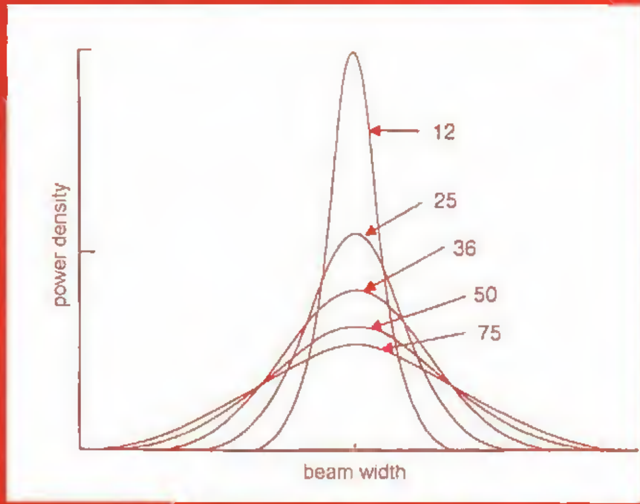

Fig. 2 — Widening of power density distribution with increasing working distance.

Although electron beam welds produced directly in atmosphere (using nonvacuum electron beam welding, or NVEBW) aren't usually capable of exhibiting fusion zone characteristics identical to those accomplished when some sort of vacuum environment is employed, nonvacuum EB welds exhibit a fairly high aspect ratio and relatively low total energy input, especially at the higher welding speeds that have been demonstrated as achievable with the NVEBW process.

Because of its ability to reliably and repeatedly produce acceptable welds at very high part-production rates, the NVEBW process has been successfully utilized in the U.S. automotive industry for close to 40 years. During that time span, the process has been employed on upward of 100 welding systems that have a combined production output numbering in the hundreds of millions of parts. Some examples of the variety of parts that have resulted from this mass production utilization of the NVEBW process are torque converters, catalytic converters, steering column jackets, tailored blanks (used for providing deep-drawn frame segments), planetary gears, timing gears, and die-cast aluminum manifolds (Ref. 1).

Besides two U.S.-originated units installed in France some 25 years ago, the first European enterprises that pioneered the use of the NVEBW joining method for mass production were in Germany — first in 1995, then with more installations in 1999 and 2001. The current number of German NVEBW installations will soon increase, since more facilities are adding the process to their production lines. All of these new European NVEBW production applications are being used for aluminum part fabrication. This is not only due to the importance placed on the use of aluminum in modern day automotive production, but also because of the outstanding weld quality the NVEBW process provides under high-volume production conditions for high-speed welding of this challenging-to-weld material.

Process Basics and Equipment Overview

The electron beam used for NVEBW processing is generated in a high-vacuum environment. An electron gun is used to produce the beam through electrostatic collimation and acceleration of thermal electrons emitted from an incandescent filament. Upon exiting the gun area, the beam, which consists of electrons accelerated up to an operating voltage level of about 175 kV, is electromagnetically focused down through a set of orifices separating a series of increasing pressure-level vacuum stages. Therefore, in NVEBW, the beam is initially generated under high-vacuum conditions, but is then extracted out of this ideal environment, and applied to a workpiece located directly in atmosphere. This is accomplished by employing a series of differentially pumped vacuum stages (all isolated from each other and atmosphere by a set of axially aligned orifices) that the beam passes through in its travel route out into the ambient atmosphere.

Upon exiting the NVEBW gun column assembly and entering the surrounding atmosphere, the beam of electrons begins to broaden due to collisions with gas molecules in the ambient environment. This then causes the beam's diameter to gradually increase with distance traveled out into the surrounding atmosphere. The degree to which the beam diameter increases as a result of these collisions depends both on the makeup of the surrounding gas (i.e., heavier gases, such as air, will produce a more rapid broadening effect than lighter ones, such as helium) and the distance the beam travels in this ambient atmosphere before striking the workpiece (i.e., the length of exit orifice-to-workpiece spacing). Irrespective of this beam dispersion effect, since NVEBW equipment commercially available today is easily able to provide 25 kW of beam power or more, the power density being delivered to the workpiece is still of a high enough magnitude to allow keyhole-type welds to be readily achieved at "standoff" (i.e., exit orifice-to-workpiece spacing) distances ranging up to 30 mm in length (Fig. 2) (Ref. 2).

Although this beam dispersion effect ultimately limits the maximum standoff distance that can be utilized when applying the process, it simultaneously helps reduce the degree of part preparation needed for employing the process. This is due to the fact that the beam divergence and resulting beam spot size increase at the workpiece. This dispersion effect allows gaps, mismatches, and beam-to-joint misalignments resulting in poor joint fitup values in the range of 0.5-mm-magnitude to be welded. In addition, although a metal vapor plasma

Fig. 3 — Examples of NVEB welds in steel: A — fillet weld, 5.7 + 6.7 mm, 6.4 m/min, 26 kW; B — seam weld, 2.4 + 3.5 mm, 6.4 m/min, 15 kW; C — butt joint weld, 25 mm, 0.5 m/min, 30 kW.

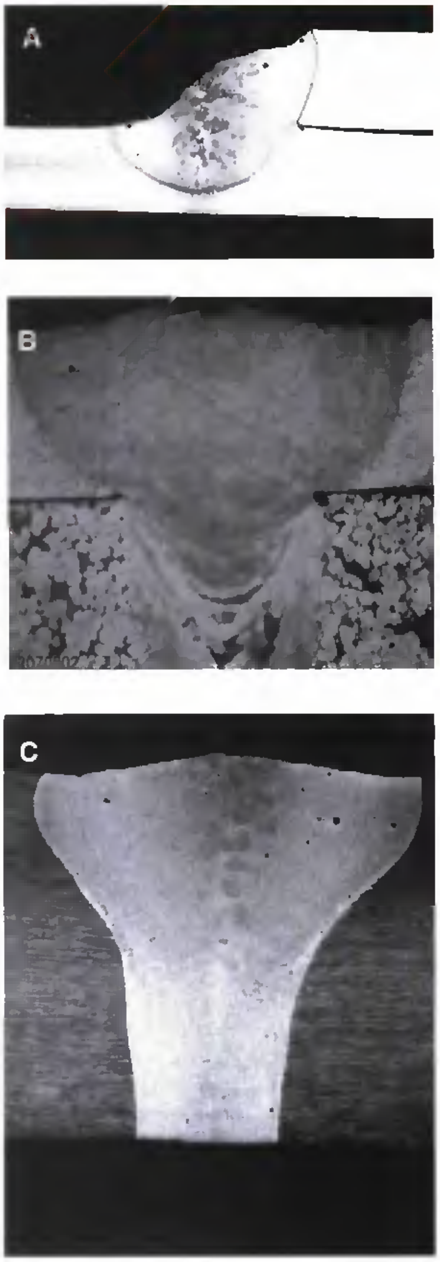

Fig. 4 — Examples of NVEB welds in aluminum: A — fillet weld, Al-3%Mg, 2×2.5 mm, 7.6 m/min, 10.7 kW; B — seam weld, Al-3%Mg, 2.4 mm + Al-7%Si-0.15%Mg, 3.5 mm, 10.2 m/min, 3.7 kW; C — butt joint weld, Al-2%Mg-0.8%Mn, 5 mm, 7.5 m/min, 11.7 kW.

results from employing a keyhole method of welding, this plasma neither interferes with nor detracts from the NVEBW process's ability to produce a satisfactory weld. Thus, as a consequence of this plasma being "transparent" to an electron beam, it need not be disposed of (i.e., forcefully blown out of the beam's path) as is required in the case of laser beam welding. The NVEBW process can also be used to join any conventionally weldable metal without fear of a negative influence from the material's surface texture condition and/or reflectivity value, nor as a result of the degree of beam impact angle being employed.

The weld depth achievable in a single pass with the NVEBW process spans the range from 0.5 to 25 mm — with the attainable result ultimately dependent on the material being welded, as well as the standoff distance and weld speed being employed. Figures 3 and 4 indicate the type of weld profiles (i.e., weld depth and depth-to-width ratio) achievable from employing the NVEBW process under various conditions. These figures illustrate the variety of welds (seam, flange, fillet, butt, etc.) that can readily be accomplished with the process. The process is also capable of providing weld speeds from less than 0.5 to greater than 50 m/min, depending on type and thickness of material being welded and standoff distance being employed.

It should be noted that the NVEBW process sometimes employs a "helium blowdown" technique. This is a method that generates a stream of helium in such a manner that it blows out into the ambient atmosphere coaxially with the beam's travel path. This directed flow of helium tends to partially shield the beam from the ambient atmosphere, thereby helping reduce the rate at which beam broadening occurs. Utilization of helium blowdown is not a requirement for employing the process, and whether or not to use this technique is evaluated on a case-by-case basis.

In addition, although NVEBW can normally be accomplished without the need to utilize some type of adder material, either for acting as a deoxidizing agent or as a filler material (to help accommodate excessively poor joint fitup conditions), the process is quite adaptable to having material continuously fed into the melt zone during welding, should the need to employ such a tactic ever arise.

Each NVEBW machine is comprised of three primary systems:

Beam Generating System — This consists of the beam generation gun column assembly, plus the high-voltage power supply, vacuum pumps, control units, etc., utilized for operating the assembly.

Part Clamping and Motion System — This depends on the size and shape of workpiece to be welded, and can vary from a system providing straight linear transfer of parts in and out of the weld area and production of a simple circular weld path during welding, to a system employing complex part-transfer means and providing three-dimensional weld path motion. In general, since the beam generator column can weigh on the order of 400 kg, welding motion is normally accomplished through movement of the part only. However, various applications have employed an integrated motion of both column and part to perform the weld task required.

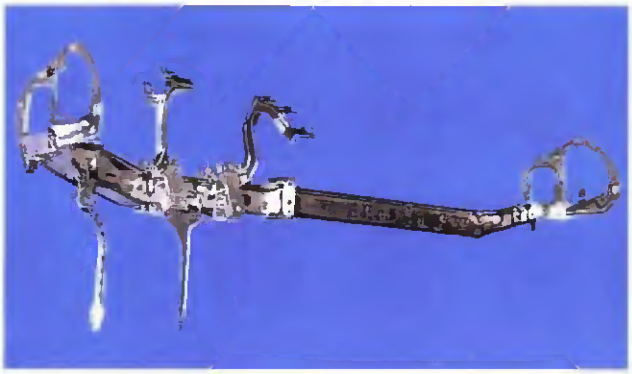

Fig. 5 — Nonvacuum electron beam-welded aluminum structural beam for a car's instrument panel, here completed by GMA-welded attachments.

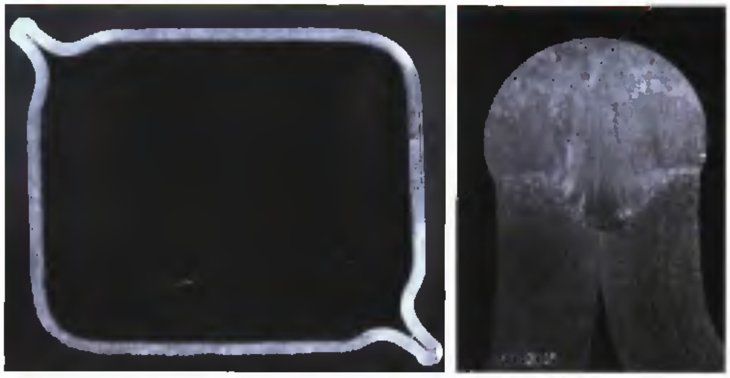

Fig. 6 — Macro section of the NVEB weld (12 m/min, 19.3 kW) at the flange of 2 × 2.5 mm Al-3%Mg deep-drawn shells.

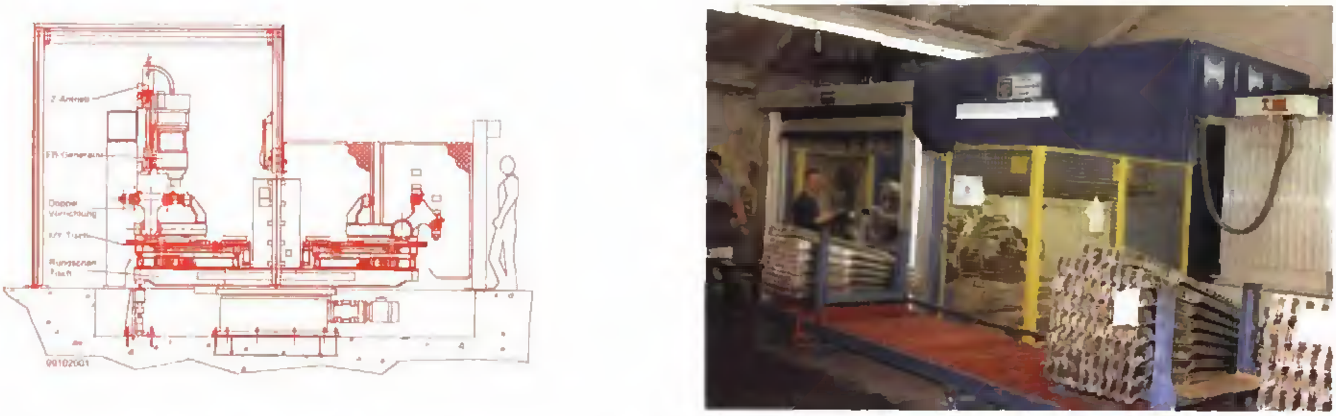

Fig. 7 — Project scheme and photograph of the round table NVEBW machine for structural beam production (1995).

X-Ray Protection System— This also depends on size of the workpiece being processed, as well as on the complexity of the part transfer and weld path mechanisms being utilized. Thus X-ray protection systems can vary in size from very small (desk size) to very large (room size) structures, as outlined in Ref. 14. In all cases, however, the design of these safety structures is such that no hazard exists to workers engaged in operating the units, nor to any other workers in the immediate vicinity of these units.

Present Use of NVEBW for Large-Scale Production of Aluminum Structural Beams

Some years back, the Audi/VW group determined that if an aluminum instrument panel beam (produced by using two formed and welded half shells manufactured from 2.5-mm-thick Al-3%Mg material) were used as a direct replacement for the steel one that was then being utilized (which was produced by gas metal arc [GMA] welding together two sections formed from 1.5-mm-thick steel sheets), then a 40% reduction in this part's weight could be achieved, resulting in an almost 3-kg weight saving per car — Fig. 5. Consequently, an investigation was conducted into how these aluminum half shells could reliably and repeatedly be joined in production. After an extensive evaluation of all the various joining methods available, which involved comparing the adaptability of each of these methods to the joint geometry and fitup tolerances associated with the formed parts to be welded (in addition to examining the stiffness and finished weld properties of the finally welded components, maximum weld speeds achievable, etc., resulting from each joining method), it was determined that nonvacuum EB welding was the best process for manufacturing these parts (Refs. 5, 6).

Based on the results of tests done on the NVEBW sample welds, the following conclusions were reached regarding the process (all of which have now been reaffirmed by several years of daily use in production):

- Welding is possible without need for degreasing or pickling the aluminum half shells.
- Edge welding of the beam's two flanged joints (Fig. 6) can be accomplished without need for using filler wire — even when root openings up to 0.5 mm, mismatches up to 1 mm, and lead/lag angles on the order of 30 degrees are involved.
- Welding can be performed using air only, but is presently being done in production utilizing a helium blowdown, thereby allowing a greater work distance to be employed, which results in a broader melt zone being produced as well as in helping increase the operating lifetimes of both filament and orifices.
- "Burn away" of the 3% Mg content of the base material could be reduced (a remaining value of 2.6% in the fusion zone is presently attainable) by utilizing an energy input of only 900 J/cm, thus alleviating the risk that cracking would occur.
- Weld speeds on the order of 18 m/min could be achieved when doing

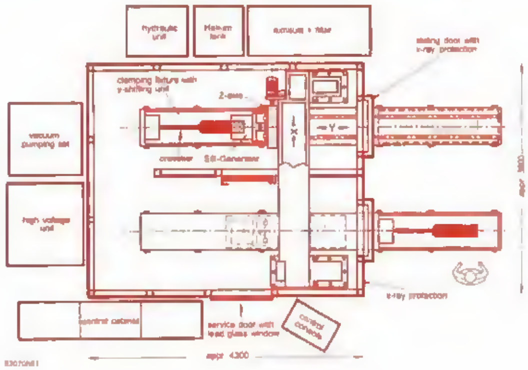

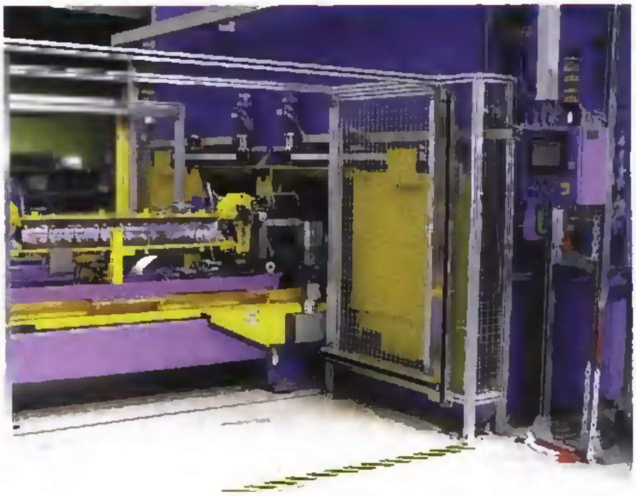

Fig. 8 — Project scheme and photograph of the linear-axes NVEBW machine for structural beam production (1999).

Fig. 9 — Nonvacuum electron beam welding of die-cast aluminum manifolds: 6 mm welding depth, 10 m/min, 21.7 kW (1978).

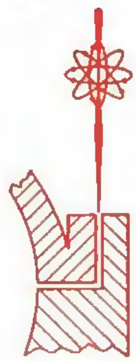

straight-line weld samples, but speeds more on the order of 12 m/min are used for doing the three-dimensional parts being welded in production.

■ Fatigue test comparisons showed the NVEBW continuous welds in aluminum to have a better performance than the previous GMA intermittent welds in steel.

In order to meet mass production requirements (i.e., producing upward of 2000 parts per day, with every part needing two 1359-mm-long welds) the various manufacturers utilizing this process in production investigated numerous methods for cyclically producing these parts and ultimately chose the following two schemes:

1) An indexing table with two workstations, each of which contained an x-y table — Fig. 7.

2) Two parallel linear y-axes, each carrying a table — Fig. 8.

In both cases, installed on the tables (for parts holding) are automated hydraulic clamping units suitable for loading and unloading via manual or robotic means. Also, in each case, the EB gun column assembly is gantry-mounted (vertically orientated, above the tables). In the first scheme, the EB gun is equipped with z-axis motion capability only, while in the second scheme it is equipped with both x- and z-axis motion capability. The specific X-ray protective housing concept used depended on which tooling scheme was being employed.

For welding the 3-D joint contours involved, the workpiece and EB gun column are simultaneously moved under computerized numerical control (CNC). No motion of beam inclination angle, however, is required to accommodate the up to 60 degree "slopes" contained in the beam's travel path, and only z-axis adjustment of the EB gun column assembly is required to address these vertical variations. Up to seven seconds are needed to accomplish a single joint weld, and each part contains two joints to be welded. Including all "idle times" associated with part-transfer functions (i.e., turning parts, moving joint to joint, alternating tables, opening and closing the X-ray housing, access ports, etc.), two fully welded parts can be produced every 65 seconds, resulting in a production rate capability of approximately 110 parts per hour (PPH). Based on the success (both in quantity and quality of parts produced) experienced by the production installations that have been operating for some years now, additional similar facilities are being started up in Europe.

It should be noted that, although the NVEBW systems delivered for this production joining task were specifically designed and built to be capable of operating in a continuous fashion under fairly stringent high-volume production conditions, end users of the equipment were obliged to recognize that it was still necessary to incorporate a mandatory preventive maintenance schedule (similar to that conventionally employed with other high-tech equipment being operated at their facility) in order to ensure the units were able to achieve this goal.

Use of NVEBW for Welding Die-Cast Aluminum Manifolds

Confirmation of NVEBW's ability to be employed for high-production joining applications even under the most stringent of industrial conditions dates back to the 1970s, when the process was used in the United States for welding engine inlet manifolds fabricated from die-cast aluminum Alloy 380 — Fig. 9. Its successful employment for welding both the four- and six-port version of this type of manifold, coupled with a demonstrated capacity to successfully weld different styles and materials of automotive components since its original introduction to U.S. industry during the 1960s, have helped solidify the process's reputation as a totally viable production tool.

To weld these manifolds, two half shells are positioned (one seated atop the other to form a vertical edge-weld style joint around the entire periphery of the part as shown in Fig. 9) in a clamping fixture at the operator's station, located outside the lead room housing the weld area. The transfer pallet on which this clamping fixture is mounted is then transferred inside to the weld area by means of a power-and-free conveyor. Upon reaching the weld area, a pick-and-place device grasps this clamping fixture and moves it off the transfer pallet and onto a CNC x-y table assembly. This x-y table assembly then traverses the part in a two-dimensional (x-y contour style) fashion to accurately trace the complex peripheral joint to be welded underneath a fixed, vertical EB gun column assembly. Thus, this x-y table automatically traverses the entire joint path to be welded underneath the beam, a total length of some 2.5 m on the fairly large six-port manifolds. Utilizing approximately 22 kW of beam power and an average weld speed of about 8 m/min (weld speed is programmed to automatically slow down during short-radius path segments, and speed up during the more straight-line path segments, and thus varies from 5 to 11 m/min), a part throughput of some 200 PPH per system is easily achievable. Because of NVEBW's inherent beam characteristics, the process can readily melt enough of the sacrificial joint-forming edge material provided (by design as shown in Fig. 9) to produce a satisfactory weld even when root openings greater than 0.5 mm in width occur as a result of the two cast half shell parts not fitting together well.

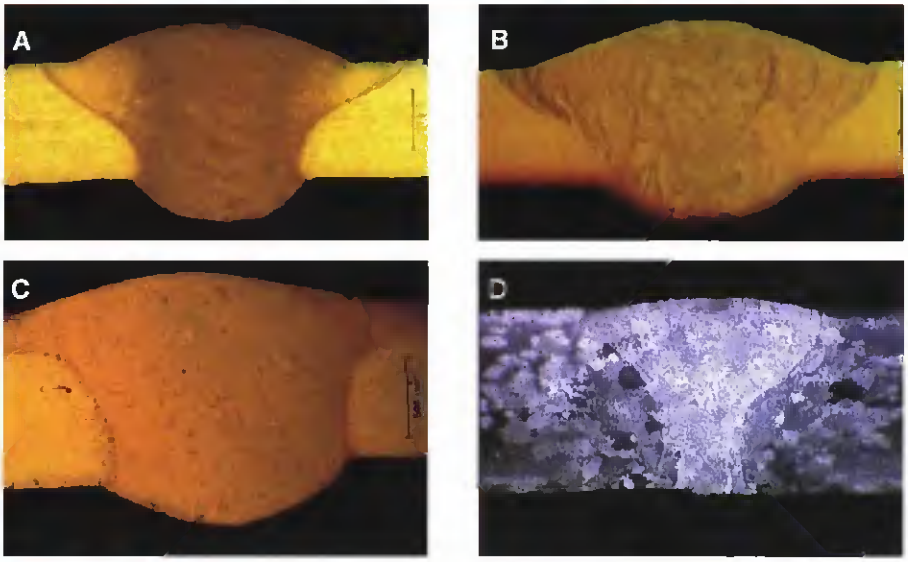

Fig. 10 — Nonvacuum electron beam welds in butt joints on different alloys, prepared with sheared edges, using suitable filler wires. A — Al-5%Mg-Mn (1 mm) + wire Al-4.5Mg-Mn, 30 m/min welding speed; B — Al-0.4%Mg-1.2%Si (1 mm) + wire Al-4.5%Mg-Mn, 30 m/min welding speed; C — Al-0.4%Mg-1.2%Si (1 mm) + wire Al-12%Si, 60 m/min welding speed; D — Al-Mg-0.7%Si (4 mm) + wire Al-5%Si, 10 m/min welding speed.

Fig. 11 — Nonvacuum electron beam welds on Al-0.4%Mg-1.2%Si transition zone to base metal, different magnifications.

Potential Future Employment: Welding Other Aluminum Alloys

Various institutes have investigated the feasibility of employing NVEBW for a range of other of aluminum alloys, as well as the mechanical properties of weld samples produced in this fashion. The spectrum of tests encompassed welding both with and without filler metal (as means for influencing metallurgy and/or filling root openings), joining both thin sheet and heavy section components, utilizing a variety of joint configurations (butt, lap, edge, etc.), and welding at very high speeds (> 50 m/min). The conclusion was that no other approach to aluminum welding could be envisioned that would involve such little trouble and yet yield such excellent results with regard to quality, integrity, and strength of weld (Ref. 9).

Results indicated that welds can be produced that are free of pores and cracks, with a grain structure (in both the weld zone and heat-affected zone) that is fine and shows smooth transitions. In addition, the welds demonstrate mechanical property values close to that of the base material while simultaneously exhibiting good deep-draw characteristics. While not providing a complete picture of all results achieved, the self-explanatory examples

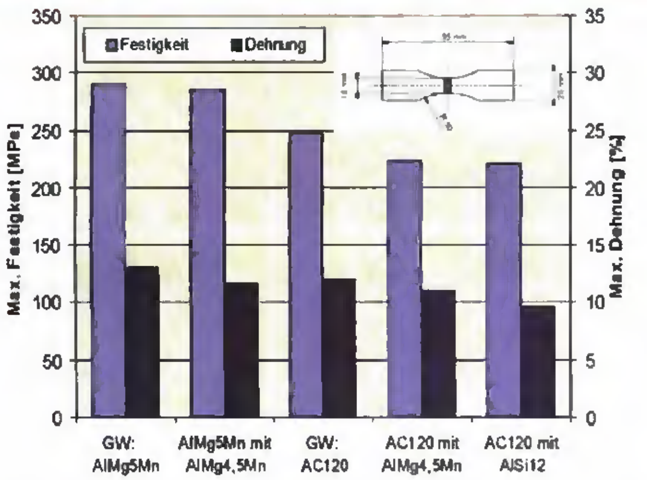

*Fig. 12 — Tensile strength (*Festigkeit*) and elongation (*Dehnung*) of different aluminum alloys in base material (GW) and NVEB welds.*

provided in Figs. 10–12 (Refs. 10–13) give some insight into what results are possible, including the potential for being able to employ processing speeds greater than 60 m/min, as well as to readily weld magnesium alloys in a excellent fashion.

Summary and Outlook

The NVEBW process, since first being introduced to industry some 40 years ago, has been utilized to weld a wide variety of high-volume production components for the automotive industry, and, as such, has clearly demonstrated its inherent ability to readily adapt to the broad range of workpiece conditions and operating environments that the industry has come to recognize as "common practice," and which they generally assume all equipment being supplied will conform to.

Consequently, recent investigations into employing the process have been aimed at widening the field of NVEBW applications both inside the automotive sector (based on its plans to utilize "platform" concepts to extend production volumes) and outside of it (by tapping into the ship, rail, and other industries). The intent of this application-broadening investigation was not to compete with the well established and quite different form of welding, "deep penetration welding," being performed in vacuum by the high-vacuum electron beam welding (HVEBW) process, but rather to present the nonvacuum EBW method as an "alternative form" of beam technology that all industries should at least consider.

As a result of these investigations, the aluminum alloy joining abilities of the NVEBW process have been so convincingly demonstrated that more and more manufacturers involved with materials of this nature have begun to direct their attention to the process — fully recognizing that, in order for the process to be economically competitive to other means for joining such parts, the following must be realized:

■ The number of similar parts to be welded must be of a sufficient quantity to ensure that the NVEBW machine is utilized to the fullest.

■ Welding to be done must be of sufficient length to ensure that the time needed for welding greatly exceeds the cumulative idle time resulting from operating in a cyclic production fashion. (However, it should be noted that one German manufacturer now employing NVEBW for producing large aluminum parts states that, even though weld times do not greatly exceed idle times in their present operation, the quality and repeatability of the welds produced are so much better than what was attainable from other production joining methods investigated that they are now looking into using the process on even smaller parts — regardless of the fact that this would make weld and idle times even closer in value.)

Thus the NVEBW process's demonstrated potential for increasing productivity while also helping lower operating costs and raising weld quality consistency has now gained the attention of those producing components in the following industrial areas:

- Structural-style automotive parts manufacturing.
- Aluminum tailored-blank production.
- Railroad car panel manufacturing.
- Component manufacturing for ship construction.
- Component manufacturing for aircraft production.
- Container and tank production.
- Special tube manufacturing. ◆

References

1. Powers, D. E., et al. 1980. Progress of nonvacuum electron beam welding. *DVS-Berichte* 63:70–77.
2. Gajdusek, E. 1980. Advances in nonvacuum electron beam technology. *Welding Journal* 59(7): 17–21.
3. Powers, D. E. 1994. Schweissen mit dem elektronenstrahl an atmosphaere. *Der Praktiker* 46(10): 526–528.
4. Powers, D. E., and LaFlamme, G. R. 1992. How high-energy-density beam welding manufactures transmission components. *Welding Journal* 71 (6): 47–52.
5. Schulze, K. R. 1997. Nonvacuum electron beam welding for automotive suppliers. *Proceedings IIW/Comm. XII Seminar, Wels.* 163–171.
6. Gomes-Buco, J., et al. 1997. Nonvacuum-elektronenstrahlschweissen von aluminiumtraegern in der grossserie des automobilbaus. *DVS-Berichte* 186:59–62.
7. Hinrichs, J. F., et al. 1974. Production electron beam welding of automotive frame components. *Welding Journal* 53(8): 488–493.
8. LaFlamme, G. R., and Schubert, G. 1996. Welding of tailored blanks in atmosphere with the electron beam. *Proceedings IBEC, Detroit* 11–120.
9. Hauser, F., Keitel, S., and Marquardt, E. 1997. Vergleich der verfahren laserstrahlschweissen, elektronenstrahlschweissen an atmosphaere und plasmaschweissen beim fuegen von aluminumlegierungen. *DVS-Berichte* 186: 179–181.
10. Draugelates, D., Bouaifi, B., and Ouaissa, B. 2000. Hochgeschwindigkeits — Elektronenstrahlschweissen von aluminiumlegierrungen unter atmosphaerendruck. *Schweissen & Schneiden* 52(6): 333–339.
11. Draugelates, D., Bouaifi, B., Ouaissa, B., and Schulze, K.-R. 2001. Elektronenstrahlschweissen an der atmosphaere — Verfahrenspotential und industrielle anwendung. *DVS-Berichte* 216:13–20.
12. Bach, F.-W., Versemann, R., Niemeyer, M., Szelagowski, A., and Zelt, M. 2001. Nonvacuum-elektronenstrahlschweissen an Al- und Mg- feinblechen. *Proceedings 5, Konferenz Strahltechnik, Halle* 46–53.
13. Schubert, G., and Joaquin, A. 2001. Electron beam process delivers consistent welds. *Welding Journal* 80(6): 53–57.
14. Schulze, K.-R. 2001. Nonvacuum-elektronenstrahlschweissen in der industrie: mit vielfalt der anlagenkonzepte zu hoher wirtschaftlichkeit. *Proceedings 5, Konferenz Strahltechnik, Halle* 60–66.


Would you allow welding without a helmet?
Then don't let your staff work without the NEWEST D1.1 Steel Code
If you don't have this, you don't have the latest welding requirements for quality fabrication.
The industry reference since 1928, the 2004 edition covers:
▪ Design of Welded Connections
▪ Prequalification of Welding Procedure Specifications
▪ Qualification for Procedures and Personnel
▪ Fabrication
▪ Inspection
▪ Stud Welding
▪ Strengthening and Repair of Existing Structures
NEW for 2004
▪ Clarifies when an engineer's approval is needed
▪ Details newest allowable stress range formulae
▪ Latest restrictions on prequalified FCAW and GMAW power sources
▪ Most current tolerances for PJP and CJP groove welds
▪ Adjusts welder qualification essential variables
▪ Adjusts pre-qualification figure details
▪ Latest revision of the prequalified base metal list
Order today. Call us at 800.854.7179 or visit global.ihs.com to get your copy.
ANSI approved, Department of Defense adopted, NASA preferred, U.S. customary and metric units of measurement.
NON-MEMBER
AWS MEMBER
D1.1/D1.1M:2004 (Web Order Code: D1.1/D1.M) $344 $258
D1.1/D1.1M:2004 CD (Web Order Code: D1.1/D1.1M CD) $375 $281
Full D1.1-2004 text, as well as graphics and tables now on a CD-ROM. Find specific provisions fast with five convenient search methods.
D1.1/D1.1M COMBO (Web Order Code: D1.1/D1.1M Combo) $616 $462
Buy the hardcopy D1.1 and companion CD ROM and SAVE.
Sales, fulfillment and customer service managed by Global Engineering Documents
© American Welding Society 2004 TEC10538
AWS D1.1/D1.1M:2004
An American National Standard
Structural Welding Code—Steel
American Welding Society
ANSI
AWS
American Welding Society
Founded in 1919 to Advance the Science, Technology and Application of Welding
To become an AWS member, call 800.854.7179 or visit our website at http://www.aws.org
Circle No. 16 on Reader Info-Card

Friction Welding of Aluminum Cuts Energy Costs by 99%

Mazda develops alternative to resistance spot welding

BY ROSS HANCOCK

Close-up photo of a completed friction spot weld in an RX-8 aluminum rear door.

Engineers of Mazda Motor Corp. have introduced a new welding technology in the production of the RX-8 sports car. The aluminum rear doors and hood of the car are joined using spot friction welding

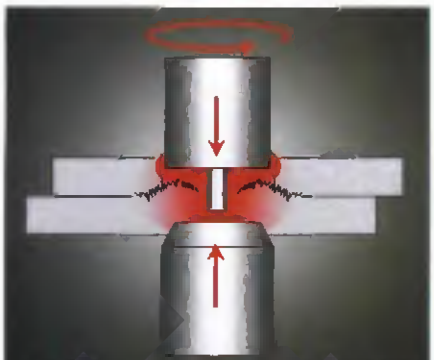

Mazda's process uses a spinning pin to generate welding heat in aluminum panels.

where resistance welding would usually be performed.

For joining these panels, Mazda uses welding robots controlling a friction welding gun. The gun grips the parts from both sides and plunges a spinning pin, which creates frictional heat, softening the metal and forming a welded joint in the aluminum panels.

Because they conduct electricity and heat better than steel, aluminum panels are somewhat difficult to spot weld with arc or resistance welding processes.

Mazda says it has reduced electricity consumption by 99% using the method, which, unlike resistance spot welding, does not need coolant, compressed air, or large electric current. Furthermore, the equipment involves 40% less capital investment compared to resistance welding apparatus for aluminum.

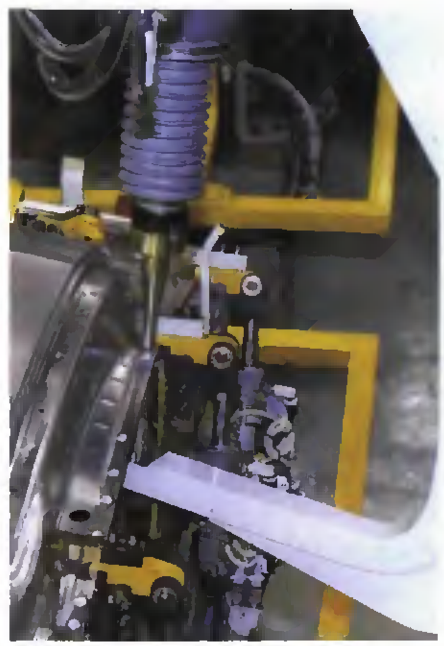

Body panels are pinched together while a spinning pin is plunged into the workpieces.

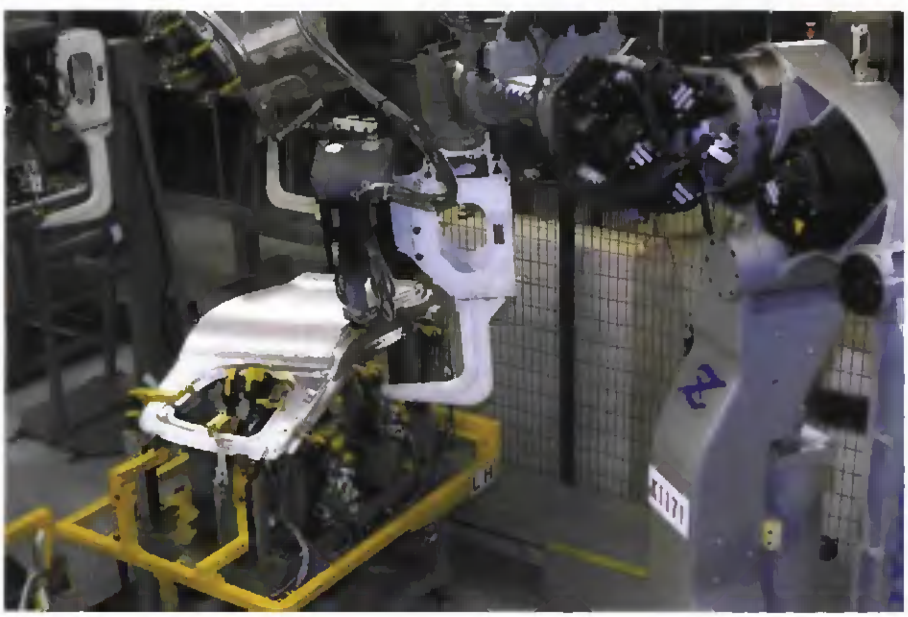

A robot controls the friction spot welds in an aluminum door.

The new process does not require precleaning of the workpieces, and does not generate fumes or spatter.

The Mazda RX-8 incorporates aluminum body parts to increase its fuel economy and performance. The company says it can adapt friction welding to other large body parts in the future. ◆

ROSS HANCOCK (rhancock@aws.org) *is Associate Editor of the* Welding Journal.

NEW SEMINAR DAYS AND TIMES

American Welding Society

Founded in 1919 to Advance the Science, Technology and Application of Welding

AWS Certification is the welding industry's most respected sign of approval.

SEMINAR AND EXAM SCHEDULE FOR FEBRUARY 2004 THROUGH APRIL 2004

FEBRUARY 2004	SEMINAR DATES	EXAM DATES
Denver, CO	2/1-6	2/7/2004
Seattle, WA	2/1-6	2/7/2004
Ontario, CA	2/1-6	2/7/2004
Birmingham, AL	2/8-13	2/14/2004
Louisville, KY	2/8-13	2/14/2004
Miami, FL	Exam Only	2/19/2004
Columbus, OH	2/16-20 at NBBPVI	2/21/2004
Norfolk, VA	2/22-27	2/28/2004
Chicago, IL	2/22-27	2/28/2004
Corpus Christi, TX	Exam Only	2/28/2004
Indianapolis, IN	2/29-3/5	3/6/2004
Hartford, CT	2/29-3/5	3/6/2004

MARCH 2004	SEMINAR DATES	EXAM DATES
Rochester, NY	Exam Only	3/6/2004
Las Vegas, NV	3/7-12	3/13/2004
Perrysburg, OH	Exam Only	3/13/2004
Miami, FL	Exam Only	3/18/2004
Mobile, AL	Exam Only	3/20/2004
Houston, TX	3/14-19	3/20/2004
New Orleans, LA	3/14-19	3/20/2004
San Francisco, CA	3/21-26	3/27/2004
Anchorage, AK	3/21-26	3/27/2004

APRIL 2004	SEMINAR DATES	EXAM DATES
Miami, FL	Exam Only	4/15/2004
Portland, ME	4/18-23	4/24/2004
Roanoke, VA	4/18-23	4/24/2004
Corpus Christi, TX	Exam Only	5/1/2004
Detroit, MI	4/25-30	5/1/2004
Bakersfield, CA	4/25-30	5/1/2004

Seminar and Exam Schedule

Course	Schedule
D1.1 Code Clinic	Sunday; 1 p.m.- 5 p.m.
	Monday; 8 a.m.- Noon
API 1104 Code Clinic	Monday; 1 p.m.- 5 p.m.
Welding Inspection Technology	Tuesday-Thursday; 8 a.m.- 5 p.m.
Visual Inspection Workshop	Friday; 8 a.m.- 5 p.m.
Exam	Saturday; report for exam at 7:30 a.m.

Circle No. 5 on Reader Info-Card

To register or for more information on an exam prep course, call (800) 443-9353, ext. 229; to request an application for CWI exam qualification, call ext 273.

To find out about AWS Customized In-House Training and Quality Assurance Programs for your company, call AWS, toll-free at 1-800-443-9353, ext. 482, or check the box on the registration form.

Visit our website www.aws.org for additional dates.

AWS reserves the right to cancel or change the published date of an exam preparation seminar listed if an insufficient number of registrations are received. Prices are subject to change without notice.

BY TONY ANDERSON

Q: I am having problems passing the guided bend tests for my procedure qualification tests. I am working to AWS D1.2 *Structural Welding Code — Aluminum*. My base material is 6061-T6 and my filler metal is ER4043. I am using the plunger-type guided bend jig. I am passing the reduced section tension tests on the same test specimen, and there would appear to be no relevant discontinuities in the weld and, therefore, no apparent reason for the bend tests to fail.

A: The guided bend test has been around for many years and is a common method of testing the integrity of welds made in many different material types. Where properly used, it can be very revealing; however, when testing aluminum, the testing methods used must be thoroughly understood in order for the test results to be meaningful.

The guided bend test is a relatively quick and, usually, a comparatively economical method of establishing the soundness of a groove weld. This test is designed to help determine whether the weldment tested contains discontinuities such as cracks, incomplete fusion, incomplete joint penetration, or severe porosity. Various types of bend tests are used to evaluate welds. Guided bend specimens may be longitudinal or transverse to the weld axis and may be of the root bend, face bend, or side bend type. The type of bend test (root, face, or side) is determined by which surface of the weld sample (root, face, or side) is on the convex (outer) side of the bent specimen and, consequently, subjected to tension load during the testing operation. Probably the most common combination of bend tests used for welder performance and welding procedure test samples are two transverse root bend tests and two transverse face bend tests per test plate.

Fig. 1 — Guided bend test samples. Top sample shows a side bend section prior to full preparation and bending. Lower sample shows a completed side bend specimen.

Bend Testing Aluminum Is Different than Bend Testing Steel

Most guided bend testing of steel is conducted with the use of a die and plunger arrangement often referred to as the plunger-type guided bend test. The plunger-type guided bend test is not recommended for testing aluminum. The heat-affected zones of welds in aluminum alloys, and particularly in the heat-treatable aluminum alloys, are significantly softer and weaker than the surrounding material. If these welds are bent around a plunger, the bend sample usually bends sharply in the heat-affected zones and kinks and breaks without adequately bending the weld metal, resulting in a test failure. In order to avoid such meaningless test failures, the wraparound bend test fixture should always be used for testing aluminum. This testing method forces the test specimen to bend progressively around a pin or mandrel so that all portions of the weld zone achieve the same radius of curvature and, therefore, the same strain level.

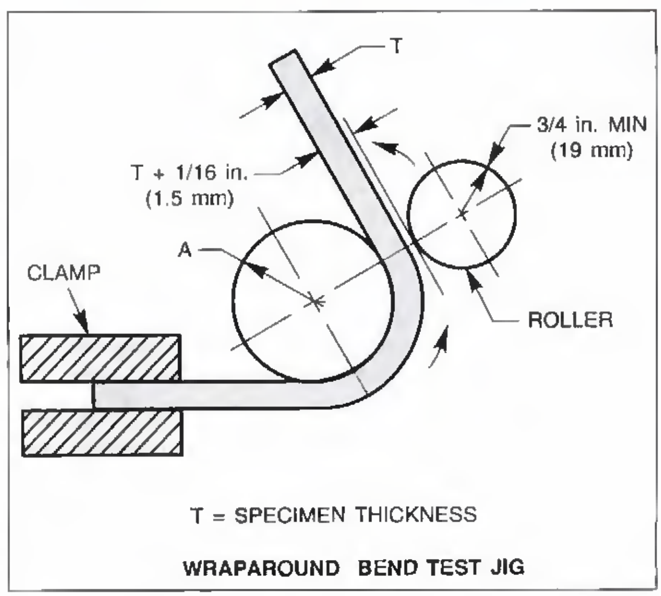

Fig. 2 — The mechanism for the wraparound bend test fixture, the preferred method of bend testing aluminum weldments. The "A" dimension shown on the drawing will vary depending on plate thickness and base metal/filler metal being tested.

There are a number of other pitfalls to avoid when bend-testing aluminum. We should be concerned about bend test sample preparation prior to bending. A common mistake is to leave the corners of the sample square. Most codes allow up to a 1/8-in. (3-mm) radius on the corners of the test specimens. For best results, samples should have a smooth surface, free of sharp notches that may provide stress concentration during the bending operation.

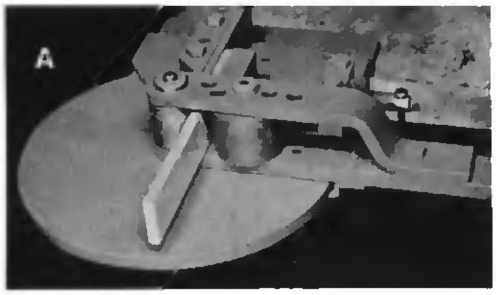

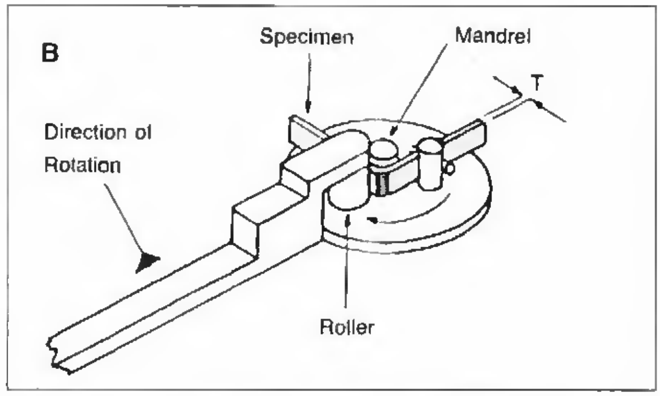

Fig. 3 — A — Wraparound testing machine with an aluminum test sample loaded and ready to be tested; B — basic design of a wraparound testing jig.

Special Bending Conditions for Aluminum Alloys

We should be aware that most codes, and certainly AWS D1.2, stipulate special bending conditions for various base and filler metals. Test samples of base metals within the 6xxx series (M23) or other base metals welded with the 4xxx series (F23) filler metals are required to be tested under either of two special bending conditions: as-welded or annealed. If testing is to be conducted in the as-welded condition, the test specimen is required to be reduced from the standard 3/8-in. (10-mm) thickness to 1/8 in. (3 mm) prior to bending, and then bent over a diameter of 16⅔ T. If annealed prior to testing, the standard 3/8-in. (10-mm) specimen is required to be bent over a 6⅔-T diameter.

The specified annealing practice contained in AWS D1.2 is to heat the bend specimens to 775° F (410° C), hold them at this temperature for 2–3 hours, then control-cool at 50°F/h (28°C/h) down to 500°F (260°C). The rate of cooling below 500°F (260°C) is unimportant.

Welds made with the 2219 base material (M24) are required to be annealed and bent over an 8-T diameter. Welds made with 7005 base material (M27) are required to be bend-tested within two weeks of welding. This requirement for 7005 materials is based on the ability of this alloy to gain substantial tensile strength over time, and, consequently, suffer a reduction in ductility through natural aging.

It is obvious that there are many requirements that need to be considered if we expect to obtain the desired results from our guided bend testing procedures. It is most important to understand the following:

- The preparation of test samples prior to bend testing is very important.
- There is an optimum method of bend testing aluminum (the wraparound bend test).
- There are major differences between the testing procedures used, which are often dependent on base material and filler metal types being tested.

If test samples are prepared correctly and test procedures specific to the material and filler metal being tested are used, we can go a long way toward assuring that we have no questionable test results. ◆

TONY ANDERSON is Technical Director of AlcoTec Wire Corp., Traverse City, Mich. He is Chairman of the Aluminum Association Technical Advisory Committee on Welding and Joining; Chairman of the AWS Committee for D10.7 Gas Shielded Arc Welding of Aluminum Pipe; Chairman of the AWS B8.14 Committee for Automotive and Light Truck Components — Aluminum; Chairman of the AWS D3.7 Guide for Aluminum Hull Welding; and Vice Chairman of the AWS Committee for D1.2 Structural Welding Code — Aluminum. Questions may be sent to Mr. Anderson c/o Welding Journal, 550 NW LeJeune Rd., Miami, FL 33126; e-mail tanderson@alcotec.com.

BY R. L. PEASLEE

Q: We vacuum furnace braze dental equipment with BNi-5 and are unable to obtain the smooth fillets that the customer requires. Our fillets are rough and porous. How can we obtain smooth fillets?

A: The question about surface quality of fillets is one that comes up frequently. The solution requires the understanding of many variables, one or more of which can cause the rough porous fillet.

1) Rough porous fillets have caused considerable confusion when penetrant inspecting. Many times, porosity is taken for cracks, as the bleeding fluid from the pores comes together to form a line. For this reason, AWS C3.6 *Specification for Furnace Brazing* includes the following; "These inspection techniques are not suitable for inspection of brazed fillets because they routinely give false results."

2) *Fillet size vs. porosity.* In general, the larger the fillet size the more porosity and roughness occurs. For this reason, the smaller the fillet, the less porosity and roughness will form.

3) *Brazing temperature vs. porosity.* Generally, higher brazing temperatures yield more porosity and roughness. This is caused by the brazing filler metal dissolving more of the base metal, resulting in the liquid filler metal at the brazing temperature having a wider melting range. For best results, the brazing temperature should be as low as practical.

4) *Time at heat vs. porosity.* The longer the time at heat the more base metal is dissolved into the filler metal resulting in more porosity.

5) *Location of the filler metal vs. porosity.* Apply the filler metal on the opposite side of the joint from where the smooth fillet is desired, preferably on the inside or lower part of the joint.

6) *Atmosphere vs. porosity.* BNi-5 is one of the filler metals more sensitive to atmosphere quality. Vacuum pressure is only one of many things that makes up atmosphere quality. Therefore, a very good atmosphere quality is required to minimize porosity. The application of the T-specimen in the furnace is a good indicator of atmosphere quality

7) *Filler metal solidus-to-liquidus range vs. porosity.* In general, the wider the melting range, the more porosity can be expected.

8) *Solubility of base metal vs. porosity.* As a general rule, the more base metal that dissolves into the filler metal, the wider the melting range of the filler metal. Thus, more porosity is present.

9) *Cooling rate vs. porosity.* Slow cooling allows dendrites to form first, and on further cooling, the remaining liquid portion pulls back into the joint exposing the rough, porous fillet.

10) *Eutectic filler metals vs. porosity.* Eutectic filler metals are better, and have less porosity, assuming that one or more of the above variables do not enter into the brazing cycle.

11) An element that has a single melting point will dissolve other elements from the base metal during brazing, and can result in fillet porosity and roughness, depending on the variables listed above.

To produce fillets with little or no porosity will require exercising very careful control of the variables mentioned above. ♦

R. L. PEASLEE is Vice President, Wall Colmonoy Corp., Madison Heights, Mich. Reader may send questions to Mr. Peaslee c/o Welding Journal, 550 NW LeJeune Rd., Miami, FL 33126 or via e-mail to bobpeaslee@wallcolmonoy.com.

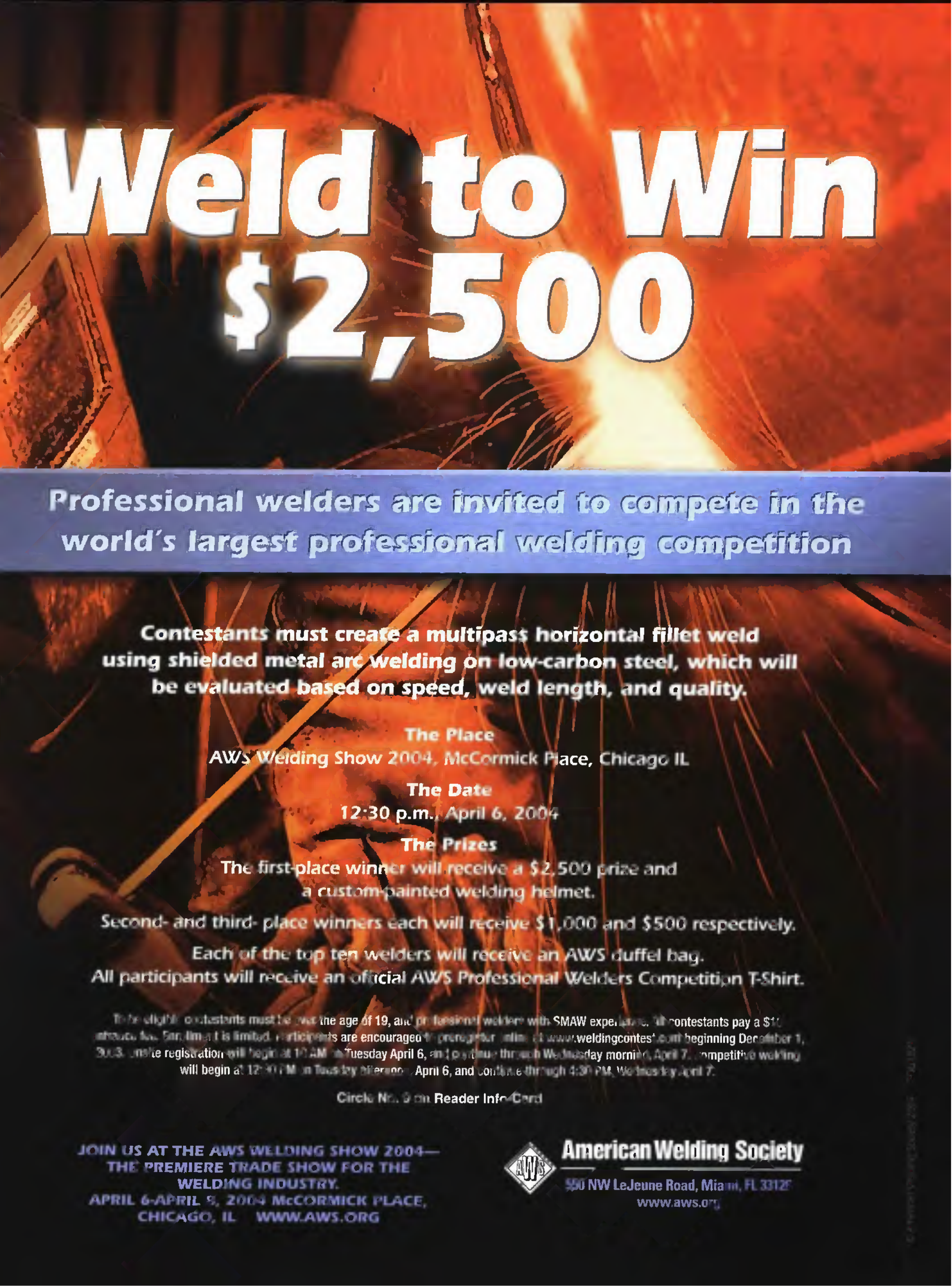
Weld to Win $2,500
Professional welders are invited to compete in the world's largest professional welding competition
Contestants must create a multipass horizontal fillet weld using shielded metal arc welding on low-carbon steel, which will be evaluated based on speed, weld length, and quality.
The Place
AWS Welding Show 2004, McCormick Place, Chicago IL
The Date
12:30 p.m., April 6, 2004
The Prizes
The first-place winner will receive a $2,500 prize and a custom-painted welding helmet.
Second- and third- place winners each will receive $1,000 and $500 respectively.
Each of the top ten welders will receive an AWS duffel bag.
All participants will receive an official AWS Professional Welders Competition T-Shirt.
Circle No. 9 on Reader Info-Card
JOIN US AT THE AWS WELDING SHOW 2004— THE PREMIERE TRADE SHOW FOR THE WELDING INDUSTRY. APRIL 6-APRIL 8, 2004 McCORMICK PLACE, CHICAGO, IL WWW.AWS.ORG
American Welding Society
550 NW LeJeune Road, Miami, FL 33126
www.aws.org

BY A. E. GICKLER AND F. H. LePREVOST, JR.

Tips for Soldering Aluminum

Aluminum soldering can be simple but has a number of critical areas that need tight process control. Tenacious aluminum oxide makes most attempts to solder using conventional means difficult. In addition, care must be taken regarding alloy choice due to potential galvanic corrosion consequences because of aluminum's dissimilarity with many conventional solders. The varieties of aluminum alloys, gauges, and tempers often display widely varying soldering results, and how aluminum accepts or rejects heat during soldering must be carefully studied for each individual job.

Soldering can be done with either soft solders (Sn-based, lower temperature) or hard solders (Zn-based, higher temperature) and with appropriate fluxes to fit processing temperature ranges. By definition, soldering is a low-temperature joining process. Therefore, less distortion of the aluminum component is expected by soldering than by brazing, welding, or other fusion joining processes. Soldering temperatures of 225 to 490°C are well below the 661°C aluminum melting temperature, although 490°C is above the annealing point. Stresses in the aluminum from shearing, drawing, and heat treating are changed by the localized heating encountered during soldering, and distortion may result. Preheating, noncontinuous joints, and careful selection of joint geometry becomes critical.

Various aluminum alloys have different solderability: 1xxx, 2xxx, 3xxx, 4xxx, and 7xxx are easier to solder than the 6xxx series alloys. Due to their magnesium content, 5xxx series alloys are the most difficult to solder.

Methods or processes in aluminum soldering involve mechanical rubbing of aluminum with solder, ultrasonic bath soldering, thermal spray (these three do not use fluxes), heating the assembly by induction, flame, infrared, hot plate, furnace, soldering iron, laser, and arc lamp (all of which usually involve the use of fluxes). Soldering aluminum requires an adequate volume of heat on the component, not the solder. Because of the high thermal conductivity and reflectivity of aluminum, the heat source must be tailored to the job.

A. E. GICKLER and F. H. LePREVOST, JR., are with Johnson Manufacturing Company, Princeton, Iowa.

Coupons of Alloy 6111, 2 × 4 × 0.036 in. with 2-in. overlap. The top coupon has a 0.125-in. hole centered in the overlap area to facilitate introduction of Zn/15Al hard solder wire. Solder flows to every edge providing complete wetting of the joint.

Close-up confirms total wetting. Appearance changes where reaction occurs between the flux and surface oxidation, yet residues are considered noncorrosive. Joints of this type are generally stronger than the base material.

Use of Flux

The rapid formation of an aluminum oxide layer and the difficulty in removing that oxide layer so the solder can wet the aluminum are the reasons for the use of flux. In "normal" soldering of copper, removal of the copper oxide is relatively easy with mild organic and inorganic fluxes. Aluminum oxide is not so easily removed and may require stronger fluxes such as an organic amine-based flux (up to 285°C), inorganic fluxes (chloride or fluoride up to 400°C), and complex fluoroaluminate salts (above 550°C). The use of mechanical rubbing, ultrasonics, or thermal spray depends upon using the molten zinc to abrade or blast away the aluminum oxide layer and allowing subsurface wetting of the aluminum. No flux is used. Tin/zinc soft solders are typically used with the first two fluxes since their melting point is under 330°C and the zinc portion helps in preventing galvanic corrosion. Zinc-based hard solders use fluxes that offer higher melting temperatures to activate. The residues of some soft soldering fluxes may be still active after soldering and must be removed. Solders used for aluminum generally contain zinc with some lead, cadmium, tin, copper, or aluminum. However, any solder that contains tin may cause an electrochemical corrosion problem due to its galvanic potential. With the anticipated worldwide ban on lead in solder, most industries have already or are switching to lead-free solders. This removes some of the more ductile and/or higher-temperature soft solders available. Cadmium-bearing solders have been effectively banned due to worker health issues.

Additives

Lead-free and cadmium-free alloys that are commonly used to solder aluminum include 91Sn9Zn, 70Sn30Zn, and 98Zn2Al. Other alloys in the Zn/Al fami-

Coupons of Alloy 6111 soldered using Zn/15Al and a flux based on complex fluoroaluminate salts. For the purpose of this test, one length of 0.093-in.-diameter solder was placed on one side of the joint, then pulled through to the opposite side with heat.

ly include 85Zn/15Al, 90Zn/10Al, and 97Zn/3Al. Other variations are 60Sn/40Zn and 80Sn/20Zn, which are in the Sn/Zn family.

Aluminum often has other elements added to improve strength, rigidity, corrosion resistance, machinability, and formability. Some additives cause no problem for soldering, but magnesium is the exception. Magnesium-containing aluminum alloys (e.g., 5xxx and 6xxx series) are used for extending the strength-to-weight ratio and to provide better corrosion resistance in some applications. However, the authors are not aware of any solder or flux that is very effective with magnesium-containing aluminum alloys. The magnesium oxide reforms very quickly and does not allow solder wetting to take place. Titanium and some exotic additives such as vanadium and chromium may also cause problems. The 1xxx (99% Al or higher), 2xxx (copper added), 3xxx (manganese added), 4xxx (silicon added), and 7xxx (zinc added) series are generally solderable. The 5xxx (magnesium added) series is probably not solderable and the 6xxx (silicon and magnesium added) series may or may not be solderable depending upon the individual alloy. The 6061 alloy is definitely solderable and the 2xxx series in sheet form may have a 6xxx cladding that could change its solderability.

Close-up confirms good fillets on both sides. Zn-based hard solders may not be as pretty as soft solders, yet they are not susceptible to galvanic corrosion when soldering aluminum, as are Sn-based alloys.

Cladding or Coatings

In some cases the aluminum can be clad with a more solderable alloy, plated with nickel, or coated with zinc by thermal spray or other methods. This surface is then more solderable and eases the above problem since they are both easier to solder than just aluminum. Soldering aluminum to other metals (steel, galvanized steel, copper, brass, stainless, etc.) is also done, but with some difficulty since the joint design must allow for differential thermal expansion and many fluxes do not work for both metals. The simple job of heating the assembly at the joint area becomes difficult since the aluminum conducts heat away from the joint very rapidly vs. other metals' tendency to conduct heat away much more slowly (stainless steel comes to mind). A general rule of thumb in soldering is "heat the component, not the solder." This allows the substrate to transfer heat to the solder and melt the solder once it is up to the melting temperature. Fluxes can insulate the solder from the substrate and cause the reactivity of the flux to expire before the solder melts or, perhaps, leave a hard residue that the solder cannot penetrate in order to wet the substrate. Cored soft solders may be used to eliminate this problem since the flux is not released until the solder melts; however, not all aluminum solders are available with flux cores.

Dangers of Overheating

Due to its low melting temperature, aluminum may be annealed or tempered at temperatures as low as 325–350°C in a relatively short time. This suggests that any joining process approaching these temperatures for more than a brief interval may begin to alter the properties of the base metals being joined. Overheating may result in stress relieving, sagging or warping panels, altering hardness, temper, surface condition, re-alloying of the base metal in the immediate joint area, hot cracking, or even a dreaded meltdown.

Generally speaking, soft solders do not pose much of a risk to the base materials from heating, provided the parts are not held at soldering temperatures for an extended period of time. However, in some cases, exposure of aluminum to a molten zinc alloy for even a short period of time may result in re-alloying of the base metal within the heat-affected zone (HAZ). This may change its properties and cause what appear to be heat cracks that emanate beyond the HAZ.

One final tip: Working in the laboratory can aid in process, alloy, and flux selection. A mock-up might be helpful to determine the type, location, and volume of heat required to accomplish the desired result. As in other processes, preheating or hybrid heating may be helpful and may change the original process selection. Cooldown times and delay before handling may vary substantially from the laboratory to the production floor. Aluminum soldering is not difficult, but neither is it very forgiving. Control the process tightly. ◆

Works Consulted

Metals Handbook, 10th Ed.,Vol. 2. 1990. Properties of wrought aluminum and aluminum alloys. Materials Park, Ohio: ASM International, pp. 102–103.

ASM Desk Editions Online — Metals Handbook Desk Edition. Brazing and soldering. Retrieved August 1, 2002, from *http://www.asminternational.org/asm/servlet/Navigate.* Materials Park, Ohio: ASM International.

Fenton, E. A. 1963. *Brazing Manual.* New York, N.Y.: American Welding Society. p. 9.

Rivard, John D., Sabau, Adrian S., and Schwartz, M. M. 1987. *Brazing.* Metals Park, Ohio: ASM International.

NOTE: A DIAMOND (♦) DENOTES AN AWS-SPONSORED EVENT.

♦Eighth Robotic Arc Welding Conference and Exhibition. February 9–10, Grosvenor Resort in the Walt Disney World Resort, Orlando, Fla. Sponsored by the American Welding Society. Contact AWS Conferences, 550 NW LeJeune Rd., Miami, FL 33126, (800) 443-9353 ext. 449 or, outside the U.S., (305) 443-9353 ext. 449, FAX: (305) 443-1552; *www.aws.org*.

♦D1.1 Code Week. D1.1 Road Map, February 16; D1.1 Design of Welded Connections, February 17; D1.1 Qualifications, February 18; Fabrication, February 19; Inspection, February 20. Grosvenor Resort in the Walt Disney World Resort, Orlando, Fla. D1.1 Road Map seminars are also available in April, May, September, October, and November. Sponsored by the American Welding Society. Contact AWS Conferences, 550 NW LeJeune Rd., Miami, FL 33126, (800) 443-9353 ext. 449 or, outside the U.S., (305) 443-9353 ext. 449, FAX: (305) 443-1552; *www.aws.org*.

SOUTH-TEC Charlotte. March 2–4, Charlotte Convention Center, Charlotte, N.C. Sponsored by the Society of Manufacturing Engineers (SME). Cosponsored by the American Machine Tool Distributors Association and the Association for Manufacturing Technology. For additional information and to register, visit the SME Web site at *www.sme.org*.

12th Annual Automotive Laser Applications Workshop. March 8–11, St. John's Golf and Conference Center, Plymouth, Mich. Sponsored by the University of Michigan, College of Engineering, Center for Professional Development. For registration and more details, visit *http://cpd.engin.umich.edu*.

Advanced Surface Engineering for Gears Symposium. March 9, Detroit, Mich. Sponsored by ASM International. For further information, visit *www.asminternational.org/events*.

WESTEC Advanced Productivity Exposition. March 22–25, Los Angeles Convention Center. The WESTEC Conference will be held concurrently with cooperation from Boeing. Both events sponsored by the Society of Manufacturing Engineers (SME). For additional information and to register, visit *www.sme.org*.

♦AWS Welding Show 2004. April 6–8, McCormick Place, Lakeside Center, Chicago, Ill. Exhibition of the latest and best technology in the welding industry. For information, contact: AWS Convention and Exhibition Dept., 550 NW LeJeune Rd., Miami, FL 33126, (800) 443-9353 ext. 256 or, outside the U.S., (305) 443-9353 ext 256, FAX: (305) 441-7451. To register for free,visit *www.aws.org/expo*.

♦AWS Detroit Section's Sheet Metal Welding Conference. May 11–14, Sterling Heights, Mich. Sponsored by the AWS Detroit Section. Contact (810) 231-2502 ; *www.sheetmetalwelding.org*.

♦2004 International Conference on Aluminum Structural Design (INALCO 2004). June 2–4, The Lincoln Electric Co., Cleveland, Ohio. Cosponsored by The Lincoln Electric Co., the American Welding Society, the Aluminum Association, ASCE Structural Engineering Institute, the Japanese Light Metal Welding and Construction Assn., and Univ. Prof. Dr. D. Kosteas, Light Metal Structures and Fatigue, Technical University of Munich. For information on submitting papers on aluminum structural design research and practice, contact *randy.kissell@tgbpartnership.com*.

Educational Opportunities

Emmet A. Craig Resistance Welding School. April 5-6, McCormick Place, Lakeside Center, Chicago, Ill. Sponsored by the Resistance Welder Manufacturers' Assn. (RWMA). Contact RWMA, 1900 Arch St., Philadelphia, PA 19103-1498, (215) 564-3484, FAX: (215) 564-2175, e-mail: *rwma@fernley.com*; *www.rwma.org*.

Hobart Institute of Welding Technology. Welding for the Non-Welder, February 15, May 24, August 16, or October 11. Fundamentals of Visual Inspection, February 3, April 13, July 7, or September 8. Classes are held at the Hobart Institute of Welding Technology, Troy, Ohio. For further information and 2004 schedules, call (800) 332-9448 or e-mail *hiwt@welding.org*; *www.welding.org*.

Unitek Miyachi Corp. Training Services. Unitek Miyachi's Applications Labs offer personalized training services to customers desiring further education regarding resistance and laser welding and laser marking. For more information, contact Unitek Miyachi's Applications Labs at (626) 303-5676 or via e-mail at *info@unitekmiyachi.com*; *www.unitekmiyachi.com*.

EPRI NDE Training Seminars. EPRI offers NDE technical skills training in Visual Examination, Ultrasonic Examination, ASME Section XI, UT Operator Training, and more. For specific information, contact Sherryl Stogner, (704) 547-6174, e-mail: *sstogner@epri.com*.

Victor 2004 Training Seminars. Victor Equipment Co. will be conducting training programs for gas apparatus and service repair technicians, end users, and sales personnel in 2004. For a complete schedule, contact: Aaron Flippen, (940) 381-1217; *www.victorequip.com*.

The Fabricators & Manufacturers Assn., Int.(FMA), and the Tube and Pipe Assn., Int. (TPA), Courses. A course schedule is available by calling (815) 399-8775; e-mail: *info@fmametalfab.org*; *www.fmametalfab.org*.

Malcom Plastic Welding School. A comprehensive two-day, hands-on course that leads to certification in accordance with the latest European DVS-approved plastic welding standards for hot gas and extrusion welding techniques. Contact: Sheila Carpenter, Administration, Malcom Hot Air Systems, 1676 E. Main Rd., Portsmouth, RI 02871, (888) 807-4030, FAX: (401) 682-1904, e-mail: *info@malcom.com*; *www.plasticweldingtools.com*.

Hellier NDT Courses. A course schedule is available from Hellier, 277 W. Main St., Ste. 2, Niantic, CT 06357, (860) 739-8950, FAX: (860) 739-6732.

NACE International Training and Certification Courses. Course description, dates, and registration forms are available from NACE Membership Services, (281) 228-6223, FAX: (281) 228-6329, e-mail: *msd@mail.nace.org*,; *www.nace.org*.

Educational Opportunities

AWS Schedule — CWI/CWE Prep Courses and Exams

Exam application must be submitted six weeks before exam date. For exam information and an application, contact the AWS Certification Dept., (800) 443-9353 ext. 273. For exam prep course information, contact the AWS Education Dept., (800) 443-9353 ext. 229.

Cities	Exam Prep Courses	CWI/CWE Exams
Anchorage, Alaska	March 21–26 (API 1104 Clinic also offered)	March 27
Birmingham, Ala.	February 8–13 (API 1104 Clinic also offered)	February 14
Chicago, Ill.	February 22–27 (API 1104 Clinic also offered) (CRAW Seminar February 26–27)	February 28
Columbus, Ohio	February 16–20	February 21
Corpus Christi, Tex.	EXAM ONLY	February 28
Dallas, Tex.	March 8–13 9-YEAR RECERTIFICATION COURSE	
Detroit, Mich.	February 9–14 9-YEAR RECERTIFICATION COURSE	
Hartford, Conn.	February 29–March 5 (API 1104 Clinic also offered)	March 6
Houston	March 14–19 (API 1104 Clinic also offered)	March 20
Indianapolis, Ind.	February 29–March 5 (API 1104 Clinic also offered)	March 6
Las Vegas, Nev.	March 7–12 (API 1104 Clinic also offered)	March 13
Louisville, Ky.	February 8–13 (API 1104 Clinic also offered)	February 14
Miami, Fla.	EXAM ONLY	February 19
Miami, Fla.	EXAM ONLY	March 18
Miami, Fla.	EXAM ONLY	April 15
Mobile, Ala.	EXAM ONLY	March 20
New Orleans, La.	March 14–19 (API 1104 Clinic also offered)	March 20
Norfolk, Va.	February 22–27	February 28
Ontario, Calif.	February 1–6 (API 1104 Clinic also offered)	February 7
Perrysburg, Ohio	EXAM ONLY	March 6
Portland, Maine	April 18–23 (API 1104 Clinic also offered)	Arpil 24
Rochester, N.Y.	EXAM ONLY	March 6
San Francisco, Calif.	March 21–26 (API 1104 Clinic also offered)	March 27
Seattle, Wash.	February 1–6 (API 1104 Clinic also offered)	February 7

AWS 2004 International Schedule — CWI/CWE Prep Courses and Exams

MEXICO

CWI Training: March 8–12, June 21–25, November 8–12
Examinations: March 13, June 26, November 13
Location: DALUS, S.A., Monterrey, N.L.
Contact: Lorena Garza
Telephone: 52 (81) 8386 1717
FAX: 52 (81) 8386 4780
E-mail: *info@dalus.com*

VENEZUELA

CWI Training: June 9–13
Examination: June 14
Location: Centro Internacional de Education y Desarrolo
Contact: Carlos Quintini
Telephone: 582 906 4694
FAX: 582 906 4690
E-mail: *quintinic@pdvsa.com*

INDIA

CWI Training: June 14–18
Examination: June 19
Location: Industrial Quality Concepts
Contact: V. Raghavendran
Telephone: 44 2 499 3826
Fax: 44 2499 3826
E -mail: *iqc.in.org@vsnl.com*

— *continued on page 73*


A 2-day conference and exhibition designed to help you decide if robotics is a good match for your application. If you've already integrated robotics, learn how to extract more precision from your operation.
• 16 EXPERTS • CASE STUDIES • TAKE-HOME CD-ROM
Special Features
CD-ROM take-homes: One contains the presentations, participants, and exhibitor contacts; the second is a video showing successful robotic applications.
Free Session that is a rundown for robotic investigators and a refresher for those with current robotic operations who might not know it all.
16 Experts ready to spend off-line time with attendees.
Case Studies revealing the cross-industry fundamentals of robotics: steel, aluminum, filler materials, power sources, fixturing, controls, monitoring, and true weld costs.
Register Today!
ROBOTIC ARC WELDING
February 9-10, 2004 • Orlando, Florida
Grosvenor Resort • Walt Disney World
2-Day Conference & Exhibition
online
www.aws.org/robotic or call 1-800-443-9353 ext. 449
sponsored by
AWS
American Welding Society
endorsed by
FMA
Fabricators & Manufacturers Association, International
Circle No. 7 on Reader Info-Card

NJC Materials Joining Technology Presented at DMC 2003

The Defense Manufacturing Conference (DMC), hosted by the U.S. Air Force in conjunction with the Joint Defense Manufacturing Technology Panel (JDMTP), was held in Washington, D.C., December 2003. Based on the theme "Defense Manufacturing Technology: Transitioning Affordable Combat Power to Our Warfighters," the conference provided an overview of government and industry programs as well as a vision for the future of defense manufacturing and sustainment needs. The Navy Joining Center and more than 75 other organizations exhibited to more than 700 attendees at the conference. The various exhibits showcased state-of-the-art government, industry, and academic capabilities and successes for transformation of U.S. warfighters. The NJC participated in both Technical and Poster Sessions, and shared information with attendees on a number of development activities under way at the center.

The NJC's contribution to the Poster Session highlighted Friction Stir Welding for Defense Applications. Friction stir welding (FSW) can improve the weld performance and reduce distortion when compared to conventional welding methods. The NJC has developed manufacturing procedures for aircraft engines, aircraft structures, and combat vehicles. Highlighted within the session was the development of FSW procedures in 2519 aluminum armor structures for the Marine Corps Expeditionary Fighting Vehicle (EFV). This system was formerly known as the AAAV. The results of this activity demonstrated improved productivity, reduced acquisition costs, and maximized performance of the aluminum armor material.

The Navy presented its vision for future warfighting capability during the JDMTP Technical Subpanel and Agency Status Briefings. Within this technical session, the NJC presented a short briefing on the "Large Marine Composite-to-Steel Adhesive Joints" project. The increased use of composite materials has brought about a need to develop new joining techniques for large composite-steel structures. This development activity is directed at meeting the new design and performance criteria for the DD(X) multi-mission surface combatant as well as other defense acquisition programs requiring the use of composite/steel bonded joints. The NJC is developing adhesive joining technology that is producible, cost effective, and meets the functional requirements of the structures, signatures, and longevity. Once developed, the NJC will support transition of the technology to the shipyards.

Navy Joining Center staff exhibits at DMC 2003.

The NJC exhibit presented several development activities aimed at transitioning technology to the warfighter in support of the DOD tri-services. Demonstration hardware was presented showing translational friction welding (TFW) for fabrication of a dual-alloy titanium airfoil (BLISK), a laser beam welded titanium wing spar assembly, adhesive bonding of composite structures for aircraft primary structures, and adhesive bonding of a full-scale composite-to-steel joint for the DD(X). Each of these applications is providing new materials joining solutions to enhance the performance, affordability, and cost requirements for our nation's warfighters.

For more information, contact Larry Brown at (614) 688-5080 or *larry_brown@ewi.org*. ♦

Mark Your Calendar:

NJC to Exhibit at AWS Welding Show 2004

Visit the NJC at Booth #5050 at the AWS Welding Show in Chicago, Illinois, April 6–8. The show will be held at McCormick Place Lakeside Center. Brochures and articles will be available highlighting NJC projects. Navy Joining Center staff will be available for discussion of various project development activities.

NJC
Operated by
EWI

The Navy Joining Center
1250 Arthur E. Adams Dr.
Columbus, OH 43221
Phone: (614) 688-5010
FAX: (614) 688-5001
e-mail: *NJC@ewi.org*
www: *http://www.ewi.org*
Contact: Larry Brown

Preparing Aluminum for Welding

Cutting. Sawing, shearing, and other mechanical methods are commonly used for cutting aluminum. The cutting is done dry whenever possible, but cutting lubricants may be used when necessary. Cutting wax is not recommended for use on blades because of the difficulty of its complete removal from the weld area.

Sawing aluminum requires relatively coarse teeth and high blade speeds. Band saws can be used for cutting small pieces. The blades should have 2 to 4 teeth per in. (8 to 16/cm), and a blade speed of at least 6000 ft/min (1800 m/min) under load. A typical band saw blade for aluminum is shown in Fig. 1. Circular

Carbide-tipped blades are good, especially where blade lubrication isn't allowed.

saws fitted with high-speed blades are run at 8000 surface ft/min (2400 m/min) or faster. For other tool steel blades, the speed is at 4000–6000 surface ft/min (1200–1800 m/min). Carbide-tipped blades are good, especially where blade lubrication is not allowed.

If shearing is used, it should be clean and sharp with correct clearances between blades for the metal thicknesses. Properly sheared edges can be welded satisfactorily up to 3/16 in. (4.88 mm). The edges should be clean whether they are welded "as-sheared" or after dressing. Shearing is not recommended for aluminum alloys containing 3.5% or more Mg because the edges become sensitive to stress corrosion cracking.

Plasma arc cutting is fast and accurate, although the equipment can be expensive. There is cost justification with the process in conditions that require cutting of one-inch or thicker plate, stack cutting of thin plate, or with quantities of identical parts.

Edge Preparation. The preparation of edges is often done as the sheet or plate is cut to size and shape. Below 3/16 in. (4.8 mm) thickness, a square edge may be satisfactory. Above this thickness, a single or double-bevel, or J-shape edge geometry may be required. Typical butt joint configurations are shown in Fig. 2. Edge preparation should be in accordance with the welding procedure specification. If air-operated tools are used, the air supply should be free of oil, moisture, and dirt since any of these materials could contaminate the weld area. High-speed milling machines, routers, planers, and various types of saws can be used for edge preparation. Heavy-duty industrial tools are recommended. The use of sanding or grinding is not generally recommended, but if used, the abrasives should be approved for the job. Remove any residue left from sanding or grinding to avoid weld contamination and porosity. If the cutting operation leaves a rough surface, a secondary operation should follow to provide adequate smoothness for proper cleaning before welding.

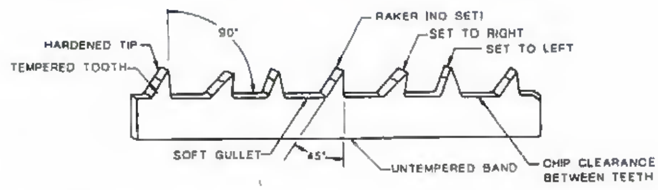

Fig. 1 — Typical band saw blade design for aluminum.

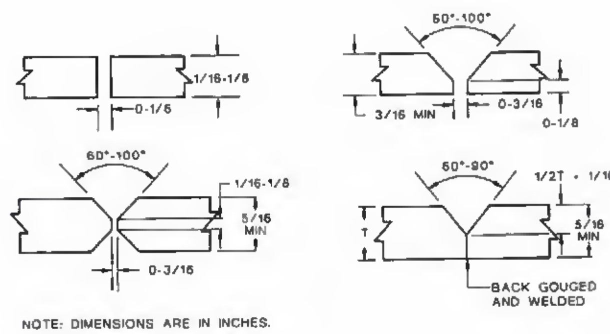

Fig. 2 — Typical joint designs for gas shielded arc welding of aluminum.

Cleaning for Welding. Common cleaning procedures for aluminum consist of degreasing followed by hand or power wire brushing. Degreasing is usually done with a commercial solvent by wiping, spraying, dipping, or vapor degreasing. Such solvents may be toxic, therefore welding and cleaning operations should be done in well-ventilated areas. It is good practice to degrease all surfaces for a distance of 3 to 6 in. from the joint edge.

Wire brushes should have stainless steel bristles from 0.005 to 0.015 in. (0.13 to 0.38 mm) in diameter. They should be degreased periodically to prevent contamination. Pressure on the brush should be light to avoid burnishing the surface or imbedding foreign matter.

For very tightly adhering contaminants or very thick oxide, methods such as machining, scraping, filing, grinding, or sanding may be required. Chemical methods include the use of caustic soda, acids, and proprietary solutions. When mixing solutions, the chemical should always be added slowly into the water or solvent while stirring.

Cleaning should be done before joint fitup because it is difficult to remove solvents or solution from assembled joints. Weld joint surfaces may become contaminated again if they are exposed to the shop atmosphere for more than eight hours.

Excerpted from AWS D3.7, *Guide for Aluminum Hull Welding.*

SOCIETY NEWS

BY SUSAN CAMPBELL

VOLUME 83 • NUMBER 2 • FEBRUARY 2004

Students Create a Wonder in Metal

The bald eagle is crowned with thousands of handmade stainless steel feathers.

The massive arched base support for the eagle is decorated with 32 layers of various metals to create the colored images.

The eagle is nearly ready for mounting on its base.

Middlesex County Vocational and Technical High School students in Piscataway, N.J., are close to completion of an incredible work of art they have named *Fierce Allegiance*.

The 6800-lb metal project when completed will be a monumental sculpture fabricated entirely of numerous metals selected for their colors and textures. The basic materials include mild steel, stainless steel, brass, bronze, copper, and aluminum.

The sculpture consists of two major components: the eagle and a massive vividly decorated supporting base.

The eagle's wingspan measures 18 ft from tip to tip; and it towers 14 ft from wing tip to talon. Joseph Gess, Jr., the designer of the sculpture and a teacher at Middlesex Vo-Tech, said he designed the eagle to be anatomically correct in its stance, proportions, and textures.

"I planned its construction to make it relatively light yet strong for its size."

The eagle's 800-lb body has some surfaces exposed to permit natural oxidizing; other surfaces are protected to keep a lasting luster. The bird's wings and body are fabricated from mild steel, which will oxidize to a deep brown color. The head and tail feathers are made from surgical-quality stainless steel, to ensure its bright luster indefinitely. The beak and talons are brass, coated to retain its gold luster.

All of the eagle's parts, components, and its 2000 feathers were individually handcrafted by the students.

The front view of the base presents American scenic wonders, adding interest and proclaiming the sculpture's patriotic theme. As viewed from the rear, the base is seen to be a massive supporting structure, adorned with stars and stripes, to hold the eagle aloft.

The frontal art was created using 32 layers of various ferrous and nonferrous metal pieces, hand cut and shaped to picture the sun, moon, stars, and clouds. Pictured too, are snow-capped mountains, cliffs, forested foothills, a mountain lake, and waterfalls. Metallic oxidation will eventually transform the materials into various shades of green, brown, and gray.

The supporting base is 8 ft tall and 16 ft wide. It weighs about 6000 lb; serving as a counterbalance for the weight of the cantilevered eagle that will be mounted at the top.

The height and space restrictions in the high school's shop restricted the students from mounting the eagle in its final position. As pictured, the eagle is currently mounted on a work stand. At the time of installation, the eagle will be permanently affixed on the base structure with a unique design that gives the illusion the eagle is in free flight with no apparent mounting point to the base.

Stars and stripes adorn the rear of the arched base support.

Clenched in the eagle's beak will be a streaming red, white, and blue banner.

When finally assembled, the sculpture will stand 21 ft high and weigh approximately 6800 lb.

At the time of this writing the sculpture is nearly completed. A few more weeks of hard work and the project will be finished and ready for its permanent home, to be announced.

John Gess, Jr., and his students take pride that their hard work has resulted in a stunning monument that will soon inspire many observers with its beauty and strength through the science of metallurgical technology. ◆

AWS Foundation Announces Its Fourth Annual Silent Auction

The AWS Foundation is proud to announce the current donors to its Fourth Annual Silent Auction, April 6–8, at McCormick Place Lakeside Center in Chicago, Ill.

The auction benefits the AWS Foundation's scholarship programs. Companies wishing to donate items for the auction ($240 minimum value), please call Vicki Pinsky at (800) 443-9353 ext. 212 or e-mail to *vpinsky@aws.org*.

To bid in advance, visit the American Welding Society's Web site at *www.aws.org/foundation/auction/* or contact the AWS Foundation at (800) 443-9353 ext. 212 with the item name and your bid, complete name, address, and telephone number. To bid on an item while attending the AWS Welding Show, please go to the AWS Foundation booth.

Welding Engineering Supply Co.
2520 lb ⅙ diameter × 60 lb Coils of Tri-Mark Triple 7 Flux Cored Arc Welding Wire
Retail Value: $3150 ($1.25 per lb)
Minimum Bid: $1600
Bid Increment: $100

Malcolm Gilliland
600-A CV Welding Power Source
Retail Value: $3000
Minimum Bid: $1500
Bid Increment: $100

Nelson Stud Welding
Series 4000 Model 300 Stud Welding System
Retail Value: $2950
Minimum Bid: $1500
Bid Increment: $75

Thermadyne Industries, Inc.
Thermal Arc 185TSW Portable/ Shielded Metal Arc Welding Machine
Retail Value: $2100
Minimum Bid: $1000
Bid Increment: $75

Nordan Smith Welding
E71T1 FCAW Wire
Retail Value: $1731
Minimum Bid: $900
Bid Increment: $50

Select Arc, Inc.
1 Pallet of 1200-lb Welding Wire, Select 720.052
Retail Value: $1600
Minimum Bid: $800
Bid Increments: $60

Quality I Welding & Consulting Inc.
Welder Training Fixture
Retail Value: $1295
Minimum Bid: $650
Bid Increment: $30

ESAB Welding & Cutting Products
Miniarc 150 APS Power Supply
Retail Value: $937
Minimum Bid: $500
Bid Increment: $50

ESAB Welding & Cutting Products
Purox GT-350 Deluxe Gas Welding and Cutting Outfit
Retail Value: $500
Minimum Bid: $200
Bid Increment: $20

Welder Training & Testing Institute
AWS CWI Prep Course
Retail Value: $950
Minimum Bid: $475
Bid Increment: $15

Applied Robotics
QS-AWSDNP - Robotic Collision Sensors
Retail Value: $845
Minimum Bid: $450
Bid Increment: $15

Miller Electric Mfg. Co.
Millermatic® 175 All-in-One GMA Welding Machine
Retail Value: $793
Minimum Bid: $400
Bid Increment: $50

Sonesta Beach Resort
Two-Night/Three-Day Stay for Two
Retail Value: $750
Minimum Bid: $375
Bid Increment: $20

Calco Controls, Inc
McIlrath Electric Gas Heater
Retail Value: $660
Minimum Bid: $330
Bid Increment: $20

Saf-T-Cart
552-16FE
Retail Value: $607
Minimum Bid: $300
Bid Increment: $20

ITW Hobart Brothers
$600 Training Equipment
Retail Value: $600
Minimum Bid: $300
Bid Increment: $20

Harris Calorific, Inc
Harris Port-A-Torch
Retail Value: $566
Minimum Bid: $300
Bid Increment: $20

The Lincoln Electric Co.
Two Front Straight Tickets for the NASCAR Winston Cup in 2004.
Retail Value: $500
Minimum Bid: $250
Bid Increment: $25

AWS Foundation Announces Its Fourth Annual Silent Auction

Jackson Products
HSL 100 American Eagle Welding Helmet with NexGen™ EQC® Lens
Retail Value: $409
Minimum Bid: $188
Bid Increment: $20

PFERD, Inc.
50 each PFERD POLIFAN Flap Discs
Retail Value: $400
Minimum Bid: $200
Bid Increment: $15

Hyatt Regency McCormick Place
Two-Night Weekend Stay for Two
Retail Value: $384
Minimum Bid: $175
Bid Increment: $20

District 5 Director
Jackson Nexgen EQC Welding Shield
Retail Value: $375
Minimum Bid: $188
Bid Increment: $20

Earl Lipphardt, AWS Treasurer
1 Set of Golf Clubs
Retail Value: $350
Minimum Bid: $160
Bid Increment: $20

Inweld Corp.
Medium-Duty Welding and Cutting Kit
Retail Value: $340
Minimum Bid: $170
Bid Increment: $15

IWDC (Weldmark)
Weldmark Medium-Duty Deluxe Welding & Cutting Kit
Retail Value: $340
Minimum Bid: $170
Bid Increment: $15

Steiner Industries
Welder's Safety Kit
Retail Value: $340
Minimum Bid: $170
Bid Increment: $15

Jerry Uttrachi
AWS Vice President
Gas Saver System
Retail Value: $328
Minimum Bid: $164
Bid Increment: $15

Metabo Corp.
W10-150 Quick 6 deg Angle Grinder
Retail Value: $321
Minimum Bid: $160
Bid Increment: $15

Four-Points by Sheraton
Two-Night Stay for Two Including Dinner in York, Pa.
Retail Value: $320
Minimum Bid: $150
Bid Increment: $15

AWS Central-Pennsylvania Section
Welded Brass Bonsai Tree Sculpture
Retail Value: $300
Minimum Bid: $125
Bid Increment: $15

JAZ USA, Inc.
Wire Brushes and Abrasive Wheels
Retail Value: $300
Minimum Bid: $150
Bid Increment: $20

The Lincoln Electric Co.
Washington Redskins Racing Helmet Signed by Joe Gibbs
Retail Value: $300
Minimum Bid: $150
Bid Increment: $20

Lancaster County Career & Technical Center
Brass & Pewter Chess Set Complete with Board
Retail Value: $300
Minimum Bid: $125
Bid Increment: $15

AWS St. Louis Section
Sony DSC-P52 Digital Still Camera
Retail Value: $277
Minimum Bid: $135
Bid Increment: $15

Revcu Industries, Inc.
Tool Handz™ Series Glove Package
Retail Value: $275
Minimum Bid: $140
Bid Increment: $15

The Lincoln Electric Co.
Black Leather NASCAR Bomber Jacket
Retail Value: $260
Minimum Bid: $130
Bid Increment: $20

ArcOne Welding & Safety Products
I 80 STS
Retail Value: $250
Minimum Bid: $137
Bid Increment: $15

AWS San Antonio Section
Gift Certificate from Victoria's Secret
Retail Value: $250
Minimum Bid: $160
Bid Increment: $15

AWS York Central Section
Patriotic Cylinder Bell with Stand
Retail Value: $250
Minimum Bid: $125
Bid Increment: $10

Flexovit Abrasives
Metal Hog Basket
Retail Value: $250
Minimum Bid: $125
Bid Increment: $10

Dressel Welding Supply Co.
ArcMaster Head Shield
Retail Value: $249
Minimum Bid: $125
Bid Increment: $10

Laser Quest of Austin
Two Birthday Party Gift Certificates
Retail Value: $240
Minimum Bid: $75 each
Bid Increment: $10 each

Abicor Binzel
Two sets of Alpha MIG Guns
Retail Value: $250 each set
Minimum Bid: $180
Bid Indrement: $15

Hornell
Speedglas Protop with 9000V Lens
Retail Value: $356
Minimum bid: $180
Bid Increment: $15

Sellstrom Mfg. Co.
Five themed Titan with Attitude Welding Helmets with Striker Autodarkening Filter.
Retail Value: $143 each
Minimum Bid: $75
Bid Increment:$10

AWS Welcomes New Supporting Companies

New Educational Institutions

Institute for Construction Education
2240 E. Geddes Ave.
Decatur, IL 62526

Neo Welding Institute
Modern Erectors, Gravipuram
Kollam, Kerala 691 011
India

Virginia College Technical
2790 Pelham Parkway
Pelham, AL 35124

William J. Dean Technical High School
1045 Main St.
Holyoke, MA 01040

New Supporting Companies

Vaughn's, Inc.
3960 Boone Rd. S.E.
Salem, OR 97301

AWS Membership

Member Grades	As of January 1, 2004
Sustaining Companies	414
Supporting Companies	211*
Educational Institutions	318
Affiliate Companies	217
Welding Distributor Companies	44
Total Corporate Members	**1,204**

** During the month of March, the Society launched the Welding Distributor Company Membership. Those Supporting Company Members identified as welding distributors were upgraded to this new corporate member category.*

Individual Members	43,350
Student Members	4,438

Total Members ... 47,788

Sustaining Member Company

Stillwater Technologies, Inc.
1040 S. Dorset Rd.
Troy, OH 45373
Phone: (800) 338-7561
www.stlwtr.com

Stillwater Technologies, Inc., has experienced sufficient growth and development over the last 45 years to place the company firmly in the position of being one of the top suppliers of resistance welding tip-dressing equipment throughout the domestic and international automotive marketplaces. Stillwater Technologies' diverse selection of electric and pneumatic tip dressers in both single and dual-head models offers a wide variety of choices unmatched in the field. These tip dressers, matched with the company's new automated tip-changing system, can provide a hands-off solution to users of robotic resistance welding cells.

By maintaniing control of all machining and fabricating in-house, Stillwater can service many of its customers' resistance welding needs for gun arms, tips, shanks, and specially designed tooling and fixturing.

The company's mission statement says it all:
"To serve our customers with professionalism, integrity, quality, and value." ♦

AWS Welcomes New Affiliate Member Companies

AMG, Inc.
301 Jefferson Ridge Parkway
Lynchburg, VA 24501

Don Foss Fabrications
2356 Ethel Porter Dr.
Napa, CA 94558

Pipe & Tank Erection Ltd.
27C Rousseau Rd.
Kingston 5, Jamaica

RPM & Associates, Inc.
333 Concourse Dr.
Rapid City, SD 57703

Serimer Dasa North America
10777 Clay Rd.
Houston, TX 77041

Solar Atmospheres
1969 Clearview Rd.
P.O. Box 64476
Souderton, PA 18964

Specialty Welding, Inc.
P.O. Box 1101
Moses Lake, WA 98837

Valco Fabricating & Machining
1235 St. Luke Rd.
Windsor, Ontario N8Y 4W7
Canada

Wilborn Steel Company Ltd.
P.O. Box 10208
San Antonio, TX 78210

AWS Life Members Receive Free Registration for the Welding Show's Professional Program

As longtime supporters of the American Welding Society (AWS), AWS Life Members are being offered complimentary registration to the AWS Welding Show 2004 and the complete Professional Program (a $325 value).

The Professional Program will take place April 6–8 in Chicago, Ill., at the McCormick Center, with the Welding Show occurring on the same dates.

Registration to the Professional Program entitles AWS Life Members to attend any of the seminars or sessions occurring over the three-day period. Please be sure to include any applicable fees for special events or spouse attendance when you register. Registration forms will be available in upcoming issues of the *Welding Journal* as well as in the Advance Program, which was mailed to members in January.

To register, please mark "AWS Life Member: FREE Registration" at the top of the registration form, then fax both sides to Cassie Burrell, Associate Executive Director, Membership, at (305) 443-5647; or mail the form to AWS, 550 NW LeJeune Road, Miami, FL 33126. ♦

SECTION NEWS

Shown at the Green & White Mountains Section meeting November 13 are (from left) Wesley Mekurt, Ron Williams, and John Corrado.

Shown at the Boston Section's Welders' Night program, Steve Flowers (right) and his students received a plaque in appreciation for their continuing support.

DISTRICT 1

Director: Russ Norris
Phone: (800) 559-9353

GREEN & WHITE MOUNTAINS

NOVEMBER 13
Speakers: **John Corrado, Ron Williams, Wes Mekrut**
Affiliation: Filler Metals LLC
Topic: Aluminum welding techniques
Activity: **Kevin McGloughlin, Mark Walzak,** and **Geoff Putnam** received their 25-year AWS membership awards.

BOSTON

DECEMBER 1
Activity: **Steve Flowers**, metal fabrication instructor, Southeastern Regional Vocational High School, and his students presented a Welders' Night program jointly with members of the local chapter of American Society for Nondestructive Testing. **Tom Ferri** received recognition for his services as outgoing Section Chair.

DISTRICT 2

Director: Alfred F. Fleury
Phone: (732) 868-0768

NEW YORK

NOVEMBER 17
Speaker: **Bill Polanski**, sales rep.
Affiliation: G-Tec Natural Gas Systems
Topic: Oxygen cutting and soldering
Activity: The meeting was held at Buckley's Restaurant in Brooklyn.

Bill Polanski (left) receives the New York Section's speakers award from Vice Chair Bob Waite at the November 17 meeting.

New York Section Chair Ray Henderson II (left) presents the 35-year AWS Membership Award to Richard Couch, Jr.

John Otto was honored at the Philadelphia Section program in December.

PHILADELPHIA

DECEMBER
Activity: **John Otto** was named the Section's first Student of the Month. A student at Gloucester County Tech Institute welding program, Otto is also active in the SkillsUSA-VICA program.

DISTRICT 3

Director: Alan J. Badeaux, Sr.
Phone: (301) 934-9061

LEHIGH VALLEY

OCTOBER 21
Speaker: **Colin Phelps**, QA technician.
Affiliation: Alstrom Power, Inc.
Topic: Documentation for welders for pressure vessels, including PQRs, WPSs.

READING

OCTOBER 16
Activity: The Section held its Past Chairmen's Recognition program at Crystal Springs Restaurant in Sinking Spring, Pa. **Dick Unger** (1983–1984) hosted the nostalgic event.

Reading Section Past Chairs shown at the October 16 meeting are (from left) Francis Butkus, Dick Unger, Paul Levengood, Joseph Progin, Merilyn McLaughlin, Larry Heffner, John Miller, Dennis Hornberger, and Dave Hibshman.

Shown with their District 4 awards at the Tidewater Section meeting November 13 are (from left) Steve Harris, John Gomez, District Director Ted Alberts, Jon Cookson, and Gary Roy.

Members of the York-Central planning committee pose at the December 21 meeting.

Winners in the Southwest Virginia June golf outing were (from left) Coy Stennette, Leon Bryant, Matt Pisenti, Chair Bill Rhodes, and Kyle Deal.

Speaker Dick Unger (left) is shown with Reading Section Chair John Miller at the October 16 meeting.

Lehigh Valley Section Chair Frank Wemet (right) presents the speaker award to Colin Phelps at the October 21 meeting.

CUMBERLAND VALLEY

NOVEMBER 11
Speaker: Carlu Rosati
Affiliation: FBI, Laboratory Div.
Topic: Applied metallurgy as used in crime investigations.
Activity: The meeting was held at Richardson's Restaurant in Hagerstown, Md.

YORK CENTRAL PENNSYLVANIA

NOVEMBER 17
Activity: The Section participated in the York County School of Technology's Open House Career Night program.

DECEMBER 17
Activity: The York-Central Pennsylvania Section held its Image of Welding meeting at Hoss's Steak House.

DISTRICT 4

Director: Ted Alberts
Phone: (540) 674-3600, ext. 4314

District 4 Director Ted Alberts (back row, far right) headed the AWS Richmond Section reactivation committee in November.

Dayton Section members participated in a forging, blacksmithing, and forge welding demonstration at the County Fairgrounds in Troy, Ohio, November 11.

SOUTHWEST VIRGINIA

JUNE 20

Activities: The Section held its golf outing at Countryside Golf Course in Roanoke, Va. Also in June, the Section participated with John W. Hancock, Jr., Inc., in the American Cancer Society's Relay for Life program.

NOVEMBER 13

Speaker: **Dick Holdren**

Affiliation: Edison Welding Institute

Topic: Enhanced welding productivity through technology

Activity: **Gary Roy** and **Jon Cookson** received the Private Sector Educators Award. **John Gomez** and **Steve Harris** received the District Meritorious Award from District 4 Director **Ted Alberts**.

RICHMOND

NOVEMBER

Activity: The Section held its reorganization meeting headed by District 4 Director **Ted Alberts**. Elected to offices were **Brett Clarke**, chairman; **John Dillard**, vice chair; **Lisa Campbell**, secretary; **Marcus Swailes**, treasurer; and **George Reynolds**, educational chair.

TIDEWATER

OCTOBER 9

Activity: The Section held its annual golf tournament at Cypress Creek Golf Course in Smithfield, Va. Eighty players participated. Ron Davis once again masterminded the event for the Section.

DISTRICT 5

Director: Wayne J. Engeron
Phone: (404) 501-9185

NORTH CENTRAL FLORIDA

OCTOBER 14

Speaker: **Bill Myers**, senior welding engineer, AWS Past President 2001

Affiliation: Dresser-Rand Turbo Products Div. (ret.)

Topic: AWS A5.1, *Specification for Carbon Steel Electrodes for Shielded Metal Arc Welding*

Activity: The meeting was held at Holox Restaurant in Ocala, Fla.

South Carolina Section Chair Gale Mole is shown with speaker Tim Dangerfield at the November 20 program.

Pittsburgh Section Chair Carl Ott presents Gabriel Centofanti an appreciation gift for conducting the Section's tour of H.B.C. Barge Co. on November 11.

SOUTH CAROLINA

NOVEMBER 20

Activity: The Section toured American Pipe, Inc., in Hanahan, S.C. **Tim Dangerfield**, operations manager, conducted the tour.

DISTRICT 6

Director: Neal A. Chapman
Phone: (315) 349-6960

DISTRICT 7

Director: Robert J. Tabernik
Phone: (614) 488-7913

PITTSBURGH

NOVEMBER 11

Activity: The Section toured H.B.C. Barge Co., in Brownsville, Pa. **Gabriel E. Centofanti**, president, conducted the tour, and explained the fabrication of various types of barges, the welding processes used, and how the finished barges were maneuvered into the river.

DAYTON

NOVEMBER 11

Speakers: **Steve Roth** and **Al Minneman**

Shown at the New Orleans Section program November 19 are (from left) District 9 Director John Bruskotter, speaker Ryan Baker, Shelton Ritter, George Fairbanks, Chair David Foster, Joe Golemi, O. J. Templet, and Mike Skiles.

District 9 Director John Bruskotter and wife, Donna, are shown at the New Orleans Section holiday party December 18.

Affiliation: The Southern Ohio Forge and Anvil Assn. (SOFA)
Topic: Forging, blacksmithing, and forge welding
Activity: The SOFA staff demonstrated how to make fancy twists, leaf making, and texturing. Afterward, the Section members had a hands-on opportunity to try forge welding techniques.

DISTRICT 8

Director: Wallace E. Honey
Phone: (256) 332-3366

GREATER HUNTSVILLE

October 20
Activity: The Section hosted a student welding contest led by **Larry Smith,** welding instructor, Blount County Area Vocational Technical Center. Sixty-one people participated in the event.

DISTRICT 9

Director: John Bruskotter
Phone: (504) 367-0603

BATON ROUGE

November 20
Activity: **Barry Landry,** and **Glenn Ingrassia** led a tour of the AKA Volks Construction Co. fabrication shop to learn the procedures used to manufacture pressure vessels. Featured were the various types of welding involved to meet the ASME Code requirements.

NEW ORLEANS

November 19
Speaker: **Ryan Baker**, district manager
Affiliation: Harris Calorific, Daphne, Ala.

ASQC Chair Kelly Hered (left) chats with speaker Jackie Morris at the Mobile Section program November 20.

Shown at the Baton Rouge Section program November 20 are (from left) Terry Babin, Dave Poydock, John Bruskotter, Davis Rayburn, Mark Kevin, and George Fairbanks.

Topic: Oxyacetylene gas safety and the state of the welding industry
Activity: The program was held at Boomtown Casino in Harvey, La.

December 18
Activity: The New Orleans Section joined with the local chapter of American Society for Nondestructive Testing to cohost a Christmas dinner for 91 attendees at Boomtown Casino in Harvey, La.

MOBILE

November 20
Speaker: **Jackie Morris**, QA manager

Darren Haas (center) presents the Pascagoula Section speaker awards to Ken Inabinette (left) and James Ivy at the November 20 program.

Affiliation: Bender Shipbuilding and Repair Co., Inc.
Topic: Details on the AWS Certified Welding Supervisor (CWS) program
Activity: This joint meeting with members of the local chapter of American Society for Quality Control was held at Bay Beach Inn in Gulf Breeze, Fla.

PASCAGOULA

November 20
Activity: The Section hosted a Students Night program at Mississippi Gulf Coast Community College. Speakers included **James Ivy**, training manager, Northrup Grumman Ship Systems; and **Ken Inabinett**, QC vice president, Signal International. They discussed welding job opportunities.

DISTRICT 10

Director: Victor Y. Matthews
Phone: (216) 383-2638

NORTHWESTERN PENNSYLVANIA

October 14
Speaker: **Damian Kotecki,** AWS National Vice President, and technical director, stainless steel

Damian Kotecki (left) is welcomed to the Northwestern Pennsylavania Section program by Educational Chair Steve DeHart.

Speaker Brad Shaw (right) accepts a speaker gift from Northwestern Pennsylvania Chair Chet Wesley November 11.

Milwaukee Chair John Kozenieki (left) is shown with speaker Marty Johnson November 13.

Affiliation: The Lincoln Electric Co.
Topic: Fundamentals of welding austenitic stainless steels
Activity: This Northwestern Pennslvania program was held at Tri State Welding Lab for 58 attendees.

November 11
Speaker: **Brad Shaw**, senior welding engineer
Topic: Steel and welding issues related to high-speed, 300-mph rail transportation systems
Activity: This Northwestern Pennsylvania Section program was held at Tri State Welding Lab for 59 attendees.

DISTRICT 11

Director: Eftihios Siradakis
Phone: (989) 894-4101

DETROIT

December 4
Activity: The Section held its holiday dinner. The proceeds from the Detroit Red Wings ticket auction were donated to the Salvation Army.

DISTRICT 12

Director: Michael D. Kersey
Phone: (262) 650-9364

MILWAUKEE

November 13
Speaker: **Marty Johnson**, wildlife biologist
Affiliation: Wisconsin Dept. of Natural Resources
Topic: Deer hunting and the impact of chronic wasting disease for the season
Activity: Thirty-five people attended the program.

Shown at the Milwaukee Christmas party are (from left) District 12 Director Michael D. Kersey, Bob Schuster, Chair John Kozeniecki, Jay Wilson, and Gerald Blaski.

November 13
Activity: The Milwaukee Section held its annual Christmas party at Sprecher Brewery in Milwaukee, Wis. The event included a tour of the Rathskellar Museum to see displays of artifacts from historic Milwaukee-area breweries.

DISTRICT 13

Director: J. L. Hunter
Phone: (309) 888-8956

DISTRICT 14

Director: Tully C. Parker
Phone: (618) 667-7744

LEXINGTON

November 20
Speakers: **Edward Varekojis**, and **Lou Vitucci**
Topic: Welding aluminum with inverter technology
Activity: The meeting, attended by 60 people, was held at Central Kentucky Vocational Technical School.

The Lexington Section hosted an aluminum welding seminar.

Indianapolis Past Chair Bennie Flynn (left) is shown with presenters Fern Deckard and Mike Anderson at the November 10 school welding program.

Arrowhead Section Chair Loren Kantola (right) is shown with tour guides John Penaz and Scott Udenberg during the Section's tour of Sercoloaders November 20.

The Northern Plains Section members are shown during their tour of Fargo Tank and Steel facilities in December.

INDIANAPOLIS

NOVEMBER 10
Activity: This student night program, held at Warren Central High School, featured welding topics related to auto racing. Instructor **Mike Anderson** hosted the event.

DISTRICT 15

Director: J. D. Heikkinen
Phone: (218) 741-9693

ARROWHEAD

NOVEMBER 20
Activity: The Section toured the Sercoloaders facility in Two Harbors, Minn., to study the manufacturing techniques used to build various industrial loading and lifting equipment. **Scott Udenberg**, plant superintendent, conducted the tour.

NORTHERN PLAINS

DECEMBER
Activity: The Section toured the Fargo Tank and Steel facilities in Fargo, N.Dak. The tour guides included **Jim Rudland**, shop superintendent, and **Bruce Palmer**, structural lead man.

DISTRICT 16

Director: C. F. Burg
Phone: (515) 294-5428

MID PLAINS

DECEMBER 3
Activity: The Section held its meeting at the North Platte High School to demonstrate the proper use of small household-type welding machines. Everyone had an opportunity to make welds using the equipment.

KANSAS

SEPTEMBER 29
Activity: The Section held its meeting at Whiskey Creek Restaurant in Wichita, Kans. The topic for discussion was the AWS D1.1, *Structural Welding Code — Steel.*

OCTOBER 28
Activity: The Kansas Section members toured the Big Dog Motorcycle manufacturing facility in Wichita, Kans. **Mr. Shaw** discussed the need for precision welding of the various parts.

DISTRICT 17

Director: Oren P. Reich
Phone: (254) 867-2203

CENTRAL TEXAS

DECEMBER 9
Speaker: **Dave Culwell**, Sr. tech rep.
Affiliation: J. W. Harris Co., Inc.
Subject: Filler metals
Activity: This meeting, fully sponsored by Dupuy Oxygen and Supply Co., was held at Texas State Technical College with the Section's Student Chapter in attendance.

OKLAHOMA CITY

OCTOBER 16
Speaker: **Ron Walker**, district sales manager.
Affiliation: Hobart Brothers
Topic: Metal core welding
Activity: This meeting was held at Boardman, Inc., in Oklahoma City. Following the talk and a slide presentation, the members had a hands-on demonstration of the advantages of using metal core filler metals compared with basic GMAW consumables.

NOVEMBER 13
Activity: The Section toured the Trinity Industries facilities in Oklahoma City, to study the production welding procedures used for the manufacture of refrigerated railroad cars. Ninety people participated in the event.

HOUSTON

NOVEMBER 19
Activity: The Section hosted its Student Night and awards presentation program at Brady Landing Restaurant. In attendance were members of the Texas A&M Student Chapter. Honored were **Chau Hoang**, Private Sector Instructor Award; **John Husfeld**, Section Educator Award; **Ed Malmgren**, **Dennis Eck**, and **Larry Smith**, Section Meritorious Awards; **Randy Sipes**, District Meritorious Award; **John Pearson**, Section-level Dalton E. Hamilton Memorial CWI of the Year Award; and **Ron Theiss**, District-level Dalton E. Hamilton CWI of the Year Award. Special District Director awards were presented to **Dan Jones**, **Kim Smith**, **Asif Latif**, and **Dave Smith**; and Special Houston Section Meritorious Awards were bestowed upon **Ron Theiss**, and **Daryle Morgan.**

EAST TEXAS

NOVEMBER 20
Activity: The Section toured the LeTourneau, Inc., factory in Longview, Tex., to study the construction of large front-end loaders and other earthmoving equipment.

DISTRICT 18

Director: John Mendoza
Phone: (210) 860-2592

DISTRICT 19

Director: Phil Zammit
Phone: (509) 468-2310 ext. 120

SPOKANE

DECEMBER 17
Activity: The Section met at the Spokane Skills Center where two shifts of students study welding using the AWS S.E.N.S.E., Entry Level Welder, program of instruction. **Andrew Snyder**, welding instructor, conducted the tour.

DISTRICT 20

Director: Jesse A. Grantham
Phone: (303) 451-6759

DISTRICT 21

Director: Les Bennett
Phone: (805) 929-2356

KERN

SEPTEMBER 18
Activity: The Section toured Valley industrial X-Ray & Inspection Services, Inc., in Bakersfield, Calif. Jack Wright demonstrated ultrasonic shearwave examination techniques. The members experienced hands-on demonstrations of various nondestructive examination procedures, including magnetic particle, liquid penetrant, ground-penetrating radar, and magna flux leakage.

OCTOBER 16
Activity: Praxair hosted the Kern Section to a barbeque dinner and a presentation by Lincoln Electric Co. representatives on changes to FEMA structural steel fabrication requirements.

NOVEMBER 20
Activity: The Kern Section held its meeting at Flowserve Hot-Tap and Line Stopping. **John More** was presented the AWS Silver Membership Award for his 25 years of service to the Society.

DISTRICT 22

Director: Kent S. Baucher
Phone: (559) 276-9311

FRESNO

SEPTEMBER 26
Activity: The Section held its annual trap shoot at Fresno Trap & Skeet Club. First place honors went to **Brian Visher**; second place was taken by **Josh Meyers**. More than 40 participated in the event.

OCTOBER 30
Speaker: **James Vela**, CWI
Topic: Prequalified WPSs
Activity: **Brad Bosworth** received the Fresno Section CWI of the Year Award.

SACRAMENTO VALLEY

NOVEMBER 19
Activity: The Section toured the Gayle Manufacturing facility in Woodland, Calif., to study its innovative procedures for fabricating structural steel products.

John More (right) accepts his Silver Membership Award from Kern Section Chair Brent Welsh November 20.

Nominations Sought for National Offices

AWS members who wish to nominate candidates for President, Vice President, and Director-at-Large on the AWS Board of Directors for the term starting June 1, 2005, may either:

1) Send their nominations before February 15, 2004, to Ernest D. Levert, National Nominating Committee Chairman, American Welding Society, 550 NW LeJeune Road, Miami, FL 33126.

or

2) Present the nomination in person at the open session of the National Nominating Committee Meeting scheduled for 10:00 to 11:00 A.M., Tuesday, April 6, 2004, at McCormick Place, Chicago, Illinois, during the AWS 2004 Welding Show.

Nominations must be accompanied by biogaphical material on each candidate, including a written statement by the candidate as to willingness and ability to serve if nominated and elected, and a 5 X 7-in. black and white or color photograph.

Notice of Annual Meeting American Welding Society

The Annual Meeting of the members of the American Welding Society will be held on Monday, April 5, 2004, beginning at 9:00 A.M. at McCormick Place, Chicago, Illinois.

The regular business of the Society will be conducted, including election of officers and nine members of the Board of Directors. Any business properly brought before the membership will be considered.

2003–2004 Member-Get-A-Member Campaign

Listed below are the people participating in the 2003–2004 Member-Get-A-Member Campaign. For campaign rules and a prize list, please see page 53 of this Welding Journal.

If you have any questions regarding your member proposer points, please call the Membership Department at (800) 443-9353 ext. 480.

Winner's Circle

(AWS Members sponsoring 20 or more new Individual Members, per year, since June 1, 1999.)

J. Compton, *San Fernando Valley*****
E. H. Ezell, *Mobile***
S. McGill, *Northeast Tennessee**
J. Merzthal, *Peru***
B. A. Mikeska, *Houston**
R. L. Peaslee, *Detroit**
W. L. Shreve, *Fox Valley**
G. Taylor, *Pascagoula***
T. Weaver, *Johnstown/Altoona**
G. Woomer, *Johnstown/Altoona**
R. Wray, *Nebraska**

**Denotes the number of times an Individual Member has achieved Winner's Circle status. Status will be awarded at the close of each membership campaign year.*

President's Guild

(AWS Members sponsoring 20 or more new Individual Members between June 1, 2003, and May 31, 2004.)

President's Round Table

(AWS Members sponsoring 11–19 new Individual Members between June 1, 2003, and May 31, 2004.)

R. Purvis, *Sacramento* — 14
P. Evans, *Chicago* — 12
T. Hart, *Mobile* — 12

President's Club

(AWS members sponsoring 6–10 new Individual Members between June 1, 2003, and May 31, 2004.)

J. Powell, *Triangle* — 9
W. Drake, Jr., *Ozark* — 8
G. Taylor, *Pascagoula* — 7
J. Compton, *San Fernando Valley* — 6
C. Daily, *Puget Sound* — 6
P. Walker, *Ozark* — 6

President's Honor Roll

(AWS members sponsoring 1–5 new Individual Members between June 1, 2003, and May 31, 2004. Only those sponsoring 2 or more AWS Individual Members are listed.)

D. St.-Laurent, *Northern Alberta* — 5
B. Suckow, *Northern Plains* — 5
C. Wesley, *Northwestern Pa.* — 5
C. Dynes, *Kern* — 4
J. Smith, *Columbus* — 4
S. Abarca, *Illinois Valley* — 3
K. Campbell, *L.A./Inland Empire* — 3
C. Chilton, *Ozark* — 3
B. Franklin, *Mobile* — 3
J. Greer, *Chicago* — 3
T. Nichols, *West Tennessee* — 3
J. Cantlin, *Southern Colorado* — 2
S. Colton, *Arizona* — 2
A. DeMarco, *New Orleans* — 2
E. Duplantis, *San Antonio* — 2
S. Henson, *Spokane* — 2
R. Johnson, *Detroit* — 2
P. Krishnasamy, *India* — 2
G. Mulee, *Rochester* — 2
J. O'Neal, *Ozark* — 2
R. Painter, *Holston Valley* — 2
S. Schrecengost, *Pittsburgh* — 2
T. Shirk, *Tidewater* — 2
R. Warner, *Utah* — 2
D. Wright, *Kansas City* — 2
R. Wright, *Southern Colorado* — 2

Student Sponsors

(AWS members sponsoring 3 or more new AWS Student Members between June 1, 2003, and May 31, 2004.)

R. Olson, *Siouxland* — 36
M. Pointer, *Sierra Nevada* — 27
C. Donnell, *Northwest Ohio* — 25
S. Sivinski, *Maine* — 24
M. Arand, *Louisville* — 23
C. Overfelt, *Southwest Virginia* — 23
M. Wilkes, *Mahoning Valley* — 23
D. Combs, *Santa Clara Valley* — 21
D. Kettler, *Williamette Valley* — 21
W. Kielhorn, *East Texas* — 21
F. Juckem, *Madison-Beloit* — 20
D. Scott, *Peoria* — 19
F. Wernet, *Lehigh Valley* — 19
B. Chesney, *Green & White Mountains* — 17
J. Daugherty, *Louisville* — 16
D. Hatfield, *Tulsa* — 16
A. Reis, *Pittsburgh* — 16
T. Baldwin, *Arrowhead* — 15
R. Norris, *Maine* — 15
D. Roskiewich, *Philadelphia* — 15
M. Anderson, *Indiana* — 14
J. Hepburn, *Johnstown-Altoona* — 13
L. Davis, *New Orleans* — 13
G. Euliano, *NW Pennsylvania* — 13
W. Harris, *Pascagoula* — 13
K. Ellis, *Central Pennsylvania* — 12
A. Badeaux, *Washington, D.C.* — 12
R. Tupta, Jr., *Milwaukee* — 11
P. Walker, *Ozark* — 11
R. Williams, *Ozark* — 11
J. Boyer, *Lancaster* — 10
M. Koehler, *Milwaukee* — 10
T. Strickland, *Arizona* — 10
A. Vidick, *Wyoming* — 10
D. Weeks, *Southwest Virginia* — 10
G. Gammill, *Northeast Mississippi* — 9
J. Mendoza, *San Antonio* — 8
J. Pelster, *Southwest Nebraska* — 8
J. Smith, Jr., *Mobile* — 8
J. Compton, *San Fernando Valley* — 7
R. Gallagher, Jr., *Lehigh Valley* — 7
W. Galvery, Jr., *Long Beach/Orange Cnty* — 6
C. Kipp, *Utah* — 6
M. Tyron, *Utah* — 6
D. Vranich, *North Florida* — 6
J. Carney, *Western Michigan* — 5
T. Kienbaum, *Colorado* — 5
A. Mattox, *Lexington* — 5
W. Miller, New Jersey — 5
S. Williams, *Central Arkansas* — 5
R. Douglas-Wells, *Atlanta* — 4
F. Henry, *L.A./Inland Empire* — 4
J. Olivarez, Jr., *Puget Sound* — 4
R. Richwine, *Indiana* — 4
D. Smith, *Niagara Frontier* — 4
W. Wilson, *New Orleans* — 4
D. Zabel, *Southeast Nebraska* — 4
T. Bur, *Northern Michigan* — 3
J. Ciaramitaro, *North Central Florida* — 3
J. Crosby, *Atlanta* — 3
R. Grays, *Kern* — 3
R. Huston, *Olympic* — 3
J. Livesay, *Nashville* —3
J. Morash, *Boston* — 3
A. Ochoa, *San Francisco* — 3
H. Rivera, *South Florida* — 3
T. Shirk, *Tidewater* — 3 ♦

Nominations For AWS District Directors

The term of office for District Directors in the following Districts will terminate on May 31, 2005. As District Nominating Committees will be appointed this spring, it is time to be thinking of position nominations. For further information, use your current District Director's contact information given below.

District 3

Alan J. Badeaux, Jr., Instructor
Charles County Career & Tech Center
7775 Marshall Corner Rd.
Pomfret, MD 20675
Telephone: (301) 934-9061
FAX: (301) 934-0165
e-mail: *abadeaux@ccboe.com*

District 6

Neal A. Chapman, Welding Engineer
Entergy Nuclear Northeast
15491 McIntyre Rd.
Sterling, NY 13156
Telephone: (315) 349-6960
FAX: (315) 349-6625
e-mail: *chapman@redcreek.net*

District 9

*** John C. Bruskotter**
Dynamic Industries, Inc.
2804 Peters Rd. (70058)
P.O. Box 44
Harvey, LA 70059
Telephone: (504) 363-5900
FAX: (504) 363-5920
e-mail: *jbruskotter@dynamicind.com*

District 12

*** Michael D. Kersey**, Technical Sales Representative
The Lincoln Electric Company
W223 N798 Saratoga Drive #H
Waukesha, WI 53186
Telephone: (262) 650-9364
FAX: (262) 650-9370
e-mail: *michael_d_kersey@lincolnelectric.com*

District 15

*** Jack D. Heikkinen,** President
Spartan Sauna Heaters, Inc.
7484 Malta Rd.
Eveleth, MN 55734
(218) 741-8433
e-mail: *spartans@cpinternet.com*

District 18

John Mendoza
City Public Service
3319 Kashmuir
San Antonio, TX 78223-1612
Telephone: (210) 532-9098
e-mail: *mendoza727@aol.com*

District 21

Les J. Bennett
Associate Professor
Allan Hancock College
1020 Fairway Vista Dr.
Santa Maria, CA 93455
(805) 348-1838
e-mail: *lesweld@aol.com*

* Denotes current District Director is not eligible for reelection to another three-year term.

Standards Notices

Standard for Public Review

AWS was approved as an accredited standards-preparing organization by the American National Standards Institute (ANSI) in 1979. AWS rules, as approved by ANSI, require that all standards be open to public review for comment during the approval process. This column also advises of ANSI approval of documents. The following standards are submitted for public review. A draft copy may be obtained by contacting Rosalinda O'Neill at AWS, Technical Services Business Unit, 550 NW LeJeune Rd., Miami, Fl 33126; telephone (800/305) 443-9353 ext. 451, e-mail: **roneill@aws.org.**

D16.1M/D16.1:200X, *Specification for Robotic Arc Welding Safety*. New standard. $7. [ANSI public review expires February 10, 2004.]

Technical Committee Meetings

All AWS technical committee meetings are open to the public. Persons wishing to attend a meeting should contact the staff secretary of the committee as listed below at AWS, 550 NW LeJeune Rd., Miami, FL 33126; telephone: (800) 443-9353 or, outside the United States, (305) 443-9353.

February 4–5, International Standards Activities Committee. Miami, Fla. General meeting. Staff contact: A. R. Davis, ext. 466.

February 5–6, Technical Activities Committee. Miami, Fla. General meeting. Staff contact: A. R. Davis, ext. 466.

February 11, D16 Committee on Robotic and Automatic Welding. Orlando, Fla. Standards preparation and general meeting. Staff contact: P. Howe, ext. 309.

February 26–27, C3 Committee on Brazing and Soldering. Miami, Fla. Standards preparation and general meeting. Staff contact: C. Jenney, ext. 304.

February 26–27, B2F Subcommittee on Plastic Welding Qualification, Miami, Fla. Standards preparation meeting. Staff contact: A. R. Davis, ext. 466.

March 14–19, D1 Committee on Structural Welding. Atlanta, Ga. Standards preparation meeting. Staff contact: J. L. Gayler, ext. 472.

March 29, C2 Committee on Thermal Spraying. New Orleans, La. General meeting. Staff contact: A. R. Davis, ext. 466.

March 29, G1A Subcommittee on Hot Gas Welding and Extrusion Welding. New Orleans, La. General meeting. Staff contact: A. R. Davis, ext. 466.

March 30, A5K Subcommittee on Titanium and Zirconium Filler Metals. New Orleans, La. General meeting. Staff contact: A. R. Davis, ext. 466.

March 30, G2D Subcommittee on Reactive Alloys. New Orleans, La. General meeting. Staff contact: A. R. Davis, ext. 466. ♦

GUIDE TO AWS SERVICES

550 NW LeJeune Rd., Miami, FL 33126
Phone (800) 443-9353; (888) WELDING
FAX (305) 443-7559; *Internet: www.aws.org*
Phone extensions appear in parentheses.
E-mail addresses are available on the AWS web site.

AWS PRESIDENT
Thomas M. Mustaleski
BWXT Y-12 LLC
P.O. Box 2009
Oak Ridge, TN 37831-8096

ADMINISTRATION
Executive Director
Ray W. Shook ....(210)

Deputy Executive Directors
Jeffrey R. Hufsey ....(264)
John J. McLaughlin ....(235)

Chief Financial Officer
Frank R. Tarafa ....(252)

Corporate Director of Quality Management Systems
Linda K. Henderson ....(298)

Executive Assistant for Board Services and IIW
Gricelda Manalich ....(294)

HUMAN RESOURCES
Director
Luisa Hernandez ....(266)

DATABASE ADMINISTRATION
Corporate Director
Jim Lankford ....(214)

INTERNATIONAL INSTITUTE OF WELDING
Information ....(294)

Provides liaison activities involving other professional societies and standards organizations, nationally and internationally.

GOVERNMENT LIAISON SERVICES
Hugh K. Webster
Webster, Chamberlain & Bean
Washington, D.C.
(202) 466-2976
FAX (202) 835-0243

Identifies sources of funding for welding education and research and development. Monitors legislative and regulatory issues important to the industry.

WELDING EQUIPMENT MANUFACTURERS COMMITTEE
Mary Ellen Mills ....(444)

WELDING INDUSTRY NETWORK (WIN)
Mary Ellen Mills ....(444)

CONVENTION & EXPOSITIONS
Exhibiting Information .... (242, 295)

Managing Director of Convention Sales
Jeff Weber ....(246)

Director of Convention & Expositions
John Ospina ....(462)

Organizes the week-long annual AWS International Welding and Fabricating Exposition and Convention. Regulates space assignments, registration materials, and other Expo activities.

PUBLICATION SERVICES
Department Information ....(275)
Director
Andrew Cullison ....(249)

WELDING JOURNAL
Publisher
Jeff Weber ....(246)

Editor/Editorial Director
Andrew Cullison ....(249)

National Sales Director
Rob Saltzstein ....(243)

WELDING HANDBOOK
Welding Handbook Editor
Annette O'Brien ....(303)

Publishes AWS's monthly magazine, the *Welding Journal*, which provides information on the state of the welding industry, its technology, and Society activities. Publishes *Inspection Trends*, the *Welding Handbook*, and books on general welding subjects.

MARKETING
Corporate Director
Bob Bishopric ....(213)

Plans and coordinates marketing of AWS products and services.

MARKETING COMMUNICATIONS
Senior Manager
George Leposky ....(416)

Manager
Amy Nathan ....(308)

MARKET RESEARCH AND DEVELOPMENT
Corporate Director
Debrah C. Weir ....(482)

Investigates and/or proposes new products and services. Researches effectiveness of existing programs.

MEMBER SERVICES
Department Information ....(480)

Associate Executive Director
Cassie R. Burrell ....(253)

Director
Rhenda A. Mayo ....(260)

Serves as a liaison between Section members and AWS headquarters. Informs members about AWS benefits and other activities of interest.

EDUCATIONAL PRODUCT DEVELOPMENT
Director
Christopher B. Pollock ....(219)

Information on education products, projects, and programs. Responsible for the S.E.N.S.E. program for welding education, and dissemination of training and education information on the Web.

CONFERENCES & SEMINARS
Director
Giselle I. Hufsey ....(278)

Responsible for national and local conferences/exhibitions and seminars on industry topics ranging from the basics to the leading edge of technology. Organizes CWI, SCWI, and other seminars designed for preparation for certification.

CERTIFICATION OPERATIONS
Managing Director
Wendy S. Reeve ....(215)

Director
Terry Perez ....(470)

Information and application materials on certifying welders, welding inspectors, and educators. ....(273)

INTERNATIONAL BUSINESS DEVELOPMENT
Director
Walter Herrera ....(475)

AWS AWARDS, FELLOWS, AND COUNSELORS
Managing Director
Wendy S. Reeve ....(215)

Coordinates AWS awards and AWS Fellow and Counselor nominees.

TECHNICAL SERVICES
Department Information ....(340)

Andrew R. Davis ....(466)
Director Technical Operations and International Standards Development, Welding in Marine Construction, Inspection, Mechanical Testing of Welds

Stephen P. Hedrick ....(305)
Safety and Health Manager, Metric Practices, Friction Welding

Engineers
John L. Gayler ....(472)
Structural Welding, Personnel and Facilities Qualification

Rakesh Gupta ....(301)
Filler Metals and Allied Materials, International Filler Metals, Instrumentation for Welding, Sheet Metal Welding

Harold P. Ellison ....(299)
Resistance Welding, High-Energy Beam Welding and Cutting, Oxyfuel Gas Welding & Cutting, Automotive Welding, Aircraft and Aerospace

Peter Howe ....(309)
Arc Welding & Cutting, Piping & Tubing, Machinery and Equipment, Robotics and Automatic Welding, Food Processing Equipment

Cynthia Jenney ....(304)
Definitions & Symbols, Brazing & Soldering, Filler Metals for Brazing and Braze Welding, Technical Editing

Technical Publications
Senior Manager
Rosalinda O'Neill ....(451)

AWS publishes more than 160 volumes of material, including standards that are used throughout the industry.

With regard to technical inquiries, oral opinions on AWS standards may be rendered. However, such opinions represent only the personal opinions of the particular individuals giving them. These individuals do not speak on behalf of AWS, nor do these oral opinions constitute official or unofficial opinions or interpretations of AWS. In addition, oral opinions are informal and should not be used as a substitute for an official interpretation.

WEB SITE ADMINISTRATION
Director
Keith Thompson ....(414)

Nominees for National Office

Only Sustaining Members, Members, Honorary Members, Life Members, or Retired Members who have been members for a period of at least three years shall be eligible for election as a Director or National Officer.

It is the duty of the National Nominating Committee to nominate candidates for national office. The committee shall hold an open meeting, preferably at the Annual Meeting, at which members may appear to present and discuss the eligibility of all candidates.

To be considered a candidate for positions of President, Vice President, Treasurer, or Director-at-Large, the following qualifications and conditions apply:

President: To be eligible to hold the office of President, an individual must have served as a Vice President for at least one year.

Vice President: To be eligible to hold the office of Vice President, an individual must have served at least one year as a Director, other than Executive Director and Secretary.

Treasurer: To be eligible to hold the office of Treasurer, an individual must be a member of the Society, other than a Student Member, must be frequently available to the National Office, and should be of executive status in business or industry with experience in financial affairs.

Director-at-Large: To be eligible for election as a Director-at-Large, an individual shall previously have held office as Chairman of a Section; as Chairman or Vice Chairman of a standing, technical or special committee of the Society; or as District Director.

Interested parties are to send a letter stating which particular office they are seeking, including a statement of qualifications, their willingness and ability to serve if nominated and elected, and 20 copies of their biographical sketch.

This material should be sent to Ernest D. Levert, Chairman, National Nominating Committee, American Welding Society, 550 NW LeJeune Rd., Miami, FL 33126.

The next meeting of the National Nominating Committee is currently scheduled for April 2004. The term of office for candidates nominated at this meeting will commence June 1, 2005. ♦

Honorary-Meritorious Awards

The Honorary-Meritorious Awards Committee has the duty to make recommendations regarding nominees presented for Honorary Membership, National Meritorious Certificate, William Irrgang Memorial, and the George E. Willis Awards. These awards are presented in conjunction with the AWS Exposition and Convention held each spring. The descriptions of these awards follow, and the submission deadline for consideration is July 1 prior to the year of presentation. All candidate material should be sent to the attention of John J. McLaughlin, Secretary, Honorary-Meritorious Awards Committee, 550 NW LeJeune Rd., Miami, FL 33126.

National Meritorious Certificate Award: This award is given in recognition of the candidate's counsel, loyalty, and devotion to the affairs of the Society, assistance in promoting cordial relations with industry and other organizations, and for the contribution of time and effort on behalf of the Society.

William Irrgang Memorial Award: This award is administered by the American Welding Society and sponsored by The Lincoln Electric Co. to honor the late William Irrgang. It is awarded each year to the individual who has done the most to enhance the American Welding Society's goal of advancing the science and technology of welding over the past five-year period.

George E. Willis Award: This award is administered by the American Welding Society and sponsored by The Lincoln Electric Co. to honor George E. Willis. It is awarded each year to an individual for promoting the advancement of welding internationally by fostering cooperative participation in areas such as technology transfer, standards rationalization, and promotion of industrial goodwill.

International Meritorious Certificate Award: This award is given in recognition of the candidate's significant contributions to the worldwide welding industry. This award should reflect "Service to the International Welding Community" in the broadest terms. The awardee is not required to be a member of the American Welding Society. Multiple awards can be given per year as the situation dictates. The award consists of a certificate to be presented at the award's luncheon or at another time as appropriate in conjunction with the AWS President's travel itinerary, and, if appropriate, a one-year membership to AWS.

Honorary Membership Award: An Honorary Member shall be a person of acknowledged eminence in the welding profession, or who is accredited with exceptional accomplishments in the development of the welding art, upon whom the American Welding Society sees fit to confer an honorary distinction. An Honorary Member shall have full rights of membership. ♦

TELEWELD
FAX: (305) 443-5951

PUBLICATION SALES & ORDERS
Global Engineering Documents
(800) 854-7179 or (303) 397-7956

REPRINTS
To order quality custom reprints, contact Claudia Stachowiak at FosteReprints at (866) 879-9144 ext. 121

It is the intent of the American Welding Society to build the Society to the highest quality standards possible. We welcome any suggestions you may have.

Please contact any of the staff listed on the previous page or AWS President Thomas M. Mustaleski, BWXT Y-12 LLC, P.O. Box 2009, Oak Ridge, TN 37831-8096.

AWS MISSION STATEMENT

The mission of the American Welding Society is to provide quality products and services to its members and the industry that will advance the science, technology, and application of materials joining throughout the world.

AWS FOUNDATION, INC.
550 NW LeJeune Rd.
Miami, FL 33126
(305) 445-6628
(800) 443-9353, ext. 293
Or e-mail: *bobw@aws.org*
General Information
(800) 443-9353, ext. 689

Chairman, Board of Trustees
Ronald C. Pierce

Executive Director
Ray W. Shook

Director of Development
Robert B. Witherell

The AWS Foundation is a not-for-profit corporation established to provide support for educational and scientific endeavors of the American Welding Society. Information on gift-giving programs is available upon request.

2004 Catalog Presents Miller's Full Line

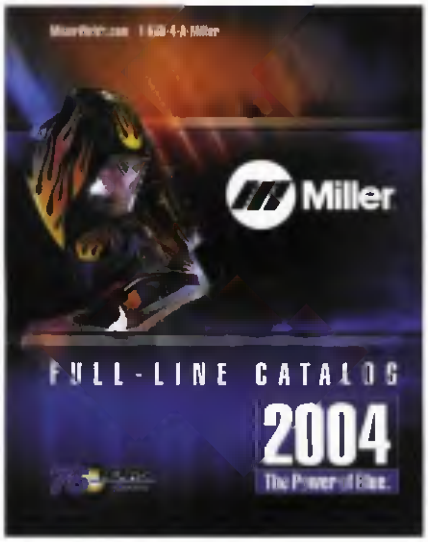

The company's 84-page, full-color 2004 catalog includes its full line of welding and plasma arc cutting products with specifications and suggested accessories. A glossary of welding terminology is included.

Miller Electric Mfg. Co. 114
P.O. Box 100, Lithonia, GA 30058

Design Guides Cover Steel Construction Topics

A series of guides on steel construction topics for architects and engineers has been published by the American Institute of Steel Construction (AISC). The guides are available for purchase or download from *www.aisc.org* or by calling AISC at (800) 644-2400.

Brochure Features 3-D Laser Beam Cutting

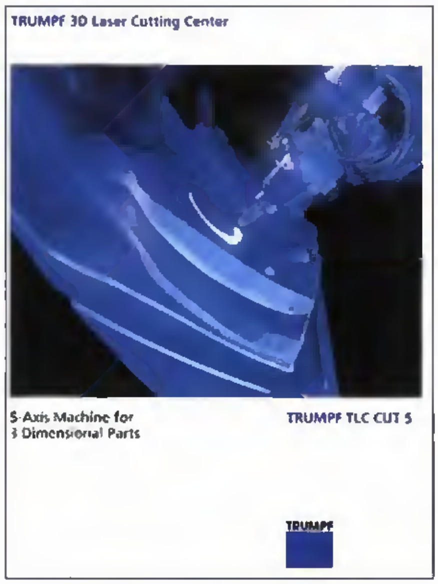

A full-color, four-page brochure for the TLC CUT 5 describes the five-axis progammed laser beam cutting center. The three-dimensional cutting system is available with CO_2 lasers from 2000 to 3200 Watts.

Trumpf Inc. 115
47711 Clipper St., Plymouth, MI 48170

Standard for Avoiding Refinery Piping Cracks Published

NACE Standard RP0403-2003, *Avoiding Caustic Stress Corrosion of Carbon Steel Refinery Equipment and Piping*, has been released. This standard provides guidance to those designing, fabricating, and/or maintaining carbon steel equipment and piping that are exposed to caustic environments. The publication includes the "Caustic Soda Service Chart." The price is $33 list, $25 for NACE members. It can be purchased at *www.nace.org* or (281) 228-6223.

Brochure Describes Storage Boxes for Pickup Trucks

A six-page color brochure features the Rollerbox™ line of utility storage boxes for pickup trucks. The diamond plate aluminum units are mounted on rails via the truck's stake pockets, allowing them to slide from cab to tailgate and back as needed.

Slide Systems 116
125 Rasbach St., Canastota, NY 13032

Textbook Introduces Welding, European-Style

The 200-page paperback textbook,

Welding Processes Handbook by Klas Weman, introduces the student or novice welder to the major welding processes. The book covers requirements referred to in European standards, and can be used as a textbook for the combined courses of the European Federation of Welding, Joining and Cutting and the International Institute of Welding. Price is $70 (available online from *www.woodhead-publishing.com*).

NEWS OF THE INDUSTRY

— *continued from page 12*

ager, directs the office's operations. Technical sales staff will provide sales, service, and support for all MKS products in China.

■ American Torch Tip Co., Bradenton, Fla., recently invested $1 million in new equipment. The state-of-the-art CNC machines will be used to produce some of the more than 16,000 plasma, laser, GMAW, GTAW, thermal spray, oxyfuel, and multiuse replacement parts the company sells for use on torches, guns, and machines for welding, cutting, and metal treating.

■ Wall Colmonoy, Madison Heights, Mich., is celebrating its 65th year of business. The company was founded in 1938 under the trade name Colmonoy® by metallurgists Norman Cole and Walter Edmonds. Soon after, A. F. Wall, owner of a large industrial gas company, purchased the firm, named it Wall Colmonoy Corp., and moved the operation from California to Detroit. Today Wall Colmonoy manufactures nickel-based hard-surfacing alloys and brazing filler metals, and operates five contract processing facilities across the United States and Europe.

■ The U.S. Navy recently awarded Northrop Grumman's Ship Systems sector a $419 million contract to build an *Arleigh Burke* class Aegis-guided missile destroyer. The destroyer is the third of a four-ship multiyear procurement contract awarded to Ship Systems in September 2002. The contract includes an opportunity for a fifth ship, for a total potential contract value of more than $2 billion.

NEW PRODUCTS

— *continued from page 23*

bevel and face, or bevel and bore, the pipe. Pipes from 1.575-in. I.D. to 8.625-in. O.D. can be handled.

ESCO Tool 111
P.O. Box 530, Medfield, MA 02052

Carbide Burrs Available in Specialized Shapes

The company's carbide burrs are produced in a wide variety of shapes and sizes for weld preparation, metal removal, deburring, creating radii, etc. They are available in standard, double, nonferrous, and heavy-duty cuts, with ⅛-in. and ¼-in. shanks.

Rex-Cut Products, Inc. 112
P.O. Box 2109, Fall River, MA 02722

Helmet Features 30% Larger Window, More Sensors

Big Window Elite™ autodarkening welding helmets have a 30% larger window than standard helmets. The helmets feature four independent arc sensors for good response to low-amperage and out-of-position welding. Their twin replaceable, solar-assisted lithium batteries run for 3000 hours.

Miller Electric Mfg. Co. 113
P.O. Box 100, Lithonia, GA 30058

COMING EVENTS

— *continued from page 50*

Shielded Metal Arc Welding of 2-In. Pipe in the 6G Position — Uphill. Hobart Institute of Welding Technology, Troy, Ohio. This course is designed to develop welding skills necessary to produce quality multipass welds on 2-in.-diameter, schedule 160 mild steel pipe (0.436-in. wall thickness) in the 6G position using E6010 and E7018 electrodes. For further information, contact: Hobart Institute of Welding Technology, 400 Trade Square East, Troy, OH 45373, (800) 332-9448, FAX: (937) 332-5200; *www.welding.org*.

2004 Motor Sports Welding School. Classes are scheduled at Lincoln Electric headquarters in Cleveland, Ohio. For more information and a complete schedule, contact: Lincoln Electric Motor Sports Welding School, 22801 St. Clair Ave., Cleveland, OH 44117, (216) 383-2461, FAX: (216) 383-8088, e-mail: *lori_bollas@lincolnelectric.com*; *www.lincolnelectric.com*.

Boiler and Pressure Vessel Inspectors Training Courses and Seminars. Courses and seminars cover such topics as ASME Code Sections I, IV, V, VIII (Division 1), IX, and B31.1; Writing Welding Procedures; Repairing Pressure Relief Valves; Understanding How Boilers and Pressure Vessels Are Constructed and Inspected; and more. To obtain a 2004 schedule of training courses and seminars conducted by the National Board of Boiler and Pressure Vessel Inspectors at its Training and Conference Center in Columbus, Ohio, contact: Richard McGuire, Manager of Training, (614) 888-8320, e-mail: *rmcguire@nationalboard.org*; *www.nationalboard.org*.

Welding Skills Training Courses. Courses include weldability of ferrous and nonferrous metals, arc welding inspection and quality control, preparation for recertification of CWIs, and others. For a complete 2004 schedule, contact: Hobart Institute of Welding Technology, 400 Trade Square E., Troy, OH 45373, (800) 332-9448 or, outside the U.S., (937) 332-5000, FAX: (937) 332-5200; *www.welding.org*.

Structural Welding: Design and Specification Seminars. Conducted by the Steel Structures Technology Center (SSTC). For 2004 schedule and locations, contact: SSTC, (248) 344-2910, FAX: (248) 344-2911; *www.steelstructures.com*.

RED HOT Products

Alpha Automatic MIG Guns

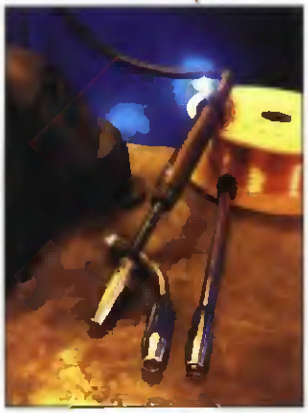

Circle No. 120

ABICOR Binzel introduces the newest member to their line of quality MIG-Gun products – the ALPHA Automatic MIG-Guns. The new "AUT" guns feature the modular swanneck assemblies for fast replacement and interchangeability, incurring less downtime as the result of collision damage or necessary parts replacement. Popular universal rear connector kits available.

ABICOR BINZEL Corp.
650 Research Dr., Ste 110
Fredrick, MD 21703-8619
(800) 542-4867
FAX: (301) 846-4497

Introducing CenterLine® Resistance Welding Product Guide - Version 7.0 from CenterLine (Windsor) Limited

Circle No. 124

"CenterLines Resistance Welding Product Guide — Version 7.0" outlines our full range of cold formed electrodes, patented weld nut electrodes and consumables. CenterLine provides cost effective solutions for virtually every resistance welding requirement. This product guide is available at www.cntrline.com; by e-mail at info@cntrline.com; or by calling us toll-free at 800-249-6886.

Centerline Windsor Limited
595 Morton Drive
Windsor, ONT
Canada, N9J 3T9
(800) 249-6886
FAX: (519) 734-0016

Capacitor Discharge Welders

Circle No. 121

Aelectronic Bonding Inc. Celebrating 20 years, makes capacitor discharge welders utilizing resistance, pulse arc and fusion technologies. These inexpensive welders are used in the jewelry, dental, medical, auto and electronics industries. Applications from butt-welding wires, thermocouple leads, stud, optical frames, jewelry repairs, cathode de-burring of similar and dissimilar metals, tack weld positioning amongst many. ABI 888-494-2663. Visit our website at www.abiusa.net.

Aelectronic Bonding Inc.
1655 Elmwood Ave., Bldg #7
Cranston, RI 02910
(401) 461-4140
FAX: (401) 461-5250

General-Purpose TIG Filter with Sensitivity and Grind Mode

Super Singles™ 240

ArcOne's NEW Super Singles 240 auto-darkening filter is the first 2x4 filter specifically designed for Tig welding with features such as sensitivity and delay only available in more costly products. An additional grinding mode negates the need for a more costly flip front helmet. The Super Singles comes with a dark state of 10.5 and a light state of 2.5, is completely Solar powered so there are never any batteries to change, water and dust resistant, and up to shade 16 UV/IR protection. Available in the Vision and Hawk helmet.

Circle No. 122

Cored Welding Wire Guide

Circle No. 126

This brochure shows Cor-Met's wide offerings of sizes and alloys in Cored Welding Wires, Stick Electrodes and TIG wires (both spools and cut lengths). It includes descriptive, classification and physical data on low alloy steels, cobalt-base and nickel-base alloys, tool and stainless steels, and hard-facing alloys. Alloys are available for resistance to high temperatures, erosion and corrosion; cored wires, electrodes and TIG and MIG solid alloy steels; cast iron and stainless steel.

Cor-Met Inc.
12500 E. Grand River
Brighton, MI 48116
(800) 848-2719
FAX: (810) 227-9266
Website: www.cor-met.com

Atlas Model 500 Welding Positioner

Circle No. 123

The Atlas Welding Positioner is designed for strength and stability in handling and welding loads of up to 500 pounds when properly balanced in the horizontal position. • 1/4 hp DC motor • 400 amp welding ground circuit • Dynamic Braking rapidly stops table rotation • Full speed advanced for stitch welding • 14" x 5/8" thick rotary table • On/off foot switch • Front panel speed and rotation controls

Atlas Welding Accessories
Troy, MI 48099
(800) 962-9353
FAX: (248) 588-3720
Email: atlaswelding@ameritech.net • www.atlasweld.com

WeldOffice® Software

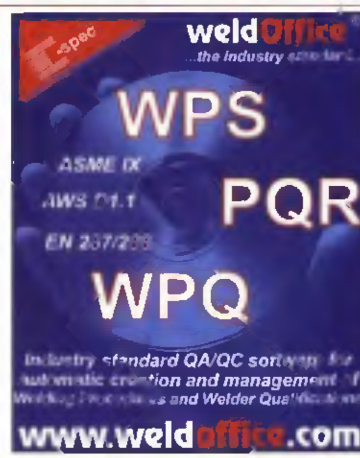

Circle No. 127

Automatic creation and management of welding procedures, welder qualifications and NDE reports. ASME IX, AWS D1.1 and EN code validation supported by knowledgeable welding engineers and code committee members. Complete solutions for QA/QC management of plants, fabrication shops and construction projects.

C-spec
P.O. Box 27604
Concord, CA 94527
(888) 673-9777 toll free
FAX:(925) 930-8223
E-Mail: software@cspec.com
Website: www.cspec.com

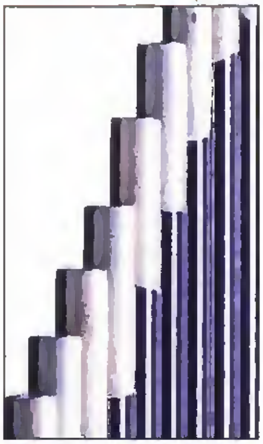

Circle No. 128

Tri-Mix™ Tungsten

Diamond Ground Products, Inc., offers Tri-Mix™ tungsten. This premium quality tungsten material is non-radioactive and offers superior performance in TIG and plasma welding applications. It is blended with three rare earth elements that scientifically balance the migration and evaporation rates to extend service life with increased number of arc starts and fewer misfires. Its lower work function requires less energy to start and also runs cooler. Free samples available on request.

Diamond Ground Products, Inc.
2550 Azurite Circle
Newbury Park, CA 91320
(805) 498-3837
FAX: (805) 498-9347
E-mail: sales@diamondground.com
Website: www.diamondground.com

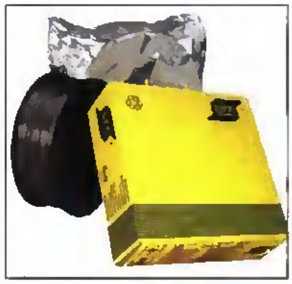

Circle No. 132

New & Improved Stainless Cored Wire

ESAB's newly reformulated Shield-Bright X-tra, flat & horizontal stainless cored wire has been re-engineered to provide the latest developments in slag system technology. The product's arc characteristics have been enhanced to include better feed ability, improved arc direction, and more acceptable bead appearance. These modifications add up to improve the overall performance characteristics designed to meet or exceed competitive products worldwide.

ESAB Welding &
Cutting Products
Florence, SC 29501-0545
(800) ESAB-123
Website: www.esabna.com

Circle No. 129

Divers Academy International Offers A Career That Will Take You Places.

Take your topside welding skills underwater and go places. Outstanding career opportunities await graduates of Divers Academy International, known world wide for training commercial divers and underwater welders to work on some of the worlds largest bridges, nuclear power plants and oilrigs. Our state of the art commercial diving program includes, underwater welding, non-destructive testing, HAZWOPER and remotely operated vehicle training. Divers Academy International is federally accredited and offers financial assistance if qualified, a student housing program and a career placement program. Our admissions coordinators are available to personally assist you.

Divers Academy International
2500 Broadway
Camden, NJ 08104
(800) 238-DIVE
FAX: (856) 541-4355
E-mail: diver@diversacademy.com

Circle No. 133

Aristo Systems Combine "Intelligence" and Power

Ideal for a wide range of industrial welding needs, including shipbuilding, mobile machinery, offshore construction, automotive, power generation, civil construction and more. Modular in nature, Aristo Systems can be "built" with ideal components to meet demands of your operation – and – they are upgradable. Choose from AristoMig, AristoTig or AristoArc in the 400 or 500 series.

ESAB Welding &
Cutting Products
Florence, SC 29501-0545
(800) ESAB-123
Website: www.esabna.com

Circle No. 130

Plasma Power Packed

From the plasma leaders, ESAB's PowerCut Plasmarc cutting packages feature the revolutionary PT-32EH torch for higher production rates with lower costs. These lightweight machines have super-sturdy composite cases for roughest use. Models include: PowerCut 875 (cuts 7/8", severs 1-1/4"); PowerCut 1250 (cuts 1-1/4", severs 1-1/2"), PowerCut 1500 (cuts 1-1/2", severs 1-3/4").

ESAB Welding &
Cutting Products
Florence, SC 29501
(800) ESAB-123
Website: www.esabna.com

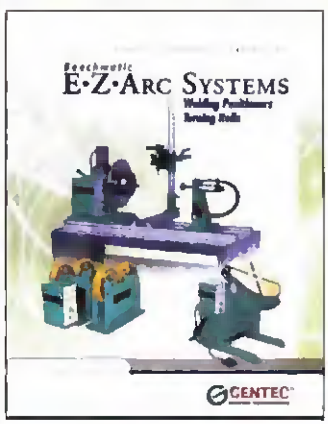

Circle No. 134

EZ ARC Welding Systems

GENTEC offers affordable solutions to work station design. The EZ ARC product line includes complete welding workstations that accommodate a wide variety of part configurations. Components are attached to base rail system fixture parts for optimum results on a repetitive basis. Automation may be achieved using optional Sequencer. The product line also includes Welding Positioners and Turning Rolls.

Genstar Technologies Co.
4525 Edison Ave.
Chino, CA 91710
(909) 606-2726
E-Mail: sales@genstartech.com
Website: www.genstartech.com

Circle No. 131

OXWELD Gas Products Have Lifetime Warranty

Buy an OXWELD gas torch or regulator, and you'll be making a lifetime investment. All OXWELD gas regulators, welding and cutting torches and cutting attachments, as well as complete welding and cutting outfits such as the TradeMaster, are covered by a lifetime warranty. Plus, OXWELD gas equipment leads the industry in quality and safety, with many unique built-in safety features.

ESAB Welding &
Cutting Products
Florence, SC 29501-0545
(800) ESAB-123
Website: www.esabna.com

Circle No. 135

Plate Bevelers

The Bevel-Mill plate bevelers produce fast, clean bevels for weld preparation. The machines use a milling type cutter with inexpensive standard carbide inserts. Depth of cut adjustable up to 13/16". Variable angle from 15 to 45 degrees. Lightweight and portable with new added power. Several models to choose from including floor models and bench models for ultra precision bevels.

Heck Industries, Inc.
P.O. Box 425
Hartland, MI 48353
(810) 632-5400
FAX: (810) 632-6640
Website: www.heckind.net

Custom Made Stringers For Spiral Staircases: Rolled/Formed/Fabricated To Your Specifications

Circle No. 136

Hodgson Custom Rolling Inc. is one of North America's largest plate rolling, forming, section rolling and fabricating companies, servicing numerous industries including the energy sectors of hydro, petro chemical, atomic, gas, oil, wind, etc. in addition to those in heavy manufacturing, steel pulp & paper, mining , marine forestry, etc. Hodgson has the expertise to roll curved structural sections into a wide range of shapes and sizes (angle, wide flange beam, channel, bar, tee section, pipe, tubing, rail, etc.), specializing in custom made Spiral Staircase Stringers.

HODGSON CUSTOM ROLLING INC.
5580 Kalar Road, Niagara Falls, ON
CANADA L2H 3L1
(800) 263-2547 FAX: (905) 356-6025
E-Mail: hodgson@hodgson.on.ca

Power MIG™ 300

Circle No. 140

The Power MIG 300–a single phase, multi-process, synergic wire feeder welding package for the professional welder. This ready-to-weld package is unbeatable when it comes to superior multi-process welding. The synergic design, traditionally only available in more expensive welders, gives you ultimate control over the arc by automatically aligning wire feed speed and voltage. It also offers top quality aluminum welds with push-pull wire feed capability, not usually available in competitive models. True MIG pulsing and Pulse-on-Pulse™ capabilities ensure that superior feeding is matched by high quality arc performance.

The Lincoln Electric Company
22801 St. Clair Ave.
Cleveland, Ohio 44117
(216) 481-8100
Website: www.lincolnelectric.com

Pro-Cut 55

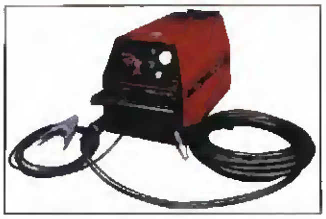

Circle No. 137

The Pro-Cut 55 plasma cutter packs the highest cutting performance in the industry into a portable, 55 lb. unit. 60 amps of power allow cutting up to 3/4" while the PCT 80 torch and VORTECH™ technology consumables provide speed and capacity. The unit's power source incorporates "dual winding technology" which makes the Pro-Cut 55 the easiest to use in the industry. Arc transfer is faster and dross levels at the start are lower, and gouging performance is unparalleled for a unit this size. Patented full-flow cooling delivers the longest consumable life in the industry.

The Lincoln Electric Company
22801 St. Clair Ave.
Cleveland, Ohio 44117
(216) 481-8100
Website: www.lincolnelectric.com

New Oxy-Acetylene — Hose Reels Industrial Design, Priced To Sell!

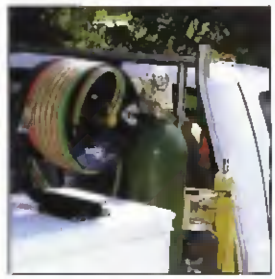

Circle No. 141

New Oxy-Acetylene Hose Reels from Rapid Reel make hose handling easy. With all-steel construction, powder-coat paint, and top-grade components, you won't find a higher quality hose reel on the market today. Mounting options available for trucks, flatbeds, walls, carts, and more. 50' to 300' hose capacity. Priced from $120 to $345 MSRP. Contact Rapid Reel for more information.

Reel Quick, Inc.
P.O. Box 22640
Lincoln, NE 68542-2640
800-523-4321
FAX: 800-548-3203
Website: www.RapidReel.com

Invertec® V205-T AC/DC

Circle No. 138

Get precise TIG welding wherever you need it with the Invertec V205-T AC/DC TIG Welder. This rugged unit is lightweight (just 33 lbs.) and portable, making it ideal for shop or field. Full-featured TIG controls give you command of AC or DC output on a wide variety of material types and thicknesses. It stick welds, too. Lincoln's advanced inverter technology optimizes arc performance, while adjustable AC frequency lets you focus the arc for critical applications. The 115/230V auto-reconnect and line voltage compensation add flexibility.

The Lincoln Electric Company
22801 St. Clair Ave.
Cleveland, OH 44117
(216) 481-8100
Website: www.lincolnelectric.com

Ready Welder II – Worlds Best Selling Spool Gun!

Circle No. 142

An incredibly powerful MIG welder offering solid performance, quality built and totally portable. Using batteries the RWII can single pass 1/2" steel, aluminum or stainless metals. When connected to a welding machine, the RWII is the best balanced and most versatile spool gun–period. Ideal welding solution for maintenance, repair, industrial, recreational, agricultural and construction...weld virtually anywhere!

Ready Welder Corporation
1891 N. Gaffey Street #A
San Pedro, CA 90731
(800) 935-3644
FAX: (310) 832-9958
Website: www.readywelder.com

Precision TIG™ 275

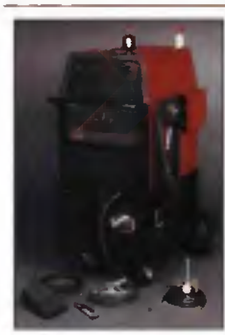

Circle No. 139

This is the one you have been waiting for–The Precision TIG 275 is the mainstay in the next generation of the Square Wave family of machines. Patent-pending Micro-Start™ Technology provides unrivaled and revolutionary arc performance ideal for critical AC or DC welding in fabrication, aerospace, production, motorsports, and vocational applications. Available in both machine-only models or in a convenient Ready-To-Weld Package, the Precision TIG 275 combines both outstanding value-added features, with precision arc performance to meet all of your welding needs.

The Lincoln Electric Company
22801 St. Clair Ave.
Cleveland, Ohio 44117
(216) 481-8100
Website: www.lincolnelectric.com

Welding Electrodes Catalog

Circle No. 143

Select-Arc, Inc. has issued a new 40-page catalog which describes the company's complete line of tubular welding electrode products. Welding applications, characteristics, classifications, diameters, positions, shielding gases, typical mechanical properties and typical deposit compositions are provided for each electrode product.

Select-Arc, Inc.
P. O. Box 259
Fort Loramie, OH 45845-0259
(800) 341-5215
FAX: (937) 295-5217
Website: www.select-arc.com

Improved Plasma Cutting

Circle No. 144

Contaminants in your compressed air system — dust, scale, condensed moisture and oil mist — seriously affect the quality of your plasma cuts. Installation of a Motor Guard Sub-Micronic Air Filter on your plasma machine will effectively remove these contaminants; eliminating arc-sputter and producing cleaner, faster, smoother cuts. Motor Guard Filters virtually pay for themselves by reducing wear and prolonging the life of expensive tips and electrodes. Ask your welding equipment supplier for a Motor Guard Filter today.

Motor Guard Corporation
580 Carnegie Street
Manteca, CA 95337
(800) 227-2822
FAX: (800) 237-7581
Website: www.motorguard.com

Trailing Shield Kit

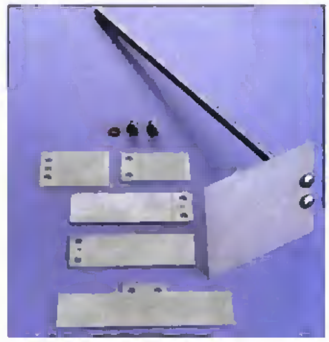

Circle No. 148

The Weld Hugger Trailing Shield kit is an inert cover gas system designed to uniformly flow cover gas over and behind the weld pool to reduce part oxidation and discolorization. The kit's all stainless steel nozzles and manifold tube can be bent to conform to the geometry of many parts. The complete kit price is $249.95. To order, call toll-free or visit our website.

Weld Hugger LLC
7201 West Oakland St.
Chandler, AZ 85226-2434
(877) 935-3447
FAX: (480) 940-9366
Website: www.weldhugger.com

Thermal Arc®, Launches New Portable Inverter

Circle No. 145

Thermal Arc, is fielding a new team of inverter arc welding power supplies geared especially for portable STICK (SMAW), TIG (GTAW) and MULTI-PROCESS construction and maintenance welding duties. A new, simplified, push button control panel with digital meter is standard on all models. The control panel is weather protected to stand up to on-site rigors associated with construction and maintenance environments. Machine setup is simple with easy to follow graphics that lead operators through the controls to make fast, accurate selections. The new case design allows units to be stacked for convenience and space saving. All units include a Voltage Reduction Device (VRD) that reduces OCV when the power supply is not in use, eliminating the chance of accidental electric shock.

Thermal Arc, A Thermadyne Company
16052 Swingley Ridge Rd, Suite 300
St. Louis, MO 63017
(636) 728-3000
Website: www.thermalarc.com

Fixturing Kits for Welding Offer Many Solutions

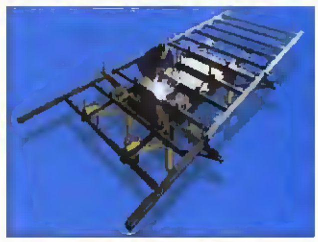

Circle No. 149

The Demmeler modular fixturing system for welding comes with a full range of components to fixture virtually any part. Angles, spacer blocks, clamps, positioning and clamping bolts and a complete family of universal stops can be assembled into a ready-to-use welding fixture in a matter of hours. The five-sided table has surfaces that are flat and square 0.0004"/ft and bores that are located +/-0.001". More than 30 different kits are offered.

Bluco Corporation
509 Weston Ridge Dr.
Naperville, IL 60563
(800) 535-0135
Website: www.bluco.com

New CUTMASTER' 1 Series Plasma Cutting Systems

Circle No. 146

Thermal Dynamics, has introduced a new family of CUTMASTER' 1Series air plasma cutting systems, featuring the company's revolutionary 1Torch' plasma torch and patent pending ATC' (Advanced Torch Connector) quick disconnect. All 1Series machines take advantage of the 1Torch start (non-HF) capability that eliminates electronic interference. Each system is suitable for cutting materials including aluminum, stainless steel, and mild steel in applications ranging from construction to fabrication to manufacturing.

Thermal Dynamics
A Thermadyne Company
16052 Swingley Ridge Road, Suite 300
St. Louis, MO 63017
(636) 728-3000
Website: www.thermal-dynamics.com

Technical Books

Circle No. 150

American Technical Publishers is America's only employee-owned career and technical book publisher. Catalog covers books for the metals, electrical and building trades, written by and for trades people.

American Technical Publishers, Inc.
1155 W. 175th Street
Homewood, IL 60430
(800) 323-3471
FAX: (708) 957-1101
Website: www.go2atp.com

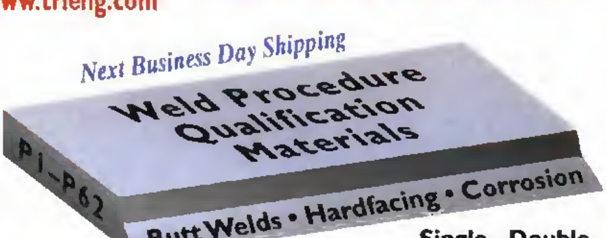

Circle No. 147

New 4ft Table Blaster Incorporates All the Industry's Best Features

Circle No. 151

Viking Blast & Wash Systems announces the release of its newest evolution of the 4-ft airless table blaster, the 48T. The 48T incorporates a wrap-around door feature, and an angle-mounted wheel. Cast chrome/moly plates protect the cabinet from direct impingement while manganese alloy protects the rest of the cabinet. Viking employs more than 25% more standard cleaning capability than competitor models using a 20HP direct drive blast wheel versus competitors' 15HP or less.

Viking Blast & Wash Systems
3810 N. Toben
Wichita, KS 67226
(800) 835-1096
Website: www.vikingcorporation.com

EMPLOYMENT

MFG REPS and SALES REPS

Large manufacturer of industrial gas apparatus and industrial flow control equipment seeks experienced reps calling on welding supply industry. Large protected territories and great commission rates. Forward resume or line card to Fax: **909-612-1927**

AWS JobFind

Post Jobs.
@ Find Jobs.
www.aws.org/jobfind

Job categories for welders, engineers, inspectors, and more than 17 other materials joining industry classifications!

CERTIFICATION/TRAINING

Begin 2004 With REAL Training From Real Educational Services, Inc.

CWI PREPARATORY

Guarantee - Pass or Repeat FREE!

SAT–FRI COURSE (7 DAYS)
EXTRA INSTRUCTION TO GET A HEAD START
Pascagoula, MS Mar. 13–19 Jun. 12–18
Houston, TX Feb. 21–27 May 1–7
Houma, LA Apr. 10–16

MON–FRI COURSE (5 DAYS)
GET READY - FAST-PACED COURSE!
Pascagoula, MS Mar. 15–19 Jun. 14–18
Houston, TX Feb. 23–27 May 3–7
Houma, LA Apr. 12–16

2 WEEK COURSE (10 DAYS)
MORE HANDS-ON/
PRACTICAL APPLICATIONS
Pascagoula, MS Mar. 8–19 Jun. 7–18
Houma, LA Apr. 5–16
(Test follows on Saturday at same facility)

CONTINUE YOUR EDUCATION WITH:

APPLICATIONS OF VISUAL WELDING INSPECTION
Pascagoula, MS Apr. 26–30

FILM INTERPRETATION AND WELDING PROCEDURES
Houston, TX Mar. 29–Apr. 2
Get 40 hours of useful training

MT/PT LEVEL I & II
Pascagoula, MS Feb. 16–19
Houma, LA Mar. 1–4

UT LEVEL I
Pascagoula, MS Mar. 22–26

For our entire class schedule, call or e-mail
1-800-489-2890
or
info@realeducational.com

The AWS Certification Committee

Is seeking the donation of sets of Shop and Erection drawings of high-rise buildings greater than ten stories with Moment Connections including Ordinary Moment Resistant Frame (OMRF) and Special Moment Resistant Frame (SMRF) for use in AWS training and certification activities. Drawings should be in CAD format for reproduction purposes. Written permission for unrestricted reproduction, alteration, and reuse as training and testing material is requested from the owner and others holding intellectual rights.

For further information, contact:
Joseph P. Kane
631-265-3422 (office)
516-658-7571 (cell)
joseph.kane11@verizon.net

BUSINESS FOR SALE

BUSINESS FOR SALE

Established 1983. Make small stored energy welding equipment. Pulse arc, spot resistance and fusion percussion mini stud welder. International markets through distributors, reps and direct sales. Miniature tech joining of similar and dissimilar metals for medical, dental, optical, jewelry, crafts, appliance, auto, aircraft, and electronics industries. Very strong gross profit @84%, before tax earnings @26% and after tax profits of 15%. Strictly confidential, please write:

Business 4 Sale
PO Box 893
E. Greenwich, RI 02818

DON'T FORGET

The March 2004 issue of Welding Journal highlights the AWS Welding Show. This issue has the largest readership of the year. Call now to reserve your advertising space.

Rob Saltzstein 800-443-9353, ext 243
Lea Garrigan 800-443-9353, ext 220

EQUIPMENT TO BUY OR SALE

EQUIPMENT SALES/RENTAL

EQUIPMENT USED

SERVICES

CAREER OPPORTUNITIES

Tregaskiss
WELDING PRODUCTS

We are an international manufacturer of high quality and innovative welding products. Due to growth demands, an opportunity exists on our Sales Team for an exceptional sales professional to join as a

REGIONAL BUSINESS MANAGER

This representative will be based in the PA, NJ area and required to manage and profitably grow our distribution throughout the NY, NJ, PA, MD and VA markets.

The successful candidate will possess the following qualifications:

- A college education or equivalent professional work experience
- Excellent oral, written and presentation skills.
- Experience managing and selling through distribution channels
- Consultative selling skills to various end users segments
- Computer skills and knowledge of Microsoft applications
- Broad welding applications and equipment knowledge and skills, MIG gun sales experience an asset.
- Ability to work in a cohesive team environment
- Time management skills and ability to travel

The Rewards... The successful candidate will join a motivated, focused sales team. The position offers a salary, benefits and commission package that have great potential for personal financial growth.

If you have the initiative, drive and desire to be a part of our team in a progressive growth environment, please forward your resume and salary expectations in confidence to Human Resources by February 14, 2004:

2570 North Talbot Road
Windsor, Ontario N0R 1L0
Fax: 1-800-665-0400
hr@toughgun.com
Please reference job number 01/04

We thank all applicants in advance, and advise that only those candidates under consideration will be contacted. No telephone inquiries or agencies please.

ADVERTISER INDEX

IFC = Inside Front Cover
IBC = Inside Back Cover
OBC = Outside Back Cover
RI = Reader Information Card

SUPPLEMENT TO THE *WELDING JOURNAL*, FEBRUARY 2004
Sponsored by the American Welding Society and the Welding Research Council

An Investigation of Ductility-Dip Cracking in Nickel-Based Weld Metals — Part III

The characteristics of weld-metal grain boundaries associated with elevated-temperature fracture are investigated

M. G. COLLINS, A. J. RAMIREZ, AND J. C. LIPPOLD

ABSTRACT. In Part I of this investigation of ductility-dip cracking (DDC) in nickel-based filler materials, the strain-to-fracture (STF) test (Ref. 1) was used to quantify the DDC susceptibility of two Ni-based filler metals, Filler Metal 52 and Filler Metal 82. Ductility-dip cracking susceptibility was related to the nature of the migrated grain boundaries in these weld metal deposits and the effect of grain boundary "tortuosity" on the mechanical locking of these boundaries at elevated temperature. Part II of this investigation used scanning electron microscopy to examine the DDC fracture surfaces in order to relate fracture mode to temperature, composition, interstitial content (hydrogen), and microstructure. Part III of this investigation uses optical microscopy, high-resolution scanning electron microscopy, and electron backscattered diffraction (EBSD) techniques to further explore the factors that contribute to DDC in Ni-based weld metals. Based on this analysis and the results from Parts I and II of this investigation, a DDC mechanism is described that involves the complex interplay of alloy composition, interstitial and impurity element additions, grain boundary segregation, triple-point grain boundary junctions, grain growth, grain boundary sliding, precipitation, recrystallization, boundary orientation relative to the applied strain, and the contribution of grain boundary misorientation and accumulated local strain. Insight is provided to optimize elevated-temperature ductility in order to avoid DDC in Ni-based weld deposits and other austenitic alloys.

Introduction

From a mechanistic standpoint, relatively little is known or understood about DDC, a solid-state cracking mechanism. Ductility-dip cracking occurs below the effective solidus temperature and separation of grain boundaries has been reported to be characteristic of materials susceptible to DDC (Refs. 2, 3). A number of factors have been reported to contribute to the development of DDC, including specific alloy, impurity, and interstitial element content, segregation, large grain size, grain boundary precipitation, orientation relative to the applied strain, and high levels of weld restraint. The DDC mechanism is still not well understood, nor is the individual effect of these factors. Furthermore, preventive methods for avoiding DDC in highly restrained weldments have proven elusive.

Part I of this investigation (Ref. 4) quantified DDC susceptibility in Filler Metals 52 and 82. Additionally, hydrogen and sulfur additions to the weld metal were evaluated with the STF test and found to increase weld metal DDC susceptibility. Part II of this investigation (Ref. 5) used optical and scanning electron microscopy to study the ductility-dip fracture surfaces, identifying the fracture mode dependence on temperature and microstructure. These two previous studies provided an initial insight into the factors responsible for promoting DDC in highly restrained weld metals. Part III of this investigation uses optical microscopy, high-resolution scanning electron microscopy, and electron backscattered diffraction techniques to further expand on the understanding of the DDC phenomenon. Part III of the investigation has combined the results of the first two parts with the advanced characterization results to provide insight into the mechanism of DDC. The mechanistic aspects of DDC discussed here are thought to apply not only to the Ni-based Filler Metals 52 and 82, but also more broadly to other austenitic alloys, including the austenitic stainless steels.

This investigation has provided further evidence that the Gleeble strain-to-fracture test is an effective, robust test technique for evaluating DDC susceptibility in weld metals. The ability to determine the strain-temperature relationships for DDC as a function of composition has been invaluable for studying elevated-temperature behavior in these alloys.

KEY WORDS

Ductility-Dip Cracking
Nickel-Based Filler Metals
Grain Boundary Characteristics
Strain
Elevated-Temperature Ductility

M. G. COLLINS, A. J. RAMIREZ, and J. C. LIPPOLD are with The Ohio State University, Columbus, Ohio.

Experimental Procedures

Advanced characterization was conducted on STF samples of both Filler Metals 52 and 82. The compositions of these filler metals are provided in Table 1. The STF test techniques and test results are reported in Part I (Ref. 4). In this study, grain boundary characteristics of DDC were investigated in more detail than in Part I.

Strain-to-fracture samples were sectioned and mounted in a conductive phenolic powder for advanced characterization using optical and high-resolution scanning electron microscopy, along with X-ray energy-dispersive spectrometry (EDS) and electron backscattered diffraction (EBSD), also known as orientation image microscopy (OIM™). The samples were polished and then electrolytically etched with 10% chromic acid at 2.5 V for 15–20 s. During polishing, an effort was made to minimize material removal, as many cracks were relatively shallow. The polished and etched samples were examined using a Nikon metallograph, and digital photomicrographs were taken with a Hitachi CCD camera. Additionally, a Philips XL-30 field emission gun (FEG) scanning electron microscope (SEM) was

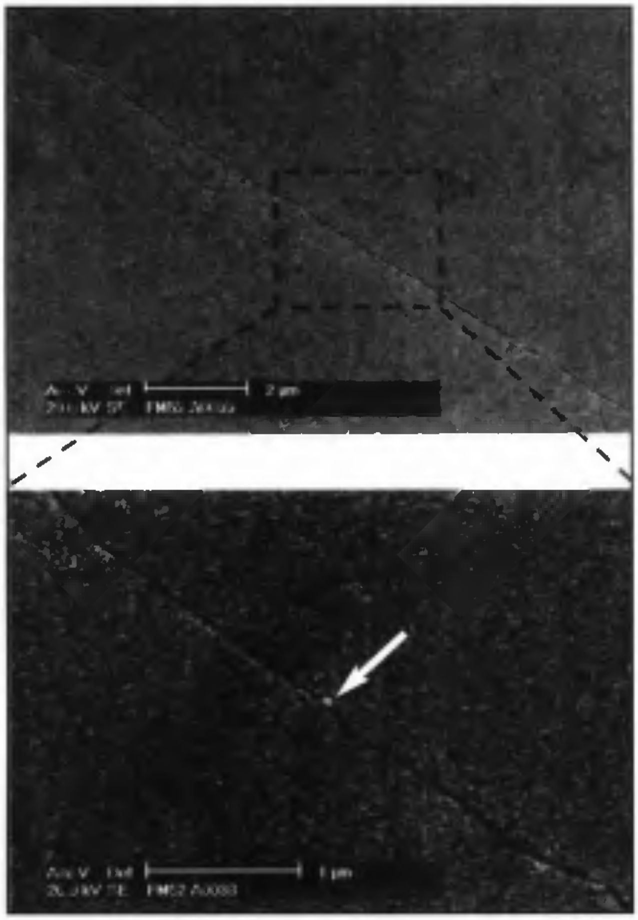

Fig. 1 — Migrated grain boundary in Filler Metal 52 at 986°C and 2.6% strain. (Arrow indicates small particle along boundary.)

Fig. 2 — Precipitation and microsegregation along solidification subgrain boundaries in Filler Metal 52 at 986°C (lower photo reveals boundary migration from "pinning points" at solidification subgrain boundary.)

Table 1 — Chemical Composition of Filler Materials (wt-%)

Element	Filler Metal 52 Heat NX9277	Filler Metal 82 Heat YN6830	Filler Metal 82 Heat YN7355	Filler Metal 82 Heat YB7724
C	0.026	0.04	0.04	0.041
Mn	0.25	2.86	2.75	2.79
Fe	8.88	1.18	0.70	0.90
S	0.0037	0.01	0.002	0.001
Si	0.17	0.12	0.07	0.06
Cu	0.011	0.09	0.07	0.04
Ni	60.12	72.75	72.8	72.98
Al	0.71	N/A	N/A	0.05
Ti	0.50	0.37	0.47	0.45
Cr	29.09	20.1	20.1	19.98
Cb + Ta	0.02	2.3	2.6	2.7
Mo	0.05	N/A	N/A	N/A
P	0.0044	0.007	0.01	0.004
Pb	0.0001	0.004	0.002	0.002
Co		0.05	0.04	0.01

used to analyze the mounted DDC specimens at higher magnifications. The chemical compositions of the precipitates were measured by EDS analysis.

The grain boundary character distribution and local strain distribution were determined on the SEM using EBSD. Electron backscattered diffraction is a widely used technique that collects crystallographic data from a surface with submicron resolution. Because this technique uses the electron beam on an electron microscope, most commonly an SEM, a direct relationship can be established between the microstructure and the crystallographic information (Ref. 6), making it an excellent tool for fracture analysis (Ref. 7). The samples to be used for the EBSD analysis were ground and polished using the same procedure previously described. However, special precautions were taken to minimize the grinding deformation artifacts. After polishing, the samples were lightly electrolytically etched with 10% chromic acid at 1.5 to 2.0 V for 15 s. Electron backscattered diffraction dedicated software, Channel 5™ by HKL Technology, was used for the automated EBSD data acquisition and analysis. The low-angle (1–15 deg) grain boundary distribution was determined based on the EBSD maps. Finally, this low-angle grain boundary information was also used to obtain plastic strain distribution maps in the microstructure (Ref. 8).

Results

Grain Boundary Characterization — SEM

In Part I of this investigation, optical microscopy was used to characterize DDC behavior of Filler Metal 52 and Filler Metal 82. To develop a better understand-

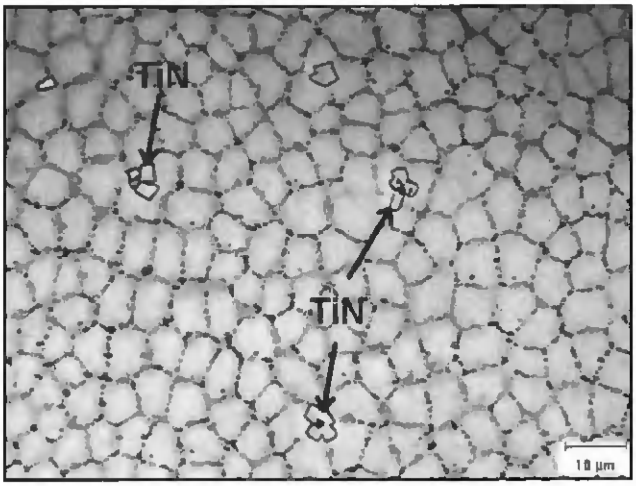

Fig. 3 — Second phases precipitated in the Filler Metal 52 weld metal.

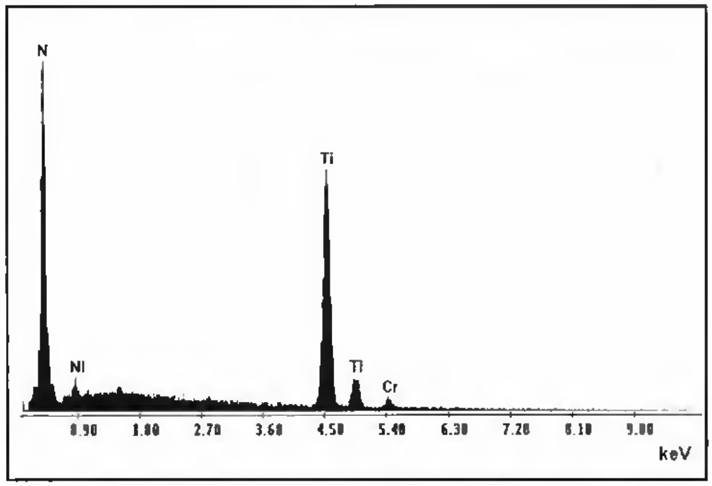

Fig. 4 — Energy-dispersive spectrometry spectra of cuboidal second phases observed in the Filler Metal 52 weld metal.

ing of the factors contributing to DDC, the SEM was used to characterize Filler Metal 52 and Filler Metal 82 grain boundaries at much higher magnifications. It is anticipated that these results, in combination with the metallographic results shown previously in Part I and the fractography analysis presented in Part II of this investigation, would further elucidate the factors contributing to DDC formation.

Filler Metal 52

Migrated grain boundaries in Filler Metal 52 weld deposits exhibit both long/straight and tortuous segments. Under low strain levels, cracking occurred primarily along the straight sections of these boundaries. Examination of the weld-metal microstructure using optical and scanning electron microscopy revealed interdendritic second phases. In addition, clear evidence of grain boundary pinning caused by these interdendritic precipitates was observed. However, these precipitates were not consistently distributed throughout the weld-metal microstructure. Consequently, the regions free of these precipitates underwent more grain boundary migration, resulting in the straight boundaries most susceptible to DDC. Figure 1 illustrates a long, straight migrated grain boundary in a Filler Metal 52 multipass weld. Both the boundary and the microstructure clearly lack any impediments (precipitates or second phases) to "lock" the boundary in place, or to "pin" boundary movement, resulting in uninhibited boundary migration and the consequent grain boundary straightening, grain growth, and increased susceptibility to DDC.

Figure 2 clearly reveals solidification subgrain boundaries, migrated grain boundaries, and DDC along migrated grain boundaries. The solidification subgrain boundaries exhibit both segregation (as revealed by the contrast) and two different types of precipitates, shown in Fig. 3. The large precipitates are cuboidal TiN particles, approximately 5 µm in their largest dimension. Figure 4 shows a typical EDS spectrum for this precipitate, indicating that Ti and N are essentially the only elements present. The small Cr and Ni peaks probably reflect the surrounding matrix. The size and location of these large precipitates suggest they did not form as a result of the weld solidification process. Rather, it appears these particles were transferred into the weld pool from the welding wire. To confirm this, Fig. 5 shows the microstructure of the Filler Metal 52 wire, where even larger TiN particles were observed. The larger size of the precipitates in the welding wire suggests that the nitrides partially dissolved once they were injected into the molten pool. Since the welds were made using the gas tungsten arc welding (GTAW) process with cold wire feed, it is possible for these particles to survive in the molten pool and then become entrapped in the microstructure during weld solidification.

The other precipitates, evident along the solidification subgrain boundaries in Fig. 3, are smaller (less than 1 µm in diameter), but are also rich in Ti and N. Analysis of these particles in the transmission electron microscope verified that they are TiN. Because these smaller precipitates are slightly elongated and perfectly aligned along the solidification subgrain boundaries, it is apparent that their formation is directly related with solidification segregation. It is hypothesized that these particles are the result of a eutectic reaction at the end of solidification, or may form in the solid state on cooling from the solidification range or during reheating in the multipass weld. Further study is necessary to clarify the nature of these particles.

Initially, these precipitates were thought to be MC carbides, Laves phase, or a mixture, which precipitate at the end of the solidification as a result of eutectic reactions (Ref. 9). Depending on the chemical composition of the alloy, MC carbide precipitation or MC carbide plus Laves phase may form in Ni-based weld metals, as proposed by DuPont and coworkers (Ref. 9). Figure 6 shows the schematic solidification path for an Nb-bearing Ni-based alloy, which leads to the formation of MC carbides (NbC in this case) and possibly Laves phases eutectic constituents during solidification. Compositionally, Laves phase can form from several elements in the basic form [$(Ni, Fe, Co)_2(Nb, Ti, Mo)$]. Energy-dispersive spectrometry analysis of the precipitates did not indicate any combination of Ni or Fe and Ti, which could be the most probable if Laves was present. Based on this cursory analysis, it appears that the predominant particle in the Filler Metal 52 weld microstructure is a Ti-rich nitride approximating TiN.

The detail of the grain boundary in Fig. 2 shows they have clearly migrated away from the solidification subgrain boundaries that are free of the TiN precipitates. Ductility-dip cracking is predominant along these "clean" migrated grain boundaries. The bottom photo in Fig. 2 is a higher magnification of the boxed area in the upper photo of Fig. 2, clearly illustrating the lack of precipitation or second phases along the migrated grain boundary, whereas the large TiN particles appear as single large cuboidal particles, as

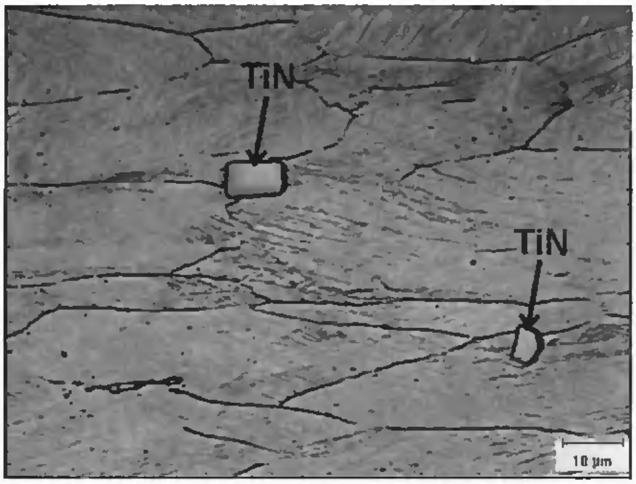

Fig. 5 — Second phases precipitated in the Filler Metal 52 weld metal.

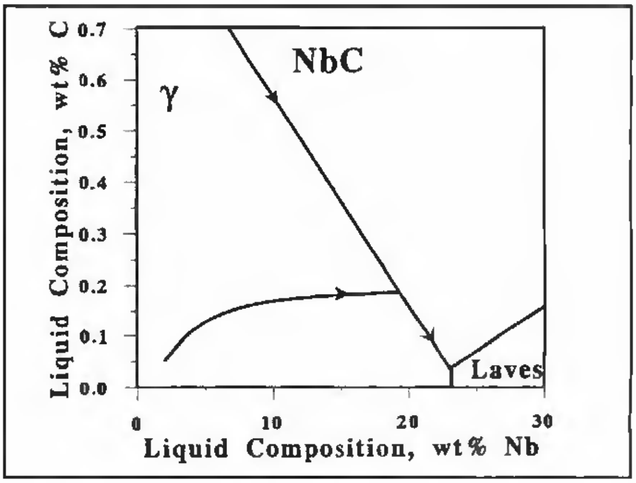

Fig. 6 — Schematic solidification path for a Nb-bearing superalloy leading to the formation of MC carbides and possibly Laves phases eutectic constituents (Ref. 5).

Table 2 — Filler Metal 82 Chemical Composition Comparison (wt-%)

Element	Ni-Cr-Fe-Nb Weld Deposit 12	Filler Metal 82 Heat YN6830	Differential (+ or –)
C	0.031	0.040	+0.009
Mn	0.20	2.86	+2.66
Fe	7.04	1.18	–5.86
S	0.007	0.01	+0.003
Si	0.16	0.12	–0.04
Cu	0.035	0.09	+0.055
Ni	73.85	72.75	–1.1
Al	0.12	N/A	—
Ti	0.26	0.37	+0.11
Cr	15.7	20.1	+4.4
Nb + Ta	1.58	2.3	+0.72
Mo	N/A	N/A	—
P	N/A	0.007	—
Pb	N/A	0.004	—
Co	N/A	0.05	—

shown in Fig. 3, and discrete small particles (see left portion of bottom photo in Fig. 2). Some other elongated phases appear continuous (see right portion of bottom photo in Fig. 2) along some of the solidification subgrain boundaries. The ductility-dip crack follows a migrated grain boundary path that both transects and directly follows a solidification subgrain boundary.

The grain boundary highlighted and detailed in Fig. 2 migrated from the relatively "clean" solidification subgrain boundary to its left. Since the precipitates were not prevalent along this particular solidification subgrain boundary, the impediment to boundary motion was low enough to allow the boundary to migrate. Migrated grain boundaries move away from the compositional portion of a solidification grain boundary in the solid state due to simple grain growth or a boundary straightening mechanism. Throughout the Filler Metal 52 microstructure, some regions reveal decreased microsegregation along the solidification subgrain boundaries and decreased second phases than do other regions. The "clean" grain boundaries or the grain boundaries absent of such constituents preferentially migrate and crack under sufficient levels of strain. Under low levels of applied strain, these "clean" boundaries are most likely the sites of DDC initiation with propagation possible along more tortuous boundary segments. The tortuous paths appear to assist in arresting DDC propagation, probably due in part to a mechanical "locking" effect.

Filler Metal 82

In comparison to Filler Metal 52, Filler Metal 82 migrated grain boundaries are always tortuous in nature, which contributes to an increased resistance to DDC (Ref. 4). Filler Metal 82 weld deposits contain large amounts of MC carbides (FCC crystal structure) of the type NbC and/or (Nb,Ti)C, which pin the grain boundaries. Thus, grain growth is inhibited resulting in increased grain boundary area and a subsequent increase in the strain necessary to cause cracking. The interdendritic position of these carbides suggest they are the result of a eutectic reaction occurring at the end of solidification, as schematically shown in Fig. 6. The solidification process in this alloy starts as L→γ with the interdendritic region or liquid becoming enriched in C and Nb, until the composition of this liquid achieves the twofold saturation between γ and NbC. At this point the solidification continues by the simultaneous formation of γ and NbC by a eutectic-type reaction as the remnant liquid follows the twofold saturation line shown in Fig. 6. If the solidification process ends along this twofold line, the only interdendritic-formed phase would be NbC. However, if solidification continues to the triple eutectic point (where γ, NbC, and Laves phases are in equilibrium) it will form Laves phase in addition to γ and NbC (Ref. 9). In the case of the Filler Metal 82 chemical composition (Table 2), the low Fe content limits the Laves formation and the results show that in this case the solidification ends along the twofold saturation line before the triple eutectic point is reached. As a result, only the NbC second phase is formed during solidification of Filler Metal 82.

In Filler Metal 82, eutectic carbides are evenly distributed throughout the microstructure, residing at solidification grain and subgrain boundaries. Figure 7 shows eutectic MC carbides consistently distributed throughout the Filler Metal 82 microstructure with several of the constituents effectively pinning the grain boundary from further motion, thereby restricting grain growth. Additionally, Fig. 7 illustrates a number of smaller intergranular and intragranular carbides (see boxed area in lower photo of Fig. 7). These smaller precipitates were found to be associated with the interdendritic regions and gathered around the larger carbides. In contrast, the Filler Metal 52 weld deposit microstructure appears to be free of these groups of smaller precipitates when observed in the SEM.

EDS analysis of the large precipitates (Fig. 8) showed Nb and Ti peaks, characteristic of an Nb-Ti-rich MC carbide (Nb,Ti)C. The Ni and Cr peaks result from the electron beam interaction with the matrix due to the small size of the analyzed particle. The particles observed in the boxed area in the lower photo of Fig. 7 were too small to identify in the SEM, but have been identified independently as (Nb,Ti)C (Ref. 10).

Figure 9 reveals further definitive evidence of grain boundary pinning by the MC eutectic carbides. Again the large eutectic constituents are (Nb,Ti)C formed at the end of solidification. The smaller precipitates (in the boxed area and along the grain boundary) are most likely (Nb,Ti)C or some other type of MC-carbide particles.

Electron Backscattered Diffraction

Electron backscattered diffraction was used to determine the point-to-point local lattice orientation over the sample surface. Based on these data, information regarding the grain boundary misorientation, special orientation relationships such as coincident site lattice (CSL) grain boundaries, and accumulated plastic local strain was extracted from several STF samples in both the cracked and uncracked conditions.

Special Grain Boundaries. In general terms, the grain boundary character distribution (GBCD) determined using EBSD showed a small fraction of low-Σ CSL grain boundaries in the microstructure. The highest measured fraction of Σ_3–Σ_{29} was about 17%, which is not far away from the expected value for an as-welded austenitic material. However, this fraction is slightly higher than the 9.1% reported for as-cast, pure nickel (Ref. 11).

The GBCDs measured on the STF samples of Filler Metal 52 and Filler Metal 82 (Heat YN6830) are summarized in Table 3. The data in this table should be analyzed carefully because important differences exist among different regions of the samples. Measurements 2, 5, and 6 were conducted on cracked samples but in regions where cracks were not present. All the other measurements were taken in regions where many cracks were present.

When the measurements were performed in uncracked regions (measurements 2, 5, and 6 in Table 3) or over larger regions where the cracked area represented a lower fraction (measurement 4), the low-Σ CSL grain boundary fraction was lower, as can be seen when measurement 3 is compared with measurements 5 and 6, or when comparing measurements 3 and 4 (larger region with lower cracked area). The only exception was measurement 2, where the uncracked region of Filler Metal 52 had a relatively high (12.2%) fraction of low-Σ CSL grain boundaries. This result was probably due to the poor statistics of measurement 2, resulting from the large grain size. However, this sample was tested at high temperature (1160°C) where the higher fraction of low-Σ CSL grain boundaries may be explained by the observed dynamic recrystallization.

The GBCD data show that the special grain boundaries are mainly associated with the regions that have cracks and not with the uncracked regions. This result appears to be contradictory with the accepted higher cracking resistance of these special grain boundaries. However, the special grain boundaries observed around the cracks were formed during the dynamic recrystallization process suffered by these highly deformed regions around the intergranular cracks. It should be noted that the fraction of special grain boundaries in the microstructure was too low to significantly influence the crack nucleation.

The misorientation between the grains where intergranular cracking occurs was measured in the samples subjected to EBSD analysis. The results of these measurements are presented in Table 4. The angle between these grains varied between 9 and 60 deg, with the average approximately 40 deg. This value is close to the maximum misorientation frequency, expected to be about 45 deg, for a theoretical random set of misorientations. Therefore, the cracked grain boundaries were random grain boundaries. In addition, an EBSD orientation map reconstruction, by extrapolation of the grain orientations around the cracks, verified that the cracked grain boundaries were not low-CSL grain boundaries, as expected, due to the reported high cracking resistance of these grain boundaries.

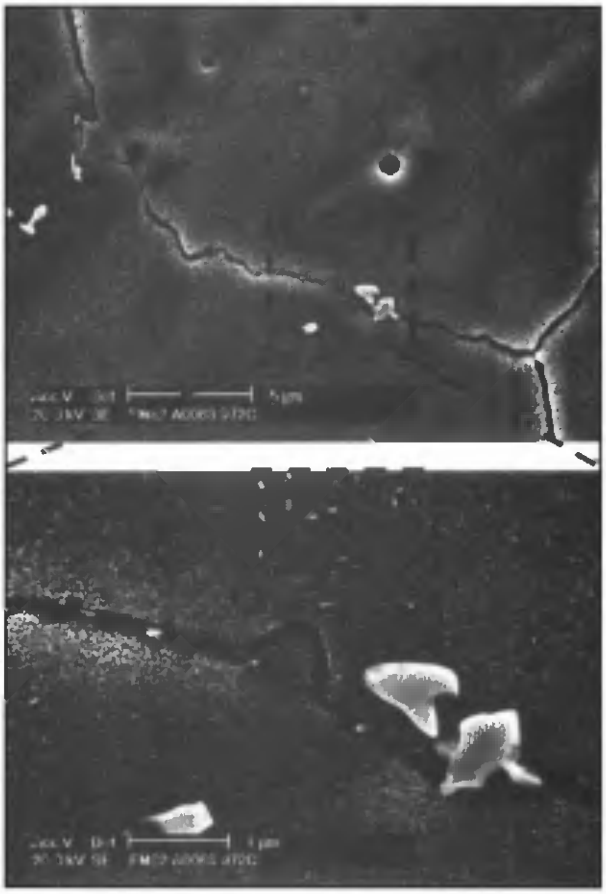

Fig. 7 — Tortuous boundary in Filler Metal 82 resulting from "pinning" by eutectic particles. (Boxed area in lower photo shows small particles prevalent throughout the Filler Metal 82 weld-metal matrix.)

Strain Distribution

The EBSD technique also allows the local strain distribution in the microstructure to be estimated, allowing strain maps to be plotted. The strain maps from STF specimens revealed strain concentration at or very near the grain boundaries, especially at the triple-point junctions. When cracked regions were mapped, as shown in Fig. 10, strain concentration around the cracks was evident. Figure 10 presents the strain map in an STF specimen of Filler Metal 52 heated to 986°C and strained 2.6%. In this map, the thin lines represent the high angle grain boundaries and the black regions are the open cracks from which EBSD information is not obtained. The color pattern represents the strain distribution, with blue representing the lowest and red the highest strains in this map. In all the strain maps developed

Table 3 — Grain Boundary Character Distribution of STF Samples

Measurement	1	2	3	4	5	6	7	8
Alloy	FM-52	FM-52	FM-82	FM-82	FM-82	FM-82	FM-82	FM-82
Temperature (°C)	986	1160	972	972	984	984	1147	1147
Strain (%)	2.6	2.9	7.5	7.5	8.1	8.1	11.3	11.3
Area (mm x mm)	0.4 x 0.3	0.4 x 0.3	0.4 x 0.3	2.0 x 1.8	0.7 x 0.5	0.4 x 0.3	0.4 x 0.3	0.4 x 0.3
Cracks	Yes	No	Yes	Yes	No	No	Yes	Yes
CSL Σ_{3-29} fraction of the high angle grain boundaries (angle > 15 deg) [%]								
Σ3	3.9	2.1	5.9	2.9	0.3	0.3	10.3	8.7
Σ5	2.2	—	—	1.6	0.1	1.3	0.3	0.4
Σ7	—	—	0.5	0.9	—	0.7	1.2	—
Σ9	2.5	—	0.2	0.6	—	—	0.4	0.3
Σ11	0.3	0.1	0.1	0.5	—	—	—	-
Σ13	0.1	—	1.1	0.4	3.4	—	1.1	—
Σ15	0.3	—	1.6	0.2	—	0.5	0.1	1.6
Σ17	2.0	—	—	0.4	—	—	0.2	0.4
Σ19	0.1	3.4	0.6	0.1	—	—	0.7	0.9
Σ21	0.1	6.5	0.3	0.2	—	—	0.4	0.7
Σ23	0.1	—	0.2	0.3	—	—	—	—
Σ25	—	—	0.8	0.2	—	—	0.1	0.4
Σ27	0.1	—	0.2	0.7	—	0.1	0.1	0.4
Σ29	—	—	0.1	0.3	2.8	4.4	2.3	2.5
Total (%)	11.6	12.2	11.5	9.2	6.7	7.3	17.0	16.4

Table 4 — Grain Boundary Misorientation in STF Samples

Measurement	1	3	4	7	8
Alloy	FM-52	FM-82	FM-82	FM-82	FM-82
Heat	NX9277	YN6830	YN6830	YN6830	YN6830
Temperature (°C)	986	972	972	1147	1147
Strain(%)	2.6	7.5	7.5	11.3	11.3
Area (mm x mm)	0.4 x 0.3	0.4 x 0.3	0.2 x 1.8	0.4 x 0.3	0.4 x 0.3
Misorientation between grains where cracking occurred (degrees)					
Minimum	9	20	21	19	11
Maximum	54	60	52	57	59
Average	40 ± 10	40 ± 5	34 ± 3	40 ± 5	39 ± 4

from STF specimens of Filler Metals 82 and 52, the strain was found to be concentrated at the grain boundaries with essentially no strain in the grain interiors. The highest strains were associated with the crack tips, where high stress concentrations would be expected.

Discussion

Based on the results presented here and those from Parts I and II of this investigation, it is clear that DDC is a complex phenomenon that is influenced by multiple factors, to be reviewed and discussed in the following sections. Reference to Parts I and II of this investigation are suggested in order to understand the entire context of this discussion.

Alloy Element Effects

Based on the results of STF tests presented in Part I of this investigation, significant differences in DDC susceptibility were observed when comparing Filler Metals 52 and 82. Data in the literature support the observed differences based on the composition of the weld metal. A number of Ni-based alloy welds were tested by Heuschkel (Ref. 12) to determine their elevated-temperature ductility response. In that study, Ni-Cr-Fe-Nb weld deposits achieved the best ductility, with a minimum elongation of 34% observed. Conversely, Ni-Cr-Fe-Ti and Ni-Cu-Ti type weld deposits exhibited the lowest ductility, with a minimum elongation of 10% reported. The 649°–1093°C low-ductility temperature range reported for the Ni-Cr-Fe-Nb weld deposits is similar to the STF results for Filler Metal 82 (Ref. 4), which contains Nb and forms a NbC eutectic constituent. Interestingly, the Ni-Cr-Fe-Ti weld metal contained only 0.47% Nb while the Ni-Cu-Ti weld deposits contained no Nb additions whatsoever. Table 2 compares the composition of the Ni-Cr-Fe-Nb weld deposits from Heuschkel (Ref. 12) with that of Filler Metal 82 (Heat YN6830).

Overall, the compositions of the two filler metals (Table 2) are strikingly similar. Note especially the Nb, Cr, and C contents. From his studies of a number of differently alloyed Ni-Cr-Fe weld deposits, Heuschkel (Ref. 12) reported the best results for those weld deposits containing Nb additions and made with argon shielding gas. Additionally, Sadowski (Ref. 13) summarized the effects of Nb on weld-metal hot cracking susceptibility of 25%Cr-20%Ni based on reports by several authors and reported Nb content to be deleterious up to 0.25% while beneficial at 1.38–2.90%. This is precisely the Nb range for both filler metals in Table 2. Furthermore, based on hot ductility testing of 25%Cr-20%Ni and 18%Cr-8%Ni, Haddrill and Baker (Ref. 14) reported that Nb-containing weld deposits increased the observed ductility minimum significantly compared to weld deposits free of Nb additions.

Carbon content has been reported by a number of researchers to have a significant effect on DDC susceptibility (Refs. 2, 14–16). Haddrill and Baker (Ref. 14) observed less cracking along migrated grain boundaries as carbon content was increased from 0.06 to 0.125 wt-% in reheated regions of 25%Cr-20%Ni austenitic weld metal. They suggested that the reduction in cracking susceptibility with the increased interstitial element content could be related with the morphology and distribution of the intergranular carbides and with the segregation of solute elements to the dislocations. In support of this, Matsuda et al. (Ref. 15) and Arata et al. (Ref. 16) reported a much narrower DTR and an increased minimum strain

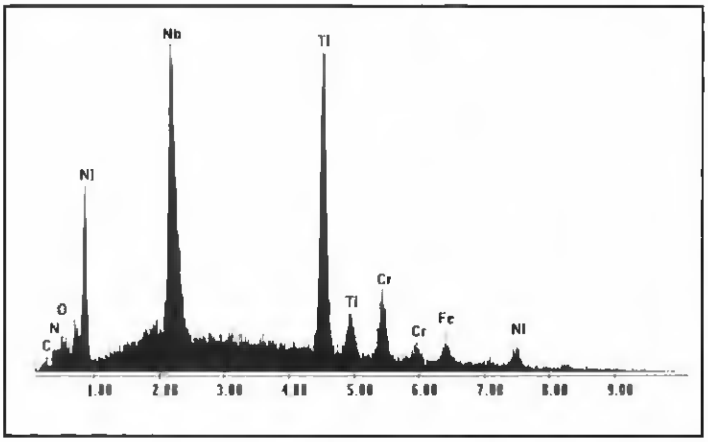

Fig. 8 — EDS analysis of large eutectic constituents along the migrated grain boundaries in Filler Metal 82.

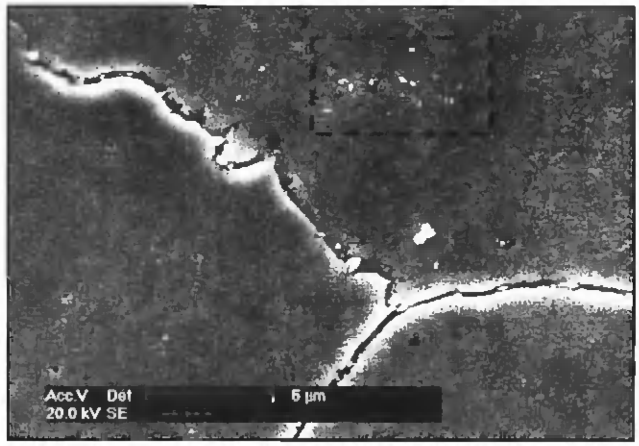

Fig. 9 — Triple-point migrated grain boundary intersection with eutectic grain boundary "pinning" in Filler Metal 82 tested at 1147°C.

(E_{min}) to cause cracking in fully austenitic 310S when carbon contents were increased, with no DTR phenomena observed whatsoever when carbon contents ranged between 0.43 and 0.53%. This improvement in ductility was attributed to an increase in the formation of eutectic M_7C_3 carbides that restrict grain growth and grain boundary mobility (Refs. 12, 17).

Nickel-based alloys containing Nb can form both MC carbides and Laves phase eutectic constituents during solidification (Ref. 9). However, thermodynamic calculations showed that for the chemical compositions of Filler Metals 52 and 82, the formation of eutectic Laves phase is not expected. In the case of Filler Metal 52, the calculations showed that the slightly higher content of Ti, along with the N content, promotes TiN (FCC structure) precipitation in the liquid and its continuous precipitation along the entire solidification range. The chemical composition of this precipitate gradually changes from TiN at temperatures well above the alloy liquidus to NbC (FCC structure) at the end of the solidification. Thermo-Calc™ estimates of the simulated solidification paths revealed the mass fraction of TiN+(Nb,Ti)C at the end of the solidification to be approximately 0.25% for Filler Metal 82 and 0.1% for Filler Metal 52 (Ref. 10). The actual fraction of eutectic constituents was not measured, but a qualitative analysis shows there is a large difference in the fraction of these interdendritic precipitates, being much smaller and less uniformly distributed in Filler Metal 52.

Based on observations made during this investigation, it is postulated that the difference in STF DDC susceptibility between Filler Metal 52 and Filler Metal 82 is explained, in part, by the different contents of Nb and C. These contents are higher for Filler Metal 82, and therefore its ability to form MC-type carbides is increased. The interdendritic constituents inhibit grain boundary motion in the solid state resulting in smaller grains and increasingly tortuous grain boundary paths that are resistant to cracking. These constituents along the boundary also inhibit grain boundary sliding, which has been reported to be most prevalent along "clean" grain boundaries (Refs. 18–22).

Hydrogen Effects

Hydrogen was shown to have a pronounced negative effect on the STF behavior of Filler Metal 82, as discussed in Part I and II of this investigation (Refs. 4, 5). Hydrogen cracking is typically not a concern in fully austenitic structures based on the high solubility of hydrogen and its low diffusivity in the austenitic (FCC) matrix. Regardless, atomic hydrogen is an extremely mobile interstitial species and hydrogen cracking may occur in austenitic materials if sufficient hydrogen is present (Ref. 23). Part II of this investigation (Ref. 5) contained a discussion of the two different H-embrittlement mechanisms, hydrogen-enhanced local plasticity (Ref. 24) and hydrogen-induced decohesion (Ref. 25), and that may be acting in the DDC temperature range of these filler metal deposits. The high incidence of triple-point cracking along with the planar slip evident in the fractography of the STF samples with intentional hydrogen additions suggests that both hydrogen embrittlement mechanisms may be operative during DDC of Ni-based alloys. The level of hydrogen necessary to reduce ductility in addition to the effect of grain boundary structure and precipitation on hydrogen mobility is the subject of continuing research.

Eutectic Constituent Effects

In addition to the large cuboidal TiN transferred from the weld wire (Figs. 3 and 5), Filler Metal 52 formed small nitrides during solidification. Based on thermodynamic calculations, the eutectic phase formed at the end of solidification was the isomorph MC carbide, having the same crystal structure as TiN with very similar lattice parameters. The gradual change of the precipitated phases from TiN to MC has been previously reported during the solidification of N-bearing Ni-based superalloys (Ref. 26). The weight fraction of the interdendritic phases in Filler Metal 52 was very low (about 0.1% according to thermodynamic calculations) and its distribution within the weld metal microstructure was very inconsistent (Figs. 1 and 2) resulting in relatively large areas across the weld metal microstructure that were absent of boundary "locking" and/or "pinning" constituents. As a result, Filler Metal 52 exhibited many long, straight, "clean" migrated grain boundaries that crack under low levels of strain (<2%).

In contrast, Filler Metal 82 forms abundant MC-carbide eutectic constituents of the type (Nb,Ti)C. The calculated weight fraction of this carbide for Filler Metal 82 was approximately 0.25% (Ref. 10). The carbides were distributed relatively consistently throughout the weld metal microstructure (see Figs. 7 and 9) further inhibiting boundary motion and grain growth, and thus decreasing cracking susceptibility.

It is apparent that boundary tortuosity plays an important role in the DDC susceptibility of the weld metal, especially at low levels of applied strain. In these filler metals, tortuosity is associated with the (Nb,Ti)C eutectic carbide when higher levels of carbon and Nb are present in the filler material. Increased eutectic constituents in the microstructure reduce grain growth, increase grain boundary tortuosity, and significantly suppress grain boundary sliding resulting in increased resistance to DDC initiation and propagation. Based on the STF results for these

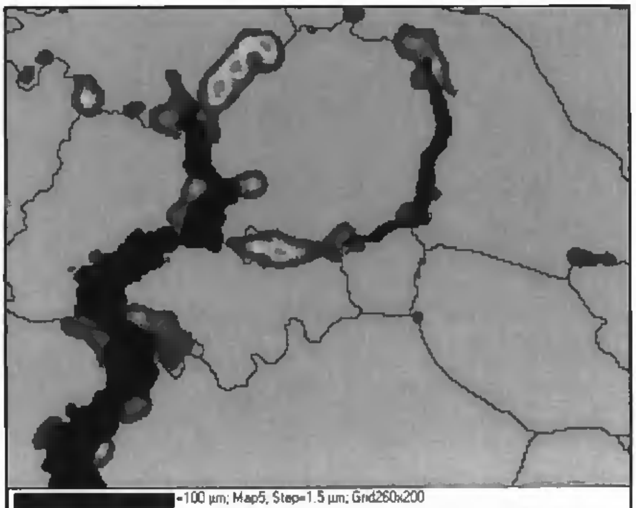

Fig. 10 — Strain distribution map in the STF specimen of Filler Metal 52 heated to 986°C and strained 2.6%. The thin lines represent the high angle grain boundaries. The black regions are the open cracks. The colored contouring shows the strain distribution with blue representing the lowest and red the highest strains.

filler metals, a strong contributing factor to the higher resistance of Filler Metal 82 to DDC is the preponderance of tortuous migrated grain boundaries. These tortuous boundaries provide a mechanical locking effect as the adjacent crystals attempt to slide past each other with applied strain at elevated temperature.

The specific effect of different interdendritic particles, i.e., nitrides, carbides, or other particles, on the variation in cracking behavior between Filler Metals 52 and 82 is not clear. It is possible that certain particles are more effective in reducing DDC relative to others based on their size, distribution, or morphology. This effect is also the subject of ongoing research.

Segregation Effects

In Part I of this investigation, the detrimental effect of sulfur on DDC was clearly shown. Although detailed grain boundary analysis was not performed, it is anticipated that the segregation of sulfur to the migrated grain boundaries was responsible for this degradation. In addition, as described previously, the accumulation of hydrogen at grain boundaries also appears to be detrimental.

Migrated grain boundaries move more easily through the weld metal microstructure when fewer eutectic constituents are present to "lock" and/or "pin" grain boundary motion. During multipass welding, multiple thermal cycles promote additional boundary migration and segregation. During migration, impurity and interstitial elements can be swept into the boundary as they have high diffusivities and high affinities for grain boundaries. As the impurity and interstitial content in the boundary approaches a critical level, a "drag effect" is imposed upon the boundary. The boundary is no longer highly mobile but is now highly enriched in impurity and interstitial element content. This enrichment may have negative implications as some impurity and interstitial elements are detrimental to ductility. Thus, in the event that impurity and interstitial segregation play roles in the DDC mechanism, less grain boundary area brought about by increased grain size will lead to higher impurity and interstitial concentrations at the grain boundaries, possibly lowering cohesion between grains. Such an increase in segregation could further weaken the grain boundaries, encouraging grain boundary sliding under low orders of strain, subsequently resulting in intergranular cracking.

Effect of Triple-Point Junctions

The presence of triple-point grain boundary intersections in polycrystalline materials has been shown to influence several material properties, including ductility, grain boundary migration, sliding, and recrystallization (Refs. 11, 27). Watanabe (Ref. 11) used a computer simulation of intrinsic stress distributions at triple-point grain boundary intersections to show that uncompensated stresses exist at these intersections, supporting the hypothesis that triple-point grain boundary intersections are highly stressed regions conducive to crack initiation.

Masubuchi and Martin (Ref. 18) and Haddrill and Baker (Refs. 14, 22) describe cracking along triple-point grain boundary intersections and attribute the cracks to a combination of increased stress concentration at the intersection and grain boundary sliding. Masubuchi and Martin (Ref. 18) stated that sliding along grain boundaries might take place at a low stress since the inherent grain boundary flow stress is very low. Thus, the high stress concentration at the intersection initiates intergranular fracture with propagation of the fracture a function of sliding along the low flow stress grain boundary. Ductility-dip cracking appears to either initiate or terminate at these intersections. The strain maps obtained by EBSD, such as the one presented in Fig. 10, clearly reveal strain concentration at triple points. It is possible that cracking initiates at these triple-point grain boundary intersections, as these are sites of high stress concentration, thereby lowering the "global" stress necessary to initiate cracking.

Dynamic Recrystallization

A combination of accumulated deformation and thermal energy promotes recrystallization. High local strains at the crack tip lower the amount of thermal energy necessary to induce recrystallization. The strain maps obtained from the cracked samples reveal recrystallization occurring at the strain-concentrated regions of the microstructure, either in front of the cracks or at the triple-point junctions along the crack path. Figure 10 shows two regions of strain concentration where recrystallization has initiated, one of them in front of the smaller crack and the other where the larger crack changed its propagation direction due to a triple point. Additionally, strain concentrates along grain boundaries that have not separated. As temperature increases, recrystallization occurs more easily at these strained grain boundaries. Based on observations during this investigation, it is postulated that the combination of applied strain, stress concentration at the grain boundary, high local strains at the crack tip, and applied thermal energy increases the likelihood of dynamic recrystallization. Therefore, it is possible that the appearance of dynamic recrystallization within the microstructure signals the onset of ductility recovery in the high-temperature region (1050°–1200°C) of the overall DTR.

Boundary Orientation Relative to the Applied Strain

It is apparent that grain boundary orientation to the applied strain is a factor in DDC formation. Previous studies by Bowers (Ref. 28) and Kikel and Parker (Ref. 29) using the double-spot Varestraint test showed that orientation relative to the applied strain has a significant effect on DDC susceptibility. In this investigation, STF samples were tested in both the as-welded (multipass weld) and spot-welded condition. The as-welded condition results in a more random grain boundary pattern resulting from epitaxial nucleation and columnar grain growth in the multipass weld. When a spot weld is made within the weld metal in the STF sample, a radial grain boundary pattern is created with boundaries ranging from 0 to 90 deg relative to the applied strain. For Filler Metal 52, the as-welded STF behavior showed a threshold strain of 2.5%, but when spot-welded samples were tested the threshold strain for cracking dropped to 1%. There are other metallurgical influences that complicate this simple argument, such as the effect of multiple reheating in the multipass weld on the nature of the boundary. However, based on the observation that most DDC is observed in the spot welds in the angular range of 45–90 deg to the applied strain, it can be concluded that the macroscopic boundary orientation in the weld metal relative to the applied strain is a contributing factor to DDC.

Fracture Morphology

Part II of this investigation described the fracture behavior associated with DDC in STF samples of Filler Metals 52 and 82 throughout the entire 625°–1200°C DDC temperature range (Ref. 5). Ductility recovery at both extremes of the DTR is marked by ductile intergranular fracture. The ductility recovery at elevated temperature coincides with the onset of local recrystallization at the grain boundaries. In the intermediate temperature regime of the DTR, the intergranular fracture acquires a wavy pattern with crystallographic steps superimposed. These steps are clearly evidence of crystalline slip, which is thought to be related with the hydrogen-induced plasticity. The presence of precipitates was evident on the fracture surfaces. However, the exact relationship between fracture behavior and grain boundary precipitation is still not clear and is the subject of an ongoing investigation.

Grain Boundary Character Distribution

It is well known that low CSL grain boundaries (Σ_3–Σ_{29}) exhibit special properties that are associated with the relatively good atomic scale matching and consequently low energy of these grain boundaries. Among these special properties are high resistance to 1) crack propagation, 2) localized corrosion, 3) sliding and cavitation at high temperatures, and 4) lower solute segregation (Refs. 11, 27). Ductility-dip cracking is a high-temperature phenomenon and, although the difference in properties between the low-Σ CSL and the random grain boundaries decreases when temperature increases (Ref. 30), the effect of CSL grain boundaries on the DDC phenomenon was of interest.

Although a high fraction of "special grain boundaries" was not observed in either of the filler metals (Table 2), most of the boundaries identified were low Σ-CSL grain boundaries (Σ_3, Σ_5, Σ_9, and Σ_{29}), to which special properties have been reported (Refs. 11, 27). These boundary types have low activity levels in relation to grain boundary migration, sliding, vacancy generation, diffusion, and absorption while high-angle "random" grain boundaries have high activity levels in relation to these boundary characteristics (Ref. 11). Cracking did not occur along any of the "special" grain boundaries with some boundaries appearing to arrest crack propagation.

In support of this observation, Watanabe (Ref. 11) reported that "special" grain boundaries are strong obstacles to crack propagation such that intergranular fracture will arrest at these boundary types. In almost all cases, DDC was observed along "random" high-angle grain boundaries. Based on the high activity levels associated with these boundaries, fracture along these boundary types is not surprising.

Further supporting the fracture resistance of low-Σ CSL boundaries and low-angle boundaries, Palumbo and Aust (Ref. 27) reported that these boundary types would not fracture even when lying at optimal angles (45–90 deg) for operation of a grain boundary sliding assisted fracture mechanism. These angles are precisely the angular orientation range to the applied load found to be typical for DDC along random high-angle migrated grain boundaries in Filler Metals 52 and 82, further supporting fracture propensity along high-energy, high-angle migrated grain boundaries.

Grain boundary cracking resistance decreases as the boundary becomes more "random" (i.e., deviating further away from low energy configurations). At the same time, the potential for segregation of solute and impurities to this grain boundary is also enhanced (Ref. 11). The higher energy level of the boundary also improves its mobility, generating synergy between the potential for segregation of the boundary and the "sweeping" effect of impurities while it moves. This behavior lends support to increasing eutectic constituent content and decreasing impurity content in the weld-metal microstructure. Increased eutectic constituent content will inhibit boundary migration and the consequent sweeping of impurities, further minimizing the probability of grain boundary sliding and/or cracking.

In the STF samples, most of the special grain boundaries present in the microstructure were a result of the thermomechanical work, which occurred during the test itself. Many of these special grain boundaries appeared to originate during the recrystallization process in the highly strained material around the cracks. Based on this observation, low-Σ CSL boundaries have little effect on crack initiation, but may play an important role in the crack arrest process.

Insight into the DDC Mechanism

While the mechanism for DDC is still not fully understood, the STF test has confirmed many previous theories about DDC and has proven itself as a valuable method to test different conditions and produce a variety of cracked samples for evaluation. Results from this investigation confirm that DDC occurs preferentially along weld-metal migrated grain boundaries. An overwhelming majority of DDC was observed in the spot weld with cracks occurring outside the spot weld in multipass weld metal only at relatively high strains (>8%). Typically, cracks occurred on migrated grain boundaries oriented approximately 45–90 deg to the applied strain. These results agree with previous reports that grain boundary orientation relative to the direction of the applied strain is a contributing factor to formation of DDC (Refs. 15, 19, 29, 31).

The effect of intergranular precipitation on grain boundary sliding remains controversial. Mathew et al. (Ref. 21) and Dix and Savage (Ref. 32) postulated that as grain boundary precipitates form, grain boundary sliding is restricted enabling significant matrix deformation and higher ductility. Conversely, Zhang et al. (Ref. 33), Mintz et al. (Ref. 17), and Arata et al. (Ref. 16) concluded that increased intergranular precipitation lowers grain boundary ductility.

Materials containing precipitates, eutectic constituents, and/or second phases tend to restrict grain boundary motion and thereby reduce the amount and length of cracking. Furthermore, formation of eutectic constituents at the end of solidification results in tortuous grain boundary paths that are increasingly resistant to both DDC initiation and propagation when compared to straight grain boundary paths free of precipitates. Tortuous grain boundary paths result in increased grain boundary area vs. straight grain boundaries, over a given length. Grain boundary sliding is impeded by tortuous boundaries and orientation to the applied strain is increasingly random vs. a straight grain boundary oriented favorably for DDC formation.

Previous research supports the concept of Nb and C additions to the weld metal to decrease cracking susceptibility (Refs. 2, 12–16). Increased C contents in Filler Metal 82 may result in increased MC-carbide (NbC) formation along grain boundaries that further restrict grain growth and grain boundary migration ultimately resulting in increased grain boundary area to withstand higher applied strains. This investigation supports the hypothesis that grain boundary precipitates act as locking points along the boundary, thereby restricting grain boundary sliding and enabling significant matrix deformation and higher ductility (Refs. 21, 32). Furthermore, restricted boundary motion resulting from pinning by eutectic constituents in the microstructure results in reduced "sweeping" of impurities and undesirable solute elements into the boundary, further enhancing resistance to DDC.

Zhang et al. (Refs. 33, 34) revealed that fully austenitic stainless steel weld metals precipitated $M_{23}C_6$ carbides along migrated grain boundaries below 1200°C, while also observing a high density of intergranular precipitation in Fe-36%Ni weld metals. Generally, it was observed that the prevalence of precipitates increased at locations where migrated grain boundaries intersect solidification subgrain boundaries. Subsequently, it was postulated that since the solute concentration at the solidification subgrain boundary is high, migrated grain boundary precipitation should easily occur at this intersection. It was also determined that a certain region of the migrated grain boundary near the intersection could be enriched by solute elements due to rapid diffusion at the grain boundary intersection. These observations further support the hypothesis that as grain boundary precipitates form, grain boundary sliding is restricted, enabling significant matrix deformation and higher ductility.

Controlling impurity contents (S, P, etc.) may also assist in controlling formation of DDC, especially during multipass welding operations. Based on the increase in DDC susceptibility observed during STF testing of Filler Metal 82 with additions of sulfur to the spot weld, it is anticipated that minimizing S, P, and other impurity contents in Filler Metals 82 and 52 will increase the resistance to DDC. Cordea et al. (Ref. 31) concluded that after extensive grain growth, impurities became sufficiently concentrated on the grain boundaries to weaken them, resulting in crack initiation. As microsegregation of S, P, and other impurity elements easily occurs to solidification subgrain boundaries during solidification and diffusion along these boundaries is enhanced in comparison to the matrix, it is anticipated that the intersection of a migrated grain boundary with a solidification subgrain boundary will result in enrichment of impurity elements along the migrated grain boundary. This in turn will promote decohesion and facilitate grain boundary sliding along the boundary/matrix interface. Eliminating or minimizing impurity elements in the filler materials may assist in increasing the amount of strain necessary to initiate grain boundary sliding.

The potent effect of hydrogen on DDC susceptibility was initially quite surprising based on the perceived resistance of austenitic microstructures to hydrogen-induced cracking. Although the exact levels of diffusible hydrogen were not determined, it is estimated based on data gathered from multipass welds using $95Ar-5H_2$ shielding gas (Ref. 35) that the levels were on the order of 15–20 ppm. It is proposed that this hydrogen is trapped within the microstructure at trap sites such as the carbide/matrix interface and then released upon heating above 625°C. Since many of the carbides are present along the grain boundaries and stress is concentrated at these boundaries, the hydrogen accumulates in the boundary and reduces its cohesive strength and activates the localized plasticity around the grain boundaries. It is conceivable that the DDC mechanism is simply a manifestation of hydrogen-assisted cracking at elevated temperature.

Welding speed was very low for the butter passes (2 in./min) and relatively low for the fill passes (5 in./min) during STF sample preparation. Yeniscavich (Ref. 36) used the hot ductility test to study the effects of welding speed on ductility response in Ni-Cr-Fe alloy wrought materials and weld metals. The results show significant differences in the ductility responses of wrought and welded specimens, indicating that microstructure is a significant parameter affecting hot ductility. Although somewhat mixed, data from a number of heats revealed that the ductility response is a function of welding speed with ductility typically increasing as welding speed increased from 1 to 10 in./min. Higher welding speeds produced finer grain sizes in both the fusion zone and heat-affected zone resulting in greater fissure resistance. Faster welding speeds not only produced a fissure-resistant structure, but also reduced the volume of material susceptible to fissuring. Furthermore, Yeniscavich postulated that segregation decreased as the welding speed increased, decreasing the likelihood of a low ductility response.

This investigation into DDC of nickel-based alloy filler materials has identified a number of factors that contribute to DDC formation. The DDC mechanism is most likely a complex interplay amongst these contributing factors rather than a result of any single factor. The research performed in this investigation has provided increased insight into a number of variables that can be manipulated to assist in decreasing or controlling DDC formation.

Control of the DDC mechanism may be effectively described by the following: Materials containing a consistent distribution of grain boundary precipitates and/or eutectic constituents effectively "lock" and/or "pin" grain boundary motion, inhibiting grain growth. Grain boundary tortuosity is therefore increased resulting in increased boundary area per unit length (vs. a straight grain boundary) to resist applied strains while also subjecting less of the grain boundary to orientations favorable to boundary separation. Precipitation, eutectic constituent formation, and subsequent grain boundary tortuosity effectively disrupt grain boundary sliding as cohesion between grains is enhanced. Impurity and solute segregation is effectively reduced as the "locked" and/or "pinned" boundary maintains a low-angle orientation that is more resistant to solute and impurity segregation as grain boundary "sweeping" of these detrimental elements is effectively controlled. Furthermore, controlling or eliminating impurity contents and utilizing high welding speeds control intergranular segregation during multipass welding operations, further increasing resistance to grain boundary decohesion and sliding. Controlling or eliminating a single factor contributing to the DDC mechanism will assist in preventing formation of DDC, but comprehensive control of all of the contributing factors will most likely result in the most optimal ductility response in nickel-based alloy filler materials.

Conclusions

1. Ductility-dip cracking occurred along random high-angle grain boundaries, generally referred to as migrated grain boundaries in austenitic weld metal.

2. A low fraction of interdendritic constituents (TiN) and eutectic MC-carbides were inconsistently distributed throughout the microstructure of Filler Metal 52 resulting in long, straight migrated grain boundaries. These boundaries have low resistance to grain boundary sliding and thus exhibited increased susceptibility to DDC.

3. A higher fraction of eutectic constituents, particularly (Nb,Ti)C, were distributed throughout the microstructure of Filler Metal 82 resulting in formation of tortuous grain boundary paths that are more resistant to DDC. The increased resistance to DDC was a function of the eutectic constituents "pinning" grain boundary motion effectively minimizing grain growth and grain boundary sliding.

4. Sulfur and hydrogen additions were found to increase susceptibility to DDC in Filler Metal 82.

5. Triple-point grain boundary intersections act as high stress concentration regions conducive to crack initiation. The addition of hydrogen greatly increased the incidence of cracking at triple points.

6. Straight migrated grain boundaries crack under low levels of strain (<2%). Higher levels of strain (>2%) are necessary to initiate cracking along tortuous migrated grain boundaries.

7. Recrystallization was observed in the upper temperature range (1050°–1200°C) of the DTR and coincided with ductility recovery.

8. Grain boundary orientation to the applied strain is a contributing factor to

DDC formation. Boundaries oriented at 45–90 deg to the applied strain were found to be most susceptible to DDC.

9. Using the EBSD technique, it was shown that high strain concentrations are present along the migrated grain boundaries upon application of only small strains in the STF test.

Acknowledgments

The authors would like to thank Nathan Nissley, Dan Ryan, and Shu Shi, members of the Welding and Joining Metallurgy Group at The Ohio State University, for their valuable assistance during this investigation. We are grateful for the technical input and guidance of Jeff Kikel and financial support by BWX Technologies, Inc.

References

1. Nissley, N. E. 2002. *Development of the Strain-to-Fracture Test to Study Ductility-Dip Cracking in Austenitic Alloys.* MS thesis. Columbus, Ohio: The Ohio State University.

2. Hemsworth, B., Boniszewski, T., and Eaton, N. F. 1969. Classification and definition of high-temperature welding cracks in alloys. *Metal Construction and British Welding Journal*, pp. 5-16.

3. Honeycombe, J., and Gooch, T. G. 1970. Microcracking in fully austenitic stainless steel weld metal. *Metal Construction and British Welding Journal* (9): 375–380.

4. Collins, M. G., and Lippold, J. C. 2002. An investigation of ductility-dip cracking in nickel-based filler materials — Part I. *Welding Journal* 82(10): 288-s to 295-s..

5. Collins, M. G., Ramirez, A. J., and Lippold. J. C. An investigation of ductility-dip cracking in nickel-based filler materials — Part II. *Welding Journal* 82(12): 348-s to 354-s.

6. Schwartz, A. J., Kumar, M., and Adams, B. (eds.). 2000. *Electron Backscattered Diffraction in Materials Science.* Kluwer Academic/Plenum Publishers, p. 339.

7. Gourgues, A. F. 2002. Electron backscattered diffraction and cracking, *Materials Science and Technology* 18(2): 119–133.

8. Lehockey, E. M., Lin, Y. P., and Lepik, O. E. 2000. Mapping residual plastic strain in materials using electron backscatter diffraction. *Electron Backscattered Diffraction in Materials Science*, A. J. Schwartz et al. (eds.). Kluwer Academic/Plenum Publishers, pp. 247–264.

9. DuPont, J. N., Robino, C. V., and Marder, A. R. 1998. Solidification and weldability of Nb-bearing superalloys, *Welding Journal* 77(10): 417-s to 431-s.

10. Ramirez, A. J. 2002. Unpublished research performed at The Ohio State University.

11. Watanabe, T. 1988. The potential for grain boundary design in materials development. *Materials Forum* (11): 284–300.

12. Heuschkel, J. 1960. Weld metals in nickel-base alloys. *Welding Journal* 39(6): 236-s to 246-s.

13. Sadowski, E. P. 1974. Modification of cast 25Cr-20Ni for improved crack resistance. *Welding Journal* 53(2): 49-s to 58-s.

14. Hadrill, D. M., and Baker, R. G. 1965. Microcracking in austenitic weld metal. *British Welding Journal* 12(8) 411–419

15. Matsuda, F. 1990. Hot crack susceptibility of weld metal. *Proceedings of the 1st U.S.-Japan Symposium on Advances in Welding Metallurgy*. Miami, Fla.: American Welding Society, pp. 19–36.

16. Arata, Y., Matsuda, F., and Katayama. S. 1977. Solidification crack susceptibility in weld metals of fully austenitic stainless steels (Report II) — Effect of ferrite, P, S, C, Si and Mn on ductility properties of solidification brittleness. *Transactions of JWRI* 6(1): 105–117.

17. Mintz, B., Abu-Shosha, R., and Shaker, M. 1993. Influence of deformation induced ferrite, grain boundary sliding and dynamic recrystallization on hot ductility of 0.1–0.75%C steels. *Materials Science and Technology* 9(10): 907–914.

18. Masubuchi, K., and Martin. D. C. 1962. Mechanisms of cracking in HY-80 steel weldments. *Welding Journal* 41(8): 375-s to 384-s.

19. Rhines, F. N., and Wray, P. J. 1961. Investigation of the intermediate temperature ductility minimum in metals. *Transactions of the ASM* 54: 117–128.

20. Bengough, G. D. 1912. A study of the properties of alloys at high temperatures. *Journal, Institute of Metals* 7: 123–174.

21. Mathew, M. D., Sasikala, G., Mannan, S. L., and Rodriguez, P. 1993. A comparative study of the creep rupture properties of Type 316 stainless steel base and weld metals. *Transactions of the ASME, Journal of Engineering Materials and Technology* 115: 163–170.

22. Hadrill, D. M., and Baker, R. G. 1965. Heat affected zone cracking in thick section austenitic steels during post weld heat treatment. *BWRA Bulletin* 6(11): 282–288.

23. Totsuka, N., Lunarska, E., Cragnolino, G., and Szklarska-Smialnowska, Z. 1987. *Corrosion* 43(8): 515–514.

24. Estman, J., Matsumoto, T., Narita, N., Heubaum, F., and Birnbaum, H. K. 1980. Hydrogen effects in nickel — Embrittlement or enhanced ductility. *Hydrogen Effects in Metals*, M. Bernstein and A. W. Thompson (eds.). Warrendale, Pa.: TMS pp. 397–409.

25. Symons, D. M. 1999. The effect of hydrogen in the fracture toughness of Alloy X-750 at elevated temperatures. *Journal of Nuclear Materials* 265: 225–231.

26. Huang, X., Zhang, Y., Liu, Y., and Hu, Z. 1997. Effect of small amount of nitrogen on carbide characteristics in unidirectional Ni-base superalloy. *Metallurgical Transactions A* 28(10): 2143–2147.

27. Palumbo, G., and Aust, K. T. 1992. Special properties of Σ grain boundaries. *Materials Interfaces — Atomic Level Structure and Properties*, Chapter 5. Great Britain: Chapman-Hall. pp. 190–211.

28. Bowers, R. 1997. Unpublished research. Edison Welding Institute, Columbus, Ohio.

29. Kikel, J. M., and Parker, D. M. 1998. Ductility dip cracking susceptibility of Filler Metal 52 and Alloy 690. *Proceedings of the Trends in Welding Research Conference*, Pine Mountain, Ga., pp. 757-762.

30. Pumphrey, P. H. 1976. Special high angle grain boundaries. *Grain Boundary Structure and Properties*, G. A. Chadwick and D. A. Smith, (eds.). London, U.K.: Academic Press. pp. 139–200.

31. Cordea, J. N., Evans, R. M., and Martin, D. C. 1962. Investigation to determine causes of fissuring in stainless steel and nickel-base alloy weld metals. *Technical Documentary Report No. ASD-TDR-62-317, Project No. 7381*, Task No. 738102. Columbus, Ohio: Battelle Memorial Institute. pp. 1–41.

32. Dix, A. W., and Savage, W. F. 1971. Factors influencing strain-age cracking in Inconel X-750. *Welding Journal* 51(6): 247-s to 252-s.

33. Zhang, Y., Nakagawa, H., and Matsuda, F. 1985. Weldability of Fe-36%Ni alloy (Report VI) — Further investigation on mechanism of reheat hot cracking in weld metal. *Transactions of JWRI* 14(2)

34. Zhang, Y., Nakagawa, H., and Matsuda, F. 1985. Weldability of Fe-36%Ni alloy (Report V) — Behaviors of grain boundary sliding and cavity formation preceding reheat hot cracking in weld metal. *Transactions of JWRI* 14(2): 119–124.

35. Unpublished data provided by J. Kikel of BWX Technologies, Inc.. 2001.

36. Yeniscavich, W. 1966. A correlation of Ni-Cr-Fe alloy weld metal fissuring with hot ductility behavior. *Welding Journal* 45(8): 344-s to 355-s.

Liquation Cracking in Full-Penetration Al-Cu Welds

Keeping the weld-metal solute content above — not below — the solidification cracking range can prevent liquation cracking as well as solidification cracking

BY C. HUANG AND S. KOU

ABSTRACT. Liquation cracking in the partially melted zone (PMZ) of full-penetration aluminum welds was investigated, using the simple binary Alloy 2219 (Al-6.3Cu) to gain better understanding. The PMZ is the region outside the fusion zone where grain-boundary liquation occurs during welding. The circular-patch test was used to evaluate the crack susceptibility. Gas metal arc (GMA) welds were made with the weld metal containing 0.93, 2.32, 3.43, 6.30, and 7.55 wt-% Cu. The curves of temperature (T) vs. the solid fraction (f_S) were calculated for both the PMZ (same as the base metal) and the weld metal. The results were as follows: First, at 0.93% Cu liquation cracking was very severe; at 2.32% Cu liquation cracking decreased but solidification cracking appeared; at 3.43% Cu liquation cracking disappeared but solidification cracking was severe; and at 6.30 and 7.55% Cu neither type of cracking occurred. Second, liquation cracking either stopped or did not occur near solidification cracks. Third, the T-f_S curves did not intersect each other and they showed that, for the welds that liquation-cracked, the weld-metal f_S exceeded the PMZ f_S throughout PMZ solidification. Three things were proposed. First, liquation cracking is caused by the tensile strains induced in the solidifying PMZ by the solidifying and contracting weld metal that exceed the PMZ resistance to cracking. Under the same welding conditions, the tensile strains in the PMZ increase with increasing weld-metal f_S and workpiece restraint, and the PMZ resistance to cracking decreases with increasing liquation. Second, an aluminum weld metal higher in f_S than the PMZ throughout PMZ solidification can cause liquation cracking if the workpiece is restrained tightly, the PMZ is liquated heavily, and there is no solidification cracking in the adjacent weld metal to relax tensile strains in the PMZ. Third, raising the weld metal solute content beyond the solidification-cracking range can prevent liquation cracking as well as solidification cracking.

C. HUANG and S. KOU are respectively Graduate Student and Professor in the Department of Materials Science and Engineering, University of Wisconsin, Madison, Wis.

KEY WORDS

Aluminum
Alloy 2219
Solidification Cracking
Liquation Cracking
Partially Melted Zone
Circular-Patch Test
Scheil Equation

Introduction

The partially melted zone (PMZ) is a region immediately outside the weld metal where liquation occurs during welding because of overheating above the eutectic temperature (or the solidus temperature if the workpiece is completely solutionized before welding) (Ref. 1). This is illustrated in Fig. 1. Since the grain boundaries are liquated, intergranular cracking can occur under the tensile strains induced by welding. Significant tensile strains are induced in the workpiece when it is restrained and unable to contract (due to solidification shrinkage and thermal contraction) freely upon cooling during welding. Liquation cracking often occurs in the PMZ along the fusion boundary. Aluminum alloys are known to be susceptible to liquation cracking in the PMZ during welding. Liquation and liquation cracking in aluminum welds have been the subjects of great interest in welding (Refs. 1–20).

Metzger (Ref. 3) observed liquation cracking in full-penetration gas tungsten arc (GTA) welds of Alloy 6061 made with Al-Mg filler metals at high dilution ratios, but not in similar welds made with Al-Si filler metals at any dilution ratios. This was confirmed by subsequent studies on 6061 and similar alloys such as 6063 and 6082 (Refs. 5, 7–12).

Gittos et al. (Ref. 5) used the circular-patch test (Ref. 21) to study liquation cracking in an aluminum alloy close to Alloy 6082 in composition. Liquation cracking occurred in full-penetration GTA welds made with the Al-5Mg filler metal at high-dilution ratios (about 80%) but not with the Al-5Si filler metal at any dilution ratios. They proposed that liquation cracking occurs when the base metal solidus temperature is below the weld-metal solidus temperature.

Katoh et al. (Ref. 7), Kerr et al. (Ref. 8), and Miyazaki et al. (Ref. 9) used the Varestraint test (Refs. 22, 23) to study liquation cracking in GTA and GMA welds of 6000 alloys (partial penetration). Their results contradicted the cracking condition of Gittos et al. (Ref. 5).

Huang and Kou (Ref. 24) studied liquation cracking in partial-penetration aluminum welds of Alloy 2219. The papillary (nipple) -type penetration common in GMAW with spray transfer was found to oscillate along the weld and cause cracking. Various filler metals, including 1100, 2319, 4047, 4145, and 2319 plus extra Cu, were used but did not eliminate liquation cracking.

Cross and Gutscher (Ref. 25) studied the effect of Cu and Fe content on the solidification cracking and liquation in Alloy 2519 using a circular-patch test.

The present study demonstrates the significant effect of the weld-metal solute content on liquation cracking in full-penetration welds. Alloy 2219 is selected, not as the subject of investigation, but as a tool for better understanding of liquation cracking.

Experimental Procedure

The circular-patch test (Ref. 21) was used to evaluate the susceptibility to liquation cracking. As shown in Fig. 2, the workpiece was highly restrained (by being bolted down to a thick stainless steel plate) in order to prevent it from contracting freely during welding. This allows

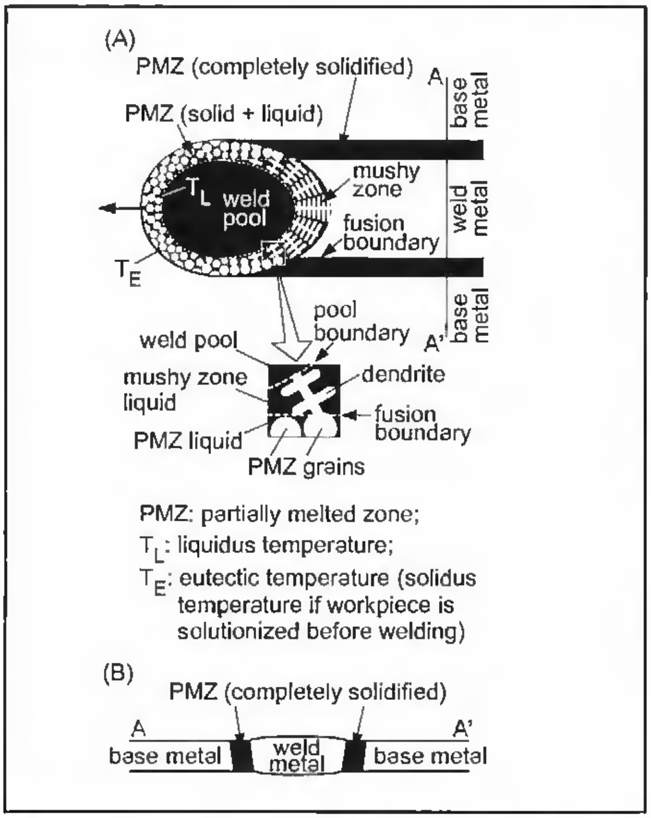

Fig. 1 — Formation of partially melted zone next to fusion boundary: A — top view; B — transverse cross section along AA' in A.

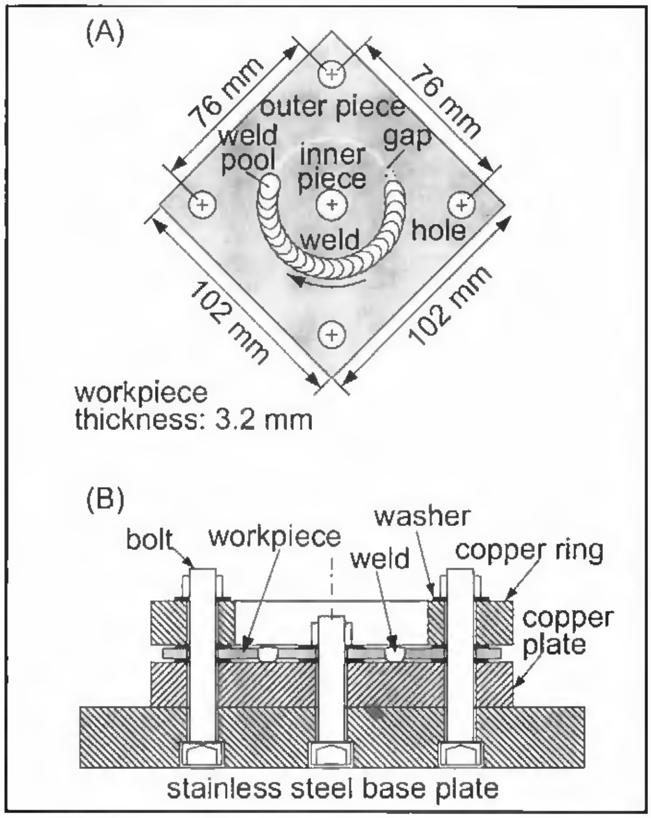

Fig. 2 — Circular-patch test. A — Top view of workpiece; B — side view of apparatus.

cracking to occur and be evaluated.

Alloy 2219-O was welded in the as-received condition, where the O-temper stands for overaging (Ref. 26). The actual compositions of the alloys and filler metals are listed in Table 1.

Table 1 — Compositions of Workpiece and Filler Metals in wt-%

	Cu	Mn	Mg	Cr	Zn	Ti	Si	Fe	Zr
					Workpiece				
1100	0.10	0.01	—	—	0.01	—	—	0.78	—
2219	6.30	0.33	—	—	0.01	0.03	0.08	0.12	0.12
					Filler Metals				
1100	0.08	0.01	—	—	0.02	—	0.08	0.52	—
2319	6.30	0.30	—	—	—	0.15	0.10	0.15	0.18

The workpiece consisted of two pieces. The outer piece was Alloy 2219, the inner piece was either Alloy 2219 or 1100, and filler metal was Alloy 1100, 2319, or 2319 plus extra Cu. By using different alloys as the inner piece and the filler metal, the weld-metal composition could be varied over a wide range.

The outer piece was 102 mm long, 102 mm wide and 3.2 mm thick, with a hole of 11.1 mm diameter in each corner. The inner piece was a circular patch 57.2 mm in diameter, with a hole of 12.7 mm at the center. The gap between the outer and inner pieces was about 0.25 mm. In one weld (Weld 2219/1100/1100B), the diameter of the inner piece (the circular patch) was changed to 50.8 mm to help adjust the weld-metal composition.

The outer piece was sandwiched between a copper plate (152 × 152 × 19 mm) at the bottom and a copper ring (19 mm thick, 83-mm ID, and 152 × 152 mm on the outside) at the top. The workpiece together with the copper plate and the copper ring were bolted down tightly to a stainless steel base plate of 203 × 203 × 25.4 mm. The bolts were tightened with a torque wrench to the same torque of 47.5 N·m to ensure consistent restraint conditions. A similar design was used by Nelson et al. (Ref. 27) for assessing solidification cracking in steel welds.

The workpiece was separated from the copper plate and the copper ring by washers (1.6 mm thick, 12.2-mm ID, and 23.5-mm OD). Without the washers, it was difficult to make full-penetration welds because of the heat sink effect of copper.

The extra Cu was a 99.999%-pure Cu wire of 1 mm diameter. When it was used, it was positioned in a 1-mm-deep groove of 50.8 mm diameter at the top surface of the circular patch. The Cu wire was placed in a 1-mm-wide groove. The extra Cu was GTA welded first to melt and mix with the surrounding base metal. The conditions for GTAW were 16 V, 75 A DCEN, and 7.4 mm/s welding speed (based on a rotation speed of 2.8 rpm and diameter of 50.8 mm) with Ar shielding. The resultant weld bead was fully penetrating and about 4 mm wide at the top, well within, and thus, fully incorporated into the subsequent GMA weld.

The welding parameters for GMAW were 4.2 mm/s welding speed (based on a 1.6-rpm rotation speed and a 50.8 mm diameter), 22-V, 140-A average current, and Ar shielding. The filler wire, 1.2 mm in diameter, was positioned at 25.4 mm from the center of the workpiece, and was fed at a speed of 93.1 mm/s. The distance between the contact tube and workpiece was about 25.4 mm, and the torch was perpendicular to the workpiece.

The macrostructure and microstruc-

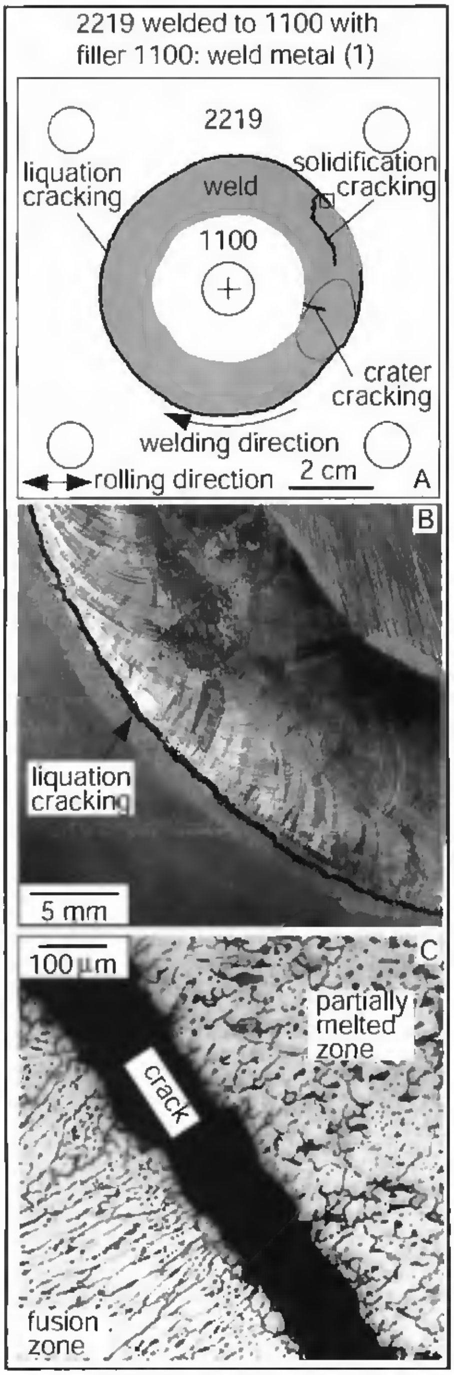

Fig. 3 — *Weld made between Alloy 2219 (outer piece) and Alloy 1100 (patch of 57.2 mm diameter) with filler metal 1100. A — Overview; B — macrograph; C — micrograph of area in square in A.*

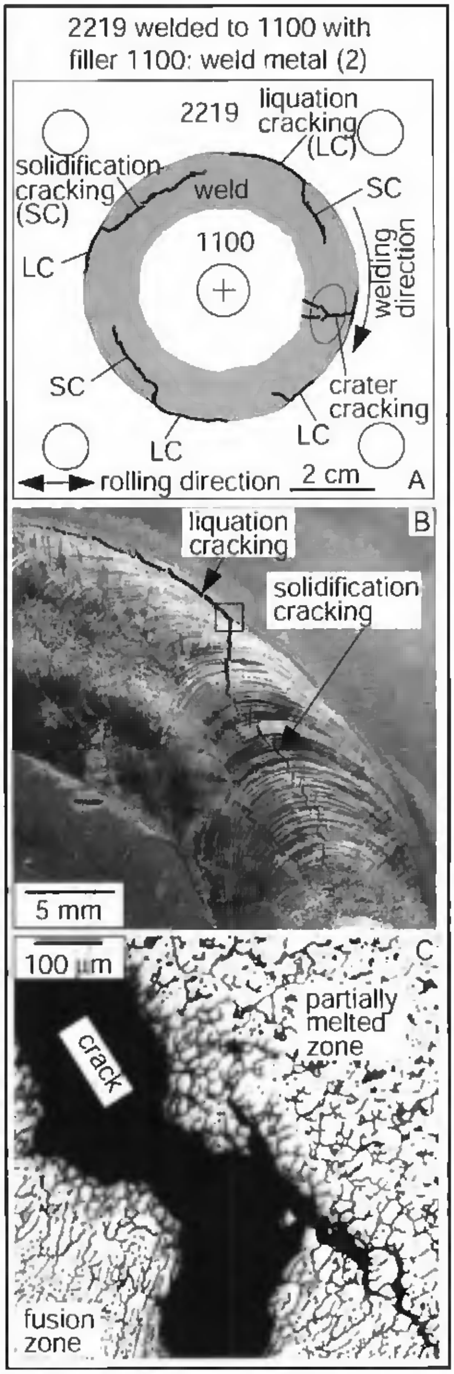

Fig. 4 — *Weld made between Alloy 2219 (outer piece) and Alloy 1100 (patch of 50.8 mm diameter) with filler metal 1100. A — Overview; B — macrograph; C — micrograph of area in square in B.*

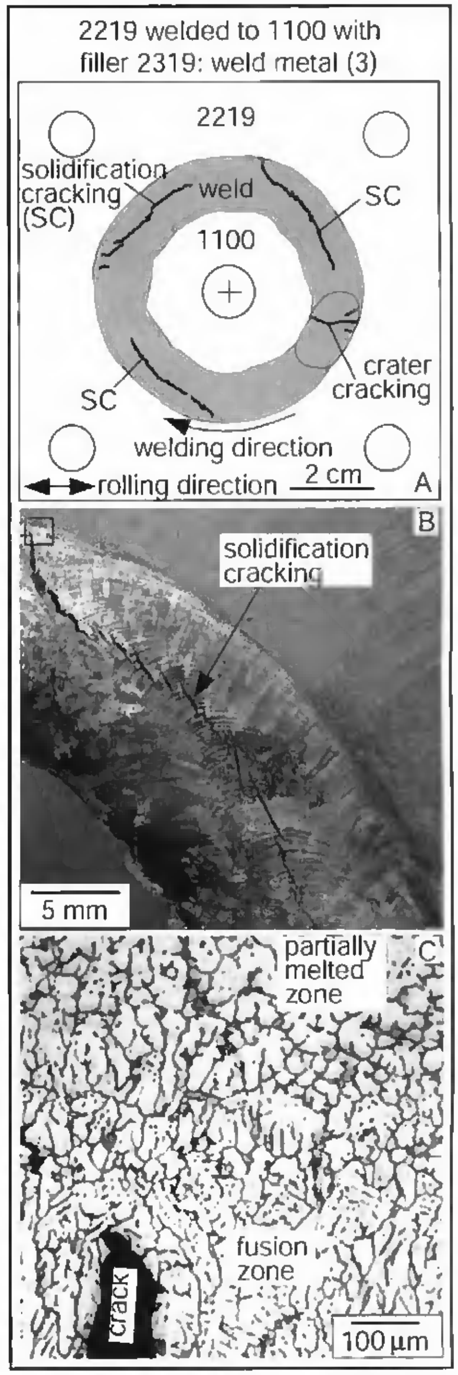

Fig. 5 — *Weld made between Alloy 2219 (outer piece) and Alloy 1100 (patch of 57.2 mm diameter) with filler metal 2319. A — Overview; B — macrograph; C — micrograph of area in square in B.*

ture of the resultant welds were examined. The surfaces of the resultant welds were cleaned with a solution of 48 vol-% HF in H_2O. Macrographs of the welds were taken with a digital camera. The welds were then sectioned and etched with a solution of 0.5 vol-% HF in water. The transverse cross-sectional area of each weld was determined with the help of computer software. The weld microstructure was examined with an optical microscope.

It has been shown that the composition of a single-pass GMA aluminum weld is essentially uniform (Ref. 28). The Lorenz force, surface-tension gradients, and droplet impingement help mix the filler metal with the melted base metal (Ref. 1). Thus, the concentration of an alloying element E in the weld metal was calculated from those in the base metals and the filler metal using the following equation:

$$\%\text{ element } E \text{ in weld metal} = [(\%E \text{ in base metal } A) \times a + (\%E \text{ in base metal } B) \times b + (\%E \text{ in filler metal } C) \times c] / (a + b + c) \quad (1)$$

where the areas a, b, and c are the areas in the weld transverse cross section that represent contributions from the base metal

A, base metal *B*, and filler metal *C*, respectively. They were determined from the area and location of the transverse cross section of the weld.

Results and Discussion

The percentage contributions from the inner piece, the outer piece, and the filler metal to the welds and the resultant weld-metal compositions are listed in Table 2. The experimental results are summarized in Table 3. For convenience, all welds are identified with a series of three numbers. The first, second, and third numbers refer to the outer piece, the inner piece (circular patch), and the filler metal used, respectively. For instance, Weld 2219/1100/2319 refers to a weld made by joining an outer piece of Alloy 2219 to an inner piece of Alloy 1100 with a filler metal of Alloy 2319.

Overviews: Macrographs and Micrographs of Welds

There were two 2219/1100/1100 welds. The one with a circular patch of 57.2 mm diameter will be called Weld 2219/1100/1100A, and the one (and the only one in the present study) with a circular patch of 50.8 mm diameter, called 2219/1100/1100B.

Figure 3A is the overview of the top of Weld 2219/1100/1100A that has been traced with the help of computer software from the digital photograph of the weld. The cracks were marked with thick lines for clarity. Such an overview was used instead of the photograph itself because cracks were too small to see at the magnification of the overview. The crater at the termination of welding was included in the figure but not the beginning of the weld (at the three o'clock position of the weld), which was welded over and replaced by the crater.

Weld 2219/1100/1100A had a weld-metal composition of Al-0.93Cu. As shown in Fig. 3A, it suffered from very severe liquation cracking (91% of the weld outer edge) and some solidification cracking (13% of the weld length). Figure 3B is a macrograph of the lower left region of the weld. Liquation cracking was evident along the outer edge of the weld, but there was no liquation cracking along the inner edge. In circular-patch welding, the workpiece is held tightly against a strong back (the stainless steel base plate in Fig. 2). This keeps the weld metal from contracting due to thermal contraction and solidification shrinkage when it cools. Consequently, the outer edge of the weld is in tension while the inner edge is in compression. This explains why liquation cracking was observed only along the outer edge of the weld.

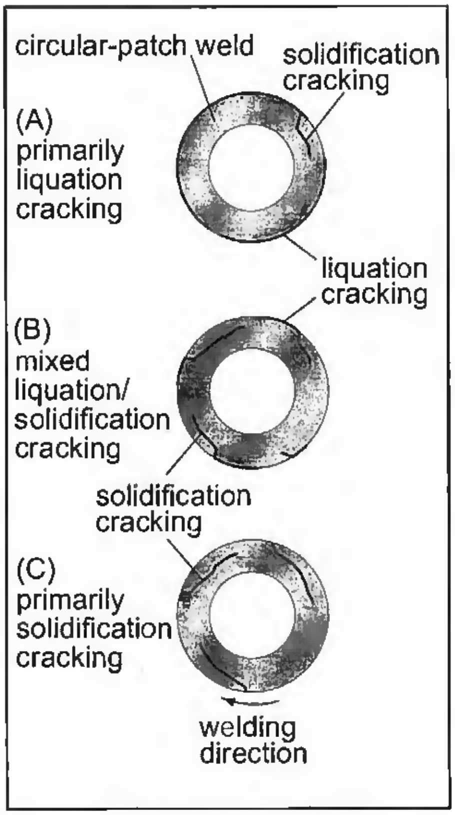

Fig. 6 — Three types of cracking observed. A — Primarily liquation cracking; B — mixed liquation/solidification cracking; C — primarily solidification cracking.

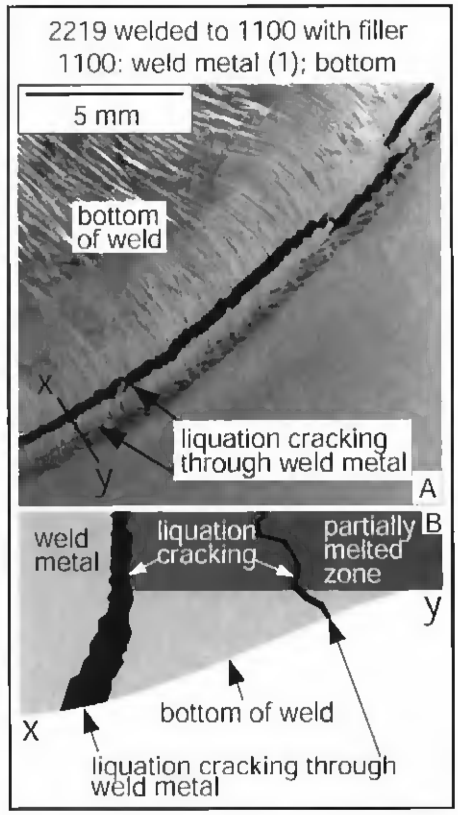

Fig. 7 — Cracking at bottom of weld. A — Bottom surface of weld in Fig. 3B; B — transverse cross section along line "xy," sketched according to micrograph observed (not shown due to space limit).

Figure 3C shows the microstructure inside the small square in Fig. 3A. The cellular/dendritic fusion zone was clearly different from the liquated PMZ. The liquation crack made a clear-cut separation of the two zones along the fusion boundary. No liquation cracking was observed inside the PMZ.

The weld-metal composition was raised to Al-2.32Cu in Weld 2219/1100/1100B to reduce liquation cracking. As shown in Fig. 4A, solidification cracking (49% of the weld length) was more and liquation cracking (28% of the outer weld edge) was less than those in Weld 2219/1100/1100A. Mixed liquation/solidification cracking was observed in four regions along the outer edge of the weld. It is interesting to note that in each region liquation cracking and solidification cracking did not coexist, that is, run side by side. Figure 4B shows cracking in the upper right region of the weld. It is evident that liquation cracking stopped at the point where solidification cracking started. This is probably because solidification cracking in the weld metal reduced the tensile strains in the adjacent PMZ significantly. In fact, a similar trend also was seen in the upper right region of Weld 2219/1100/1100A — Fig. 3A.

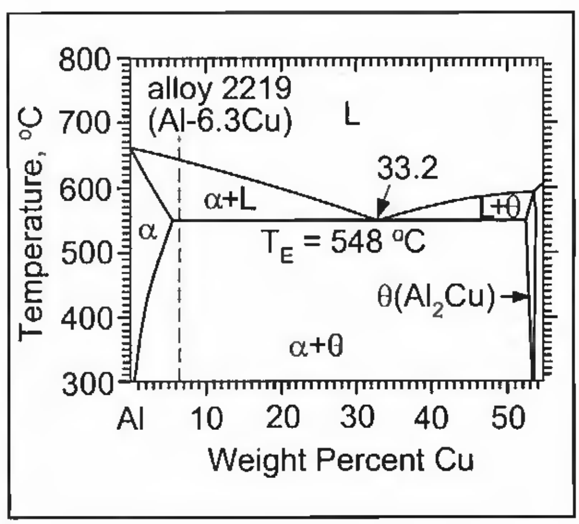

Fig. 8 — Aluminum-rich side of Al-Cu phase diagram (Ref. 30).

Table 2 — Compositions of Weld Metals

	Contribution from Outer Piece	Contribution from Inner Piece	Contribution from Filler Metal	Contribution from Extra Cu	Weld-Metal Composition
Weld metal (1) of weld 2219/1100/1100A	13.5% from 2219	52.3% from 1100	34.2% from 1100	—	Al-0.93Cu
Weld metal (2) of weld 2219/1100/1100B	36.0% from 2219	28.8% from 1100	35.2% from 1100	—	Al-2.32Cu
Weld metal (3) of weld 2219/1100/2319	21.5% from 2219	46.3% from 1100	32.2% from 2319	—	Al-3.43Cu
Weld metal (4) of weld 2219/2219/2319	65.3% from 2219 (both inner and outer pieces)		34.7% from 2319	—	Al-6.30Cu
Weld metal (5) of weld 2219/2219/2319+Cu	63.14% from 2219 (both inner and outer pieces)		35.52% from 2319	1.34% from Cu	Al-7.55Cu

Table 3 — Summary of Experimental Results

	Outer Piece/Inner Piece/Filler Metal				
	Weld 2219/ 1100/1100A	Weld 2219/ 1100/1100B	Weld 2219/ 1100/2319	Weld 2219/ 2219/2319	Weld 2219/ 2219/2319+Cu
Weld-metal composition	Al-0.93Cu	Al-2.32Cu	Al-3.43Cu	Al-6.3Cu	Al-7.55Cu
Liquation cracking (cm)	18.42	5.82	No	No	No
Liquation cracking (% of weld outer edge)	91	28	0	0	0
Solidification cracking (cm)	2.08	8.26	9.80	No	No
Solidification cracking (% of weld length(a))	13	49	60	0	0

(a) Weld length = (length of weld outer edge plus length of weld inner edge)/2.

Figure 4C shows the microstructure in the square of Fig. 4B. The solidification crack in the fusion zone was connected to the liquation crack at the weld interface. This suggests that liquation cracking can trigger solidification cracking. However, solidification cracking can also initiate within the fusion zone by itself and does not have to initiate at liquation cracks.

The weld-metal composition was further raised to Al-3.43Cu in Weld 2219/1100/2319 to reduce liquation cracking. Solidification cracking (60% of the weld length) took over completely, that is, liquation cracking disappeared. As shown in the overview in Fig. 5A, solidification cracking occurred in three different regions of the weld, each crack being about 3 to 4 cm long.

The macrograph in Fig. 5B shows solidification cracking in the upper right region of the weld. Cracking started from near the outer edge of the weld, propagated inward, and then followed the welding direction.

Figure 5C shows the microstructure of the weld inside the square in Fig. 5B, including the tip of the solidification crack near the fusion boundary. Clearly, solidification cracking initiated within the weld metal near the outer edge of the weld, and there was no liquation cracking in the PMZ.

As the weld-metal composition was increased to Al-6.30Cu in Weld 2219/2219/2319, which is the same as the composition of Alloy 2219 (Al-6.30Cu), neither liquation cracking nor solidification cracking occurred except for some solidification cracking inside the crater.

Finally, as the weld-metal composition was increased to Al-7.55Cu in Weld 2219/2219/2319+Cu, neither liquation cracking nor solidification cracking occurred, not even in the crater. Figure 6 summarizes the three types of cracking in the welds discussed above. It includes primarily liquation cracking (Fig. 3A), mixed liquation/solidification cracking (Fig. 4A), and primarily solidification cracking — Fig. 5A.

Locations of Cracking

The tensile strains in the weld are expected to be highest in the regions between the center of the workpiece and its four corners because the workpiece was bolted down at the center and near its four corners — Fig. 2. The weld could not have been subjected to uniform constraint during welding even if the washers were removed.

When liquation cracking was severe, it occurred essentially along the entire weld, as in the case of Weld 2219/1100/1100A (91% of the outer weld edge, Fig. 3A). However, when liquation cracking was less severe, it appeared to be located more or less in three regions: between the center of the workpiece and its lower left, upper left, and upper right corners. Weld 2219/1100/1100B is an example — Fig. 4A. The region between the center and the lower right corner was more complicated because of the overlapping between the beginning and the end of the weld. The rolling direction did not appear to have a significant effect on liquation cracking.

In fact, solidification cracking also appeared to be located more or less in the same three regions. Welds 2219/1100/1100A (Fig. 3A), 2219/1100/1100B (Fig. 4A), and 2219/1100/2319 (Fig. 5A) are examples. Solidification cracking can be initiated in a weld metal with a composition highly susceptible to solidification cracking when the weld pool enters the three regions. As already mentioned, when solidification cracks open up in the weld metal, tensile strains in the adjacent PMZ are greatly reduced and liquation cracking stops (or tends not to occur). This explains why liquation cracking switched to solidification cracking in Welds 2219/1100/1100A (Fig. 3A) and 2219/1100/1100B — Fig. 4A.

Bottom View of Liquation Cracking

Figure 7A shows the bottom surface of Weld 2219/1100/1100A. The crack did not look like liquation cracking because it ran parallel to but not exactly along the outer edge of the weld. It did not look like solidification cracking, either, because it did not move toward and propagate along the weld centerline. In fact, this crack was the bottom of the liquation crack shown in Fig. 3B.

The transverse cross section along line "xy" is shown schematically in Fig. 7B. During welding the molten metal at the bottom of the weld pool spread over the bottom surface of the PMZ, that is, the bottoms of the weld metal and the PMZ overlapped. The liquation crack along the

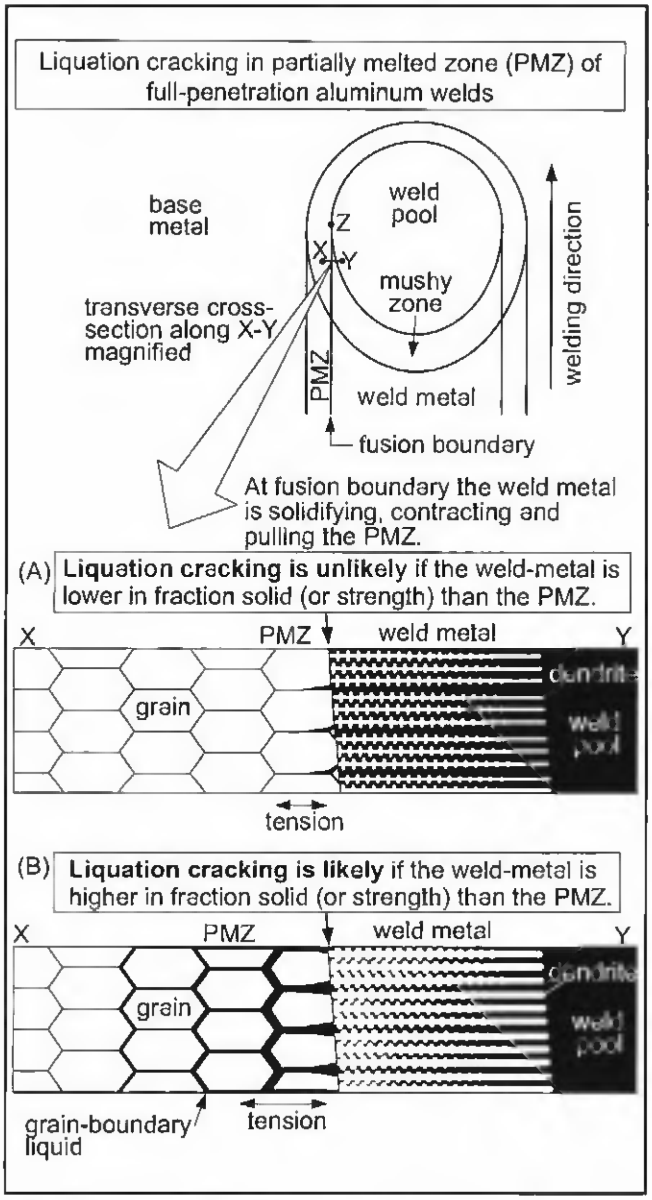

Fig. 9 — Liquation cracking in full-penetration aluminum welds: A — Liquation cracking unlikely; B — liquation cracking likely.

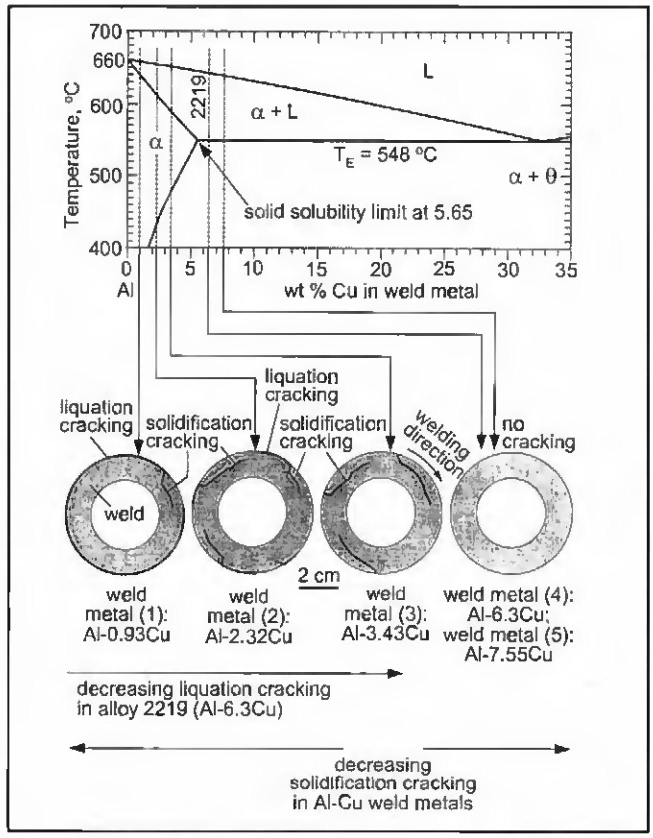

Fig. 10 — Effect of weld-metal composition on cracking in welds made in Alloy 2219.

fusion boundary propagated through the weld metal and ended up as a major crack at the bottom weld surface, while that in the PMZ also propagated through the weld metal and ended up as a minor crack at the bottom weld surface.

Mechanism of Liquation Cracking

Huang and Kou (Refs. 17, 19, 20) studied the mechanism of liquation in Alloy 2219. Figure 8 shows the Al-rich side of the Al-Cu phase diagram (Ref. 30). Cu-rich θ particles are present both along grain boundaries and within the grain interior. Upon reaching the eutectic temperature, the θ particles react with the surrounding α phase to form a eutectic liquid. Above the eutectic temperature, the eutectic liquid dissolves the surrounding α phase, increases in volume, and becomes hypoeutectic. Upon cooling, the hypoeutectic liquid solidifies first as a Cu-depleted α phase and finally as a Cu-rich eutectic.

The mechanism of liquation cracking is as follows. Liquation cracking is caused by the tensile strains induced in the solidifying PMZ by the solidifying and contracting weld metal that exceed the PMZ resistance to cracking. Therefore, liquation cracking requires the presence of both significant tensile strains in the PMZ and a susceptible PMZ microstructure.

Significant tensile strains are induced in the PMZ if the adjacent weld metal becomes stronger than the PMZ during PMZ solidification, and if the workpiece is severely restrained (for instance, in circular-patch testing) and thus unable to contract freely upon cooling. As the weld metal solidifies, it contracts because of solidification shrinkage and thermal contraction. The solidification shrinkage of aluminum is as high as 6.6% (Ref. 29). The thermal expansion coefficient of aluminum is roughly twice that of iron-based alloys. The grain-boundary liquid in the PMZ, however, does not contract significantly as it solidifies because of its much smaller volume than the weld pool. Consequently, the solidifying and contracting weld metal pulls the adjacent PMZ. The higher the solid fraction of the weld metal, the greater its strength and contraction are. For a given material, the tensile strains induced in the PMZ depend on the welding conditions, such as the heat input, welding speed, workpiece thickness, fixturing, type of weld (circular or linear), and so on. If the weld metal cracks, the tensile strains in the adjacent PMZ are relaxed. Tensile strains can also be imposed on the PMZ if external forces are applied to the workpiece during welding (for instance, in Varestraint testing).

A susceptible microstructure is present if the PMZ resistance to cracking is lowered by severe liquation. For a given material, the extent of liquation depends on the welding condition, such as the welding process, heat input, and welding speed. Therefore, for the same material under the same welding condition, the strength of the weld metal relative to that of the adjacent PMZ can have a significant effect on liquation cracking.

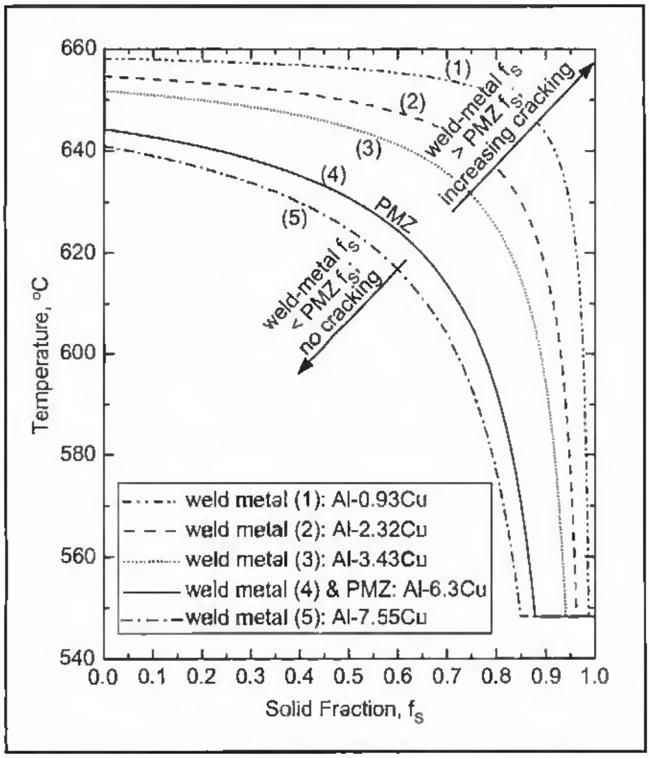

Fig. 11 — Temperature vs. solid fraction for the partially melted zone (PMZ) in Alloy 2219 and weld metals of various Cu contents.

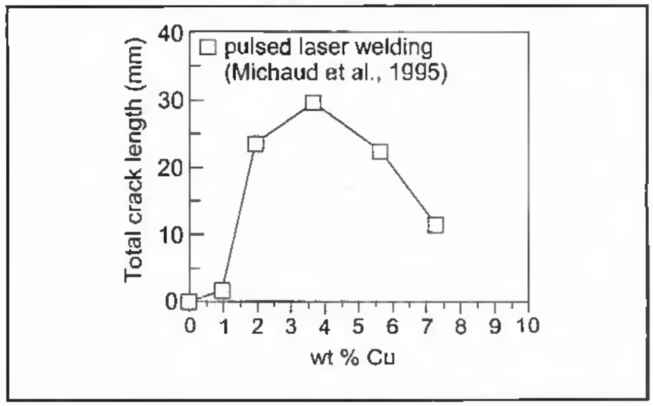

Fig. 12 — Effect of composition on solidification cracking sensitivity in pulsed laser Al-Cu welds (Ref. 33).

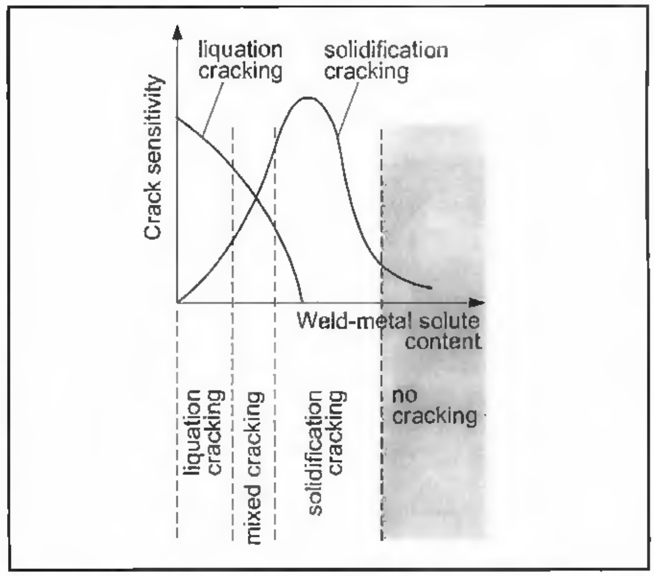

Fig. 13 — Effect of weld-metal solute content on liquation cracking and solidification cracking in full-penetration welds of a binary aluminum alloy such as 2219 (Al-6.3Cu).

Condition for Liquation Cracking

Gittos et al. (Ref. 5) proposed that liquation cracking occurs when the base-metal solidus temperature is below the weld-metal solidus temperature. However, the cooling rate during welding is too high for equilibrium solidification to exist, and solidification can continue far below the solidus temperature in an equilibrium phase diagram. A new condition for liquation cracking in full-penetration aluminum welds is proposed here.

Figure 9 shows schematically the microstructure at the fusion boundary. Consider the material at the junction between the weld pool and the fusion boundary, such as point Z. Here, the metal is completely melted both on the side of the weld pool and the side of the PMZ. As the weld pool travels a little further, the material at this point falls behind and is now at the position marked by the line XY. By now, the material has been cooling and solidifying. It consists of dendrites and interdendritic liquid on the weld-metal side, and grains and grain-boundary liquid on the PMZ side.

It is proposed that a weld metal higher in solid fraction and hence strength than the PMZ throughout PMZ solidification can cause liquation cracking if: 1) the workpiece is restrained tightly; 2) the PMZ is liquated heavily; and 3) there is no solidification cracking in the adjacent weld metal to relax the tensile strains in the PMZ. The strength of a semisolid depends primarily on the fraction of the solid phase in it, though the microstructure and the grain size can also affect the strength. Experimental data have shown that the strength of a semisolid aluminum alloy increases with increasing solid fraction (decreasing temperature) (Ref. 31).

This condition for liquation cracking in full-penetration aluminum welds is illustrated in Fig. 9. The PMZ is in tension because of the solidifying and contracting weld metal. In the case shown in Fig. 9A, at the fusion boundary the weld metal has a lower solid fraction and hence strength than the PMZ, which is only slightly liquated. Consequently, no liquation cracking occurs. In the case shown in Fig. 9B, on the other hand, at the fusion boundary the weld metal has a higher solid fraction and hence strength than the PMZ, which is severely liquated. Consequently, liquation cracking is likely to occur.

Effect of Weld-Metal Composition

Figure 10 summarizes the effect of the weld-metal composition on liquation cracking in full-penetration welds in Alloy 2219. The closer the weld-metal composition is to pure Al, the more severe liquation cracking can be. As the weld-metal Cu content increases, liquation cracking decreases.

The effect of the weld-metal composition on liquation cracking shown in Fig. 10 will be explained in the next section based on the curves of temperature vs. the solid fraction.

Temperature vs. Solid Fraction

As mentioned previously, equilibrium solidification does not exist during welding and nonequilibrium solidification needs to be considered. The simplest case of nonequilibrium solidification is that represented by the Scheil equation (Ref. 1). If the solidus line and the liquidus line of the binary phase diagram are assumed to be straight lines, the solid fraction f_S at any given temperature T can be calculated from the following Scheil equation:

$$f_s = 1 - \left(\frac{C_O}{C_L} \right)^{\frac{1}{1-k}} \quad (2)$$

where C_o is the solute content of the alloy, C_L the composition of the liquid at the solid/liquid interface at T, and k the equilibrium partition ratio. It can be shown (Ref. 32) that the Scheil equation can be rewritten as

$$f_s = 1 - \left(\frac{(-m_L)C_o}{T_m - T} \right)^{\frac{1}{1-k}} \quad (3)$$

where m_L (< 0) is the slope of the liquidus line in the phase diagram, and T_m the melting point of pure aluminum.

Consider first the effect of the weld-metal composition on liquation cracking in Alloy 2219 — Fig. 10. According to Equation 3, at any temperature T the lower the weld-metal solute content C_o, the greater the solid fraction f_S is. That is, the stronger the solidifying weld metal becomes and causes liquation cracking. This is consistent with the effect of the Cu content shown in Fig. 10. That is, the closer the weld-metal composition is to pure Al, the higher the susceptibility of Alloy 2219 to liquation cracking is, and the susceptibility decreases as the weld-metal Cu content increases.

Figure 11 shows the T-f_S curves calculated, based on the Scheil equation, for the PMZ in Alloy 2219 and weld metals of various Cu contents. As shown, Curve 1 for the Al-0.93Cu weld metal is well on the higher-f_S side of Curve 4 for the PMZ (Al-6.3Cu). This suggests that the weld metal was higher in solid fraction and hence strength than the PMZ during solidification. This helps explain why severe liquation cracking occurred in Weld 2219/1100/1100A (Weld metal 1 in Fig. 10). Similarly, Curve 2 for the Al-2.32Cu weld metal was on the higher-f_S side of Curve 4 for the PMZ, and this explains the liquation cracking in Weld 2219/1100/1100B (Weld metal 2 in Fig. 10).

Curve 3 for the Al-3.43 Cu weld metal was also on the higher-f_S side of Curve 4 for the PMZ. Surprisingly, liquation cracking did not occur (Weld metal 3 in Fig. 10). This is probably because solidification cracking occurred first, and the tensile strains in the adjacent PMZ were thus reduced significantly before liquation cracking had a chance to occur. As will be shown later, Al-Cu alloys are most susceptible to solidification cracking between 3 and 4% Cu. Since the weld metal was highly susceptible to solidification cracking and since it reached high solid fractions before the PMZ, solidification cracking occurred before liquation cracking.

The T-f_S curve for the Al-6.3Cu weld metal coincides with Curve 4 for the PMZ. Curve 5 for the Al-7.55Cu weld metal is on the lower-f_S side of Curve 4 for the PMZ. In neither case, the solidifying weld metal has a higher solid fraction and hence strength than the PMZ to cause liquation cracking. This helps explain why liquation cracking occurred neither in Weld 2219/2219/2319 (Weld metal 4 in Fig. 10) nor Weld 2219/2219/2319+Cu (Weld metal 5 in Fig. 10).

Solidification Cracking and Liquation Cracking

Figure 12 shows the curve of solidification cracking vs. composition from Michaud et al. (Ref. 33) for the pulsed laser beam welding of binary Al-Cu alloys. As shown, the maximum crack susceptibility occurs between 3 and 4% Cu, which is close to the maximum crack susceptibility at 3.43% Cu in the present study. As shown in Fig. 10, reducing liquation cracking by increasing the Cu content can encourage solidification cracking. In view of this, the weld-metal Cu content should be increased to beyond 3 to 4% Cu in order to avoid both solidification cracking and liquation cracking. This is further illustrated in Fig. 13 (shaded area).

Comparison with Partial-Penetration Welds

As already demonstrated, in full-penetration aluminum welds, liquation cracking can be eliminated by using filler metals to adjust the weld-metal composition. As shown by Huang and Kou (Ref. 24), however, in partial-penetration welds made in Alloy 2219, liquation cracking caused by oscillation of weld penetration can persist regardless of the filler metal used because penetration oscillation allows the weld metal to solidify and hence develop strength well ahead of the PMZ regardless of the weld-metal composition. Before a new penetration front arrives and liquates the PMZ grain boundaries immediately behind it, much weld metal has already been solidifying near these grain boundaries after the previous penetration front stopped.

Summary and Conclusions

In summary, in view of the susceptibility of many aluminum alloys to liquation cracking during welding, the present study was conducted to investigate liquation cracking in full-penetration aluminum welds. The simple binary Al-Cu Alloy 2219, which is easier to understand, was selected for studying liquation cracking. To test the susceptibility to liquation cracking, circular-patch welds were made by GMAW. To vary the weld-metal composition over a wide range, Alloy 2219 was welded either to Alloy 1100 or to itself with filler metals 1100, 2319, or 2319 with extra Cu. The compositions of the resultant welds varied from 0.93 to 7.55% Cu. The macrostructure and microstructure of the welds were examined. The curves of temperature (T) vs. solid fraction (f_S), were calculated for both the weld metal and the PMZ to analyze the competition between the solidifying weld metal and the solidifying PMZ.

The conclusions are as follows:

1) *Effect of weld-metal composition.* Liquation cracking can be severe when the weld-metal solute content is low and much lower than the base-metal solute content but decreases as the weld-metal solute content increases.

2) *Effect of solidification cracking.* Solidification cracking can occur if the weld-metal composition is in the range most susceptible to solidification cracking. Liquation cracking tends to be absent near solidification cracks probably because solidification cracking relaxes the tensile strains in the nearby PMZ.

3) *T-f_S curves.* The curves for the PMZ (same as the base metal) and the weld metal, which can be calculated based on the Scheil equation, do not intersect each other in binary-alloy welds such as Al-Cu welds. They show that for the Al-Cu welds that liquation-cracked, the weld-metal f_S exceeded the PMZ f_S throughout PMZ solidification. The curves, especially when coupled with the data of solidification cracking vs. composition, help understand how liquation cracking in full-penetration aluminum welds can be avoided by adjusting the weld-metal solute content.

4) *Mechanism of liquation cracking.* Liquation cracking is caused by the tensile strains, induced in the solidifying PMZ by the solidifying and contracting weld metal, that exceed the PMZ resistance to cracking. Under the same welding conditions, the tensile strains increase with increasing weld-metal f_S and workpiece restraint, and the PMZ resistance to cracking decreases with increasing PMZ liquation.

5) *Condition for liquation cracking.* A weld metal higher in f_S than the PMZ throughout PMZ solidification can cause liquation cracking in full-penetration aluminum welds if 1) the workpiece is restrained tightly; 2) the PMZ is liquated heavily; and 3) there is no solidification cracking in the adjacent weld metal to relax the tensile strains in the PMZ. This condition is different from that of Gittos and Scott (Ref. 5) based on equilibrium solidus temperatures, that is, liquation

cracking occurs when the base-metal solidus temperature is below the weld-metal solidus temperature. Equilibrium solidification does not exist in welding.

6) *Avoiding cracking.* In the case of binary-alloy welds such as Al-Cu welds, increasing the weld-metal solute content to reduce liquation cracking can encourage solidification cracking. Decreasing the weld-metal solute content to reduce solidification cracking can encourage liquation cracking. The weld-metal composition should be adjusted to where both types of cracking can be avoided, that is, beyond the solidification cracking range.

7) *Pattern of liquation cracking.* Liquation cracking initiates at, or in the PMZ near, the outer edge of the weld and propagates along the outer edge.

8) *Pattern of solidification cracking.* Solidification cracking initiates in the weld metal near the outer edge of the weld or from liquation cracks at the outer edge and moves inward to propagate more or less along the weld centerline.

9) *Liquation cracking at weld bottom.* At the bottom surface liquation cracking may not appear at the outer edge of the weld as expected but just inside the weld metal. This can occur if the weld metal spreads slightly over the bottom surface of the PMZ, thus allowing liquation cracking to propagate through the weld metal and reach its bottom surface.

10) *Comparison with partial-penetration welds.* As demonstrated in the present study, in full-penetration aluminum welds, liquation cracking can be eliminated by using filler metals to adjust the weld-metal composition. In partial-penetration aluminum welds, however, liquation cracking near the weld root caused by oscillation of weld penetration can persist regardless of the filler metal used because penetration oscillation allows the weld metal to solidify and hence develop strength well ahead of the PMZ regardless of the weld-metal composition (Ref. 24).

Acknowledgments

This work was supported by National Science Foundation under Grant No. DMR-0098776. The authors are grateful to Bruce Albrecht and Todd Holverson of Miller Electric Manufacturing Co., Appleton, Wis., for donating the welding equipment (including Invision 456P power source, and XR-M wire feeder and gun).

References

1. Kou, S. 1987. *Welding Metallurgy*, New York, N.Y.: John Wiley and Sons, pp. 239–262, pp. 137–138, and pp. 91–108.

2. Dudas, J. H., and Collins, F. R. 1966. Preventing weld cracks in high-strength aluminum alloys. *Welding Journal* 45(6): 241-s to 249-s.

3. Metzger, G. E. 1967. Some mechanical properties of welds in 6061 aluminum alloy sheet. *Welding Journal* 46(10): 457-s to 469-s.

4. Steenbergen, J. E., and Thornton, H. R. 1970. Quantitative determination of the conditions for hot cracking during welding for aluminum alloys. *Welding Journal* 49(2): 61-s to 68-s.

5. Gittos, N. F., and Scott, M. H. 1981. Heat-affected zone cracking of Al-Mg-Si alloys. *Welding Journal* 60(6): 95-s to 103-s.

6. Ma, T., and Den Ouden, G. 1999. Liquation cracking susceptibility of Al-Zn-Mg alloys. *International Journal for the Joining of Materials* (Denmark) 11(3): 61–67.

7. Katoh, M., and Kerr, H. W. 1987. Investigation of heat-affected zone cracking of GTA welds of Al-Mg-Si alloys using the Varestraint test. *Welding Journal* 66(12): 360-s to 368-s.

8. Kerr, H. W., and Katoh, M. 1987. Investigation of heat-affected zone cracking of GMA welds of Al-Mg-Si alloys using the Varestraint test. *Welding Journal* 66(9): 251-s to 259-s.

9. Miyazaki, M., Nishio, K., Katoh, M., Mukae, S., and Kerr, H. W. 1990. Quantitative investigation of heat-affected zone cracking in aluminum Alloy 6061. *Welding Journal* 69(9): 362-s to 371-s.

10. Gitter, R., Maier, J., Muller, W., and Schwellinger, P. 1992. Formation and effect of grain boundary openings in AlMgSi alloys caused by welding. *Proceedings of 5th International Conference on Aluminum Weldments*. Ed. D. Kosteas, R. Ondra, and F. Ostermann, Munchen, Germany: Technische Universita Munchen, p. 4.1.1.

11. Powell, G. L. F., Baughn, K., Ahmed, N., Dalton, J. W., and Robinson, P. 1995. The cracking of 6000 series aluminum alloys during welding. *Proceedings of International Conference on Materials in Welding and Joining*. Parkville, Victoria, Australia: Institute of Metals and Materials Australasia.

12. Ellis, M. B. D., Gittos, M. F., and Hadley, I. 1997. Significance of liquation cracks in thick section Al-Mg-Si alloy plate. *The Welding Institute Journal* (U.K.) 6(2): 213–255.

13. Schillinger, D. E., Betz, I. G., Hussey, F. W., and Markus, H. 1963. Improving weld strength in 2000 series aluminum alloys. *Welding Journal* 42: 269-s to 275-s.

14. Young, J. G. 1968. BWRA experience in the welding of aluminum-zinc-magnesium alloys. *Welding Journal* 47(10): 451-s to 461-s.

15. Lippold, J. C., Nippes, E. F., and Savage, W. F. 1977. An investigation of hot cracking in 5083-O aluminum alloy weldments. *Welding Journal* 56(6): 171-s to 178-s.

16. Huang, C., Kou, S., and Purins, J. R. 2001. Liquation, solidification, segregation and hot cracking in the partially melted zone of Al-4.5Cu welds. *Proceedings of Merton C. Flemings Symposium on Solidification Processing*. p. 229. Ed. R. Abbaschian, H. Brody, and A. Mortensen, Warrendale, Pa.: The Mineral, Metals and Materials Society.

17. Huang, C., and Kou, S. 2000. Partially melted zone in aluminum welds — liquation mechanism and directional solidification. *Welding Journal* 79(5): 113-s to 120-s.

18. Huang, C., and Kou, S. 2002. Liquation mechanism in multicomponent aluminum alloys during welding. *Welding Journal* 81(10): 211-s to 222-s.

19. Huang, C., and Kou, S. 2001. Partially melted zone in aluminum welds — planar and celluar solidification. *Welding Journal* 80(2): 46-s to 53-s.

20. Huang, C., and Kou, S. 2001. Partially melted zone in aluminum welds — solute segregation and mechanical behavior. *Welding Journal* 80(1): 9-s to 17-s.

21. Borland, J. C., and Rogerson, J. H. 1963. Examination of the patch test for assessing hot cracking tendencies of weld metal. *British Welding Journal* 8: 494–499.

22. Savage, W. F., and Lundin, C. D. 1965. The Varestraint test. *Welding Journal* 44(10): 433-s to 442-s.

23. Savage, W. F., and Lundin, C. D. 1966. Application of the Varestraint technique to the study of weldability. *Welding Journal* 45(11): 497-s to 503-s.

24. Huang, C., and Kou, S. 2003. Liquation cracking in partial-penetration aluminum welds: Effect of penetration oscillation and backfilling. *Welding Journal* 82(7): 184-s to 194-s.

25. Cross, C. E., Gutscher, D. 2003. Effect of Cu and Fe on weldability of aluminum 2519. *6th International Trends in Welding Research Conference Proceedings*, Eds. S. A. David, T. DebRoy, J. C. Lippold, H. B. Smartt, and J. M. Vitek, Materials Park, Ohio: ASM International, pp. 638–641.

26. The Aluminum Association. 1982. *Aluminum Standards and Data*. p. 15. Washington, D.C.: The Aluminum Association.

27. Nelson, T. W., Lippold, J. C., Lin, W., and Baeslack III, W. A. 1997. Evaluation of the circular patch test for assessing weld solidification cracking, I. Development of a test method. *Welding Journal* 76(3): 110-s to 119-s.

28. Houldcroft, R. T. 1954. Dilution and uniformity in aluminum alloy weld beads. *British Welding Journal* 1: 468–472.

29. Flemings, M. C. 1974. *Solidification Processing*. pp. 34–36, pp. 160–162, and Appendix B. New York: McGraw-Hill.

30. American Society for Metals. 1986. *Binary Alloy Phase Diagrams*. Vol. 1, p. 106. Metals Park, Ohio: ASM International.

31. Singer, A. R. E., and Cotrell, S. A. 1946. Properties of the Al-Si alloys at temperatures in the region of the solidus. *Journal of Institute of Metals* 73:33–54.

32. Kou, S. 2003. *Welding Metallurgy*, 2nd edition, New York, N.Y.: John Wiley and Sons, p.151.

33. Michaud E. J., Kerr, H. W., and Weckman, D.C. 1995. *Trends in Welding Research*. Eds. H. B. Smartt, J. A. Johnson, and S. A. David, Materials Park, Ohio: ASM International, p. 154.

Influence of Stress Ratio on Fatigue Crack Propagation Behavior of Stainless Steel Welds

Crack initiation and growth rates in relation to residual stresses were studied in gas metal arc welds of 316L

BY C. S. KUSKO, J. N. DUPONT, AND A. R. MARDER

ABSTRACT. The fatigue crack propagation behavior of 316L stainless steel gas metal arc welds has been investigated using the K-increasing testing procedure. A series of stress ratios from 0.10 to 0.80 was investigated in order to observe the influence of stress ratio and stress intensity range on the fatigue crack growth rate. A stress ratio of 0.55 has been shown to overcome closure for all the gas metal arc welds tested. Crack closure measurements obtained through the compliance offset method were utilized to explain the increase in crack growth rate and decrease of crack closure as the stress ratio is increased. The increase in fatigue crack growth rate, which occurs as the stress ratio is increased from 0.10 to 0.55, is generally attributed to an extrinsic crack opening effect in which higher stress ratios promote a fully open crack and corresponding higher growth rates. Continued increase in the crack growth rate that occurs as the stress ratio is increased further from 0.55 to 0.70 is attributed to a true intrinsic material response to increasing stress ratio.

Introduction

Conventional arc welds can represent stress concentrations in load-bearing structures because of geometry changes and defects associated with welding. Since welding serves as a prominent joining process for many structural applications, weld-related features can aid in the initiation of cracks. When considered in conjunction with welding residual stresses, propagation of such cracks can become a concern during service. Consequently, an understanding of the fatigue crack propagation behavior of welds is important. Maddox (Ref. 1) and Parry et al. (Ref. 2) have shown that the fatigue crack growth behavior of welds can be characterized by the well-known Paris equation, which relates the fatigue crack growth rate, da/dN, to the stress intensity range, ΔK (Ref. 3)

$$\frac{da}{dN} = C(\Delta K)^n \tag{1}$$

where a is the crack length, N is the number of cycles, and C and n are material constants. The stress intensity range, ΔK, is given by the difference between the maximum and minimum applied stress intensity of the load cycle, $\Delta K = K_{max} - K_{min}$. While the stress intensity range is the main factor that governs the crack growth rate, the stress ratio, R, (ratio of minimum to maximum applied stress intensity) can also influence the crack growth rate. The resulting effect of an increase of R on da/dN has been investigated for wrought stainless steels (Ref. 4), carbon steels (Ref. 5), alloy steels (Refs. 6–8), aluminum (Refs. 9–12), and titanium alloys (Ref. 9). Generally, an increase in R results in an increase in da/dN for a given stress intensity range, ΔK. This influence of R can essentially come from two sources — a true material dependence of crack growth rate on R (i.e., an intrinsic material effect) and/or a crack closure effect. Crack closure refers to the condition in which the crack is not fully open during the entire loading cycle. In this condition, only a portion of the applied stress serves to drive crack propagation. Crack closure is most often attributed to residual stresses. For example, if the crack enters into a compressive stress field, the compressive stress will counteract the applied tensile stress. If the compressive stress is larger than the minimum applied stress, then the crack may remain closed during a portion of the load cycle. In this case, it is useful to identify an opening stress intensity value, K_{op}, where K_{op} represents the minimum stress intensity required to keep the crack fully open. In short, if the minimum applied stress intensity, K_{min}, is below K_{op}, then the crack will be closed whenever the applied stress intensity drops below K_{op}. Under this condition, the fully applied stress intensity range, ΔK, does not contribute to crack propagation, and it is useful to define an effective stress intensity range, ΔK_{eff}, where ΔK_{eff} is given by $K_{max} - K_{op}$. Under this condition, ΔK_{eff} represents the true driving force for crack propagation. Lastly, it is important to note that one cannot separate an intrinsic crack growth rate dependence on R from a crack closure effect unless the condition at which crack closure occurs is identified during testing.

Crack closure has been applied to explain the influence of R over various regimes of da/dN (Refs. 9–11, 13–15). However, most previous research was conducted on wrought test specimens that are not subject to the residual stresses prevalent in welded samples. An investigation of alloy steel arc welded joints for R ratios of 0.00 and 0.50 showed no increase in da/dN as R increased (Ref. 16). That is, the da/dN-ΔK curves essentially overlapped for all decades of crack growth. Since the test samples were oriented such that crack propagation occurred within the weld metal along the direction of welding, such behavior has been attributed to tensile residual stresses that were encountered within the weld metal. The presence of these tensile residual stresses promotes a completely open fatigue crack at all stages of loading. That is, crack closure, or premature closure of the crack tip during loading, would not be expected to influence the crack growth behavior.

To correctly evaluate the influence of crack closure, accurate assessment of the crack opening load, P_{op}, during testing is crucial as it serves as the foundation for

KEY WORDS

Residual Stress
Crack Initiation
Crack Growth
Stainless Steel
Gas Metal Arc
K-Increasing Test

C. S. KUSKO is Research Assistant; J. N. DUPONT is Associate Professor and Director, Joining and Laser Processing Laboratory; and A. R. MARDER is Professor, Department of Materials Science and Engineering, Lehigh University, Bethlehem, Pa.

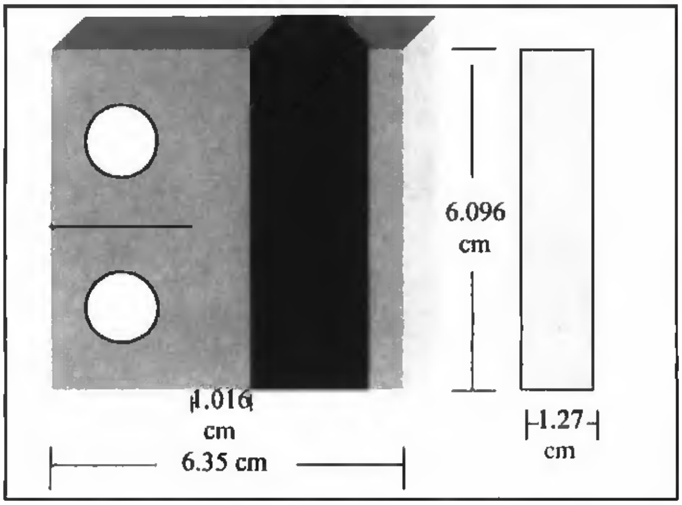

Fig. 1 — Schematic illustrations of C(T) specimens corresponding to gas metal arc weld of AB orientation.

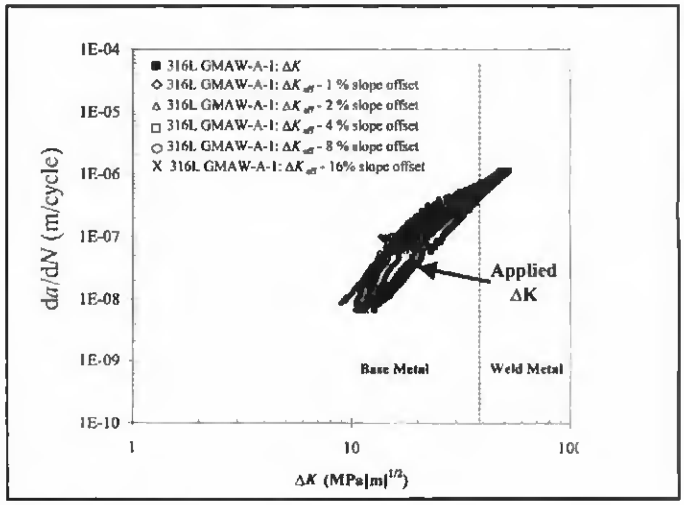

Fig. 2 — Slope offset data for 316L GMAW tested at an R ratio of 0.10.

Table 1 — Chemical Compositions (in wt-%) of 316L Base Metal and Filler Metal

	316L SS Base Metal	316L Filler Metal
Ni	10.16	12.17
Cr	16.12	18.20
Fe	68.85	64.43
Mo	2.05	2.53
Mn	1.71	1.66
Cu	0.44	0.10
Si	0.41	0.86
C	0.017	0.016
P	0.027	0.017
S	0.0011	0.014

Table 2 — Gas Metal Arc Welding Parameters

Parameter	Value
Base metal	316L
Backing bar	316L
Welding wire	316L
Welding wire diameter, mm	1.5875
Voltage, V	25–26
Current, A	280
Wire speed, cm/min	469.9
Carriage speed, cm/min	38.10
Welding position	flat
Shielding gas	98%Ar/2%O_2
Number of layers	6
Number of passes	16
Preheat temp, °C	24
Interpass temp, °C	149

K_{op} and concomitant ΔK_{eff} calculations. A standardized compliance-based slope offset method has been previously utilized for the investigation of both ΔK and ΔK_{eff} for homogeneous wrought aluminum test specimens (Ref. 17). However, this method has yet to be systematically applied to welds that are susceptible to significant residual stresses. The purpose of this research is to investigate the fatigue crack propagation behavior of stainless steel gas metal arc welds in order to observe how R influences such behavior.

Experimental Procedure

The 316L base metal and filler metal compositions used to prepare the weld samples are provided in Table 1. Weld samples were prepared by gas metal arc welding on base metals (dimensions 1.905 × 15.24 × 60.96 cm) by deposition of multiple passes on an automatic table using a 90-deg torch angle to the plate. The contact tip distance varied from 19.05 mm at the root to 12.70 mm from mid-plate to cap because of the addition of subsequent filler metal passes. Table 2 provides further details on the processing parameters.

Compact tension (C(T)) test specimens required for fatigue crack propagation testing were removed from the gas metal arc welds. Specimen dimensions conformed to those stated in American Society for Testing and Materials (ASTM) Standard E647 (Ref. 19). Figure 1 shows a schematic illustration of final dimensions, along with specimen orientation with respect to the fatigue crack starter notch and welding direction. The crack starter notch was inserted within the base metal normal to the direction of welding such that the distance from the end of the notch to the start of the weld metal on the front face was approximately 1.016 cm. The fatigue crack starter notch of length 2.54 cm, diameter 0.1524 mm, and radius of curvature 0.0762 mm was inserted by wire electrical-discharge machining (EDM). The configuration illustrated in Fig. 1 is designated as orientation AB. This two-letter system for describing weld C(T) specimen orientation was utilized by James and co-workers (Refs. 21, 22) and is based on the designations adopted for wrought specimens by ASTM in Standard E399 (Ref. 23). In this system, the first letter represents the direction of applied loading while the second letter represents the direction of crack extension. In addition, A, B, and C symbolize the direction of welding, normal to the direction of welding, and the thickness direction, respectively. It has been observed that orientation AB, for which crack propagation occurs normal to the welding direction, would be most affected by residual stresses (Ref. 22).

All fatigue crack propagation testing was conducted in accordance with ASTM E647. Compliance measurements were recorded on both loading and unloading portions of the load-displacement curve. For the C(T) specimen, the following polynomial expression was utilized for determination of the normalized crack length, a/W, as a function of compliance, $BE\delta/P$ (Ref. 24).

$$\frac{a}{W} = 1.00098 - 4.66951X + 18.4601X^2 - 236.825X^3 + 1214.88X^4 - 2143.57X^5 \quad (2)$$

where (Ref. 24)

$$X = \frac{1}{\left(\frac{BE\delta}{P}\right)^{\frac{1}{2}} + 1} \quad (3)$$

In Equation 3, E is the modulus of elasticity. The term $BE\delta/P$ is referred to as the normalized compliance and is measured as a function of N. Once a/W has been cal-

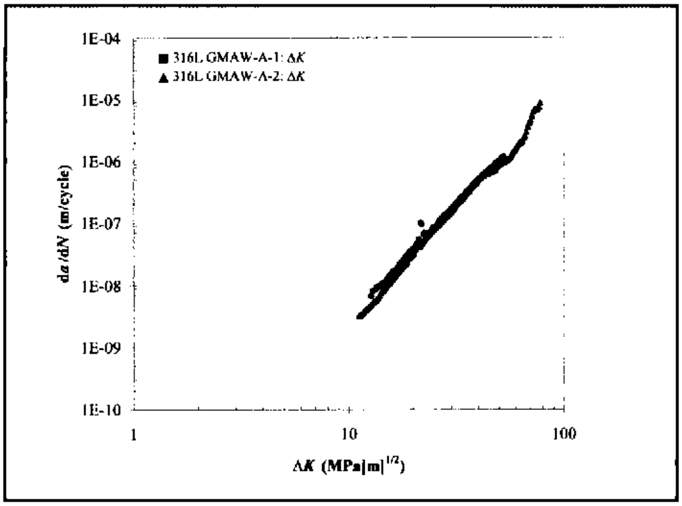

Fig. 3 — Comparison of 316L GMAW fatigue data tested at an R ratio of 0.10.

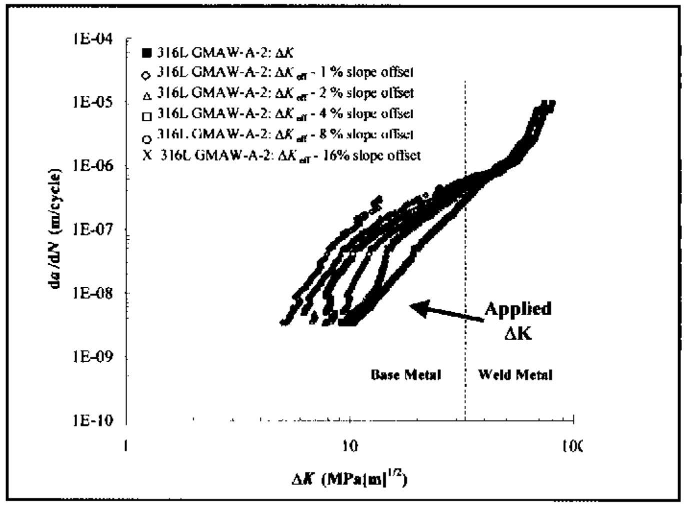

Fig. 4 — Slope offset data for 316L GMAW tested at an R ratio of 0.10.

culated from Equation 2, the following expression developed for the C(T) specimen was used to calculate K (Ref. 25)

$$\frac{KBW^{\frac{1}{2}}}{P}=\left(\frac{2+\frac{a}{W}}{\left(1-\frac{a}{W}\right)^{\frac{3}{2}}}\right)\left(\begin{matrix}0.886+4.64\left(\frac{a}{W}\right)\\-13.32\left(\frac{a}{W}\right)^{2}\\+14.72\left(\frac{a}{W}\right)^{3}-5.6\left(\frac{a}{W}\right)^{4}\end{matrix}\right) \quad (4)$$

Displacement was measured using an MTS clip gauge attached to knife-edges on the front edge of the C(T) specimen.

All testing was conducted using constant amplitude loading and a sine waveform at a frequency of 25 Hz at room temperature. Testing was performed under K-gradient control at constant R ratios of various magnitudes to determine the influence on fatigue crack growth. Data were generated using K-increasing procedures (Ref. 26), according to the equation (Ref. 24)

$$K_{\max}=K_{\max,0}\,e^{C\left(a-a_0\right)} \quad (5)$$

where C, the normalized K-gradient, represents the fractional rate of change with increasing a, such that (Ref. 27)

$$C=\frac{1}{K_{max}}\frac{dK_{max}}{da} \quad (6)$$

The K-increasing tests were run with a C value of 0.118 mm^{-1}. On all samples, precracking was conducted until the crack propagated 1.27 mm, after which, all ensuing da/dN were measured. The compliance-based crack lengths, measured as a function of N, were converted to da/dN using a modified version of the secant method (Ref. 28), which requires the calculation of the slope of a straight line connecting specified points on the a-N curve.

Results and Discussion

Fatigue Crack Propagation Results

Fatigue crack propagation data obtained from testing at an R ratio of 0.10 are shown in Fig. 2. The dotted line in the figure denotes the location where the fatigue crack crossed from the base metal into the weld metal. The solid black squares represent applied da/dN-ΔK data. The open symbols correspond to ΔK_{eff} data generated for various slope offset levels from 1% to 16% obtained from the compliance-based slope offset method, as described in Ref. 17. In this figure, the ΔK_{eff} curve for 1% slope offset level is farthest from the applied ΔK curve, while the ΔK_{eff} curve for 16% slope offset data is closest to the applied ΔK data. As explained in Ref. 17, the slope offset method may generate "artificial" crack closure information even if closure is not actually influencing crack growth. Such artificial measurements are easily identified through analysis of da/dN-ΔK and ΔK_{eff} curves for the various slope offset levels (Ref. 17) in the following manner. Once all slope offset curves are plotted, it is determined whether unique slope offset curves result for each slope offset level or a single, overlapping curve is present for all slope offset levels. Unique da/dN curves for each slope offset level, as shown for most of the crack growth rates in Fig. 2, indicate legitimate crack closure data, signifying true crack closure. However, overlap of all slope offset level curves indicates that the software has "artificially" generated crack closure data, thus indicating that the crack is fully open and the effective stress intensity range is equal to the applied stress intensity range.

In Fig. 2, unique da/dN curves are evident for each slope offset level up to da/dN of ~10^{-6} m/cycle. Thus, crack closure is significantly influencing crack growth behavior up to this level of crack growth rate at an R ratio of 0.10. At da/dN greater than ~10^{-6} m/cycle, the slope offset curves for the five offset levels begin to converge to a single ΔK_{eff} curve, indicating that the crack is fully open beyond this growth rate. Under this condition, the K_{min} has increased to a point where it exceeds K_{op} and the crack is fully open in the growth rate regime above ~10^{-6} m/cycle.

A second specimen of 316L weld was tested at an R ratio of 0.10 (over a wider crack growth rate) in order to assess the reproducibility of the results. The applied da/dN-ΔK curves for the two tests are shown in Fig. 3 and exhibit good agreement. In addition, Fig. 4 shows compliance offset data. These results are also in good agreement with Fig. 2, verifying a significant influence of crack closure during testing at R = 0.10 up to growth rates of ~10^{-6} m/cycle, at which point the curves converge, and the crack is fully open above a growth rate of ~10^{-6} m/cycle. Thus, only one specimen was tested at each of the remaining R ratios.

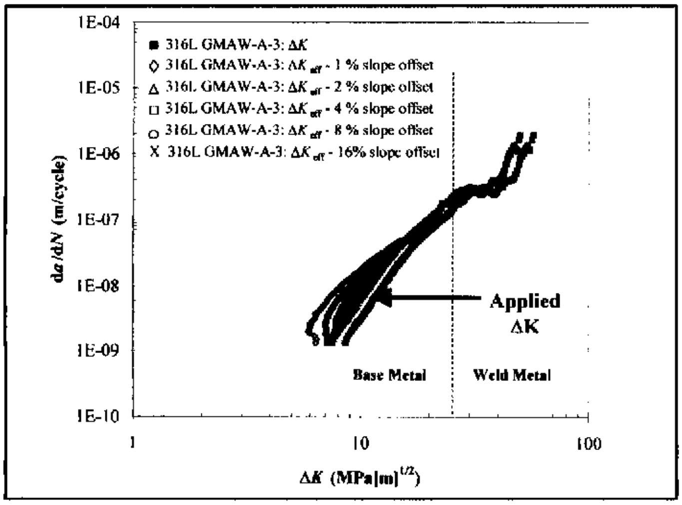

Fig. 5 — Slope offset data for 316L GMAW tested at an R ratio of 0.40.

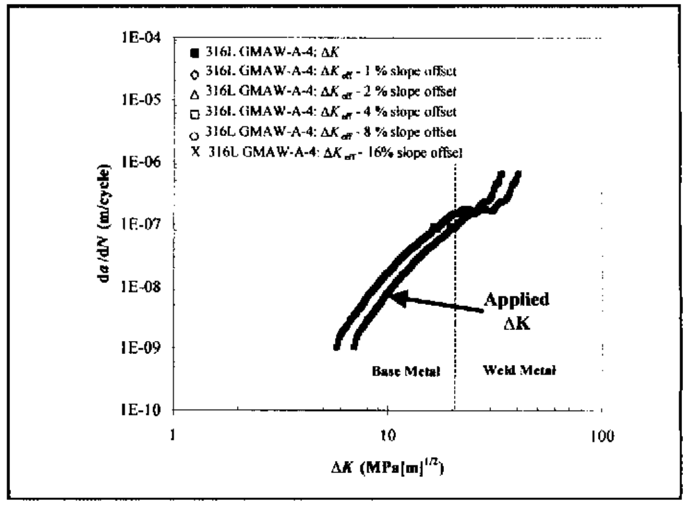

Fig. 6 — Slope offset data for 316L GMAW tested at an R ratio of 0.55.

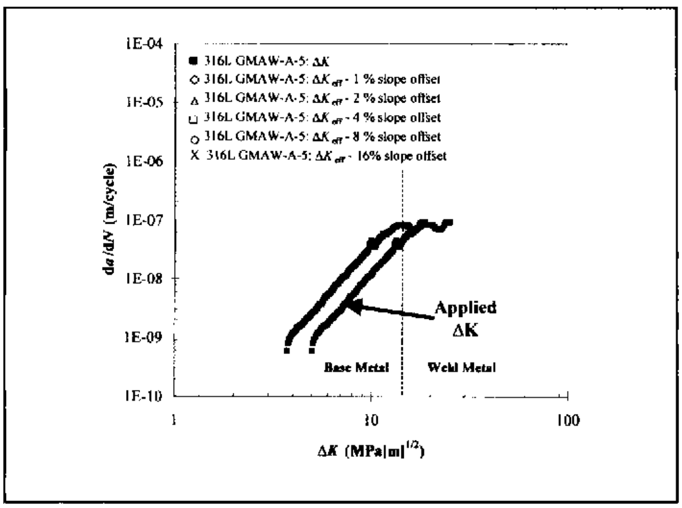

Fig. 7 — Slope offset data for 316L GMAW tested at an R ratio of 0.70.

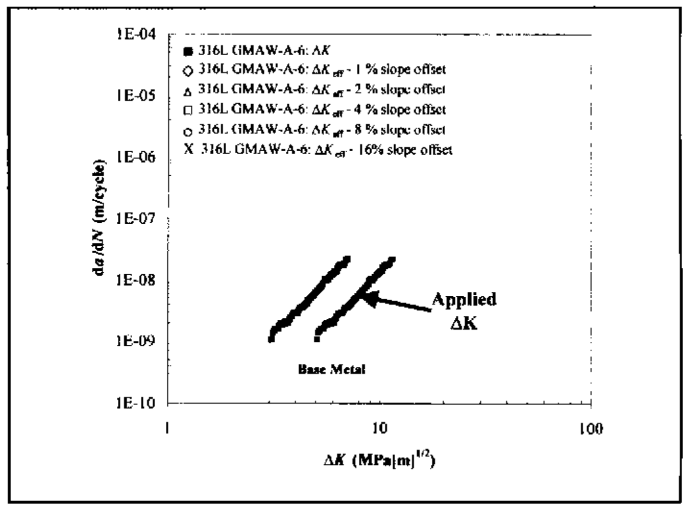

Fig. 8 — Slope offset data for 316L GMAW tested at an R ratio of 0.80.

Based on the results of Figs. 2 and 4, the R ratio was increased to higher values in an attempt to overcome closure. These results are shown in Figs. 5–8. Figure 5 ($R = 0.40$) shows a true influence of crack closure below much lower da/dN values ($\sim 5 \times 10^{-8}$ m/cycle) than Figs. 2 and 4. Thus, because of the higher stress intensity ratio, K_{min} exceeds K_{op} at much lower crack growth rates and forces the crack to remain open at lower growth rates. Figure 6 ($R = 0.55$) exhibits a single ΔK_{eff} curve for all slope offset levels (i.e., only one offset curve is visible in the figure because all the offset curves lie on top of one another), indicating the crack is always fully open and $\Delta K = \Delta K_{eff}$ over the entire growth rate regime. As exhibited in Figs. 7 and 8, closure is also overcome for all da/dN at R ratios corresponding to 0.70 and 0.80. Figure 9 shows the applied da/dN-ΔK data from Figs. 2, 3, and 5–8 on a single plot. This figure illustrates that as the R ratio increases, da/dN also increases for a given ΔK. For each respective R ratio test, this behavior occurs up to a specific da/dN at which the curves appear to coincide. The samples tested at R ratios of 0.70 and 0.80 exhibit crack growth rates that are similar over a wide range of crack growth rates.

Influence of R Ratio on Crack Growth Behavior

Figure 9 illustrates a general increase in da/dN with R for a given ΔK up to the point where $R = 0.70$. The curves corresponding to R ratios of 0.70 and 0.80 are essentially equivalent, while the curves for R ratios of 0.10, 0.40, and 0.55 show dependence on R. The dependence of da/dN on the R ratio at lower da/dN, followed by a convergence to a single curve at higher da/dN, has been previously observed for wrought aluminum alloys (Ref. 10). However, relatively little research has been conducted on stainless steel welded specimens. In addition, the condition at which the crack is partially closed is not always identified and, as a result, it is often not possible to separate an extrinsic effect of R (i.e., crack closure) from a true intrinsic, material behavior effect. In this work, identification of closure conditions permits separation of closure effects from true material dependence of crack growth rate on R. An influence of R has been observed for 304 austenitic stainless steel for a series of R ratios ranging from 0.05 to 0.75 at elevated temperatures (Ref. 4). That work was completed on wrought specimens rather than welds and did not consider crack closure measurements. Thus, based on the limited available research of austenitic stainless steel welds, it is useful to verify whether crack closure can explain the influence of R ratio on da/dN for these welded specimens.

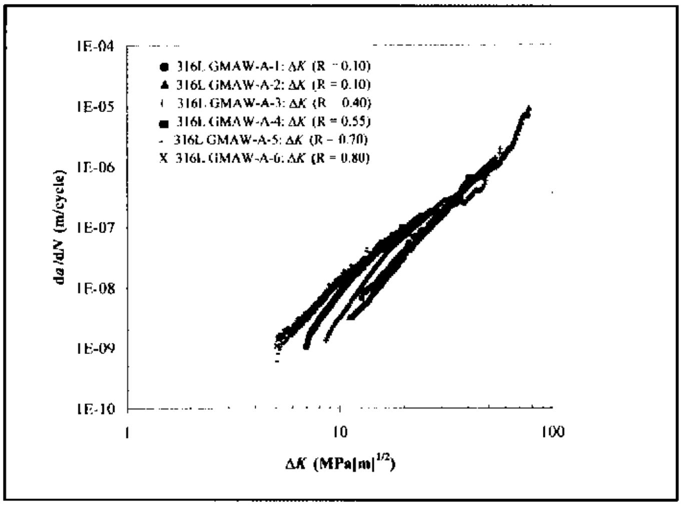

Fig. 9 — 316L GMAW data tested at a series of R ratios.

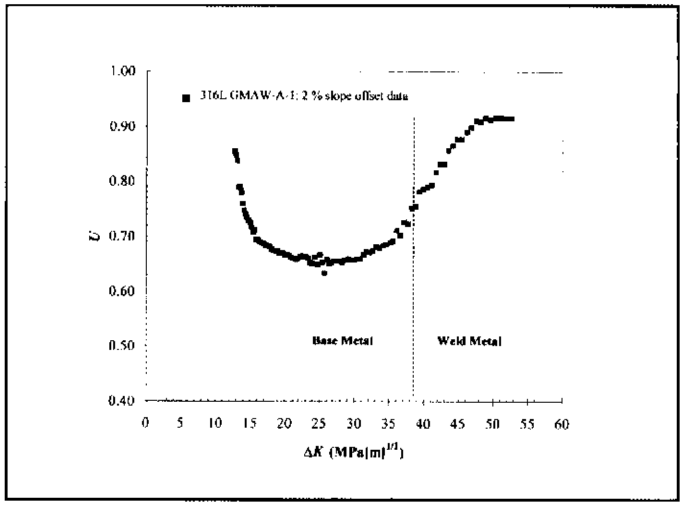

Fig. 10 — U vs. ΔK for 2% slope offset data for 316L GMAW tested at R = 0.10.

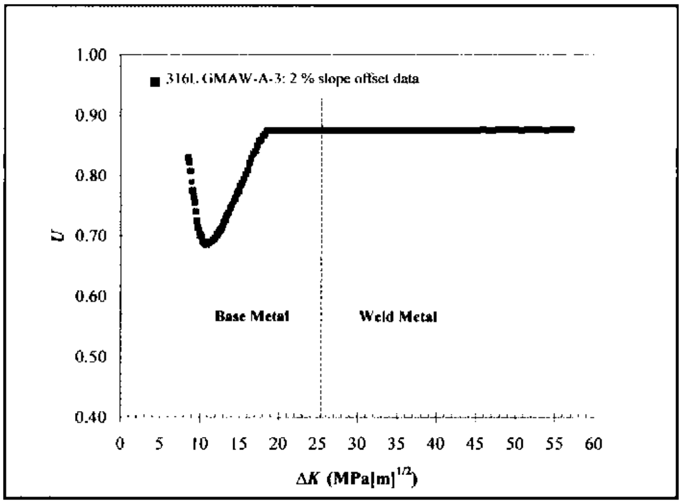

Fig. 11 — U vs. ΔK for 2% slope offset data for 316L GMAW tested at R = 0.40.

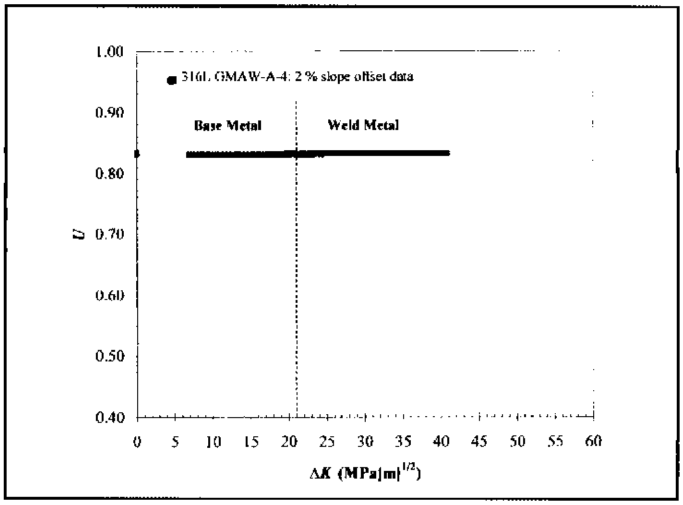

Fig. 12 — U vs. ΔK for 2% slope offset data for 316L GMAW tested at R = 0.55.

Crack closure behavior can be quantitatively characterized by the effective stress range ratio, U, which is defined as the ratio of ΔK_{eff} to ΔK (Ref. 31). As U increases toward a value of unity, the influence of crack closure diminishes. In other words, a value of U equal to one represents a completely open crack and a condition in which the applied stress intensity range, ΔK, is equal to the effective stress intensity range, ΔK_{eff}. As U decreases, the crack is closed during a larger portion of the loading cycle, and crack closure has a larger influence on the growth rate. Such knowledge can be applied to the da/dN data shown in Fig. 9 to determine if crack closure explains the da/dN dependence on R. Figure 10 illustrates the relationship between U and ΔK for the 316L weld tested at an R ratio of 0.10. In this figure, only 2% slope offset data are presented, as this offset level has been recommended as the most accurate (Ref. 17).

Since, as previously discussed, the compliance offset software generates artificial crack closure measurements even when crack closure is not actually being detected, ΔK_{eff} will appear to have a value that differs in magnitude from ΔK even when the crack is fully open. However, these values are actually equal when there is no influence from crack closure. Consequently, for the current analysis, U will never actually equal a value of one. However, closure-free conditions are easily identified when U becomes constant and nearly equal to unity. For example, in Fig. 10, a closure-free condition is identified as the horizontal portion of the curve where U is constant and equal to 0.92, which occurs over limited ΔK above approximately 50 MPa$\sqrt{m}$. This figure verifies the dominant influence of crack closure for the weld samples tested at an R ratio of 0.10. Over a significant range of ΔK (approximately 14 MPa$\sqrt{m}$ to 26 MPa$\sqrt{m}$), U decreases with an increase in ΔK. That is, the crack closure level initially increases with ΔK at lower ΔK. This can most likely be attributed to the crack entering a compressive residual stress field in the base metal from welding. However, as ΔK increases, K_{min} starts to approach K_{op} and the level of crack closure decreases (U increases). This trend continues until U = 0.92, at which point K_{min} exceeds K_{op}, closure is overcome completely, and the crack is fully open. Thus, the increase in U and corresponding decreases in crack closure can be attributed to the increase in applied ΔK and/or the crack beginning to enter a residual tensile stress field.

As shown in Fig. 9, applied da/dN-ΔK increases for a given ΔK when R increases from 0.10 to 0.40. Figure 11 shows U as a function of ΔK for 2% slope offset data for an R ratio of 0.40. This plot exhibits the same behavioral trend as Fig. 10. U initially decreases with increasing ΔK prior to reaching a ΔK at which U escalates with

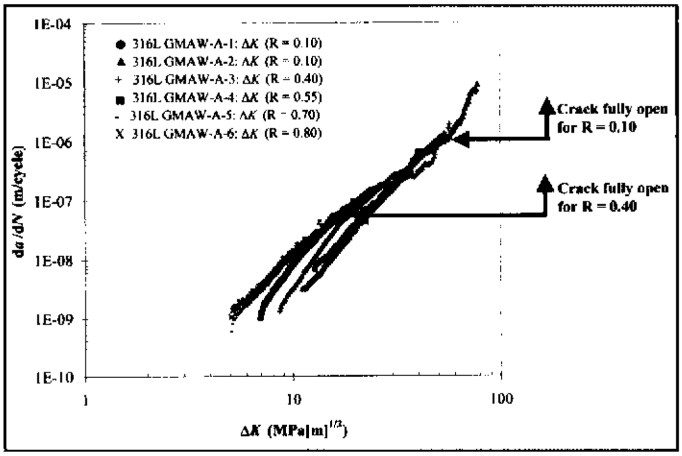

Fig. 13 — Replot of Fig. 9 showing locations where the crack becomes fully open for R ratios of 0.10 and 0.40.

ΔK. However, for an R ratio of 0.40, the ΔK at which this change occurs is approximately 10 MPa$\sqrt{}$m, which is considerably less than the ΔK of 25 MPa$\sqrt{}$m at which similar behavior transpires for an R ratio of 0.10. For comparison to the first two R ratios, Fig. 12 exhibits the U-ΔK relationship for the 2% offset level for an R ratio of 0.55. The single, horizontal line is indicative of artificial crack closure, and therefore, a completely open crack. Similar behavior was observed for R ratios of 0.70 and 0.80.

With this information in mind, a more detailed interpretation of Fig. 9 is now possible. Figure 13 shows a replot of Fig. 9. In this figure, the point at which crack closure is overcome for R ratios of 0.10 and 0.40 are noted on the figure. For an R ratio of 0.10, the crack is fully open at fatigue crack growth rates above 1×10^{-6} m/cycle. For an R ratio of 0.40, the crack is fully open at fatigue crack growth rates above 5×10^{-8} m/cycle. For the remaining R ratios, the crack is always open. First, note that the crack growth rates are essentially independent of R at growth rates above $\sim 1 \times 10^{-6}$ m/cycle, which is commonly observed since R has the largest influence on da/dN at low ΔK values. Below this growth rate, the crack is not fully open for an R value of 0.10. Thus, the increase in growth rate which occurs as R is increased from 0.10 to 0.40 can be attributed to an extrinsic effect. In other words, this increase in da/dN is caused by overcoming crack closure and is not an intrinsic material effect. A similar argument can be made for an R ratio of 0.40 at growth rates below 5×10^{-8} m/cycle, where the increase in da/dN which is observed as R is increased from 0.40 to 0.55 is due to overcoming crack closure. However, even though the crack is always open for the remaining R values of 0.55, 0.70, and 0.80, an increase in growth rate is observed as R increases from 0.55 to 0.70 up to a growth rate of approximately 3×10^{-8} m/cycle. Thus, the increase in growth rate which is observed as R increases from 0.55 to 0.70 within this growth rate regime is a true intrinsic material response to the increase in stress ratio. No significant further material response in da/dN is observed as R is increased further from 0.70 to 0.80.

Summary and Conclusions

The influence of R ratio on the fatigue crack propagation behavior of stainless steel gas metal arc welds was evaluated. The compliance offset method was applied to gas metal arc weld specimens in order to explain the influence of R ratio on crack growth behavior. For the stainless steel gas metal arc welds evaluated, an R ratio of 0.55 has been shown to overcome crack closure over all growth rate regimes. Increases in crack growth rates as R is increased from 0.10 to 0.55 can generally be attributed to an extrinsic effect in which crack closure is overcome. In contrast, the increase in crack growth rate observed for an increase in R from 0.55 to 0.70 is a true intrinsic material response. Further increase in R from 0.70 to 0.80 produces no significant enhancement in the fatigue crack growth rates.

Acknowledgments

The authors thank the United States Office of Naval Research for providing funding for this research. The authors would also like to acknowledge Mike Rex, John Gregoris, and Gene Kozma at Lehigh University for assistance with fatigue crack propagation sample preparation and testing. Preparation of the gas metal arc weld samples by Ravi Menon at Stoody Co. in Bowling Green, Ky., is also greatly appreciated.

References

1. Maddox, S. J. 1970. *Metal Construction and British Welding Journal*, Vol. 2, pp. 285–289.

2. Parry, M., Nordberg, H., and Hertzberg, R. W. 1972. *Welding Journal* 51(10): 485-s to 490-s.

3. Paris, P. C. 1964. Fatigue — An Interdisciplinary Approach. *Proc. of the 10th Sagamore Army Materials Research Conference*, Eds. J. J. Burke, N. L. Reed, and V. Weiss, pp. 107–132.

4. James, L. A. 1972. *Nuclear Technology* 14: 163–170.

5. Cooke, R. J., and Beevers. C. J. 1973. *Engineering Fracture Mechanics* 5: 1061–1071.

6. Ohta, A., and Sasaki, E. 1977. *Engineering Fracture Mechanics* 9: 655–662.

7. Ohta, A., and Sasaki, E. 1977. *Engineering Fracture Mechanics* 9: 307–315.

8. Ohta, A., Sasaki, E., Kamakura, M., Nihei, M. Kosuge, M., Kanao, M., and Inagaki, M. 1981. *Transactions of the Japan Welding Society* 12: 31–38.

9. Katcher, M., and Kaplan, M. 1974. Fracture toughness and slow-stable cracking. ASTM STP 559. American Society for Testing and Materials, pp. 264–292.

10. Brown, R. D., and Weertman, J. 1978. *Engineering Fracture Mechanics* 10: 757–771.

11. Vazquez, J. A., Morrone, A., and Ernst, H. 1979. *Engineering Fracture Mechanics* 12: 231–240.

12. Stofanak, R. J., Hertzberg, R. W., Miller, G., Jaccard, R., and Donald, K. 1983. *Engineering Fracture Mechanics* 17: 527–539.

13. Lindley, T. C., and Richards, C. E. 1974. *Materials Science and Engineering* 14: 281–293.

14. Boutle, N. F., and Dover, W. D. 1977. *Fracture 1977* 2: 1065–1071.

15. Clerivet, A., and Bathias, C. 1979. *Engineering Fracture Mechanics* 12: 599–611.

16. Ohta, A., Suzuki, N., and Maeda, Y. 1977. *International Journal of Fatigue* 19: S303–S310.

17. Donald, J. K. 1988. Mechanics of fatigue crack closure. ASTM STP 982. Eds. C. Newman, Jr., and W. Elber. American Society for Testing and Materials, pp. 222–229.

18. Banovic, S. W., DuPont, J. N., and Marder, A. R. 2001. *Metallurgical Transactions B* 32B: 1171–1176.

19. *Annual Book of ASTM Standards*. Vol. 3.01. 1996. ASTM E647 Section 3. Metals test and analytical procedures. American Society for Testing and Materials: Materials Park, Ohio, pp. 565–601.

20. Hickman, G. 2000. Allegheny Ludlum, Private communication.

21. James, L. A. 1973. *Welding Journal*, 52(3): 173-s to 179-s.

22. James, L. A., and Mills, W. J. 1987. *Welding Journal* 66(8): 229-s to 234-s.

23. *Annual Book of ASTM Standards*. Vol. 03.01. 1996. ASTM E399, Section 3: Metals test methods and analytical procedures, ASM International: Materials Park, Ohio, pp. 407–437.

24. Saxena, A., and Hudak, S. J., Jr. 1978. *International Journal of Fracture* 14: 453–468.

25. Srawley, J. E. 1976. *International Journal of Fracture* 12: 475–476.

26. Donald, J. K., and Schmidt, D. W. 1980. *Journal of Testing and Evaluation* 8: 19–24.

27. Saxena, A., Hudak. S. J., Jr., Donald, J. K., and Schmidt, D. W. 1978. *Journal of Testing and Evaluation* 6: 167–174.

28. Clark, W. G., Jr., and Hudak, S. J., Jr. 1975. *Journal of Testing and Evaluation*3: 454–476.

29. Shih, Y. W., Chen, B. Y., and. Zhang, J. X. 1990. *Engineering Fracture Mechanics* 36: 893–902.

30. Donald, K. 2002. Fracture Technology Associates, Private communication.

31. Elber, W. 1971. Damage tolerance in aircraft structures. ASTM STP 486, American Society for Testing and Materials, pp. 230–242.

32. Frost, N. E., Pook, L. P., and Denton, K. 1971. *Engineering Fracture Mechanics* 3: 109–126.

Single-Pass Laser Beam Welding of Clad Steel Plate

Trials show the possibility of a satisfactory composition and crack-free weld metal

BY S. MISSORI, F. MURDOLO, AND A. SILI

ABSTRACT. The possibility of laser beam welding (LBW) clad steel plates in one pass with a single filler metal was investigated. Two procedures, one with a single-side laser beam and the other with a dual-beam laser, were utilized for butt-joint welding of carbon steel plates clad with austenitic stainless steel. Filler metal was in the form of strips, interposed within edges prior to welding. Metallographic observations and X-ray energy dispersive spectroscopy microanalysis were performed on welded specimens. Mechanical properties were evaluated by Vickers microhardness and tensile tests. These investigations have shown the possibility of making sound welds with a satisfactory composition and crack-free weld metal with both experimental procedures.

Introduction

Plates or tubes of carbon or low-alloy steel clad with an alloyed material are an economical solution to meet the increasing demand of industrial processes for combining elevated strength with good corrosion resistance. Both base steels and cladding materials can be selected from a large variety according to specific requirements and operations. The available base steels include structural steels, pressure vessel steels for elevated temperature, and fine-grained steels. Cladding materials are provided in several classes of stainless steels, nickel alloys, copper alloys, or titanium alloys.

Cladding materials are normally applied to base steels by explosion welding, weld surfacing, solid-state welding by coextrusion, or hot rolling, obtaining strong metallurgical bonding at the interfaces. Cladding thickness may vary from 5 to 50% of the total thickness, but it is generally 10 to 20% for most applications (Ref. 1). This advantageous combination gives rise to a remarkable reduction in weight and cost savings in comparison with the utilization of solid plates.

In our experiments, we considered one of the most usual cases, that of carbon steel clad with stainless steel. It is important to remark that due to adverse metallurgical reactions, the welding techniques described below can by no means be applied to plate clad with titanium or other nonferrous alloy materials. Usually, welding of plate clad with stainless steel is carried out by arc welding processes (manual arc, submerged arc, gas metal arc, or gas tungsten arc welding). The conventional welding techniques require the following steps to be undertaken (Refs. 1–3):

1) the base steel is first welded with a filler metal;

2) the steel weld is backgouged to the sound metal, producing a groove;

3) welding of clad material can start with deposition of one or several buffer layers by using a filler metal higher alloyed than the cladding metal in order to form a layer that is tolerant of some dilution with the base metal;

4) welding is completed with filler and cover layers of cladding-like weld metal.

This welding procedure requires a quite complex practice including the use of different types of filler metals; moreover, the number of passes is the sum of passes required to weld base steel and cladding material separately plus the additional passes due to backgouging. Normally, many passes are required. Thus, it is advantageous to investigate the possibility of reducing the number of passes by high-penetration LBW. In particular, our work deals with butt-joint welding of carbon steel plates clad with stainless steel by single-pass LBW. Both single-side and dual LBW procedures were considered. Filler metal was in the form of strips or consumable inserts. It is well known that consumable inserts of several configurations (inverted T, Y, rectangular shape, etc.) are often utilized with conventional arc welding for better fitup and easier root welding of components that cannot be back welded from inside (e.g., piping). Particularly in these cases, a welding technique for clad steel that uses a single filler metal could be an interesting solution.

Investigations on welded samples included metallographic observations by optical and scanning electron microscopy (SEM), microanalysis by energy dispersive spectroscopy (EDS), microhardness tests, and tensile tests.

KEY WORDS

Clad Steel
Consumable Inserts
Laser Beam Welding (LBW)
Hot Cracks

S. MISSORI is with Dipartimento Ingegneria Meccanica, Università di Roma, Italy. F. MURDOLO and A. SILI are with Dipartimento Chimica Industriale e Ingegneria dei Materiali, Università di Messina, Italy.

Materials and Methods

Materials

The materials utilized in these welding trials were carbon steel plates (6.5 mm thick), clad with a low-carbon austenitic stainless steel (2.5 mm thick). These plates were produced by hot rolling by Voest-Alpine Stahl GmbH, Linz, Austria. The clad thickness was chosen because it was readily available from the supplier. Even though the thickness is a little greater than usual (27.7% of the total thickness), the results obtained can be extended to different thickness ratios provided that the effect of different dilution on the fusion zone (FZ) is properly taken into account in the choice of filler metal composition, as explained afterward in the discussion of results. The base material specification is H II DIN 17155, equivalent to ASTM 515 Gr. 60. The cladding metal specification is 1.4306 DIN 17440, equivalent to AISI 304. The chemical compositions of the two steels are given in Table 1.

The weld metal derives from the fusion of the filler metal and of a portion of base and cladding metals, according to the dilution and melt pool dynamics caused by the welding process. The filler metal was chosen in such a way that the weld metal is suitable to ensure the continuity of the cladding layer and its good anticorrosion properties and, moreover, does not contain structures that might develop undesirable brittleness or cracking after dilu-

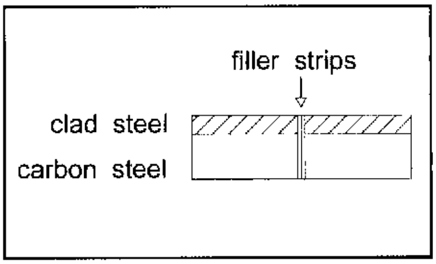

Fig. 1 — Square edge preparation of clad plates.

tion with the steel. Based on results of previous experiments in LBW of dissimilar metals (Refs. 4, 5), two different filler materials have been utilized (Table 2):

a) Nickel-based alloy (DIN 2.4806), which can tolerate high dilution with carbon steel without becoming crack sensitive. In addition, the solubility of carbon is lower by comparison to that in austenitic stainless steel, minimizing carbon migration from the ferritic steel to the weld metal during welding and while in service (Refs. 6–8).

b) Austenitic stainless steel (DIN 1.4465), with the aim of achieving a FZ composition similar to the one of clad stainless steel, free from martensite (to reduce risk of cold cracking), and with little delta ferrite, effective in preventing hot cracking in the austenitic matrix (Refs. 9–13).

Table 1 — Specifications and Chemical Composition of Plates, from Maker Certificate

Material:	Base: Carbon Steel	Cladding: Stainless Steel
Thickness:	6.5 mm	2.5 mm
DIN Specification:	H II DIN 17155	1.4306DIN17440
ASTM Equiv. Specification:	A 515 Gr. 60	A240 Type 304 L
Chemical Composition (wt-%)		
C	0.145	0.017
Mn	0.85	1.32
Si	0.20	0.39
P	0.008	0.029
S	0.001	0.003
Al	0.04	—
Cr	—	18.39
Ni	—	10.07

Table 2 — Specifications and Chemical Composition of Filler Metals, from Maker Certificate

Specification:	DIN 2.4806	DIN 1.4465
Other Designation:	AWS ERNiCr3	AWS ER310Mo Modified
Thickness:	0.4 mm	0.5 mm
Chemical Composition (wt-%)		
C	0.020	0.010
Mn	3.00	6.00
Cr	20.50	25.00
Si	0.10	0.10
Ni	bal.	22.6
Mo	—	2.10
Nb	2.50	0.01
Fe	1.5	bal.

Table 3 — Welding Parameters

	Procedure A Dual LBW	Procedure B Single-Side LBW
Power at the Workpiece:	2×10.0 kW	10.0 kW
Welding Speed:	3.0 m/min	1.6 m/min
Distance Δz:	0 mm	–1 mm
F-Number:	10/8	4
Focal Radius:	530/342 μm	250 μm
Helium Flow Rate:	2×25 L/min	20 L/min
Filler Metal:	N.3 strips ERNiCr3 alloy (0.4 mm thick)	N.2 strips ER310Mo modified (0.5 mm thick)
Position:	Plates on vertical plane with two laser beams traveling horizontally.	Plates on horizontal plane with laser beam on the clad side.
Edge Preparation:	Squared	Squared

Edge Preparations and Welding Processes

Welds in butt joints were performed on plates with square edge preparation, as shown in Fig. 1. The filler metal was put into the joint in the shape of strips. Initially, the LBW techniques were scheduled to utilize either dual laser beam or single laser beam, as well as either nickel-based alloy or austenitic steel alloy filler metal (four techniques in all), but the program could not be completed and, in fact, only the following two techniques were tested:

Procedure A: Dual LBW, with the beams traveling horizontally and the plates being positioned on a vertical plane — Fig. 2. The two laser systems were a unit UTIL 25 kW and a Rofin Sinar SR 170 (nominal power 17 kW). The focusing devices were 35-deg-off-axis paraboloids with a focal length of 682 mm each. Three strips of Ni-based alloy filler metal Type 2.4806, each being 0.4 mm thick (1.2 mm total thickness), were utilized for this procedure.

Procedure B: Single-side LBW with the plates in flat position — Fig. 3. The laser equipment was a unit UTIL 25 kW, DC, with unstable resonator configuration, nonpolarized, using CNC five-axis gantry portal. The focusing device was a 90-deg-off-axis paraboloid with a focal length of 300 mm. Two strips of the austenitic filler metal Type 1.4465 (similar to ER 310Mo), each being 0.5 mm thick (1 mm total thickness), were utilized.

The welding parameters of procedures A and B are given in Table 3. For both procedures, a diagnostic system was utilized before welding to check the features of the laser beam. The estimated Rayleigh lengths are adapted to the thickness of the workpieces. The weld pool protection and the plasma control were performed by a stream of helium gas. No preheating or postweld heat treatments were carried out.

Metallurgical Investigations

The welded plates were cut transversely to the bead to obtain samples of the welded sections. Metallographic spec-

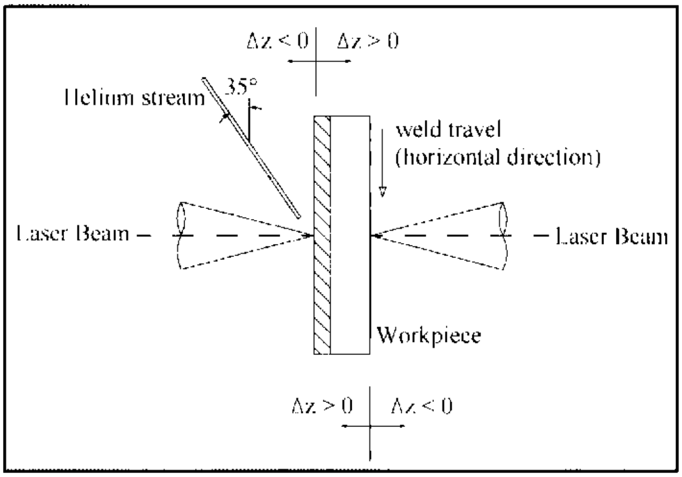

Fig. 2 — Dual LBW procedure assembly.

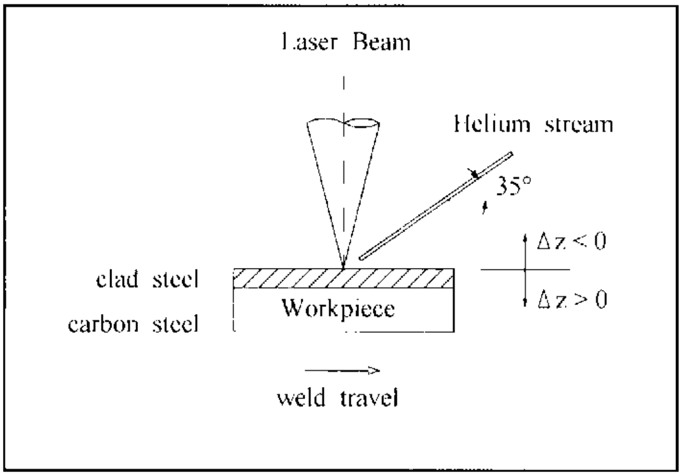

Fig. 3 — Single-side LBW procedure assembly.

imens were prepared by conventional mechanical polishing and then etched by 2% Nital or Glyceregia to reveal carbon steel and austenitic microstructures. The following experimental work was performed:

Visual inspection and macrographic examination. Welds were submitted to visual and macrographic inspection. A minimum of three macrographic samples per each procedure were cut and examined.

Optical and SEM metallurgical observations of the FZ and HAZ.

Microanalysis by energy dispersive spectroscopy (EDS). Variations in composition along the centerline of the weld zone were analyzed by a electron probe, Type JSM-35 CF, equipped with an energy dispersive spectrometer, Model EDAX 711, at an accelerating voltage of 15 kV. The analysis was performed on samples taken from both welding procedures. The content of the elements mainly influencing the formation of phases, in particular Cr and Ni, was quantitatively measured in at least ten points, located on a traverse along the weld zone crossing the full thickness of the sample.

Evaluation of fusion zone areas. The survey of the dimensions of each cross section of the welds was performed with the aid of an optical microscope by measuring the coordinates of the profile of the melt zone, divided in slices of equal height, and evaluating the area by a numerical method.

Estimation of microstructures by Schaeffler diagram (Ref. 14). The contents of Cr and Ni were taken as estimated by SEM microanalysis. Carbon and Mo contents were calculated from base and filler metal compositions, taking account of the dilution and the actual contribution of each material (base metal and filler metal) to the formation of the FZ, according to its respective melted area.

Microhardness tests. Vickers microhardness tests (100-g load, 10-s time) on metallographic samples. Microhardness values were measured on:

- a first traverse along the centerline of FZ;
- a second traverse in the middle of the clad steel thickness, parallel to the clad line;
- a third traverse in the middle of the base carbon steel thickness, parallel to the clad line.

Consequently, three hardness profiles were obtained for each welded sample.

Tensile tests. Tests were performed on specimens cut normally to the welding direction, in order to evaluate the tensile strength of welded joints. Two specimens per each welding procedure were provided.

Table 4 — Tensile Test on Welded Samples

Welding Procedure	Tensile Strength (MPa)	Failure Zone
Dual LBW	486 479	Base metal
Single-Side LBW	468 463	HAZ

Results

Visual Inspections and Macrographic Examinations

Figure 4A and B shows representative macrographs of the welded sections obtained with the two LBW procedures. Both samples showed a satisfactory appearance. No major discontinuities, such as cracks and incomplete fusion, were observed. Both welding procedures gave rise to a good bridgeability. On the sample welded with dual LBW, little porosity was observed, but no quantitative evaluation was made of size and number of pores.

In order to evaluate the extension of the FZ and heat-affected zone (HAZ), the macrographic cross-sectional areas were measured with the aid of an optical microscope. In Fig. 5 A and B, the welded sections are sketched with the indications of the FZ and HAZ sizes. No metallurgical changes were observed in the clad steel near the fusion boundary. Samples obtained by the single-side LBW procedure show a smaller extension of the FZ and HAZ.

Tensile Tests

Tensile tests show a good mechanical soundness for both procedures. The results of tensile tests on two samples per each procedure are reported in Table 4. The tensile strength values are greater than the minimum nominal tensile strength of carbon steel, equal to 410 MPa. Failure took place in the base metal for samples welded by the dual LBW procedure and in the HAZ for the single-side LBW procedure.

Vickers Microhardness Tests

The hardnesses measured on welded sections show similar profiles for both LBW procedures A and B. Representative Vickers microhardness profiles are given in Fig. 6A–C for procedure A and in Fig. 6D–F for procedure B.

a) *Traverse along FZ.* The profiles along the central line of the welded sections are fairly even and are in the range 190–240 HV for procedure A (Fig. 6A) and in the range of 180–200 HV for procedure B (Fig. 6D).

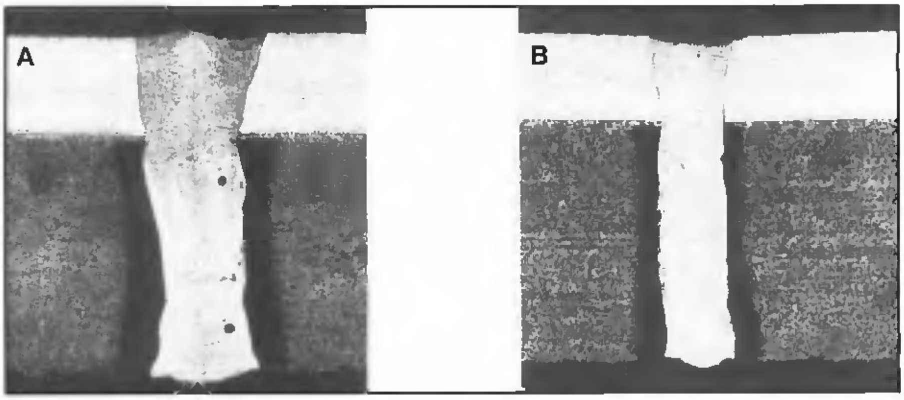

Fig. 4 — Macrographs of welded sections: A — dual LBW; B — single-side LBW.

b) *Traverse along clad steel, parallel to cladding line* (Fig. 6B and E). No significant variation of microhardness occurred along the width of the FZ or in the clad steel near the FZ (variation range of 180–210 HV). Moreover, these microhardness values are of the same order as the initial microhardness of the clad material.

c) *Traverse along carbon steel, parallel to cladding line* (Fig. 6C and F). The hardness profile along the FZ width is quite even, except for some increase in the vicinity of the fusion boundary. In the HAZ, as commonly observed in ferritic steel, the hardness decreases as the distance from the fusion boundary increases. Peak hardness values were measured near the fusion boundary line in the range of 300–400 HV. At distances greater than 3 mm, the hardness stays constant and is equal to that of the unaffected carbon steel (about 150 HV).

Metallographic Observations and Microanalysis by EDS

Microstructures the Base Metals and the Clad Steel/Carbon Steel Interface

The carbon-base steel shows a microstructure consisting of a mixture of grains of ferrite and pearlite, with pearlite disposed in longitudinal bands, typical of milled products. As pointed out in a previous work (Ref. 15), a carbon migration from the base steel toward the stainless austenitic steel occurs during the fabrication process of clad plates due to the hold time at high temperature. The carbon diffusion gives rise to microstructural changes in the two steels, near the bimetallic interface or cladding line (Fig. 7). This interface is clearly detectable as a narrow band, less than 10 μm wide. At the carbon steel side, a decarburized region about 120 μm wide, without pearlite and with ferritic grains larger than ones far from the interface, can be observed. The austenitic side is characterized by a precipitation zone, ~200 μm wide, where precipitated alloy carbides are clearly visible. In particular, the carbide concentration gradually decreases as the distance from the cladding line increases. Energy dispersive spectroscopy measurements on traverses across the cladding line have shown diffusion profiles of substitutional elements centered around the cladding line and interesting small distances of about 20 μm (Ref. 15). Welding operations do not appear to affect this initial condition.

Microstructures of the HAZ

During welding, the region closest to the weld interface undergoes a fast heating at a temperature exceeding the Ac_3 point (ferrite-austenite transformation). Consequently, complete or partial austenitization with different homogeneity of austenite occurs in the carbon steel at several distances from the weld interface, according to nucleation and growth controlled by the temperature/time history of each portion of steel. Furthermore, the subsequent microstructural transformations vary according to the cooling rate at the several distances from the weld interface.

With reference to a sample welded with procedure A, on the carbon steel side, the HAZ, less than 0.8 mm wide, is characterized by:

- first a narrow zone near the weld interface where a hard structure, probably a bainite + martensite mixture, with a microhardness peak of about 400 HV can be observed (Fig. 8);
- a second zone with greater width in which hardening structures are present mixed with untransformed ferrite (Fig. 9) with intermediate values of microhardness (200–250 HV). The amount of untransformed ferrite increases gradually with the distance from the weld interface. The microhardness decreases down to about 150 HV in the unaffected zone.

In the clad steel near the FZ, there is no evidence of structural transformations.

Microstructures of FZ

Figure 10 gives the concentration profiles of Ni and Cr by EDS measurements in the FZ along the joint thickness. The highest Ni and Cr concentrations are reached in the FZ of samples obtained with the dual-beam laser welding procedure, utilizing a high-nickel alloy as filler metal. With the single-side procedure, the alloy element concentrations in the FZ gradually decrease along the joint thickness, from the austenitic clad metal to the carbon steel side. In both procedures, metallographic observations have shown a crack-free, austenitic microstructure in

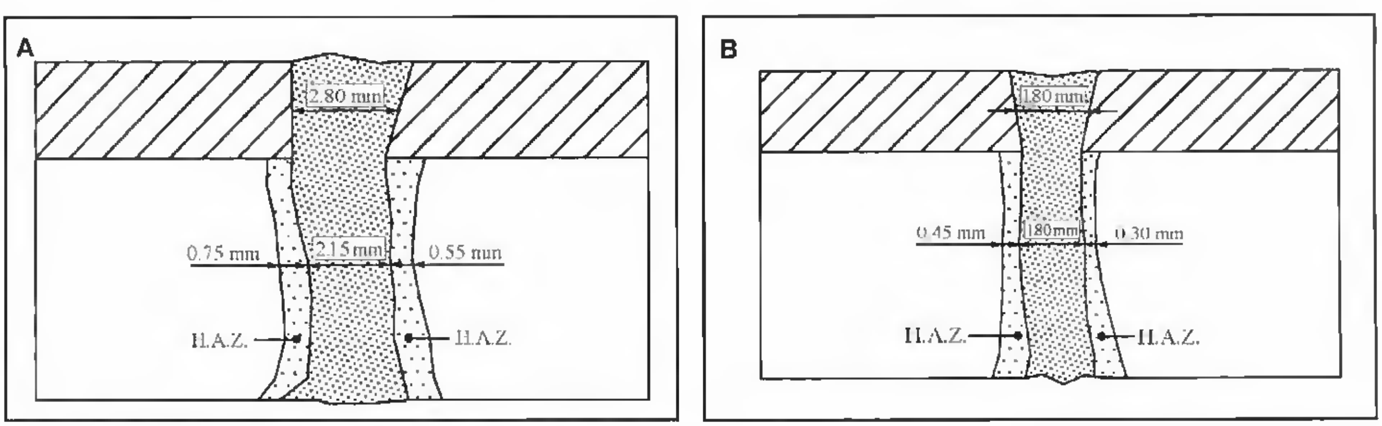

Fig. 5 — Sketches of the welded sections: A — dual LBW; B — single-side LBW.

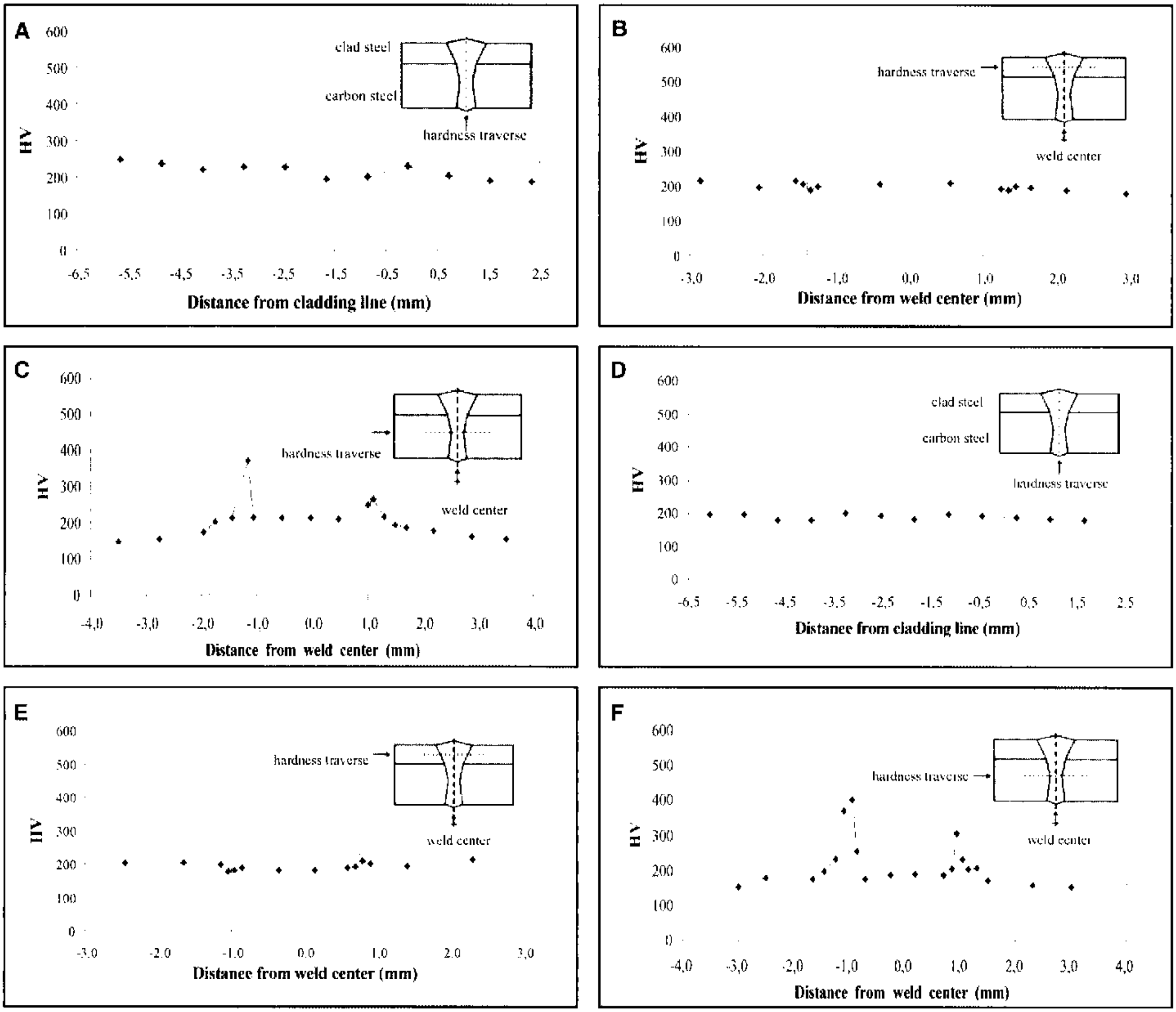

Fig. 6 — Microhardness profiles in welded sections: A, B, C — dual LBW; D, E, F — single-side LBW.

the FZ, along all the thickness of the joints. In particular, the FZ has the following characteristics according to the welding procedures utilized:

- procedure A, dual LBW: an austenitic microstructure, with high-nickel alloy composition, fairly homogeneous, with some precipitates at the grain boundary (Fig. 11);
- procedure B, single LBW: an austenitic microstructure with alloy composition close to the austenitic clad steel (Fig. 12).

Discussion

The phases in the FZ have been estimated by reporting microanalysis measurements as points on a Schaeffler diagram.

The dual-beam LBW (procedure A), which utilizes a Ni-based alloy as filler metal, gives rise to a quite homogeneous composition of the fusion zone along all the thickness, resulting in a fully austenitic phase. All the points representative of the FZ composition are in the austenitic region, typical of the alloys with high Ni composition (Fig. 13). The microhardness values are relatively low. The evaluation of average composition based on SEM microanalysis agrees with the determination based on dilution of fusion zones and material compositions. However, the Cr content, estimated by EDS, decreases along the thickness from 16% (clad steel side) to 12% (carbon steel side). Ni content is more homogeneous and is in the range of 35–40%. According to the results of microhardness tests, showing an even transversal profile, it appears reasonable to suppose that no anomalies due to incomplete mixing out of the FZ centerline should be present all along the width.

The single LBW (procedure B) with the use of filler metal Type ER 310Mo/modified shows a composition of FZ with both Cr and Ni decreasing a little along the thickness going from the clad steel to the carbon steel side. Chromium goes from 18 to 14% and Ni from 14 to 11%. On the Schaeffler diagram (Fig. 14), the points representative of Ni and Cr equivalent compositions along the weld thickness are still in the austenitic field. In particular, the points related to the compositions of the FZ at the carbon steel side fall at the boundary between the austenitic and the austenitic–martensitic regions. In any case, composition and microstructure can be considered satisfactory for this procedure as well. The hardness values are relatively low with an even profile along the fusion zone, confirming the phase estimation ac-

Fig. 7 — Micrograph of the bimetallic interface.

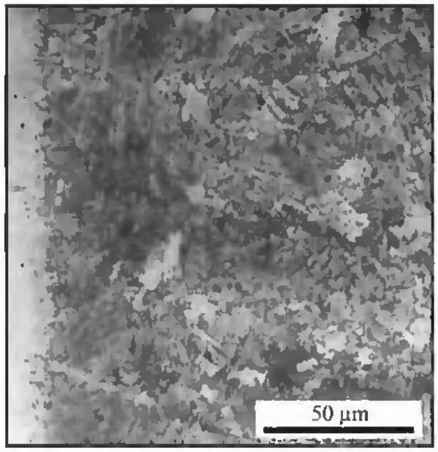

Fig. 8 — Micrograph of the carbon steel HAZ region with high hardness.

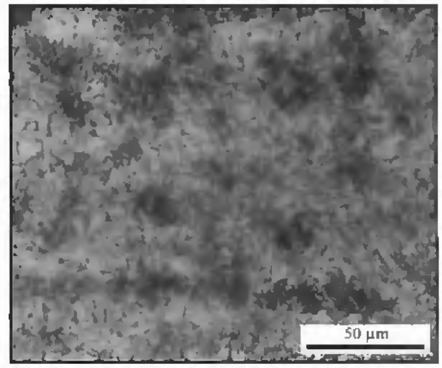

Fig. 9 — Micrograph of the carbon steel HAZ region with low hardness.

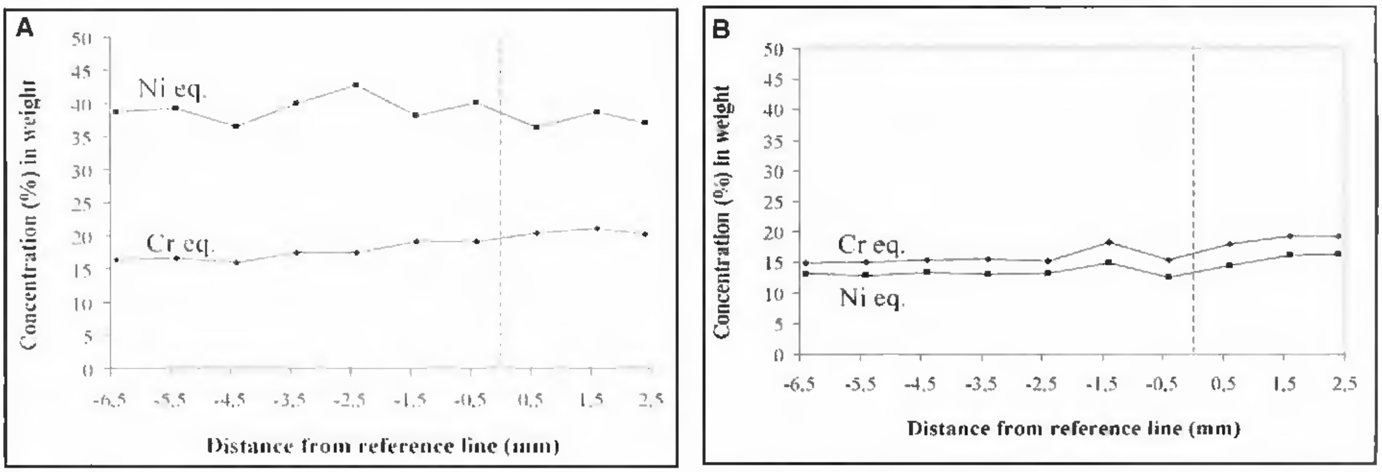

Fig. 10 — Ni and Cr concentration profiles in welded sections: A — dual LBW; B — single-side LBW.

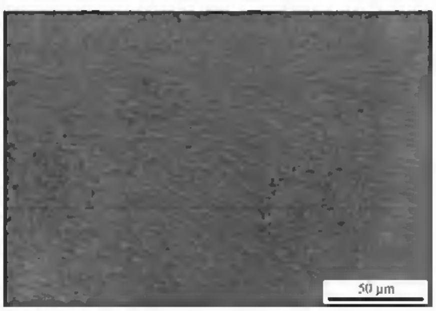

Fig. 11 — Micrograph of the FZ: dual LBW.

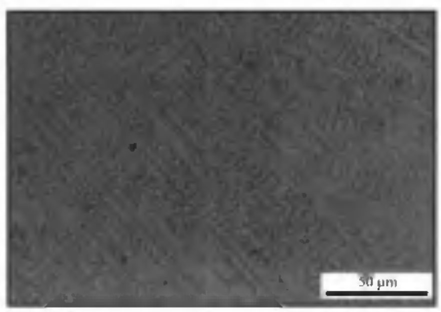

Fig. 12 — Micrograph of the FZ: single-side LBW.

cording to the Schaeffler diagram and the absence of martensitic structures.

The results obtained with the two procedures A and B are not easily compared, due to the different compositions of filler metal and different welding techniques (single or dual LB). It appears, however, that dual LBW offers more capability to fit to geometrical inaccuracies in joint preparation — also thanks to a slightly wider FZ. Moreover, the FZ composition is more even along the thickness.

Tensile tests showed good mechanical soundness of welded joints for both procedures A and B. It was found that all the welded specimens have an ultimate tensile strength not less than the minimum nominal tensile strength of the carbon steel. The failure zone is located in the base metal, out of the FZ. Therefore, the results can be considered satisfactory.

The relatively high values of hardness found in the carbon steel HAZ may be reduced by preheating and/or postweld heat treatment.

As noted in the introduction, the available clad thickness was about 27.7% of the total thickness. However, the clad thickness is usually in the range of 10–20% of the total plate thickness. To successfully apply the welding techniques tested here to cases of smaller ratios of cladding/total thickness, one should consider that the small reduction of alloy element content in the FZ, resulting from a greater contribution of carbon steel to its formation, can be easily compensated by a slightly higher Cr-Ni content in the filler metal. Under this condition, the little divergence from usual clad thickness ratio should not influence the applicability of the welding techniques.

A further improvement of the quality of fusion zones could be expected by using more appropriate filler materials, not readily available at present, to be especially provided for LBW. In particular, for single-side LBW (procedure B), filler material should have a composition slightly

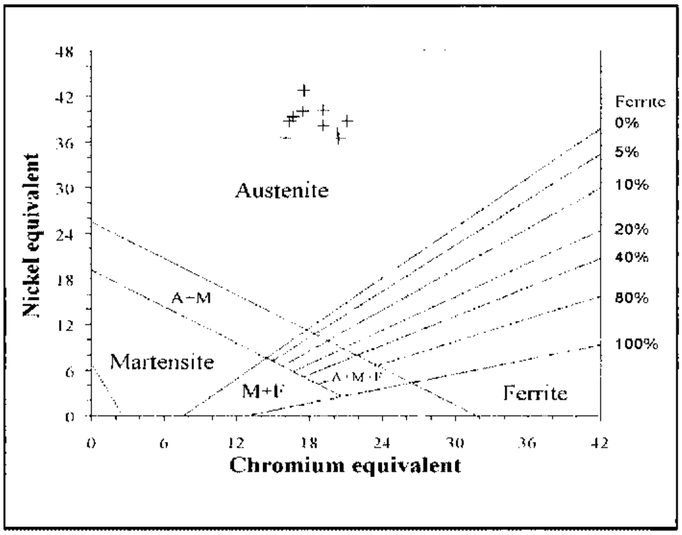

Fig. 13 — Procedure A (ERNiCr3 dual LBW procedure). Schaeffler diagram with points (+) representative of Ni and Cr equivalent compositions in the FZ.

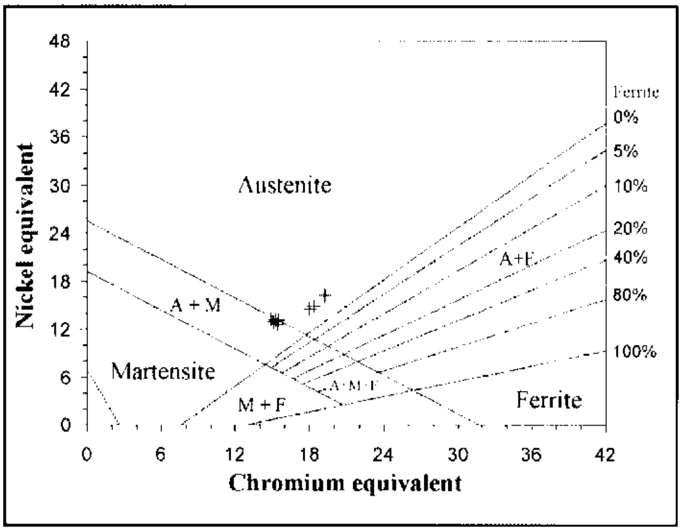

Fig. 14 — Procedure B (ER310Mo modified single-side LBW procedure). Schaeffler diagram with points (+) representative of Ni and Cr equivalent compositions in the FZ.

richer in Cr in order to better compensate for the greater dilution occurring in the base metal carbon steel side. Furthermore, for both procedures, the thickness of the filler metal strips should be increased to make possible the use of a single strip, instead of a number of packed strips. This should improve the heat flow conditions from the weld pool to the base metal and reduce the risks of incomplete fusion or penetration.

Conclusions

It is possible to draw the following conclusions:

a) Both experimental LBW procedures, named A and B, gave promising results for welding clad steel plates by a single pass as it appears feasible to weld clad steel with a satisfactory composition and crack-free FZ.

Procedure A. The dual LBW procedure showed the possibility of performing sound welds in a single pass, obtaining a homogeneous structure with high Ni content.

Procedure B. Metallographic samples of welds showed a quite homogeneous composition of the FZ all along the thickness, close to that (fully austenitic) of the clad steel. The small difference of composition between the portion of the FZ contiguous to clad metal and that contiguous to the carbon-steel metal may be compensated for by a proper increase of Cr content in the filler metal.

b) The results obtained with the procedures A and B are not easily compared, due to the different compositions of filler metal and different welding techniques (single or dual LB). It appears, however, that dual LBW offers more capability to fit to geometrical inaccuracies in joint preparation, due also to a slightly wider FZ. Moreover, the FZ composition is more even along the thickness, thus giving rise to a more homogeneous microstructure.

c) In the FZ obtained by both experimental procedures, moderate and uniform hardness values were exhibited. Mechanical strength of the joints was in all cases greater than the nominal strength of the base carbon steel.

d) The results encourage further experiments to improve the adopted welding techniques, with the aim of optimizing the composition of filler metal, with possible utilization of integral thicker filler strips.

Acknowledgments

The authors thank the Laser Welding Department of Fraunhofer Institut ILT-Aachen for its support in setting up welding procedures and providing technical assistance.

References

1. Oates, W., and Saitta, A., eds. 1998. *Welding Handbook 8th ed., Vol. 4*, pp. 370–371. Miami, Fla.: American Welding Society.

2. Funk, W. H. 1960. *Interpretative Report on Welding of Nickel Clad and Stainless Clad, Bulletin 61.* New York: Welding Research Council.

3. Voest-Alpine Stahl. 1997. *Clad Plates Catalogue.* Linz, Austria.

4. Missori, S., and Koerber, C. 1997. Laser beam welding of austenitic-ferritic transition joints. *Welding Journal* 76(3): 125-s to 134-s.

5. Missori, S., and Koerber, C. 1998. Procedure development for improved quality single and dual LBW of dissimilar metals. *Welding Journal* 77(6): 232-s to 238-s.

6. Klueh, R. L., and King, J. F. 1982. Austenitic-ferritic weld-joint failures. *Welding Journal* 61(9): 302-s to 311-s.

7. Viswanathan, R. 1985. Dissimilar metal welds in service and boiler creep damage evaluation for plant life extension. *Journal of Pressure Vessels Technology* 107: 218–225.

8. Roberts, D. I., Ryder, R. H., and Viswanathan, R. 1985. Performance of dissimilar welds in service. *Journal of Pressure Vessels Technology* 107: 247–254.

9. Brooks, J. A., Thompson, A. W., and Williams, J. C. 1984. A fundamental study of the beneficial effects of delta ferrite in reducing weld cracking. *Welding Journal* 63(3): 71-s to 83-s.

10. Singh, J., Purdy, G. R., and Weatherly, G. C. 1985. Microstructural and microchemical aspects of the solid-state decomposition of delta ferrite in austenitic stainless steels. *Metallurgical Transactions A* 16A(8): 1363–1369.

11. Kujanpaa, V. P., David, S. A., and White, C. L. 1986. Solidification cracking, formation of hot cracks in austenitic stainless steel welds. *Welding Journal* 65(8): 203-s to 212-s.

12. David, S. A., Vitek, J. M., and Hebble, T. L. 1987. Effect of rapid solidification on stainless steel weld metal microstructures and its implications on the Schaeffler diagram. *Welding Journal* 66(10): 289-s to 302-s.

13. Vitek, J. M., and David, S. A. 1988. The effect of cooling rate on ferrite in Type 308 stainless steel. *Welding Journal* 67(5): 95-s to 102-s.

14. Schaeffler, A. L. 1949. Constitution diagram for stainless steel weld metal. *Metal Progress* 56(11): 680–680B.

15. Missori, S., and Sili, A. 1997. Metallurgical transformations on hot rolled clad steel. *Proceedings of EUROMAT 97, Maastricht* 4:51–55.

WELDING Journal

Guidelines for submitting electronic files

1. Platform:
Macintosh or PC accepted

2. Files accepted:
QuarkXpress, Adobe Photoshop, Adobe Illustrator, TIFF, EPS and PDF files only.

3. Color:
Send all files in as CMYK (for color) or Grayscale (for b/w).

4. Images:
Minimum resolution required for magazine printing is 300 dpi for full color artwork or grayscale at least 1000 dpi for bitmap (B&W/line art). Images and logos from Web sites are NOT usable for printing. They are low resolution images (72 dpi). Images taken with a digital camera are not acceptable unless they meet the minimum 300 dpi requirement.

5. **Proof:**
A proof of the images should **always** be provided.

6. Electronic File Transfer:
Files larger than 68k are not acceptable as an email attachment; please CD or Zip, may also send files to the printer FTP site (a user name and password will be provided when requested)

Check list for submitting electronic files:

Colors: ❒ 4/C ❒ Grayscale ❒ B&W/line art

File Type: ❒ TIFF ❒ EPS

File sent via: ❒ Floppy disk ❒ Zip disk ❒ Jaz disk ❒ CD ❒ Email (68k limit)

❒ **Proof supplied**/faxed

❒ CMYK images at 300 dpi or higher, B&W/line art at 1000 dpi or higher.

❒ All color in all images set to CMYK process (not RGB)

When submitting ads please send them to the attention of

Frank Wilson
Advertising Production
American Welding Society
550 NW LeJeune Rd.
Miami, Fla. 33126

To receive your free literature from our advertisers, circle the numbers that correspond to the items that interest you.

Please send literature on items circled at right:

February 2004 — Card void after August 1, 2004

Name ________________ Title ________________

Company ________________

Address ________________

City ________________ State ______ Zip ________

Phone: ________________ Fax: ________________

E-mail ________________

Please circle an entry for each category:

I TYPE OF BUSINESS
1. Construction
2. Primary Metal Products
3. Fabricated Metal Products
4. Transportation
5. Wholesale Trade
6. Misc. Repair Services
7. Educational Services
8. Other

II JOB FUNCTION/TITLE
1. Corp. Management
2. Plant Mgmt. & oper.
3. Chemical and petroleum Prodn. Mgmt.
4. Welding & Cutting Oper.
5. Quality Control
6. Sales
7. Purchasing
8. Other

III PURCHASING AUTHORITY
1. Recommend
2. Specify
3. Approve

IV NUMBER OF EMPLOYEES
1. Under
2. 50 to 99
3. 100 to 499
4. 500 to 999
5. 1000 to 2499
6. 2500 to more

V ANNUAL DOLLAR VOLUME
1. Under $1 Million
2. $1 Million to 5 Million
3. Over $5 Million

VI THIS INQUIRY IS FOR
1. Immediate Purchase
2. Future Project
3. General Information

VII I HAVE CIRCLED
1. 6 Items or fewer
2. Over 6 Items

❑ AWS Member
❑ 361- Mail me List of AWS publications
❑ Non-Member
❑ 362- Information on AWS Membership

1	37	73	109	145	181	217	253	289	325
2	38	74	110	146	182	218	254	290	326
3	39	75	111	147	183	219	255	291	327
4	40	76	112	148	184	220	256	292	328
5	41	77	113	149	185	221	257	293	329
6	42	78	114	150	186	222	258	294	330
7	43	79	115	151	187	223	259	295	331
8	44	80	116	152	188	224	260	296	332
9	45	81	117	153	189	225	261	297	333
10	46	82	118	154	190	226	262	298	334
11	47	83	119	155	191	227	263	299	335
12	48	84	120	156	192	228	264	300	336
13	49	85	121	157	193	229	265	301	337
14	50	86	122	158	194	230	266	302	338
15	51	87	123	159	195	231	267	303	339
16	52	88	124	160	196	232	268	304	340
17	53	89	125	161	197	233	269	305	341
18	54	90	126	162	198	234	270	306	342
19	55	91	127	163	199	235	271	307	343
20	56	92	128	164	200	236	272	308	344
21	57	93	129	165	201	237	273	309	345
22	58	94	130	166	202	238	274	310	346
23	59	95	131	167	203	239	275	311	347
24	60	96	132	168	204	240	276	312	348
25	61	97	133	169	205	241	277	313	349
26	62	98	134	170	206	242	278	314	350
27	63	99	135	171	207	243	279	315	351
28	64	100	136	172	208	244	280	316	352
29	65	101	137	173	209	245	281	317	353
30	66	102	138	174	210	246	282	318	354
31	67	103	139	175	211	247	283	319	355
32	68	104	140	176	212	248	284	320	356
33	69	105	141	177	213	249	285	321	357
34	70	106	142	178	214	250	286	322	358
35	71	107	143	179	215	251	287	323	359
36	72	108	144	180	216	252	288	324	360

For faster processing, please FAX this card to (630) 739-9700.
Type or print the information and copy before faxing.
This fax number is for the service bureau only, not AWS.

NO POSTAGE NECESSARY IF MAILED IN THE UNITED STATES

BUSINESS REPLY MAIL
FIRST-CLASS MAIL PERMIT NO. 11992 MIAMI FL

POSTAGE WILL BE PAID BY ADDRESSEE

WELDING Journal
C/O CREATIVE DATA
519 E BRIARCLIFF RD
BOLINGBROOK IL 60440-9882


SPOTLIGHT THIS
ABIMIG®
WATER-COOLED TORCHES
ABICOR BINZEL
Chrome Nozzle Seat and Dual Cooling . . . the most updated approach to water-cooling found only in the new ABIMIG guns from ABICOR Binzel Corp. These rugged yet lightweight MIG guns now feature a chrome nozzle seat that reduces wear on the swanneck, extending service life. The dual cooling design channels water along the bolted copper inner barrel, cooling the tip, while concurrently water travels along the bolted brass outer barrel, cooling the nozzle. Dual cooling draws heat away from the source, ensuring not only longer tip life but nozzle life as well. The improved strain relief of the 500, 550 and 650 ampere Water-Cooled ABIMIG welding torches protects cable components and withstands the toughest handling.
Welding and cutting brought to the point.
8 0 0 . 5 4 2 . 4 8 6 7
ABICOR BINZEL
Circle No. 1 on Reader Info-Card
www.abicorusa.com
IBG